UNIVERSITY OF LIVERPOOL

Investigation of the importance of intestinal epithelial cell specific nuclear factor-κB subunits in regulating the response to intestinal damage-inducing stimuli

Thesis submitted in accordance with the requirements of the University of Liverpool for the degree of Doctor in Philosophy

By

Stephanie Helen James

October 2017

Declaration

I hereby declare that this thesis is a presentation of my original work. Wherever contributions of others are involved, every effort has been made to indicate this clearly, with due reference to the literature.

Work was performed under the guidance of project supervisors Dr Carrie Duckworth* and Professor Mark Pritchard*

*Gastroenterology Research Unit, Department of Cellular and Molecular Physiology, Institute of Translational Medicine, University of Liverpool

Acknowledgements

Firstly, I would like to thank Epistem Ltd and the University of Liverpool for generously funding my PhD. I am truly thankful to my supervisors Dr Carrie Duckworth and Professor Mark Pritchard for their support throughout my PhD and for the huge amount of help they have given me during my thesis write up. Thank you for your meticulous review of my work, for all the constructive criticism and all of your input. Your guidance has helped to shape my thesis into something that I am proud of. I would also like to thank Carrie for her endless wisdom, guidance and support during my years of lab work, it has been such a pleasure to learn from you!

I would like to thank the staff of the BSU for their technical help during my *in vivo* studies and for making the facility such a friendly place to work. I would like to thank all of my colleagues in the Gastroenterology research unit for their friendly welcome at the beginning of my PhD and their friendship and reassurance throughout, as well as all the help over the years. It was great sharing the lab with you for the last four years and I will miss it very much.

I would like to thank all of my friends in the Institute of Translational Medicine for their support and sympathy during the more difficult times and for all the fun over the years. It has been a great source of inspiration to see everyone making progress and working so hard even when times have been tough!

I would like to thank my mum, dad, sister and other family members and all of my dear friends for their love and support (moral, emotional and otherwise) over the years. Thank you for being so great. Additionally, thank you to the cats for being a furry source of comfort.

Finally I would like to thank Jing for always being amusing and delightful, and for his unceasing support, love and encouragement through this process.

Contents

Abstract

The epithelium of the gastrointestinal (GI) tract is highly specialised and tightly regulated to ensure efficient absorption of dietary nutrients whilst preventing invasion by luminal microorganisms that may cause local and systemic infection and inflammation. Dysregulation of this single layer of columnar epithelium is a contributing factor to several intestinal diseases and toxicities. However, mechanisms that govern the susceptibility of intestinal epithelia to damage-inducing stimuli are not currently fully understood.

NFκB signalling is known to modulate the immune system and regulate homeostasis and repair in the GI tract. The NFκB family of transcription factors consists of 5 main subunits (NFκB1, RelA, c-Rel, NFκB2 and RelB) that function as homo or hetero-dimers and is broadly categorised into the classical and alternative signalling pathways. Previous studies have indicated that the alternative (NFκB2 and RelB) NFκB signalling pathway regulates susceptibility to the onset of inflammatory bowel disease (IBD) and GI apoptosis. However, the contribution of intestinal epithelial cells and immune cells in regulating the GI mucosal response following the induction of experimental colitis was not clear from these studies. This thesis demonstrates using bone marrow reconstituted wild-type C57BL/6J and NFκB2 null mice that the alternative NFκB signalling pathway is important in both the haematopoietic cell and epithelial cell compartments in regulating GI damage following the induction of dextran sulphate sodium (DSS)-induced colitis. NFκB2 deletion in the hematopoietic compartment caused wild-type mice to experience reduced colitis severity compared with non-reconstituted wild-type mice, whereas the presence of wild-type bone marrow caused NFκB2 null mice to experience more severe colitis than that observed in NFκB2 null mice. Therefore, the susceptibility to DSS-induced colitis is mediated by both the immune and epithelial cell compartments.

As GI damage-inducing stimuli act on the epithelium by different mechanisms, this thesis explores whether NFκB signalling pathways specifically in intestinal epithelial cells are important in regulating the epithelial response to further stimuli including mucositis-inducing chemotherapy drugs (5-fluorouracil (5-FU), etoposide and irinotecan) and tyrosine kinase inhibitors (TKIs; imatinib, nilotinib, dasatinib, bosutinib erlotinib and gefitinib) that are known to cause GI toxicity. Intestinal organoid (enteroid) cultures consisting of solely epithelial cells were established from NFκB1 null, NFκB2 null, c-Rel null and RelB null mice. c-Rel deletion protected enteroids from damage induced by 5-FU and etoposide, but not against irinotecan. To validate this *in vitro* enteroid model, mice were injected intraperitoneally with 5-FU (40mg/kg) for 24 hours and c-Rel null small intestine demonstrated persistent mitosis and reduced apoptosis compared with wild-type C57BL/6J mice. Therefore, c-Rel plays a role in regulating the response to the DNA damage caused by 5-FU and the *in vivo* data supports the *in vitro* model and analysis methods established in this study.

The TKIs erlotinib, gefitinib and dasatinib caused significant increases in circularity (a measure of cell death validated against active-caspase-3 immunohistochemistry) of enteroids, while bosutinib, imatinib and nilotinib did not. This indicates that the GI side effects in erlotinib, gefitinib and dasatinib treated patients may be due to direct damage to GI epithelia. Deletion of NFκB2 protected enteroids from erlotinib-induced cell death, indicating that the NFκB2 signalling pathway may have a role in regulating the response of the intestinal mucosa to erlotinib.

Deletion of NFκB2 from intestinal epithelia therefore appears to confer a protective effect against GI damage following some damage-inducing stimuli. Further investigation of this pathway and the potential development of NFκB2 inhibitors for targeted use in the clinic is therefore warranted.

Abbreviations

2D:	Two dimensional
3D:	Three dimensional
5-ASA:	5-Aminosalicylic acid
5-FU:	5-Fluorouracil
ABL:	Abelson murine leukaemia
AID:	Autoimmune disease
AIEC:	Adherent invasive *E. coli*
ANOVA:	Analysis of variance
AOM:	Azoxymethane
APC:	Adenomatous polyposis coli
APES:	3-aminoptopyltriethoxysilane
ASO:	Antisense oligonucleotides
BCL:	B cell lymphoma proteins
BCR:	Breakpoint cluster region
BIK:	BCL interacting killer
BMP:	Bone morphogenic protein
BSA:	Bovine serum albumin
CBC:	Crypt base columnar
CD:	Crohn's disease
CDAE:	Crohn's disease associated *E. coli*
CRISPR/Cas9:	Clustered Regularly Interspaced Short Palindromic Repeats/Caspase 9

DMSO:	Dimethyl sulphoxide
DNA:	Deoxyribonucleic acid
DNBS:	Dinitrobenzene sulphonic acid
DSS:	Dextran sulphate sodium
E. coli:	*Escherichia coli*
ECL:	Enterochromaffin-like
EDTA:	Ethylenediaminetetraacetic acid
EGF:	Epidermal growth factor
EGFR:	Epidermal growth factor receptor
ESC:	Embryonic stem cells
FACS:	Fluorescence activated cell sorting
FdUDP:	Fluorodeoxyuridine diphosphate
FdUMP:	Fluorodeoxyuridine monophosphate
FdUTP:	Fluorodeoxyuridine triphosphate
FGFR:	Fibroblast growth factor receptor
FOLFIRI:	5-FU and irinotecan
FOLFOX:	5-FU and oxaliplatin
FUDP:	Fluorouridine diphosphate
FUDR:	Fluorodeoxyuridine
FdUMP	Fluorodeoxyuridine monophosphate
FUMP:	Fluorouridine monophosphate
FUR:	Fluorouridine
FUTP:	Fluorouridine triphosphate

GI:	Gastrointestinal
H+E:	Haematoxylin and Eosin
HCl:	Hydrochloric acid
HER2:	Human epidermal growth factor receptor 2
HH:	Hedgehog
IBD:	Inflammatory bowel disease
IEC:	Intestinal epithelial cell
IFN:	Interferon
IHC:	Immunohistochemistry
IHH:	Indian hedgehog
IκB:	Inhibitor of kappa B
IKK:	Inhibitor of NFκB kinase
IL:	Interleukin
iPSC:	Induced pluripotent stem cells
IROX:	Irinotecan and oxaliplatin
LPS:	Lipopolysaccharide
MAP:	Mitogen activated protein
MAPK:	Mitogen activated protein kinase
MEF:	Mouse embryonic fibroblasts
NEMO:	NFκB essential modulator
NFκB:	Nuclear factor kappa B
NIK:	NFκB inducing kinase
NKT cell	natural killer T cell

NLK:	Nemo like kinase
NRD	NIK recognition domain
NSCLC:	Non-small cell lung cancer
NSP:	Non starch polysaccharide
OPRT:	Orotate phosphoribosyltransferase
PAMP:	Pathogen associated molecular patterns
PBS:	Phosphate buffered saline
PCR:	Polymerase chain reaction
PID:	Processing inhibitory domain
PRPP:	Phosphoribosyl pyrophosphate
PUMA:	p53 upregulated modulator of apoptosis
RHD:	Rel homology domain
RNA:	Ribonucleic acid
SHH:	Sonic hedgehog
shRNA:	Short hair RNA
TCR:	T-cell receptor
TGF:	Transforming growth factor
Th1:	Type 1 T helper cell
Th17:	Type 17 T helper cell
Th2:	Type 2 T helper cell
TKI:	Tyrosine kinase inhibitor
TLR:	Toll like receptor
TLS:	Tertiary lymphoid structure

TNBS:	2,4,6-Trinitrobenzenesulfonic acid
TNF:	Tumour necrosis factor
TopoI:	Topoisomerase 1
TopoII:	Topoisomerase 2
TP:	Thymidine phosphatase
TPL-2:	Tumour progression locus-2
TUNEL:	Terminal deoxynucleotidyl transferase (TdT) dUTP Nick-End Labeling
UC:	Ulcerative colitis
VEGF:	Vascular endothelial growth factor
WT:	Wild type
ZO-1:	Zonula occludens

1 Introduction

1.1 The gastrointestinal tract

The gastrointestinal (GI) tract is the organ system which is responsible for the ingestion and digestion of food, absorption of nutrients and water and the excretion of waste. It consists of a tube which runs from the oesophagus to the anus and many attached accessory organs and glands. The inner surface of the tract is characterised by an epithelial layer which is surrounded by muscle. The walls contain muscle layers which contract and relax in a coordinated movement known as peristalsis to propel food along the GI tract, as well as non-propulsive contractions termed segmentation in order to expose food to the digestive juices secreted by the gut to aid digestion (Boron and Boulpaep, 2008). The human GI tract contains around 1150 varieties of commensal bacteria which function as an essential part of the innate immune system and the digestive process and are an essential part of the gut (Qin *et al.*, 2010; Guinane and Cotter, 2013)**.** Therefore, it is important that the gastrointestinal tract allows nutrients and water to be absorbed from food while maintaining a barrier to harmful substances and pathogenic bacteria (Artis, 2008). The GI tract has the largest mucosal surface in the body, and is often thought of as the largest component of the immune system. The GI tract is an interface between the immune system and outside pathogens which often enter the body via ingested food. It is therefore vital that the GI mucosa is able to monitor the contents of the intestinal lumen and defend against bacterial invasion (Mowat and Agace, 2014).

The organisation of the GI wall shares similarities throughout the tract (figure 1.1). The inner layer is known as the mucosa and contains invaginations which are known as crypts in the small and large intestine, and finger like projections known as villi in the small intestine, all of which are covered by a single epithelial layer. The submucosa is the supporting mesenchymal tissue of the mucosa; this layer of the GI

wall is found below the mucosa and consists of loose connective tissue and blood vessels. Surrounding the submucosa is the muscle layer which consists of two layers of smooth muscle, the inner layer being circular and the outer layer longitudinal. These layers are together known as the muscularis propria. The outer layer of the gut is known as the serosa, which is composed of connective tissue and squamous epithelial cells and functions to prevent the spread of inflammation or malignant processes to the surrounding peritoneal cavity (Allan, Richards and Shepherd, 1995; Rao and Wang, 2010).

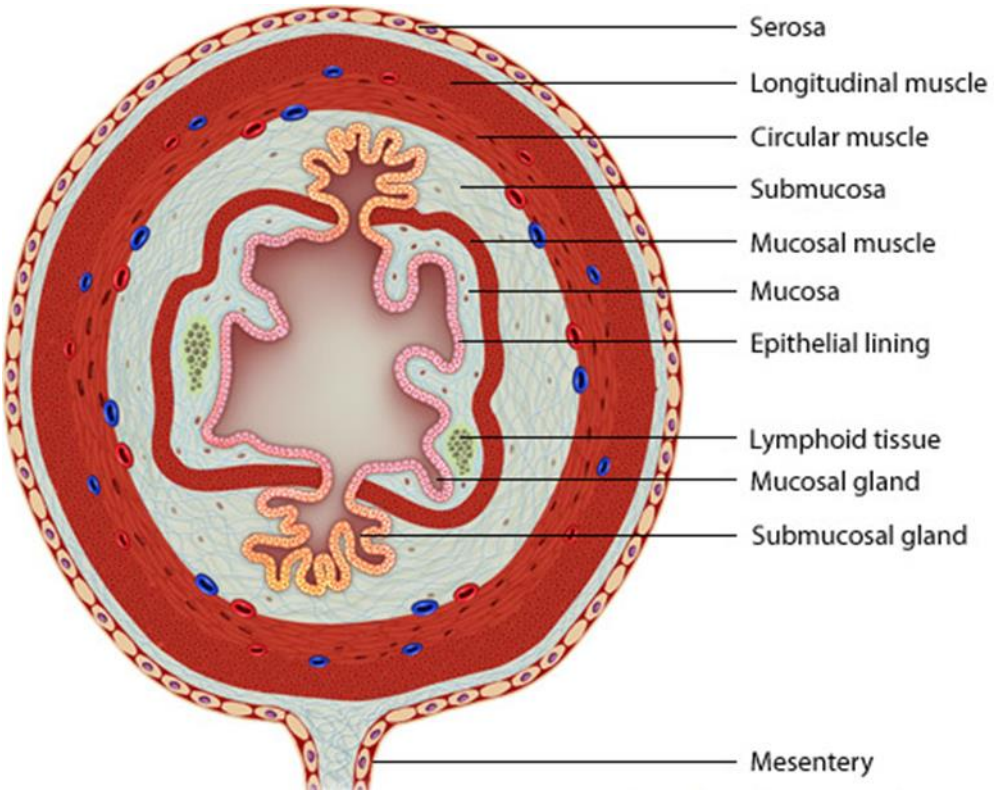

Figure 1.1 Simplified structure of the wall of the gastrointestinal tract in the small intestine and colon indicating the layers in the gastrointestinal wall. Adapted from https://www.myvmc.com/anatomy/gastrointestinal-system

1.1.1 The oral mucosa and the oesophagus

The first part of the gastrointestinal tract consists of the mouth which leads to the oesophagus. The mouth and oesophagus have a different type of epithelial lining compared with more distal regions of the GI tract. The oral mucosa is lined with tightly connected squamous epithelia, overlying a layer of squamous epithelia that proliferate to replace the surface cells which are often sloughed off. The oral mucosa can be keratinised or non-keratinised depending on its location, and has either four or two layers respectively (Presland and Jurevic, 2002). Keratinised epithelia are effectively reinforced by keratin protein fibres which attach to the cells via desmosomes (Presland and Dale, 2000). The purpose of the mouth is to chop food into small pieces, therefore the mucosa of the mouth must be specialised to endure mechanical pressure. The keratinised epithelia of the mouth are located in areas which endure more mechanical pressure such as the hard palate or the top of the mouth, and the non-keratinised epithelia are located in regions which do not endure so much stress such as the buccal mucosa and inner cheeks (Presland and Jurevic, 2002).

The next part of the gastrointestinal tract is the oesophagus. The oesophagus is important as it transmits food and liquid from the mouth to the stomach. The human oesophagus consists of an approximately 20cm long tube which has the upper oesophageal sphincter at its beginning and the lower oesophageal sphincter at its end. The oesophageal wall consists of three layers of cornified epithelia in order to withstand the mechanical pressure of swallowing (Hobson and Aziz, 2011).

1.1.2 The stomach

The stomach is a muscular bag which can hold up to around 2 litres of food and produces powerful contractions to aid digestion. Like the crypts found in the more distal parts of the gastrointestinal tract, the stomach contains invaginations termed

gastric glands. As in other areas of the gastrointestinal tract there are regional differences in the stomach. The first region of the stomach consists of the cardia which is found immediately distal to the gastroesophageal junction, the fundus is found next and is the main proximal part of the stomach, the corpus lies in the middle and the antrum is found in the distal region. The glands of the antrum and corpus contain different types of specialised cells which are unique to the stomach and unlike those found in the small intestine or colon. The glands of the corpus contain mucous neck cells, enterochromaffin like (ECL) cells which secrete histamine in response to gastrin, chief cells which secrete pepsinogen, delta (D) cells which secrete somatostatin and parietal cells which secrete hydrochloric acid (HCl) in response to histamine and enterochromaffin cells which secrete serotonin. The glands of the antrum contain mucous neck cells, gastrin (G) cells which secrete gastrin, D cells, and ECL cells. The gastric stem cells are believed to be located in the isthmus region of the gastric gland which is found in the middle of the gland wall (Boron and Boulpaep, 2008). Reserve stem cells which are identified by the expression of Lgr5 have been found in the antrum of the stomach (Barker *et al.*, 2010), additionally Lgr5 expressing cells have also been found in the base of the corpus gland in the stomach (Leushacke *et al.*, 2017).

1.1.3 Structure and function of the small intestine

The small intestine is on average around 6-7m in length in humans and 40cm long in mice (Mowat and Agace, 2014). This organ takes up a large amount of space in the abdominal cavity and consists of three distinct geographical regions. These are known as the duodenum, jejunum and ileum. Each of these regions has an inner columnar epithelium that is only one cell thick. Underneath the inner epithelial layer is the muscularis mucosae, which is the muscle layer found in the outer mucosa. The lamina propria is located in the submucosa and contains blood and lymph vessels which supply the villi (Mowat and Agace, 2014). Basal to the submucosa is the circular

muscle layer and then the longitudinal muscle layer, which is then surrounded by the serosa and the outer visceral peritoneum which functions to protect the small intestine (Boron and Boulpaep, 2008).

The small intestine is lined by invaginations termed ‘crypts’ and projections termed ‘villi’. The duodenum has been shown to have villi which are of a greater length on average than the jejunum or the ileum. In C57BL/6J wild-type mice, the villi have been found to be 370μm long in the duodenum, 250μm in the jejunum and 200μm in the ileum (Williams *et al.*, 2013). Villi are surrounded by crypts of Lieberkühn, with at least six crypts surrounding and providing cells that populate one villus (Barker, 2014). Villi maximise the surface area of the small intestine and facilitate the absorption of partially digested food that enters the duodenum directly from the stomach. Digestive enzymes are released into the duodenum in order to further digest food. Enzymes are also released by the pancreas, and their delivery is controlled by the sphincter of Oddi which is located in the duodenum and controls the release of pancreatic enzymes and bile into the small intestine. This sphincter is located between the distal bile duct and the pancreatic duct and the lumen of the duodenum (Afghani *et al.*, 2017).

There are several different differentiated cell types, each with a specialised function that are found along the crypt-villus axis (figure 1.2). The most abundant cell types found in the small intestinal epithelium are the absorptive enterocytes which are characterised by the presence of microvilli on their apical surface. These tiny brush borders further increase the surface area of the small intestine, creating a greater surface area for the absorption of the products of digestion (Abbas *et al.*, 1989). Goblet cells secrete mucus and are found throughout the small intestine, however, they are more concentrated in the distal part of the small intestine as there is a greater demand for mucus in this region to lubricate the increasingly dry food matter (Barker, 2014). Enteroendocrine cells function to secrete hormones into the circulation, for

example enterochromaffin cells which secrete serotonin using secretory granules or vesicles (Gunawardene, Corfe and Staton, 2011). Tuft cells are the least abundant of the secretory cell lineages and their function is still to be fully characterised, however there is evidence to suggest that they function in chemoreception; in particular the chemoreception of bitter, sweet and umami molecules (Gerbe, Legraverend and Jay, 2012). Paneth cells are found at the base of small intestinal crypts and secrete anti-microbial factors and support the stem cell niche (section 1.1.6).

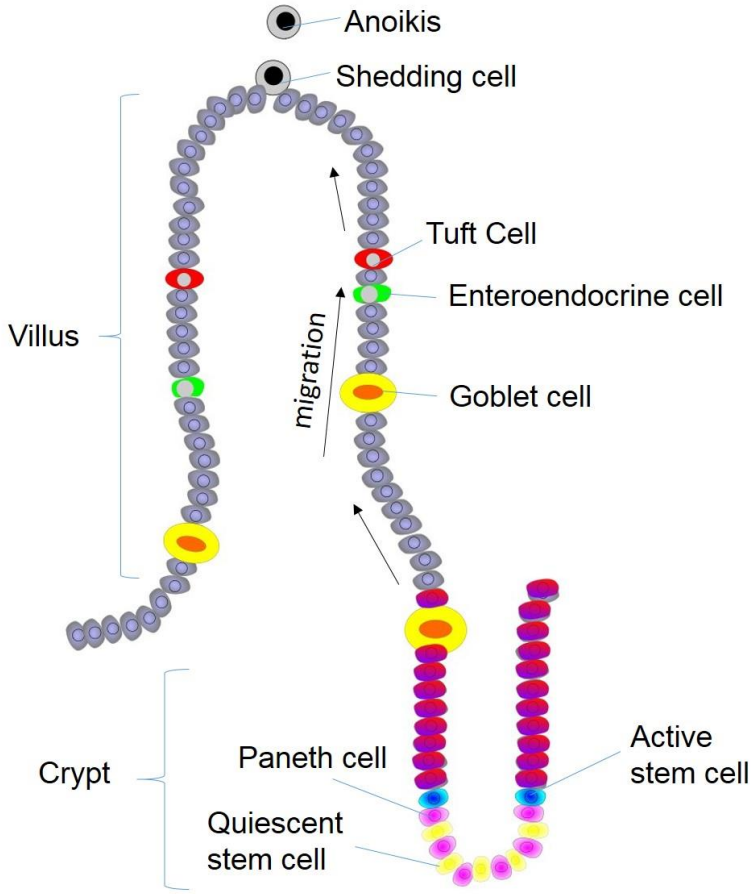

Figure 1.2 The small intestinal villus contains many different cell types. Absorptive enterocytes are shown in grey. All cell types except Paneth cells move up the crypt villus axis towards the villus tip where they are eventually shed and undergo anoikis. The bottom of the crypt is where the stem cells are located and have been found to belong to two distinct cell populations, the active stem cell which is found around the +4 position form the crypt base and the quiescent (eg Lgr5+) stem cells which are found nestled between the Paneth cells. Paneth cells are large granular cells which secrete anti-microbial peptides. In this way the stem cells at the bottom of the crypt are protected from invading bacteria. Transit amplifying cells are rapidly cycling cells which are found above the crypt base. Tuft cells are thought to be chemosensory or secretory cells (Gerbe, Legraverend and Jay, 2012), and enteroendocrine cells are involved in the hormonal regulation of the intestines (Gunawardene, Corfe and Staton, 2011).

One way in which the content of the gastrointestinal lumen is monitored is through microfold (M) cells. These cells are specialised epithelial cells that are only found overlying the lymphoid follicles of the small intestine and they function by channelling antigens from the lumen to a population of underlying immune cells in order to sample the luminal environment. This allows the immune system to appropriately respond to any threats (Mabbott *et al.*, 2013).

1.1.4 Structure and function of the colon

The colon begins at the ileocaecal valve and terminates at the anal sphincter. It consists of the caecum, the appendix, the ascending colon on the right side of the body, the transverse colon, the descending colon on the left side of the body and the rectum. The function of the colon is primarily the absorption of water and electrolytes and the conversion of waste food products into stool, which is stored in the descending colon before it is excreted. A secondary function of the colon is to absorb short chain fatty acids, which have been fermented by colonic bacteria. In humans, the colon is around 1.5m in length and it is around 8cm long in mice. In cross section, the colon is much wider than the small intestine and unlike the small intestine, villi are absent. However, like the small intestine the colon consists of an inner layer of epithelial cells which form crypts, and although the cell turnover is slower than in the small intestine the cell turnover is still high compared to most other organ tissues with full epithelial renewal every 5-7 days (Barker, 2014). The stem cells reside at the crypt base in the colon and migrate up towards the crypt table, where they are shed (figure 1.3). There are no Paneth cells in the colon, but the basic structure is the same as the small intestine in many respects, one exception being that there is a double layered mucus system which has a tightly packed inner layer. This colonic mucus is infiltrated with anti-microbial factors in order to avoid infection of the epithelial cells. The outer layer of mucus consists of a looser organisation of mucins. These mucins provide an environment for the commensal bacteria which reside in the colon and are

often advantageous to digestion. The colon is the location of most of the commensal bacteria in the intestinal tract with around 10^{12} bacteria found per millilitre. These microorganisms are contained within a complex ecosystem and abnormalities within their composition have been linked to health problems such as cancer, diabetes, autism and obesity (Zhang *et al.*, 2015). Goblet cells make up a quarter of the epithelial cells in the colon and produce mucus, for both mucus layers (Boron and Boulpaep, 2008; Mowat and Agace, 2014).

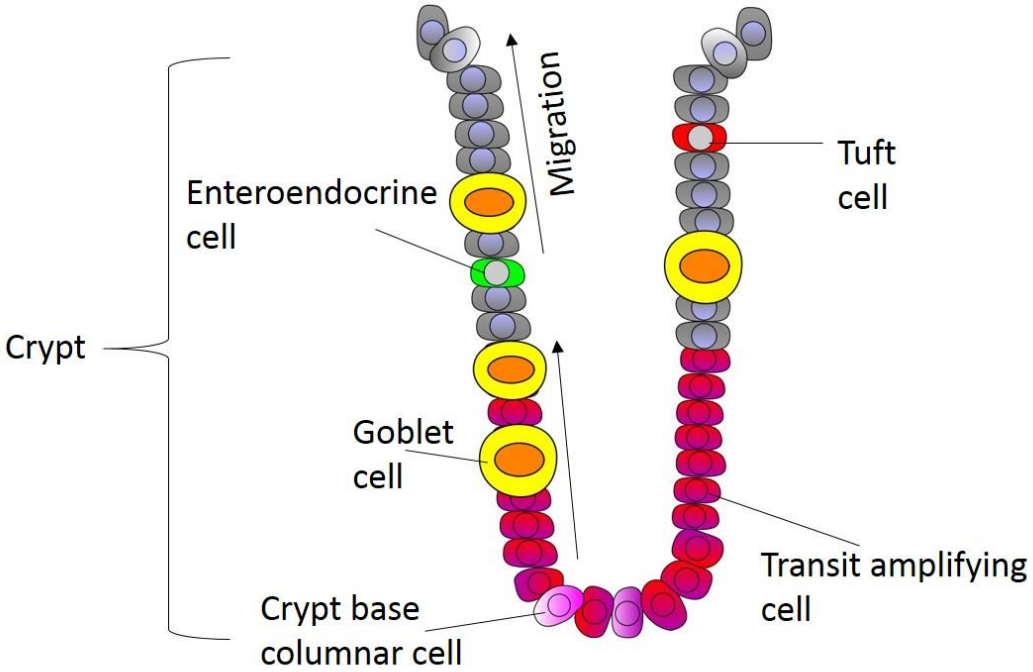

Figure 1.3 The colonic crypt contains many different cell types. Absorptive enterocytes are shown in grey. All cell types move up the crypt towards the crypt table where they are eventually undergo anoikis and are shed. Crypt base columnar cells are Lgr5 positive and make up the stem cell population of the colon. Transit amplifying cells are rapidly cycling cells which are found above the crypt base. Goblet cells secrete mucus and are numerous in the colon. Tuft cells are thought to be chemosensory or secretory cells, and enteroendocrine cells are involved in the hormonal regulation of the intestines.

1.1.5 The protective mucus of the gastrointestinal tract

From the stomach onwards, the GI tract is lined with protective mucus which functions to allow the gastrointestinal tract to digest food without digesting its own cells (Kim and Ho, 2010). The mucus in the gastrointestinal tract is produced by goblet cells in the small intestine and by both surface mucous cells and mucous neck cells in the stomach. These cells produce mucins which are highly glycosylated proteins and are created in the Golgi apparatus of the mucus secreting cells. These mucins have very hydrophilic domains which attract many water molecules in order to form the lubricating mucus. As well as protecting the intestinal wall from mechanical damage the mucus provides an environment for commensal bacteria to proliferate. In the colon and the stomach there are two layers of mucus; the outer layer provides an environment for commensal bacteria and the inner mucosal layer is tightly packed and contains antimicrobial factors which help to prevent the invasion of epithelial cells with pathogenic bacteria (Johansson, Sjövall and Hansson, 2013). In the normal gastric epithelium goblet cells do not appear. The appearance of goblet cells in the gastric epithelium is a sign that the stomach has begun to take on an intestine-like physiology and is a sign of metaplasia of the stomach. Metaplasia can happen in response to *Helicobacter pylori* infection, bile reflux, cigarette smoking and other lifestyle and diet variables. This metaplasia can predispose to adenocarcinoma of the stomach (Giroux and Rustgi, 2017).

1.1.6 Stem cells and cell turnover in the gut

Adult stem cells are multipotent, meaning that they can give rise to a limited number of differentiated cell types. For instance, in the GI epithelium the stem cells can produce the absorptive enterocytes, Paneth cells, goblet cells or enteroendocrine cells. Stem cells are also able to self-renew indefinitely (Alison and Islam, 2009). The stem cells of the small intestine exist in an environment provided by the close

proximity of the Paneth cells and also the close proximity of other intestinal stem cells. The way in which the stem cells divide has been the subject of extensive study. The first hypothesis is that the rapidly cycling stem cells produce two daughter cells which consist of a stem cell and a cell which differentiates into a transit amplifying (TA) cell which in turn is capable of producing daughter cells that then migrate up the crypt villus axis. However, another interesting theory involves the mainly symmetrical division of the stem cells, either producing two stem cells or two TA cells. (Snippert *et al.*, 2010). The experiments conducted by Ritsma *et al.* indicated that whether a cell would go on to produce transit amplifying cells or more stem cells is affected by its position in the stem cell niche. The cells found in the stem cell niche towards the upper border of the region were more likely to produce transit amplifying cells, whereas the cells which were positioned towards the middle of the stem cell niche were more likely to produce daughter cells which were stem cells (Ritsma *et al.*, 2014).

The cells of the small intestine in humans renew every 4 to 5 days (van der Flier and Clevers, 2009; Umar, 2010). These stem cells are located at the base of intestinal crypts and rapidly proliferate in order to keep up with the high rate of anoikis which occurs at the villus tip. With the exception of the Paneth cell, new small intestinal cells migrate up the crypt villus axis towards the villus tip, and approximately $2x10^8$ and 10^{11} cells are shed from the villus tip of a mouse and human respectively per day (Potten and Loeffler, 1990).

The cells which are shed from the villus tip have been shown to be shed at a speed which is faster than the speed at which cells migrate up the crypt villus axis. Therefore, these cells are shed by some form of forceful expulsion. This phenomenon has been observed in both humans and mouse models and indicates that the loss of epithelial cells from the villus tip is a very active process (Watson *et al.*, 2005, 2009).

Over the past few decades, there has been controversy over the exact location of the stem cells of the small intestine. However, it is now widely accepted that the stem cells fall into two populations; active and quiescent. The reason for the two different populations may be to safeguard the intestine against damage. Therefore, in cases where the rapidly cycling stem cells of the gut are damaged, there is a population of quiescent stem cells that can be activated (Yan *et al.*, 2012). The intestinal crypt contains around 14 actively dividing stem cells at any one time (Snippert *et al.*, 2010). The stem cells are known as the crypt base columnar (CBC) cells and are located between the Paneth cells in small intestinal crypts and at the crypt base in the colon (figure 1.2 and figure 1.3) (Krausova and Korinek, 2014). CBC cells have a slender morphology and are known to express *lgr5* and divide around once a day (Barker *et al.*, 2007). Their frequent division is demonstrated by the high occurrence of the proliferation marker Ki67 observed in immunohistochemical studies (Barker *et al.*, 2007). For many years, another population of stem cells were thought to be the true stem cells of the gut. These cells are known as the +4 stem cells and as the name suggests are found in the cell position 4 places from the crypt base (Potten *et al.*, 1978). The +4 stem cell cells are now believed to be a slower cycling population than Lgr5 expressing stem cells and are now widely thought of as the Bmi1- expressing backup stem cells, existing in the case of damage to the rapidly cycling stem cells found closer to the crypt base (Sangiorgi and Capecchi, 2008; Krausova and Korinek, 2014). Paneth cells produce factors essential for stem cells in the small intestinal crypt base such as WNT3, TGF-α and epidermal growth factor (EGF). Important factors which support the stem cells are produced by $CD24^+$ cells which rest between the *LGR5* expressing stem cells at the crypt base (Sato *et al.*, 2011). Paneth cells are known to have a life expectancy of around 2 months, making them long lived compared to the other cells of the intestinal epithelium (Ireland *et al.*, 2005).

1.1.7 Wnt signalling in the intestinal epithelium

In the foetal gut, the development of the small intestinal villi, and intestinal crypts is controlled by the hedgehog (*Hh*) proteins Indian hedgehog (*Ihh*) and sonic hedgehog (*Shh*), and depletion of both of these proteins causes defects in the formation of crypts and villi as well as the loss of the correct polarity in crypts (Madison *et al.*, 2004). However, after the intestine has formed, due to the constant renewal of the intestinal lining, homeostasis of the structure of the crypt is tightly maintained by a number of factors (figure 1.4). These are secreted by Paneth cells, by stem cells and by epithelial cells themselves. The Wnt signalling pathway is known to be very important in the homeostasis of the gut. Wnt signalling via the canonical pathway prevents β-catenin degradation in the gut. Via this mechanism Wnt signalling controls the stem cell population and the stem cell activity of the gut (Qi and Chen, 2015). Stem cells which are exposed to Wnt are able to retain stemness, which means they maintain the ability to proliferate while remaining in an undifferentiated form, while cells which are not exposed to Wnt tend to differentiate into intestinal epithelial cells such as absorptive enterocytes, goblet cells and tuft cells (Pinto *et al.*, 2003). The stem cells located at the crypt base are constantly exposed to Wnt signalling and remain de-differentiated, while the cells at the crypt table or further up the crypt-villus axis are not exposed to wnt signalling, are therefore differentiated and do not have stem cell properties. Bone morphogenic protein (BMP) also has a role to play in the control of the crypt-villus axis. Unlike Wnt, BMP is expressed at a high level at the villus tip, with BMP antagonists present in the stem cell zone to prevent any signalling of BMP in this area. BMP signalling promotes the terminal differentiation of cells, and negatively regulates the self-renewal of intestinal stem cells. EGF signalling is another factor known to increase the proliferation and survival of intestinal stem cells as well as the transit amplifying cells in the crypts. Notch signalling occurs in the stem cell and transit

amplifying cell containing regions of the crypt and prevents the cells from terminal differentiation into the secretory cell linage (Qi and Chen, 2015).

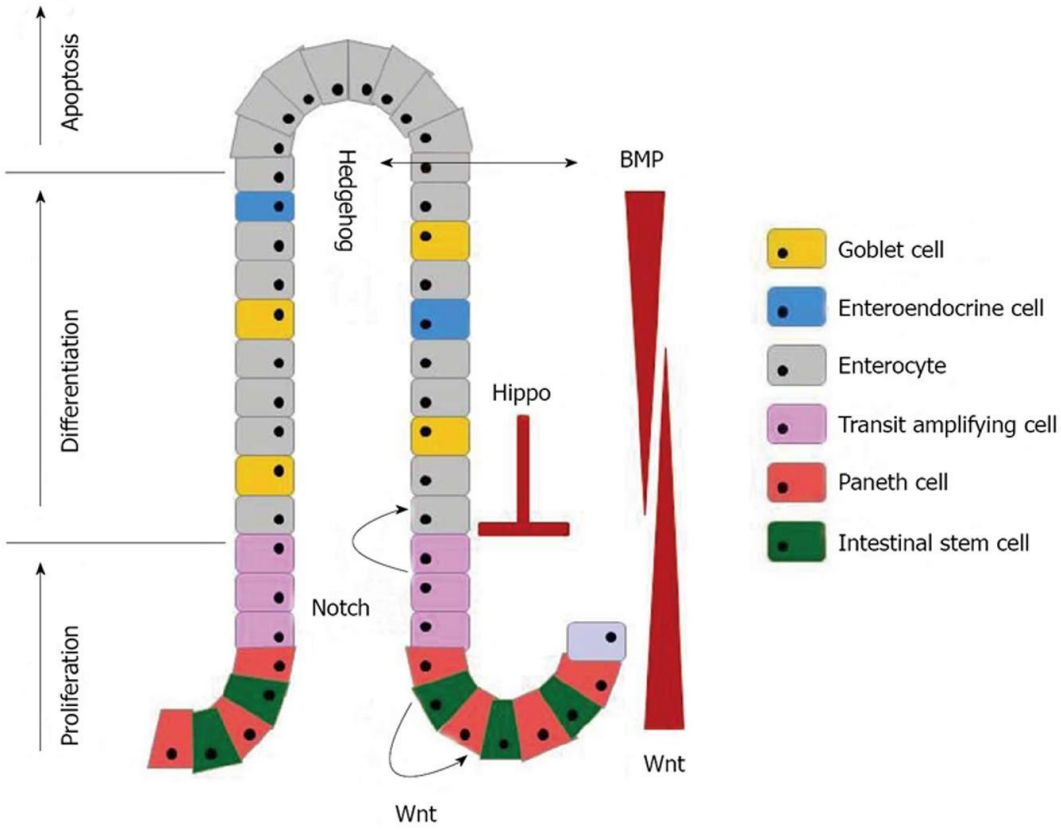

Figure 1.4 Gradients of WNT and BMP influence the homeostasis of the gut. Wnt signalling allows the maintenance of the stem cells in the intestinal crypts, and BMP signalling prevents proliferation and maintains cell locations in the crypt. Notch signalling acts to assist Wnt signalling and promotes stem cell proliferation. Hippo acts to control the proliferation of cells higher up the crypt axis in order to prevent excessive organ growth, and promotes apoptosis. Hedgehog (Hh) is involved in the formation of the villi. Adapted from Jeon *et al.*, 2013.

1.1.8 Apoptosis in the gastrointestinal tract

The gastrointestinal epithelial layer is constantly renewing itself with 10^{11} intestinal epithelial cells lost per day in humans (Leblond & Walker 1956). Apoptosis is one form of programmed cell death which occurs throughout the body. It is different from necrosis which occurs as a result of injury, for example following the cessation of the

blood supply or extreme cold (Wyllie, Kerr and Currie, 1980). Apoptosis was discovered by Kerr *et al*. in 1970 and this group also gave it the name, which comes from the Greek phrase 'falling off.' This is a particularly appropriate choice in the case of the small intestine where cells do appear to fall off the end of villi as the intestinal epithelium renews itself (Kerr, Wyllie and Currie, 1972). Apoptosis plays a very important role in the gastrointestinal tract, particularly in the small intestine and colon where the cell turnover is so rapid. Once a cell has differentiated into any cell type except a Paneth cell, it takes 2-3 days for it to reach the top of the crypt in the colon or the top of the villi in the small intestine and die (van der Flier and Clevers, 2009). The vast majority of cell loss which happens in the intestinal epithelium happens by apoptosis, and it is very important for maintaining balance with the rapid cell division which occurs in the intestinal crypts (Hall *et al.*, 1994). Cells are instructed to undergo apoptosis by death inducing stimuli (via the extrinsic pathway), for instance if a Fas ligand binds to a Fas receptor this will send an apoptosis inducing signal to the cell (Nagata and Golstein, 1995). Another way in which apoptosis may be induced is by oxidative stress (via the intrinsic pathway) or the removal of a growth factor (Buttke and Sandstrom, 1994).

1.1.9 Apoptosis at the villus tip

Cell shedding is the term used for the process by which cells are lost from the small intestinal villus tip or the colonic crypt table and occurs as cells move up the crypt-villus axis in a controlled manner before being released at the top of the villus (Bullen *et al.*, 2006). When cells detach from the epithelial layer at the villus tip, the epithelial integrity is maintained by the rapid remodelling of cell adhesions. The shedding mechanism allows the epithelial integrity of the villus to be maintained (Madara, 1990). Pathological cell shedding occurs when the rate of shedding of cells at the villus tip exceeds the rate at which proliferation occurs in the crypts (Williams *et al.*, 2015). Cell shedding contributes to the continuous renewal of the epithelium.

Proliferation occurs to ensure that cells are generated to match the rate of cell shedding at the villus tip in order to avoid gaps in the epithelium (Barker *et al.*, 2007; Potten *et al.*, 2009). When a cell is detached from the surrounding cells in an epithelial layer the cell then dies by a process known as anoikis which means 'without a home'. Anoikis is the process by which a cell dies due to lack of attachment to other cells. It is unclear whether the cells which are shed from the tip of the villus die by anoikis or are already apoptotic before they leave the epithelium (Fouquet *et al.*, 2004). Epithelial cells may already be at the early stages of apoptosis when they reach the villus tip. There is evidence to support this theory as some studies have shown that the cells at the villus tip express active caspase-3 before they are shed (Williams *et al.*, 2013). The way in which cells are expelled from the villus tip involves the rearrangement of the tight junction proteins of the surrounding cells, as tight junctions function to hold cells together in the epithelial layer. Zonula occludens (ZO-1) redistributes to form a layer underneath a shedding cell (Guan *et al.*, 2011).

1.1.10 Apoptosis in the crypts

In the healthy intestine very few apoptotic cells are found in the crypt domain of the crypt-villus axis or towards the bottom of the colonic crypt (Hall *et al.*, 1994). These cells undergo apoptosis in the proliferative zone of the crypts due to random DNA damage or an excess in cell production (Potten, Wilson and Booth, 1997).This is often referred to as spontaneous apoptosis and occurs predominantly in the stem cell region of the crypt in approximately one cell in five intestinal crypt sections (Potten, 1992). In response to radiation, stem cells in the intestinal crypts undergo apoptosis in the +4 stem cell zone (Potten, 1977). However in response to other DNA damaging stimuli such as chemotherapeutic drugs, any cell through the whole crypt can potentially undergo apoptosis; the apoptosis is not restricted to the stem cell zone (Ijiri and Potten, 1983; Ijiri and Potten, 1987). For instance in 5-FU induced crypt apoptosis

the cells which are affected are located at cell positions 6 to 8 which is the location of the transit amplifying cells of the small intestine (Pritchard *et al.*, 1997).

The bcl-2 family of proteins is involved in regulating spontaneous apoptosis and damage related apoptosis in the intestinal crypts. This family includes both pro-apoptotic members such as Bax, Bak and Bid and anti-apoptotic members such as Bcl-2, Bcl-xl and Bcl-W. The ratio of Bcl-2 family members determines whether a cell undergoes apoptosis or not (Shamas-Din *et al.*, 2013). One example of this function in the intestinal crypts is the distribution of Bcl-2 expression, which is notably absent in the stem cells in small intestinal crypts, however some colonic stem cells do express the protein hence the increased susceptibility of the small intestinal stem cells to apoptosis (Merritt *et al.*, 1995). Another anti-apoptotic family member Bcl-w has been shown to be involved in apoptosis in response to both gamma radiation and 5-FU; the deletion of this protein increases the incidence of apoptosis in response to both of these stimuli (Pritchard *et al.*, 2000). The pro-apoptotic Bcl-2 family proteins have been shown to be involved in induced apoptosis in the intestinal epithelium, for example Bak has been shown to be involved in apoptosis in response to gamma radiation and AOM (Duckworth and Pritchard, 2009).

1.2 Inflammatory bowel disease

Ulcerative colitis (UC) and Crohn's disease (CD) are the two main categories of inflammatory bowel disease (IBD). IBD results from an inappropriate inflammatory response which occurs in the gastrointestinal tract. According to the NHS, 115,000 people in the UK are living with Crohn's disease (www.nhs.uk/conditions/crohns-disease) and 146,000 people are living with ulcerative colitis (www.nhs.uk/conditions/ulcerative-colitis). Approximately 5% of IBD patients have some features of both Crohn's disease and ulcerative colitis and are diagnosed with a condition known as indeterminate colitis (Carter, 2004).

1.2.1 Ulcerative colitis

Ulcerative colitis (UC) occurs exclusively in the colon and/or rectum and is characterised by diffuse and continuous inflammation, oedema and ulceration in the mucosa. The severity of inflammation usually increases distally. Ulcers in the mucosa of UC patients can bleed or become infected which can lead to sepsis (Carter, 2004). One particularly serious complication of UC is toxic megacolon, a dilation of the colon in which inflammation occurs in the muscle layers and the serosa (Strong, 2010). This leads to the paralysis of the smooth muscle layer caused by neutrophilic infiltration and the production of nitric oxide (Sheth and LaMont, 1998).

1.2.1.1 Ulcerative colitis demographics

The global incidence of UC has increased over the past decade, especially in developing countries. Gender does not affect the likelihood of a UC diagnosis. The age at which most diagnosis of ulcerative colitis occurs is usually between 30 to 40 years (da Silva *et al.*, 2014).

1.2.1.2 Ulcerative colitis signs and symptoms

Symptoms of UC include one or more of the following: fever, cramps, the urgent urge to defecate, loose stool, diarrhoea, 10-20 bowel movements per day, blood in the stool, passage of mucus and pus, weight loss, anaemia and dehydration (Yantiss and Odze, 2006; Smith, 2017). Patients with UC may experience psychological distress and denial due to the embarrassing nature of the symptoms, which can lead to a later diagnosis and a worse prognosis.

1.2.1.3 Ulcerative colitis pathology

T helper cells are lymphocytes which express CD4, these can be categorised into T-helper cell type 1 (Th1) or T-helper cell type 2 (Th2) depending on which cytokines

they express. The expected interleukins expressed in a Th2 response are IL4, IL5 and IL13 (Strober and Fuss, 2011). The UC immune response is known as Th2 'like' because there is an increase in IL-13 and IL-5 but not IL-4. The inflammatory response involves natural killer T cells (NKT cells) which are a component of the innate immune system (figure 1.5). These cells produce large amounts of IL-13 and respond to antigens presented by the epithelial cells in the colon (Fuss *et al.*, 2004). Architectural distortion is seen on microscopic examination of a UC affected colon. This involves crypt shortening or loss, an inflammatory infiltrate present between the muscularis mucosae and the base of the crypts, the infiltration of neutrophils, neutrophilic crypt abscesses, Paneth cell metaplasia and ulceration (DeRoche, Xiao and Liu, 2014).

The precise cause of UC is unknown, although there are several theories including genetic, bacterial or viral infection and autoimmune reactions where white blood cells mistake healthy tissue for a foreign infection. It is thought that there is a genetic susceptibility element to the disease, however as families are likely to be at exposed to the same pathogens this is difficult to determine. Each flare up of UC leaves the patient at risk of complications such as perforations, strictures, rashes, eye problems, liver disease, kidney stones and a long term increased risk of cancer in the colon or rectum (Ungaro *et al.*, 2017).

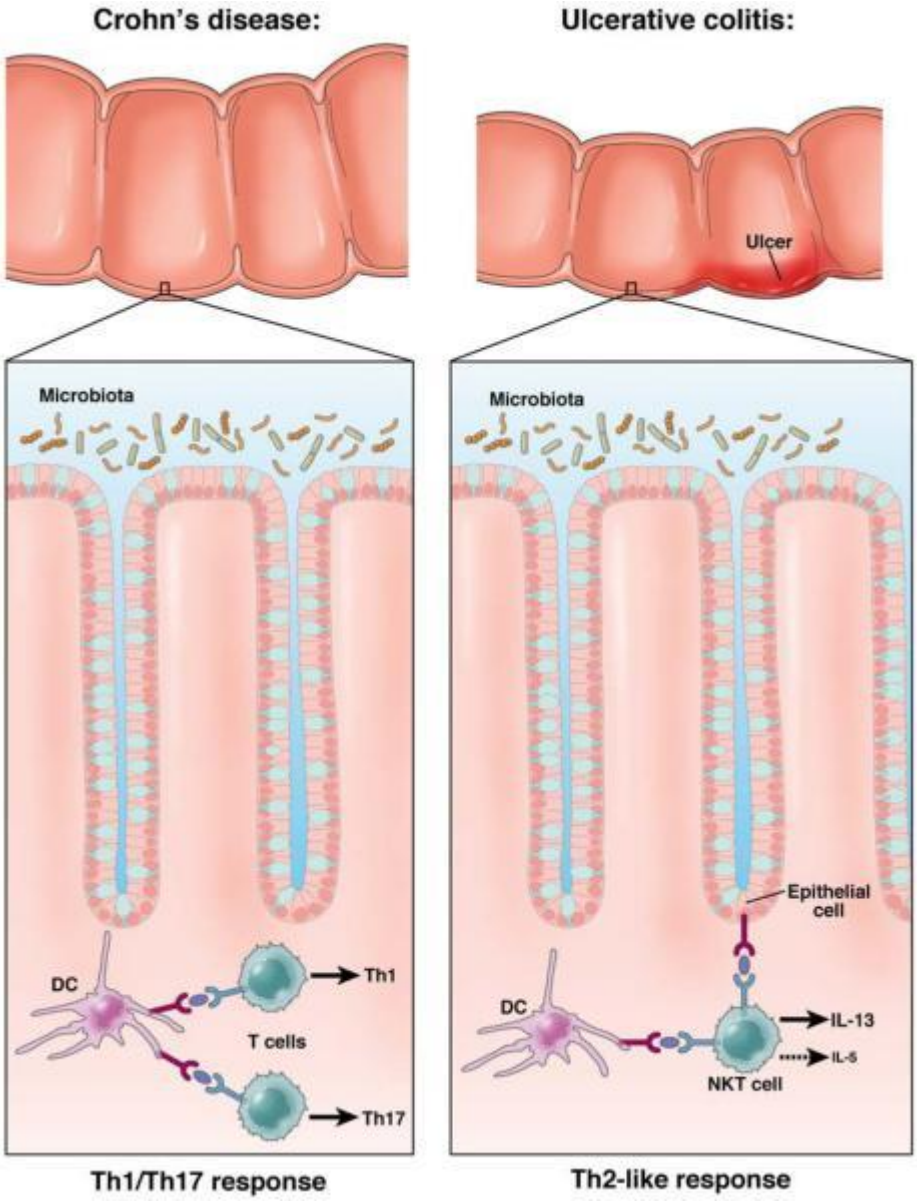

Figure 1.5 The differing T-cell responses seen in Crohn's disease and ulcerative colitis. The T helper cell response differs between the two diseases. Crohn's disease classically has a Th1/Th17 response, where there is significant upregulation in IFNγ and ulcerative colitis is associated with a Th2 like response with the natural killer T cells (NKT cells) strongly expressing the pro-inflammatory cytokine IL-13. Adapted from Strober and Fuss, 2011.

1.2.1.4 Ulcerative colitis treatments

Drugs used to treat UC need to be administered with care in order to avoid bowel dilatation. One of the most commonly used types of drugs are corticosteroids, which reduce inflammation and relieve symptoms during a flare up. Hydrocortisone and prednisolone are two of the commonly used corticosteroids. However, these also commonly cause side effects including drowsiness, Cushingoid features, osteoporosis, and delayed sexual maturation in younger patients (Smith, 2017). 5-Aminosalicylic acid (5-ASA) and derivatives such as sulphasalazine and balsalazide are frequently administered as oral and topical treatments for ulcerative colitis. Like corticosteroids they are also used to induce remission. These treatments work by down-regulating pro-inflammatory factors such as prostaglandins, inhibiting inflammatory cells and activating anti-bacterial pathways in the intestinal epithelial cells (Khanna and Marshall, 2017). Cyclosporine is an immunosuppressant drug that is occasionally given to UC patients with acute severe flare ups which works by inhibiting T-lymphocytes (Strong, 2010).

There are several other approaches which are taken by clinicians in order to prevent a flare up of UC before it happens. Azathioprine is commonly used in the maintenance of remission (Timmer *et al.*, 2016). This drug is a thiopurine which functions to prevent DNA and RNA synthesis in immune cells. Azathioprine can be used to replace steroids and has been shown to induce remission with an efficacy of 60% (Garud and Peppercorn, 2009). Preventative therapy is used to prevent the infiltration of immune cells into the colon. Another option is anti-TNF therapy such as infliximab. This drug is used in the treatment of UC and blocks TNF signalling. It is effective in causing apoptosis of inflammatory T lymphocytes which can prevent inflammation in the colon (Strong, 2010).

1.2.1.5 Ulcerative colitis surgical intervention

Surgery to remove the colon is used in severe cases of UC and 25% of patients eventually require surgery (Jess *et al.*, 2007). UC can be cured by the total removal of the colon and rectum, so usually a proctocolectomy is performed. The end of the ileum is then pulled to the surface of the abdomen to form an ileostomy. Although this surgery has a high rate of success, 20% morbidity is seen even for non-urgent elective surgery (Parray *et al.*, 2012). The formation of an ileoanal pouch is another approach and involves the surgeon creating a pouch from a segment of the small intestine, which is known as an anus attached anastomosis. Infections and mechanical failures can occur following surgery, and stomas are vulnerable to bacterial infection. In the event of surgery, although largely curative the patient will be forced to undergo a complete lifestyle change and may experience stigma associated with the stoma or abnormal bathroom habits (Smith, 2017).

1.2.1.6 Ulcerative colitis prognosis

Death from UC was high in the first half of the 20th century. Although the incidence has increased, the number of deaths from UC has been decreasing constantly since the 1950s due to modern treatment strategies. The death rate fell from 12.5 to 4.3 deaths per million living women, and 7.15 to 2.8 per million living men between the year 1950 and 1983 in England and Wales (Sonnenberg, 1986). The risk of death is higher than in the general population for about a year after the diagnosis by 2.4 fold; after this the likelihood of death is around the same in an individual with UC as that of the general population (Jess et al., 2013). Patients with disease extending further proximally throughout the colon or those with more severe lesions in the mucosa are more likely to need surgical intervention. In one study by Alkim et al, patients with proximal disease were found to be at a 14.8% risk of requiring colectomy whereas patients without proximal extension of disease were only at a 3% risk of needing a

colectomy. In some cases inflammation can spread proximally throughout the colon, which means that monitoring of patients is required as over time patients may require an increased treatment intensity (Alkim *et al.*, 2011). Extra-intestinal manifestations of disease have also been linked with a worse patient prognosis. The most common extra-intestinal manifestation is arthritis. Patients who experienced joint symptoms have been shown to have a 3.7 fold increase in the proximal extension of the disease (Farmer, Easley and Rankin, 1993).

1.2.2 Crohn's Disease

Around 41% of Crohn's disease (CD) cases involve the small intestine and the colon, 29% involve the small intestine only, 27% involve the colon only and 3% involve the anus and rectum only (Farmer, Hawk and Turnbull, 1975). When CD presents in the small intestine it is usually ileal. However, CD can occur anywhere in the intestinal tract. The disease is usually distributed in a segmental fashion (whereas UC is continuous), with the disease severity variable and not easy to predict depending on location. This inflammation can lead to stricturing in the small intestine (Carter, 2004; Yantiss and Odze, 2006)**.** The inflammation in CD is often transmural and this can cause deep fissures and fistulas to develop in the intestinal wall. One of the most serious consequences of these injuries can also be sepsis, a serious and potentially fatal outcome (Hendrickson, Gokhale and Cho, 2002; Yantiss and Odze, 2006).

1.2.2.1 Crohn's disease demographics

CD occurs most commonly in industrialised countries, with higher incidences in the Northern parts of developed countries. For example, 0.7 to 9.8 in 100,000 Europeans suffer from CD per year whereas the rate in Northern England is 144 people per 100,000 per year (Loftus, 2004). The disease can develop in children, but most commonly the first flare up of the disease is seen between ages 15 and 25. There is thought to be a second peak age of CD occurrence between 60 and 70 years of age

(Sobczac, 2017). The incidence of CD is higher in females than in males, with females having a slightly higher risk (Loftus, 2004).

1.2.2.2 Crohn's disease clinical signs and symptoms

The presentation of CD commonly includes abdominal pain over the central or right-hand side of the abdomen as well as diarrhoea, anal soreness, reduced appetite and general malaise. CD can present in a very similar way to UC, however the diseases can usually be differentiated using endoscopy and histology (Sobczac, 2017).

1.2.2.3 Crohn's disease pathology

As with UC the exact cause of CD is unknown, however the upregulation of pro-inflammatory cytokines is known to be a factor in the pathogenesis of both diseases. TNF is a pro-inflammatory cytokine which is known to be upregulated during CD (Ślebioda and Kmieć, 2014). As Crohn's disease is often associated with the invasion of adherent invasive *Escherichia coli* (AIEC) there has been significant interest in establishing whether there is a link between these bacteria and the disease (Strober, 2011). The particular *E. coli* in question are often called Crohn's disease associated *E. coli* (CDAE). Macrophages infected with these bacteria have also been found to secrete more TNFα than uninfected controls, which increases the amount of inflammation (Glasser *et al.*, 2001). This indicates that one cause of the upregulation of TNF in CD may involve infection with AIEC.

Patients with CD have a diminished acute immune response. For instance, patients have been shown to have significantly lower numbers of neutrophils accumulating at a site of injury on either the bowel or the skin. Smaller amounts of pro-inflammatory interleukins were produced in response to acute wound fluid and a significantly decreased local immune response was seen in response to *E. coli* (Marks *et al.*, 2006). Autophagy is the process of removal of unwanted microorganisms or materials

from the body by engulfment. Evidence suggests that autophagy is often defective in CD patients. Additionally NOD2 genetic variants are commonly found in CD patients (Bonen *et al.*, 2003), and NOD2 is a protein involved in the control of autophagy. (Kaser and Blumberg, 2011).

Although the acute immune response is thought to be involved, allowing larger than normal numbers of pathogens to accumulate in the mucosa of CD patients, it is the abnormal innate immune response which causes the actual damage and a prolonged Type 1 helper T cell (Th1) response is characteristic of the disease (Breese *et al.*, 1993). The Th1 response means that large quantities of interferon gamma (IFNγ) and TNFα are produced by T cells (figure 1.5). The lamina propria T lymphocytes isolated from the mucosa of CD patients produce more IFNγ than cells from healthy individuals, which was shown to be due to the presence of IFNγ secreting CD4+ T cells (Fuss *et al.*, 1996).

In addition to the Th1 response, inflammation in CD is also caused by the T helper cell type 17 (Th17) response with the production of Th17 cytokines which are involved in the exacerbation of the inflammation. However the Th17 response has less of an impact on the inflammation and it is the Th1 response which is the major source of inflammation and the major driver of disease (Strober and Fuss, 2011).

The microscopic presentation of the disease is characterised in around 25% of cases by fissuring, which appears as deep knife-like clefts into the bowel wall. Transmural inflammation is observed, with lymphoid aggregates, crypt ulcers, abscesses and granulomas often present. Widening of the submucosa and often a thickening of the muscularis mucosae are also characteristic of CD (Morson, 1968).

1.2.2.4 Crohn's disease treatments

Like UC, CD is often treated with corticosteroids such as prednisolone or hydrocortisone (Caprilli, Viscido and Latella, 2007). These corticosteroids are used

for the treatment of both UC and CD during the acute onset of disease to induce remission by reducing the inflammation. However, these treatments are not used for prevention of acute flare ups.

Heightened levels of the pro inflammatory cytokine TNF have been found in the serum and mucosa of CD patients. Therefore, anti-TNF therapies such as Infliximab can be used as treatments in order to maintain remission in CD as well as in UC (Behm and Bickston, 2008).

1.2.2.5 Crohn's disease surgical intervention

If drug treatments for CD are unsuccessful, there may be a need for more invasive forms of treatment. In the case of haemorrhage, perforation or peritonitis, surgery is also frequently required. Elective surgery usually involves resection of the damaged segment of bowel along with a primary surgical anastomosis. Alternatively, a surgeon may choose to form a stoma in order to rest a damaged segment of bowel without removing it (Strong, 2010).

1.2.2.6 Crohn's disease prognosis

The overall mortality of CD patients has been shown to increase by 50% in the long term in one Danish study (Jess et al., 2013). Other studies have also found trends towards an increased likelihood of death when compared with general populations of similar age and sex. There is an increased risk of death from GI cancer and other GI diseases and chronic obstructive pulmonary disease, although the latter is probably due to the higher incidence of smokers within the CD patient cohort (Jess *et al.*, 2006a). Over half of CD patients experience a disease relapse and patients often experience several relapses during their lifetime and, even after surgery. Patients with small intestinal disease are at the greatest risk of CD relapses, however if a patient

remains in remission for 10 years following surgery they are likely to remain in remission indefinitely (Bernell, Lapidus and Hellers, 2000).

1.2.3 Long term risks associated with IBD

CD, UC and indeterminate colitis lead to an increased risk of developing cancer (Carter, 2004). There is an increased risk of IBD related cancer in the UK and USA compared to Scandinavia, which indicates that lifestyle is also likely to be a factor in the development of the disease (Itzkowitz and Yio, 2004; Triantafillidis, Nasioulas and Kosmidis, 2009). IBD sufferers are the third most at risk group for colorectal cancer behind familial adenomatous polyposis and hereditary nonpolyposis colorectal cancer syndrome (Jess *et al.*, 2006b).

Patients suffering from CD have an overall 2.4-fold increased risk of developing colorectal cancer compared to healthy individuals (von Roon *et al.*, 2007). IBD patients are also at a higher risk of developing small bowel adenocarcinoma, intestinal lymphoma or anal cancer. Small bowel adenocarcinoma is 20 to 30 times more likely in patients with CD than those without at 8 years or more after diagnosis. Small bowel adenocarcinoma is thought to occur in cases with ileal inflammation. Intestinal lymphomas occur at an incidence of 1 per 10,000 patients per year, although like in the general population the incidence is still extremely low. Anal cancers are known to occur 10 to 20 times more frequently in patients with perineal CD (Beaugerie and Itzkowitz, 2015). In a study by Rutter *et al.* individuals with UC were shown to have a 2.5% chance of developing colorectal cancer after 20 years, a 7.6% chance after 30 years and a 10.8% chance after 40 years (Rutter *et al.*, 2006)

As well as the link between cancer and the inflammation caused by IBD, the treatments have also been linked to both an increased and decreased risk of cancer due to their effect on the immune system (Axelrad, Lichtiger and Yajnik, 2016). For instance the use of the immunosuppressant azathioprine has been linked to cancer,

with patients being shown to have an increased likelihood of developing lymphoma or urinary tract cancer (Pasternak *et al.*, 2013). Thiopurines, the drug group to which azathioprine belongs, have also been linked to an increased risk of non-melanoma skin cancer, even after their use has been stopped (Peyrin–Biroulet *et al.*, 2011). Thiopurines have also been linked to a decreased risk of colorectal cancer, with thiopurine users being 10 times less likely to develop cancer than IBD patients who did not use the drug (van Schaik *et al.*, 2012).

1.2.4 Pathological differences between ulcerative colitis and Crohn's disease

The distinction between CD, UC or intermediate colitis is important as it has a major impact on treatment options. For instance, the removal of the bowel in a patient who has CD affecting the colon, could be dangerous, as the use of a section of small intestine to create a pouch for the storage of faeces leaves the patient at risk of inflammation occurring in this reservoir. This can lead to short bowel syndrome and various complications. Pathological features of the two diseases can however often be difficult to distinguish. As well as this, several other disorders such as bacterial infections are associated with similar pathological features.

Transmural inflammation is an important pathological feature which is used to differentiate UC from CD occurring in the colon. An increased network of blood vessels develops in the colon of both UC and CD patients (Ippolito *et al.*, 2016). Increased angiogenesis occurs in the mucosa and sustains the chronic inflammation (Cibor *et al.*, 2016). As the inflammation is restricted to the mucosa in UC a normal serosa is usually seen in UC patients. However an abnormal serosa is seen in CD patients as inflammation is transmural; creeping fat (CF) can be seen to wrap around the outside of the serosa and inflammatory cells are found within the CF (Paul *et al.*, 2006). In the TNBS-induced animal model of IBD, transmural inflammation is also seen (Neurath *et al.*, 1995). Although there is little information about CF in mouse

models, it has been shown to occur in dinitrobenzene sulphonic acid (DNBS)-induced colitis (Olivier *et al.*, 2011).

Transmural inflammation as a key indicator for differential diagnosis means that endoscopic mucosal biopsies are not always sufficient for diagnosis. However mucosal differences between UC and CD are also found. In UC, severe and widespread crypt architectural distortion is seen, whereas in CD the crypt distortion is discontinuous, and normal crypts are seen surrounded by disrupted areas and vice versa (Jenkins *et al.*, 1997). In CD there is focal cryptitis which does not occur in UC, and in UC there is severe mucin depletion which is less likely to appear in CD (McCormick, Horton and Mee, 1990). A particularly strong indicator of CD that can be seen in a mucosal biopsy is the presence of epithelioid granulomas. This feature can however often be obscured by ulcers (Yantiss and Odze, 2006). The appearance of granulomas is often the most important distinguishing factor when differentiating between CD and UC. The granulomas found in CD consist of clusters of CD4 positive T cells, B cells and macrophages. These granulomas do not contain any necrotising cells, and hence they are known as non-caseating granulomas (Timmermans *et al.*, 2016). Granuloma-like structures have been observed in TNBS colitis, suggesting that this model is more akin to CD than UC (Antoniou *et al.*, 2016).

1.2.5 Causes and risk factors for IBD

Family history is associated with the likelihood of an individual developing IBD (Khor, Gardet and Xavier, 2011). Genetic factors have recently been shown to cause an increased risk of the occurrence of IBD. *CARD15/NOD2* mutations confer an increased susceptibility to inflammatory bowel disease (Carter, 2004) with 50% of CD patients carrying one of the common *CARD15/NOD2* genetic variants (Lesage *et al.*, 2002). These are associated with CD in the ileum and often lead to the accumulation of scar tissue and narrowing of the small intestine (Barreiro-de Acosta and Peña,

2007). Some genetic variants in the *ATG16L1* gene also increase susceptibility of developing CD (Hampe *et al.*, 2007). *ATG16L1* is an autophagy associated gene which is important for all aspects of autophagy and genetic variants in this gene are associated with defects in the clearance of bacteria (Khor, Gardet and Xavier, 2011). 60% of CD patients carry a genetic variant in the *ATG16L1* gene (Michail, Bultron and Depaolo, 2013). *ATG5* is another autophagy associated gene which is associated with IBD. *Atg5* null mice are susceptible to spontaneous colitis (Nedjic *et al.*, 2008; Mizoguchi and Mizoguchi, 2010).

Environmental factors can also affect whether someone will develop IBD. Increased dietary fibre has been positively associated with a decreased risk of CD but not UC (Ananthakrishnan *et al.*, 2013). Additionally the use of oral contraceptives has been previously linked to the development of IBD (Cornish *et al.*, 2008). However, a recent Swedish study found no link between the use of oral contraceptives and the incidence of IBD (Khalili *et al.*, 2016). Another theory is that increased hygiene in more developed nations causes an increased incidence of IBD, with the variety of bacteria found in the commensal gut population being depleted by 'over-cleaning' where excessive use of antibacterial agents in the home lead to less environmental bacterial exposure. In addition, a recent study has found that poor oral hygiene in childhood is inversely related to the risk of IBD indicating that the presence of oral bacteria contributes to a healthy population of commensal bacteria (Yin *et al.*, 2017). There is also an interesting relationship between smoking and IBD, with an increased risk of CD, but a decreased risk of UC being found in smokers (Calkins, 1989).

1.2.6 Animal models of inflammatory bowel disease

There are several different categories of animal models representing human inflammatory bowel disease. These animal models have allowed researchers to investigate disease process and test possible treatments. The first animal model of

inflammatory bowel disease was developed in 1957, when rabbits were sensitised to egg albumin, and subjected to formalin enemas. Subsequently over 66 models have been developed which include genetic models, adoptive transfer models and chemically induced models (Mizoguchi *et al.*, 2016).

1.2.6.1 Spontaneous inflammatory bowel disease models

Genetic models of colitis rely on genetically modified animals which are bred to spontaneously develop colitis in the absence of any other stimulus. The most widely known examples are the interleukin-10 (IL-10) deficient mouse model, the interleukin 2 (IL-2) deficient mouse model and the T-cell receptor (TCR) model of colitis. The IL-10 deficient mouse model is the most widely used of the three. This model is used to investigate CD as the inflammation is Th1 mediated and transmural which is similar to the inflammation seen in human CD. These mice are developmentally normal until they develop colitis (Kühn *et al.*, 1993), although the onset time of colitis varies between facilities depending on environmental conditions and the genetic background of the IL-10 deficient mice.

IL-2 is a cytokine which binds to a heterotrimer receptor which is involved in the activation of cell death, and the function of regulatory T cells. Mice deficient in this cytokine develop autoimmune disease which includes colitis when kept in conventional conditions, but do not develop disease in germ free housing (Sadlack *et al.*, 1993). The Th2 mediated TCR model of colitis is used to model UC. TCR-α deficient mice are deficient in the T-cell receptor. The T-cells of these animals are unable to sense pathogens, therefore this colitis model cannot be used in germ free conditions (Mombaerts *et al.*, 1993; Dianda *et al.*, 1997).

1.2.6.2 Adoptive transfer inflammatory bowel disease models

Adoptive transfer models use the transfer of T cells from a donor mouse into an immunocompromised mouse which results in IBD-like pathology. This model is useful for assessing the contribution of T cells for the development of UC and CD (Ostanin *et al.*, 2009). The adoptive transfer model of colitis has been used to investigate both Th1 and Th2 mediated inflammation (Kanai *et al.*, 2006). Naive T cells are transferred into immune deficient Rag null mice; these T cells then react to gut antigens and cause transmural neutrophilic inflammation in the colon and small intestine. The inflammation takes between 6 to 8 weeks to develop. As with other models disease development depends on the animal facility and the commensal bacteria present in the gut (Eri, McGuckin and Wadley, 2012).

1.2.6.3 Induced inflammatory bowel disease models

Chemically induced models of IBD are those which use chemicals to induce colitis in animals. Such chemicals usually have an irritating effect on the intestinal epithelium and are administered directly into the intestine via the drinking water or by enema.

Trinitrobenzenesulphonic acid (TNBS) or dinitrobenzenesulphonic acid (DNBS) induced colitis results from the rectal administration of TNBS or DNBS dissolved in ethanol to mice and the resulting pathology resembles human CD (Morampudi *et al.*, 2014; Antoniou *et al.*, 2016). Oxazolone is also administered via the rectum and is dissolved in ethanol. The mice are often pre-sensitised to oxazolone by shaving a 1cm^2 portion of their skin and applying oxazolone to sensitise the mice to the agent. The oxazolone model is notable as it was used to deduce that UC inflammation is driven by a Th2 like cell response (Heller *et al.*, 2002).

Dextran sulphate sodium (DSS) is another chemical that induces colitis in mice and rats and is administered via their drinking water. In all studies detailed in this thesis,

mice were bred on the C57BL/6J genetic background and administered 2% DSS dissolved in water. DSS is effective at inducing colitis to different extents depending on the genetic background and environmental factors encountered by mice. DSS is thought to work by disrupting the mucous layer of the distal colon and causing an immune response to the commensal bacteria. DSS is also thought to do this by the formation of nanoparticles in complexes with short chain fatty acids (Laroui *et al.*, 2012). DSS is negatively charged due to its sulphate groups. This negative charge is thought to contribute to the erosion of the colonic epithelial layer by disruption of ionic bonds at a molecular level. It allows the DSS molecules to travel though the epithelial layer and enables commensal microorganisms to make contact with the mucosal immune system (Chassaing *et al.*, 2014). When standard molecular weight DSS (36-40KDa) is administered to mice, colitis is only observed in the distal colon and this model closely resembles human UC (Yan *et al.*, 2009).

1.3 NFκB signalling

1.3.1 NFκB signalling pathways

NFκB was first discovered in 1986 in the laboratory of David Baltimore as a nucleoprotein which binds to the immunoglobulin κ chain gene at the enhancer region in B cells (Sen *et al.*, 1986). The protein was first thought to be involved in the maturation of B cells (Sen and Baltimore, 1987). However, the NFκB family has since been found to be expressed in most cell types in a context dependant manner and to have five members. These are NFκB1 (P50/P105), NFκB2 (P52/P100), RelA (P65), RelB and c-Rel. The NFκB signalling pathways have important roles in many aspects of human physiology. NFκB components can be activated by a variety of factors including bacterial proteins, viruses, factors related to the stress response and many different cytokines. There are two distinct pathways by which the NFκB proteins activate transcription, the classical (canonical) activation pathway and the alternative

(non-canonical) activation pathway. There is also a hybrid pathway which involves elements of both pathways. The strong link to inflammation means that this family of proteins is an attractive target in the study of inflammatory bowel disease (Bonizzi and Karin, 2004).

1.3.1.1 NFκB family structure

The NFκB family proteins are all transcription factors and function primarily as hetero and homo-dimers (Gilmore, 2006), and can be separated into two subgroups, the Rel subgroup which contains RelA, RelB and c-Rel and the NFκB subgroup which contains NFκB1 (P50/P105) and NFκB2 (P52/P100). The difference between the proteins in these subgroups is that those in the NFκB subgroup are characterised by the presence of a 'tail' which contains ankyrin repeats. This tail functions as an inhibitor of all members of the NFκB family. In the case of P105 and P100 (the inactive versions of NFκB1 and NFκB2 respectively), this allows the NFκB subgroup members to remain inactive, which means that they are present in the cytoplasm at all times. When the NFκB pathway is inactive, these transcription factors are inhibited either by cis inhibition or by iκBs, and inactive dimer complexes including the Rel subgroup members can occur via either form of inhibition and function to further inhibit the NFκB pathways (Pahl, 1999).

The structure of all five of the NFκB proteins includes the highly conserved rel homology domain (RHR), which functions to facilitate DNA binding and nuclear translocation, dimerisation with other NFκB subunits and interaction with inhibitors. The RHD consists of two folded domains, the amino terminal domain and the carboxy terminal domain, both of which contain an immunoglobulin like fold (Huxford and Ghosh, 2009). Additionally, out of the five transcription factors in the family, RelA, c-Rel and RelB are the members which can directly activate transcription. The remaining two transcription factors, NFκB1 and NFκB2, are only able to activate

transcription when dimerised with the other NFκB proteins. Although it is not included in the protein family, the transcriptional co-activator protein Bcl3 is also able to bind with NFκB1 and NFκB2, allowing them to activate transcription (Siebenlist, Franzoso and Brown, 1994). The transcriptionally active domain of these three proteins is known as the trans-activation domain (TAD).

1.3.1.2 NFκB signalling inhibition

The proteins belonging to the NFκB subgroup of the family are inhibited by separate proteins; these are called inhibitor of kappa Bs (iκBs). IκBs attach to the NFκB proteins by covering the nuclear localisation sequence, which means that the proteins cannot enter the nucleus. The iκB proteins therefore keep NFκB dimers in a state of tight repression in unstimulated cells. The three main members of the iκB group are iκBα, iκBβ and IκBε. The IκBs belong to the ankyrin repeat domain superfamily (Hoffmann, Natoli and Ghosh, 2006).

1.3.1.3 NFκB signalling activation

In order to activate the NFκB pathway the iκB protein on each of the subunits is degraded, uncovering the nuclear localisation sequence, which leads to the movement of the dimer into the nucleus where it can modify transcription (Pahl, 1999). The IκB proteins are vital for the tight control of NFκB signalling pathways. These proteins are continually produced and any free IκB proteins are unstable and can be degraded quickly and independently of the proteasome. However, the binding of these proteins to NFκB dimers also prevents them from undergoing constitutive degradation and non NFκB dimer bound IκBs are more rapidly targeted by the proteasome. This means that there is no unbound NFκB in unstimulated cells, the only NFκB signalling which occurs is due to activation of IKK or NIK complexes and NFκB signalling therefore occurs only when required (O'Dea *et al.*, 2007; Mathes *et al.*, 2008). When the IKK complex phosphorylates the IκB protein for degradation, the

protein is then ubiquitinated by an E3 ubiquitin ligase. For example, after phosphorylation on serine residues 32 and 36, iκBα kinases are targeted by the PIκBα-E3 ubiquitin ligase, which leads to the degradation of the protein by the 23S proteasome (figure 1.6) (Baldwin, 1996; Ben-Neriah *et al.*, 1998).

The NFκB pathway is modulated by many different factors as the pathway functions in a variety of different roles. Inhibitors of the NFκB pathway include natural products such as proteins, synthetic compounds, antioxidants, and many others.

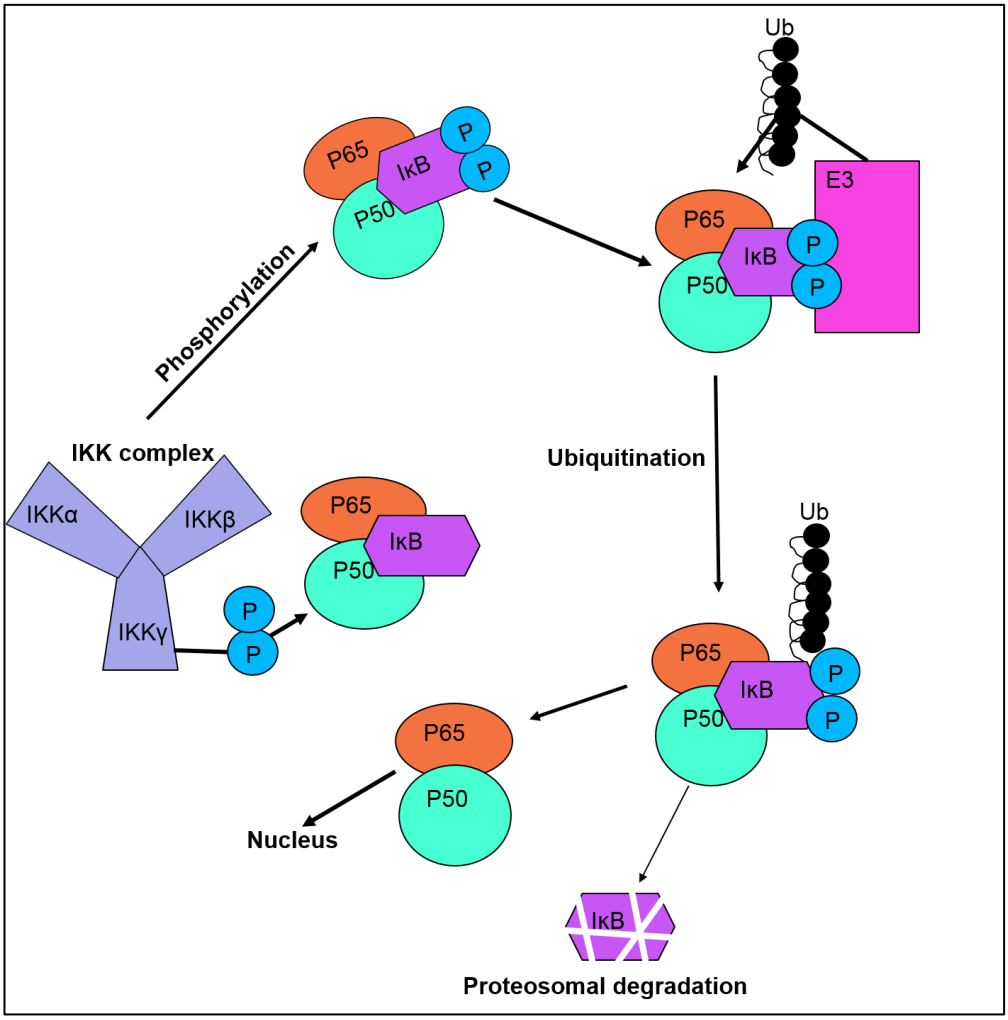

Figure 1.6 Proteasomal degradation of the IκB complex involves its phosphorylation by the IKK complex, polyubiquitination by the E3 ubiquitin ligase and degradation by the proteasome.

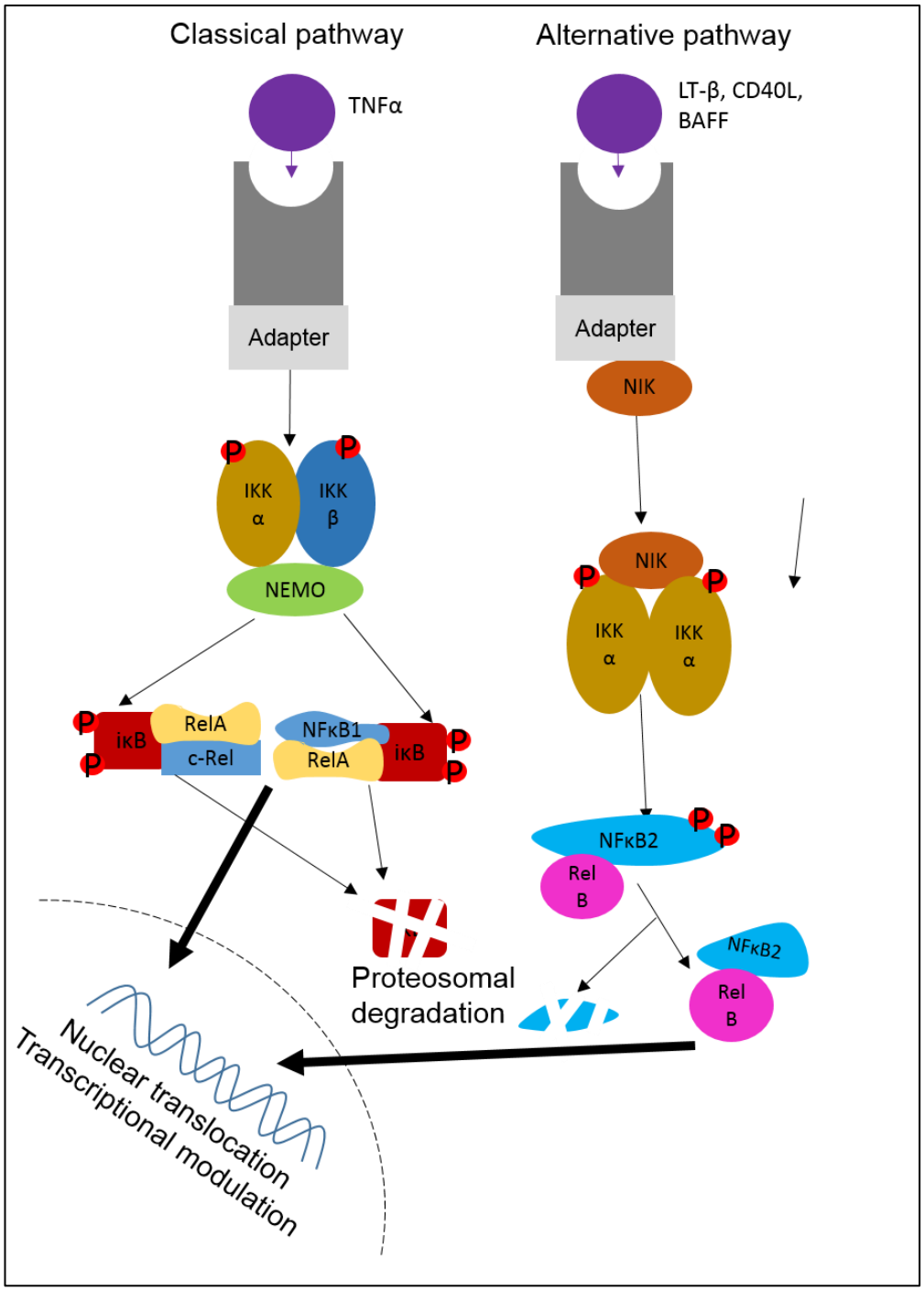

Figure 1.7 The NFκB signalling pathways. The classical NFκB signalling pathway and alternative NFκB signalling pathway.

1.3.2 Classical NFκB activation pathway

The classical NFκB activation pathway involves NFκB1, RelA (P65) and c-Rel. This pathway is triggered by activation of a dimer containing RelA, NFκB1 or c-Rel. These subunits can form homo or heterodimers, however, the RelA:NFκB1 dimer is the most ubiquitous. The first step in the pathway is activation of IKK complexes which target the inhibitors of NFκB1:RelA:iκB or other canonical dimers to the proteasome by phosphorylation and subsequent ubiquitination. This releases the complex and allows a canonical pathway dimer to translocate to the nucleus where it modulates transcription at kappa B sites in the genome (figure 1.7A) (Viennois, Chen and Merlin, 2013).

The NFκB1 precursor P105 is partially degraded by the proteasome to remove the C-terminal domain which leaves the active NFκB1 subunit (also called the P50 subunit). (Palombella *et al.*, 1994). P105 is processed by the 20S proteasome in a rapid ubiquitin dependant manner. However, there is a large pool of P105 which remains unprocessed at all times. This is due to the fact that P105 has its own separate function. The glycine rich region which is located at the C terminus of the P50 portion of the P105 protein functions as the stop signal for the proteasome (Li and Ghosh, 1996; Moorthy *et al.*, 2006). The IKK complex contains IKKα, IKKβ, and IKKγ which is also known as NFκB essential modulator (NEMO) (Gerondakis *et al.*, 2006). The IKK complex targets the IκB proteins for phosphorylation, polyubiquitination and proteasomal degradation (Karin and Ben-Neriah, 2000).

NFκB1 null mice have immune system defects which are evident when the immune system is active. However the immune system was found to be normal at rest in this strain of mice. In particular, the B cells of an NFκB1 null mouse have been shown not to proliferate in response to LPS, a protein which signals the presence of bacteria to

the immune system. These mice have defective macrophage activation, with the majority of the macrophages remaining in the spleen in response to bacterial invasion, as opposed to in a wild-type mouse, where they leave the spleen in order to combat the threat (Sha *et al.*, 1995). However, NFκB1 null mice show increased function of natural killer cells, along with increased production of interferon gamma by these cells (Tato *et al.*, 2003).

The P105 protein does not function solely to produce P50 on degradation. The inactive form of the protein also has other functions. As well as retaining other NFκB proteins inactive in the cytoplasm of unstimulated cells, P105 also functions to inhibit and hold in the cytoplasm mitogen activated protein (MAP) kinase (MAPK) and tumour progression locus-2 (TPL-2). TPL-2 is an oncogenic protein which is known to promote the transformation of cells and the progression of T-cell lymphomas (Ceci *et al.*, 1997). This inhibition actually prevents the loss of TPL-2, as without the support of the P105 protein it would be rapidly depleted (Beinke and Ley, 2004).

C-Rel is expressed in high amounts in hematopoietic cell lines. It has a role in the function of mature T and B cells, although is not essential for the development of a normal immune system (Gerondakis *et al.*, 2006). C-Rel is a transcriptionally active protein, with two transactivation domains and a rel homology domain; it is found in dimers with inactive NFκB1 or in complexes with iκB proteins. (Gilmore, 2006). Mice lacking c-Rel appear very similar to wild-type, however when an immune challenge occurs they experience an impaired immune response, with proliferative defects seen in the B and T cells. When c-Rel null immune cells are confronted with mitogenic stimuli, the MAPK (mitogen activated protein kinase) proliferative pathway does not function (Köntgen *et al.*, 1995).

1.3.3 Alternative NFκB activation pathway

The alternative NFκB activation pathway involves RelB which does not form homodimers and NFκB2 which can form homodimers as well as heterodimers with RelB. The pathway is often activated by TNF superfamily members via the NIK complex which integrates signals from various TNF receptor family members. The first event in the pathway is the activation of the NIK complex, which is dependent on the IKK alpha subunit, also found in the IKK complex (Xiao *et al.*, 2001).

When activated, the NIK complex then goes on to target the NIK recognition domain (NRD) of the P100 protein. The P100 protein consists of both P52 and an inhibitory domain containing ankyrin repeats. When the NIK complex is activated, the inhibitory domain is targeted for degradation by the proteasome. This then allows the P52 protein to dimerise with RelB, if RelB is not already present. The dimer then translocates to the nucleus to modulate transcription (Sun, 2011).

The processing of P100 to P52 is slow compared to that of P105 processing. The NIK complex induces ubiquitination by the phosphorylation of the protein at two distinct serine residues (Ser 886 and 870) (Xiao *et al.*, 2001). The C terminus of the protein is removed by proteasomal degradation. The positioning of the proteasome and the subsequent cleavage of the protein is dependent on the location of a glycine rich region, which is located at the c-terminus of the P52 protein (Heusch *et al.*, 1999).

The production of active NFκB2 is carefully controlled. The presence of P100 is important as this protein functions as an iκB in its own right, with the ankyrin repeat domain of the protein playing an important inhibitory role in the cytoplasm, which is essential for the proper development of the lymphoid organs. The deletion of the C terminus of the P100 protein in mice, causing more of the active NFκB2 protein to be present, leads to abnormalities in the stomach, and hematopoietic tissue and immune system abnormalities which cannot be normalised by other NFκB family proteins

(Ishikawa *et al.*, 1997). P52 production from P100 is tightly controlled and the presence of the inactive precursor is important for normal immune function. Unlike the processing of P105 to form P50, the processing of P100 to P52 is not constitutive, and only small amounts of the protein are active at any time (Xiao *et al.*, 2001).The processing of P100 to P52 is negatively regulated by a processing inhibitory domain (PID) found within p100 at the C terminal end downstream of the ankyrin repeats. The PID functions to avoid uncontrolled processing of the P100 protein and helps maintain the tight control required in the alternative NFκB activation pathway (figure 1.7B) (Xiao *et al.*, 2001).

The NFκB2 protein plays an important role in the immune system. The germline deletion of the NFκB2 protein in mice resulted in abnormalities with the immune system. Abnormal architecture of the spleen was seen, in particular, the complete absence of germinal centres. There was also a reduction of the B cell population in the spleen, bone marrow and in the lymph nodes, with defects in the proliferation of B cells in response to LPS and other stimuli that would normally produce an increase in the number of B cells (Caamaño *et al.*, 1998).

1.3.4 NFκB signalling in the gastrointestinal tract

In the normal gastrointestinal mucosa NFκB is thought to play a role in the regulation of the immune response to commensal and pathogenic bacteria. Toll like receptors can be activated by pathogen associated molecular patterns (PAMPs). NFκB is known to be activated when PAMPs are detected via Toll like receptors (TLRs) (Chow *et al.*, 1999). There are two different pathways of NFκB activation in response to LPS signalling; these are the Myd88 dependent (Kawai *et al.*, 1999) and the Myd88 independent or TRAF dependent pathway (Kawai *et al.*, 2001).

The classical NFκB activation pathway in the gastrointestinal tract is known to be involved in epithelial cell homeostasis and repair. Depending on the localisation of an

NFκB-activating pathogen, the epithelial cells of the gastrointestinal tract have a different response. If the antigens are detected at the apical surface, the NFκB inhibitory proteins (iκB) are stabilised and the classical NFκB signalling pathway is not activated. However, detection of a bacterium at the basolateral surface of the cell causes signalling via the classical NFκB activation pathway (Peterson and Artis, 2014).

NFκB is involved in activating the transcription of IL-8, which then attracts acute inflammatory cells to the site, providing the initial immune response to infection. It has been shown in a study using a monolayer of human intestinal epithelial cells (T84 cells), that NFκB is activated only by pathogenic bacteria such as enteropathogenic *E.coli*, and not by bacteria which are found to be commensal in the gut (Savkovic, Koutsouris and Hecht, 1997).

Intestinal injury has also been shown to cause up-regulation of NFκB. Reperfusion injury after ischaemia occurs when the blood supply has transiently been stopped and the tissue has been left without oxygen. This has been shown to cause a massive up-regulation in IKK and NFκB related genes (Chen *et al.*, 2003). Other types of intestinal injury are also worsened by inhibition of NFκB pathways. For instance sepsis related injuries are more severe in intestinal epithelial specific IKKβ null mice. Apoptosis, intestinal barrier dysfunction, villus shortening and mortality have also been shown to be worse in mice which have an enterocyte specific IKKβ deletion (Dominguez *et al.*, 2013).

NFκB is known to be involved in the response to radiation induced apoptosis in the gastrointestinal tract. Mice which are deficient in IKKβ are more sensitive to irradiation induced intestinal apoptosis and uncontrolled inflammation in response to infection (Egan *et al.*, 2004; Zaph *et al.*, 2007). The NFκB pathway is also activated in response to short wave ultraviolet radiation; interestingly, this activation does not occur as a

result of IKK activity (Li and Karin, 1998). It is thought that the mechanism of activation in this case is via inhibition of the synthesis of iκBs at the translational level (Wu and Tong, 2010).

In vitro studies have shown that some commensal bacteria are capable of down-regulating NFκB signalling (Lakhdari *et al.*, 2011). Examples include the commensal bacterium *Streptococcus salivarius* which down-regulates RelA (Kaci *et al.*, 2011) and commensal *Salmonella* bacteria which cause the down-regulation of NFκB related transcription by interfering with the IκBαs of the classical activation pathway (Neish *et al.*, 2000). *Shigella flexneri,* a pathogenic bacterium, has been shown to quickly induce classical NFκB pathway signalling by interfering with ubiquitin ligases, and *Lactobacillus casei,* which is a commensal bacteria, has been shown to be able to directly reverse this up-regulation and cause the levels of NFκB activation to return to their normal levels (Tien *et al.*, 2006). Additionally inhibition of the entire classical NFκB activation pathway in mice is known to cause spontaneous inflammatory reactions to commensal bacteria (Pasparakis, 2008). There is therefore a link between the NFκB pathway and the commensal bacteria of the gut. It was observed in chickens that the soluble non-starch polysaccharide found in plantain bananas can prevent the adhesion of bacteria to the gut wall. The plantain non-starch polysaccharide (NSP) has been shown to prevent the invasion of *Salmonella sp.* across the intestinal barrier in chickens (Parsons *et al.*, 2014). In addition, green dwarf banana (Plantain banana) flour ameliorates TNBS colitis in rats (Scarminio *et al.*, 2012). Starches found in the banana flour have been found to increase numbers of commensal bacteria such as *Lactobacillus* (Wang *et al.*, 2002), which as previously mentioned down-regulate NFκB signalling caused by other bacteria. Therefore, dietary fibres may be linked to NFκB signalling via their effects on the commensal bacteria within the gastrointestinal tract (Rahman *et al.*, 2014).

1.3.5 Potential variation of NFκB along the crypt villus axis

Given the role of NFκB subunits in modulating cellular proliferation and apoptosis, it is likely that their expressions are modulated along the intestinal crypt villus axis where different cellular compartments are either proliferative or senescent. However, to date the distributions and sub-cellular localisations of NFκB subunit expression along the intestinal crypt villus axis have not been extensively characterised in mouse or human owing to the complexities of post translational modifications of these subunits and the availability of reliable antibodies. Immunohistochemistry (IHC) has indicated that p65 expression is increased at the villus tip following the administration of inflammatory stimuli such as LPS or TNF to mice (Williams, Pritchard and Duckworth unpublished observations). Data provided on the Human Protein Atlas does not indicate any differences in RelA c-Rel, NFκB1 or NFκB2 expression along the crypt villus axis (www.proteinatlas.org). Variation in expression of RelB has been observed along the small intestinal crypt villus axis, with nuclear expression of RelB increased towards the crypt base. (Uhlen *et al.*, 2015).

1.3.6 NFκB signalling in IBD

There is a genetic element to the occurrence of IBD, as studies using monozygotic twins have shown a high concordance in not only the occurrence of CD, but also the disease location, age of onset and disease behaviour (Halfvarson *et al.*, 2003). In total 99 IBD risk loci have now been found, including genetic variants in TNF which are known to activate NFκB signalling (Anderson *et al.*, 2011). A polymorphism in the promoter region of the *NFκB1* gene which codes for P105 has been linked to UC. Patients homozygous for these genetic variants were found to be around 5 years younger than patients with UC who either did not have the mutation or were heterozygous for the mutation at the time of disease development (Borm *et al.*, 2005).

The *c-Rel* gene has also been shown to be one of the disease loci for CD and this risk locus was also found to be associated with psoriasis, another chronic inflammatory condition (Ellinghaus *et al.*, 2012).

The NFκB family of proteins has been shown to be activated in IBD (Ardite *et al.*, 1998). This is unsurprising as NFκB is important for acquired and active immunity and the immune system plays an important role in IBD (Courtois and Smahi, 2006). For instance RelA is found to be strongly up-regulated in TNBS-induced colitis and IL-10 null mice, while antisense oligonucleotides against RelA have been shown to ameliorate colitis in a TNBS-induced mouse colitis model (Neurath *et al.*, 1996). Mice which are deficient in NFκB family members can be used to examine the contributions of the NFκB pathways to colitis onset and recovery. NFκB2 null mice were protected from the induction of DSS-induced colitis in our lab (Burkitt *et al.*, 2015). The severity of murine DSS-induced colitis was also increased when the NFκB pathway initiator IKKβ was inhibited. This was true when IKKβ was inhibited for the whole DSS experiment or after the administration of DSS had been completed. Deletion of IKKβ in only the intestinal epithelial cells led to significantly worse colitis than in littermate controls (Eckmann *et al.*, 2008). This suggests that the NFκB pathway is involved in regulating the severity of chronic colitis.

The classical NFκB activation pathway cannot function at all without the presence of NFκB essential modulator (NEMO). NEMO is one of three subunits in the IKK complex, which is the complex responsible for activation of the classical NFκB pathway and contains IKKβ, IKKα and NEMO (Chu *et al.*, 1999). It has been demonstrated that when NEMO is specifically deleted in the intestinal epithelial cells (IEC) of mice, severe rectal bleeding and diarrhoea occur. Disease only occurs in the colon, and an inflammatory cell infiltrate and upregulation of pro-inflammatory cytokines are observed. The other components of the IKK complex are IKKβ and IKKα. These two proteins have been shown to have functional redundancy. If one of

the two is deleted, the classical NFκB pathway can still be activated. However, if both are deleted, a severe colonic inflammation similar to that observed in intestinal epithelial cell specific deletion of NEMO occurs (Pasparakis, 2008). Therefore, if the classical NFκB activation pathway is unable to function, mice develop severe colonic inflammation.

Several current agents that are used to treat IBD such as corticosteroids are also thought to partially exert their effects by altering NFκB signalling (Atreya et al., 2008). DSS-induced colitis has been inhibited by factors which are known to inhibit NFκB signalling. For instance, along with the upregulation in PPARγ proteins, the downregulation of NFκB signalling in mice with DSS-induced colitis is responsible for the amelioration of colitis seen in mice treated with oroxyloside (Wang *et al.*, 2016). NFκB signalling pathway activation also upregulates the inflammatory cytokines TNF and IL-1β in DSS-induced colitis (Dai *et al.*, 2013; Lee *et al.*, 2013).

Studies have shown that NFκB signalling can be controlled by a wide variety of factors. Voluntary exercise has been shown to normalise NFκB signalling in C57BL/6J mice given a high fat diet, compared to mice administered a normal diet (Liu *et al.*, 2015). The marine carotenoid astaxanthin has also been found to protect mice against DSS-induced colitis. It was shown to inhibit NFκB and pro-inflammatory cytokines (Yasui *et al.*, 2011). The botanical panax notoginseng is commonly used in herbal medicine and modulates NFκB target genes, probably through NFκB signalling. The suppression of iNOS and Cox-2(PTGS2) when panax was given to mice (Wen *et al.*, 2014) was likely to be a result of the down-regulation of RelA:NFκB1 heterodimers (Kim *et al.*, 2013).

1.3.7 NFκB signalling in IBD associated colon cancer

Although IKKβ and IKKα deletions caused no spontaneous effects, when mice with an IKKβ deletion were used in an induced colitis related cancer model, a decrease in

the severity of disease was seen. When IKKβ was deleted from the intestinal epithelial cells of mice, the number of tumours induced by the azoxymethane/DSS model was dramatically decreased. However, the size of the tumours remained the same as in control animals. When IKKβ was however deleted from myeloid cells, it was found that the size of the tumours was reduced. This indicated that the classical pathway of NFκB activation was involved in the formation of tumours as a result of inflammation, and that epithelial cells were responsible for this. It also suggested that myeloid derived haematopoietic cells are likely to be involved in regulating the growth of tumours in this mouse model (Greten *et al.*, 2004).

The alternative NFκB activation pathway has also been shown to be crucial in inflammation associated carcinogenesis as NFκB2 null mice developed less colonic tumours when subjected to the azoxymethane/DSS model of colitis associated carcinogenesis (Burkitt *et al.*, 2015). Despite showing no significant increase in colitis susceptibility, c-Rel null mice had an increased occurrence of colonic tumours, when subjected to the azoxymethane/DSS model of colitis-associated cancer (Burkitt *et al.*, 2015).

1.3.8 NFκB inhibition in treatment of inflammatory bowel disease

As the NFκB pathways have a variety of functions and components of these pathways are widely expressed, it is not surprising that NFκB mutations have been associated with several diseases. These are often diseases associated with the immune system, inflammation or cancer (Courtois and Gilmore, 2006). Sulphasalazine is a 5-ASA compound used to treat IBD and specifically targets the classical NFκB activation pathway (Wahl *et al.*, 1998). It has been shown that this drug works as an immunosuppressive agent and reduces inflammation by specifically targeting the IKKα and IKKβ components of the IKK complex (Weber *et al.*, 2000). Additionally corticosteroids are known to modulate NFκB signalling, and it is thought that in

particular suppression of NFκB1 signalling is one of the ways in which these drugs ameliorate the inflammation in IBD (Ardite *et al.*, 1998).

One new therapy which has emerged from animal studies is the use of antisense oligonucleotides against RelA (ASO-RelA) to treat colitis. This treatment was discovered to reduce the production of pro-inflammatory cytokines in mucosal cells (Murano *et al.*, 2000). In mice with DSS and TNBS-induced colitis, ASO-RelA was shown to reduce the amount of colonic inflammation (Murano *et al.*, 2000; Lawrance *et al.*, 2003). A clinical trial in 2002 where IBD patients were treated with ASO-RelA also showed significant improvements in patients compared to control groups. However this treatment has not been incorporated into routine clinical use (Loftberg *et al.*, 2002).

1.3.9 NFκB and apoptosis in the gastrointestinal tract

Intestinal crypt apoptosis occurs spontaneously and in response to DNA damaging agents. The rapidly cycling cells of the crypt are very sensitive to DNA damage and are responsible for populating the villus to replace cells that are shed from the villus tip. Egan and colleagues demonstrated that iκB ablation in small intestinal epithelial cells did not affect the amount of spontaneous apoptosis. However it did result in crypt cells being twice as sensitive to irradiation induced cell death in the +4 stem cell zone (Egan *et al.*, 2004). This indicates that signalling via the classical NFκB activation pathway is necessary for the exacerbation of crypt apoptosis that occurs in mouse models of small intestinal GI damage, but does not appear to regulate spontaneous intestinal crypt apoptosis.

GI apoptosis also occurs in response to pathogenic bacteria. The classical NFκB pathway response to LPS protects intestinal epithelial cells against apoptosis. Both RelA heterozygous mice and NFκB1 null mice have higher small intestinal crypt apoptosis in response to LPS than wild-type animals. RelA heterozygotes have

significantly more crypt apoptosis than NFκB1 null mice which indicates that RelA has the greatest protective role against LPS induced apoptosis (Gadjeva, Wang and Horwitz, 2007). Mice heterozygous for RelA are also more sensitive to a TNF challenge than wild-type, as are NFκB1 null mice. They have been shown to have significantly more apoptosis in small intestinal crypts than wild-type (Gadjeva, Wang and Horwitz, 2007).

The protective role of the classical NFκB activation pathway seen in small intestinal apoptosis does not however appear to extend to the colon. Classical NFκB signalling is known to act via the Raf kinase inhibitor protein mediated pathway to exacerbate crypt apoptosis caused by TNF, and inhibition of this pathway results in the amelioration of apoptosis (Lin *et al.*, 2017). In terms of signalling downstream from the NFκB pathway, p53 upregulated modulator of apoptosis (PUMA) is directly activated by NFκB signalling via RelA (Wang *et al.*, 2009). Studies involving this protein have indicated that it may be one of the links between NFκB signalling and crypt apoptosis and PUMA null mice show a decrease in colonic crypt apoptotic index when treated with TNBS as well as a lower apoptotic index following DSS treatment (Qiu *et al.*, 2011).This indicates that the classical NFκB pathway family members have a protective role in the small intestine, but a pro-apoptotic role in the colon in response to DNA damage in some incidences. However there does not appear to be a role for the classical NFκB activation pathway in regulating the baseline amounts of crypt apoptosis in the colon.

The NFκB signalling pathway has also been shown to regulate intestinal epithelial cell shedding. Mice which lack the classical NFκB pathway subunit RelA have been shown to have elevated levels of apoptosis in the intestinal tract, indicating that this protein is necessary for the regulation of cell shedding (Steinbrecher *et al.*, 2008). NFκB is known to be involved in anoikis, which is one of the possible mechanisms by

which shed cells undergo apoptosis. NFκB signalling has been shown to block the anoikis of rat epithelial cells in suspension and increase survival when the cells were unattached. RelA/NFκB1 was shown to be the NFκB dimer responsible for this resistance to apoptosis (Toruner *et al.*, 2006). In our lab NFκB1 and NFκB2 were shown to be involved in the regulation of cell shedding from the villus tip, with NFκB1 null mice more prone to cell shedding and NFκB2 null mice with less cell shedding (Williams *et al.*, 2013).

NFκB has also been identified as both a suppressor and an activator of apoptosis. For instance, in immature B cells, c-Rel has been found to act as a suppressor of apoptosis. The deletion of c-Rel leads to increased apoptosis in immature B cells which indicates that NFκB suppresses apoptosis in this setting (Wu *et al.*, 1996). Other examples of the anti-apoptotic function of NFκB include protective effects in MCF7 and HeLa cells against TNF induced apoptosis (Liu *et al.*, 1996). NFκB can also have an anti-apoptotic effect in response to radiation therapy or chemotherapy (Sharma, Hupp and Tepe, 2007). NFκB is also known to increase apoptosis in immune cells in response to some stimuli, for instance in the response of T cells to FasL (Kasibhatla *et al.*, 1998). NFκB has also been shown to be responsible for the apoptosis seen in serum starved cells, as seen in a study using HEK293 cells (Grimm *et al.*, 1996).

1.3.10 NFκB and DNA damage

The DNA damage response is an elaborate network of signalling pathways that has evolved in order to avoid damage to genetic material (Stilmann *et al.*, 2009). This is achieved by the prevention of the transmission of damaged genetic material to daughter cells (Bartek and Lukas, 2007). NFκB activation can be dependent on DNA damage. Double stranded DNA breakage has been shown to activate NFκB signalling in studies using topoisomerase poisons (Piret and Piette, 1996; Boland,

Fitzgerald and O'Neill, 2000). In this case, IKK signalling happens in response to the localisation of NEMO to the nucleus (Hwang *et al.*, 2015). Next, ATM kinase, a key component of the DNA damage sensing apparatus of the cell, along with a SUMO-1 ligase then SUMOlyate NEMO. The IKK complex is then activated and subsequently NFκB signalling is activated (Stilmann *et al.*, 2009). The activation of classical NFκB signalling is also known to activate cell survival pathways in response to DNA damage (Janssens and Tschopp, 2006)(figure 1.8).

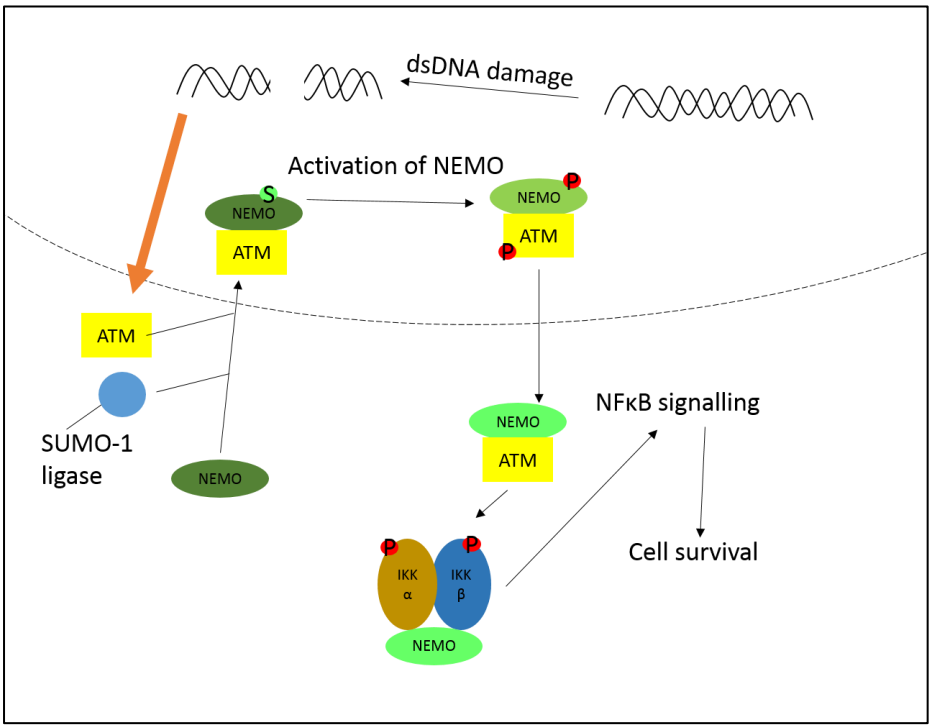

Figure 1.8 Activation of classical NFκB signalling by ATM kinase after DNA damage

The alternative NFκB pathway is also activated in response to DNA damage. Nuclear localisation of RelB is known to occur in response to radiation (Josson *et al.*, 2006). In particular, the phosphorylation and subsequent processing of the NFκB2 precursor P100 to the active form has been shown to be activated in response to DNA damage. (Xu *et al.*, 2010). This activation of the alternative NFκB

signalling pathways have been shown, similarly to the classical pathway, to promote cell survival pathways in response to DNA damage (Lessard *et al.*, 2005).

1.4 Chemotherapy induced gastrointestinal toxicity

1.4.1 Current gastrointestinal cancer treatment regimens

Cancer of the small intestine is extremely rare, however, colorectal cancer is the most common cancer of the GI tract, as well as being one of the most common cancers overall. Chemotherapy can be used to treat metastatic small intestinal and colorectal cancers. Oxaliplatin and irinotecan are commonly used in treatment and 5-Fluorouracil (5-FU) is sometimes also used in combination with radiotherapy. 5-FU is a commonly used treatment for colorectal cancer and is often used in combination with irinotecan or oxaliplatin (Longley, Harkin and Johnston, 2003). This kind of therapy is known as doublet cancer therapy, and is used in the majority of cases as opposed to single-drug therapy; often after colorectal surgery to try to stop the cancer from recurring in the areas surrounding the resection (adjuvant therapy). The combination of 5-FU and oxaliplatin (FOLFOX) or the combination of 5-FU and irinotecan (FOLFIRI) are the two most common treatments used in colorectal cancer. Both the FOLFOX and FOLFIRI approaches have been shown to improve progression free survival (André *et al.*, 2009; Sobrero, 2009; Landre *et al.*, 2015). In patients in whom 5-FU has failed, or where patients are intolerant to 5-FU, the combination of oxaliplatin and irinotecan (IROX) has been shown to improve progression free survival when compared with single agent irinotecan (Sobrero, 2009).

1.4.2 Mechanism of action of chemotherapy

Due to the rapid cell division of cancer cells, it makes sense that cancer therapies exert off target effects on intestinal epithelial cells which also proliferate extremely

rapidly. Two common chemotherapy drugs which produce these off-target effects are irinotecan and etoposide. Irinotecan targets the topoisomerase I enzyme (figure 1.9A) and etoposide is used to target the topoisomerase II enzyme (figure 1.9B). Topoisomerases introduce transient breaks in DNA molecules to avoid the DNA strands becoming tangled due to secondary structures forming. This allows different areas of the DNA strand to be wound and un-wound at different times (Seo, 2015).

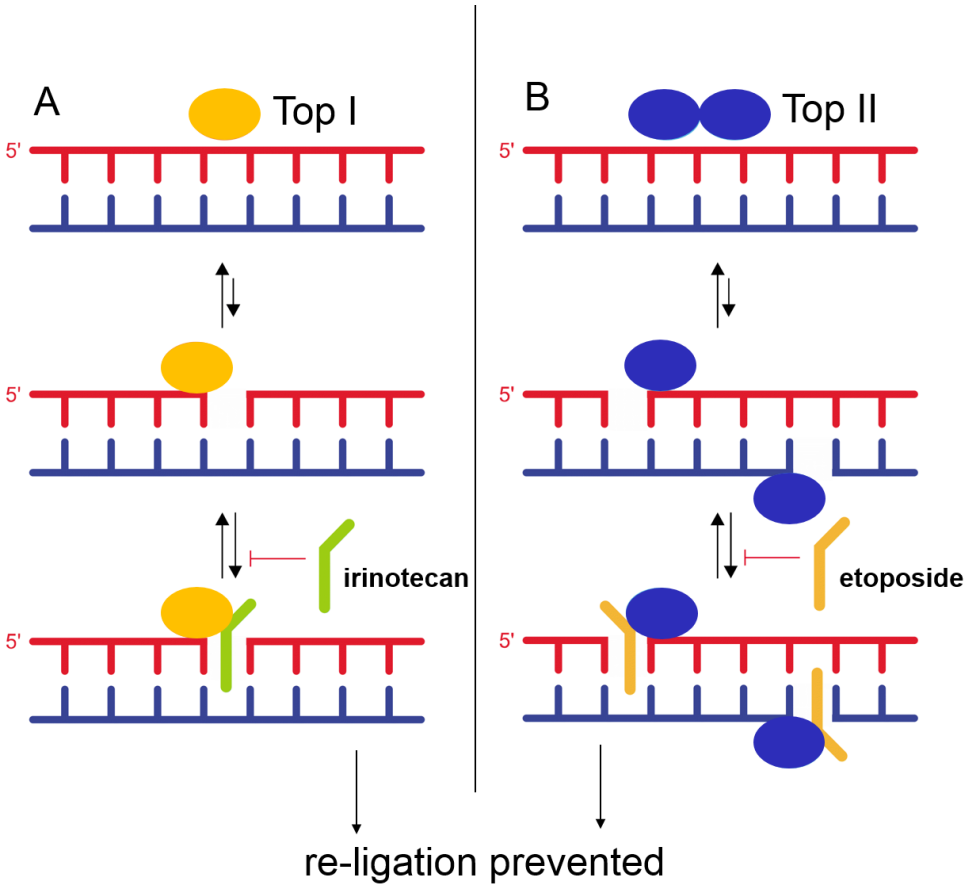

Figure 1.9 Topoisomerase poisons prevent the re-ligation of DNA strands after they have been cleaved by the topoisomerase I or topoisomerase II enzyme. Adapted from Seo, 2015.

Topoisomerase II (TopII) can ‘un-knot’, remove supercoils and separate two entangled loops of DNA from one another. Top II does this by cleaving, moving, and then re-joining a strand of DNA at a particular point. This allows the Top II enzyme to relieve the secondary structures created by the double helix of DNA. Topoisomerase I is able to reduce tension in the DNA strand by cleaving and re-sealing one of the two strands of the DNA double helix. Topoisomerases use transesterification reactions to break the DNA strands and subsequent transesterification reactions to re-seal the DNA strand. Etoposide and irinotecan work by inhibiting the ligation of the DNA strands. They stabilise the complex containing the cleaved DNA strand and cause breaks to become permanent in DNA wherever the topoisomerase proteins are working. Etoposide and irinotecan can induce the DNA damage response which occurs when a cell detects DNA damage foci. This process involves a signalling cascade, which can slow down the cell cycle or induce senescence. Irinotecan causes single stranded breaks (figure 1.9A) and etoposide initiates the formation of the double stranded breaks (figure 1.9B). These are caused by the stabilisation of topoisomerases I and II in the cleavage complexes. (Montecucco, Zanetta and Biamonti, 2015).

5-FU is an analogue of uracil with a fluorine atom at carbon 5 in place of a hydrogen. It functions to block the normal production of pyrimidine nucleotides (Diasio and Harris, 1989). 5-FU is used to treat colon cancer and is usually used when the disease has metastasised. The drug is usually administered intravenously and is metabolised into fluorodeoxyuridine monophosphate (FdUMP), fluorodeoxyuridine triphosphate (FdUTP) and fluorouridine triphosphate (FUTP) which functions to inhibit thymidylate synthetase, an enzyme involved in pyrimidine nucleotide base production(Longley, Harkin and Johnston, 2003). This leads to failed attempts to repair DNA, DNA strand breaks and cell death (Sobrero *et al.*, 2000). The 5-FU metabolite FUTP is incorporated into RNA, which disrupts RNA synthesis, translation into proteins, and

post transcriptional modifications of RNA (figure 1.10) (Pritchard *et al.*, 1997; Longley, Harkin and Johnston, 2003).

Etoposide, irinotecan and 5-FU are all known to cause DNA damage, however they work via biochemically distinct mechanisms. Etoposide stabilises the usually transient intermediate which is formed from the double stranded DNA break site and the topoII enzyme. Etoposide binds to the topoII enzyme after the enzyme has cleaved the DNA and remains bound at the 5' terminus. These double stranded breaks cause the activation of ATR (ataxia-telangiectasia mutated) and the ATR(ATM- and Rad3-Related) pathway. (Rossi *et al.*, 2006). Irinotecan binds to the topoI enzyme as opposed to topoII, and the topoI enzyme functions to relieve DNA torsion via the cleavage of only one strand of DNA and binds to the 3' end of the DNA. Although irinotecan itself has a small role in the halting of the replication fork, the active metabolic product of irinotecan known as SN-38 binds to the DNA-topoI complex (Ramesh, Ahlawat and Srinivas, 2010). Similarly to irinotecan, active metabolites of 5-FU cause the DNA damage seen in 5-FU treatment. In particular, the metabolite FdUMP interferes with thymidylate synthase mediated conversion of thymidine from uracil, which inhibits the synthesis of DNA and RNA. FdUMP binds to the nucleotide binding site of thymidine synthase and forms a stable complex, this means that uracil cannot bind and thymidine is not formed. Additionally, The 5-FU metabolite FUTP is also incorporated into RNA, which inhibits the normal function of RNA (Longley, Harkin and Johnston, 2003).

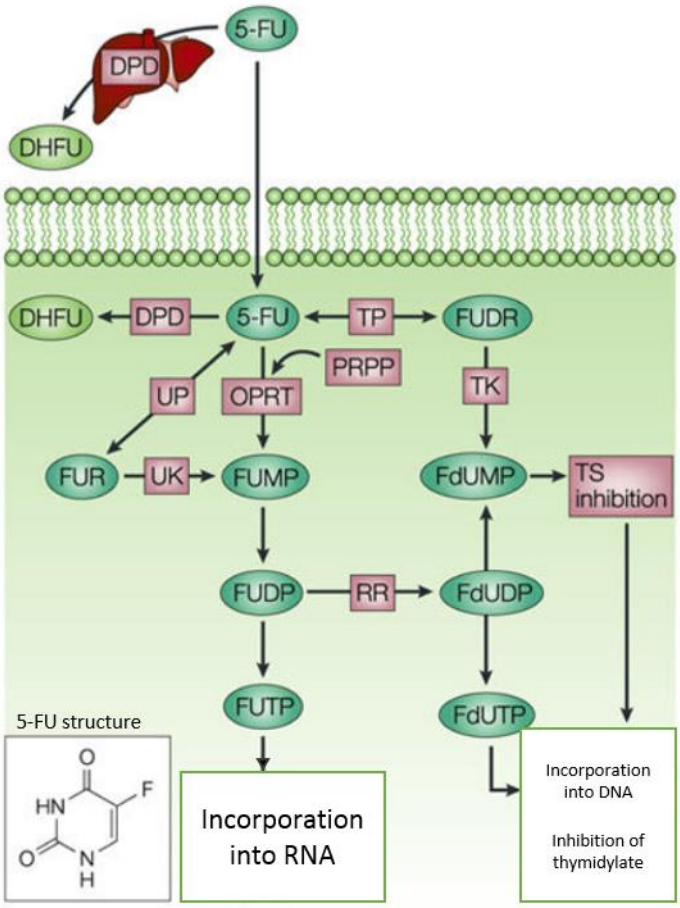

Figure 1.10 The mechanism of action of 5-Fluorouracil (5-FU). 5-FU is converted to fluorodeoxyuridine (FUDR) by thymidine phosphatase (TP) phosphorylation by thymidine kinase (TK) forms fluorodeoxyuridine monophosphate (FdUMP), which is then converted to fluorodeoxyuridine diphosphate (FdUDP) or goes on to inhibit TS and cause DNA damage. FdUDP is then phosphorylated to form fluorodeoxyuridine triphosphate (FdUTP). 5-FU is directly converted into fluorouridine monophosphate (FUMP) by orotate phosphoribosyltransferase (OPRT) and co-factor phosphoribosyl pyrophosphate (PRPP). 5-FU is converted to fluorouridine (FUR) and then FUMP through uridine phosphatase and uridine kinase. Fluorouridine diphosphate (FUDP) is formed from FUMP and is then either converted to FdUDP by ribonucleotide reductase or phosphorylated to form fluorouridine triphosphate (FUTP) which induces RNA damage. Adapted from Longley, Harkin and Johnston, 2003.

1.4.3 NFκB modulation of the effects of chemotherapy

NFκB signalling has been associated with resistance to chemotherapy drugs (Chuang *et al.*, 2002). Using genistein to inhibit classical NFκB signalling by stabilising IκBα, it has been shown that NFκB signalling plays a part in the resistance of cancer cells to chemotherapy. Cisplatin, docetaxel and doxorubicin have all been shown to induce apoptosis more effectively in cancer cells in which classical NFκB signalling has been inhibited (Li *et al.*, 2005).

Inhibition of NEMO, a key component of the NFκB pathways has been shown to increase apoptosis and inhibit the proliferation of A375 melanoma cells (Ianaro *et al.*, 2009). Additionally, in a murine model of melanoma, inhibition of the classical NFκB pathway was demonstrated to increase tumour cell death and the anti-apoptotic effect of the classical NFκB signalling pathway was reversed by inhibiting the IKK protein (Yang *et al.*, 2006). This indicates the potential role of NFκB as a pro-survival factor in carcinogenesis.

1.4.4 The effects of chemotherapy on gastrointestinal apoptosis

NFκB signalling is thought to be involved in regulating the susceptibility to gastrointestinal toxicity caused by chemotherapy (Logan *et al.*, 2009). Treatments for colorectal cancer, such as 5-FU and irinotecan are known to have direct toxic effects on the intestinal mucosa. Mucositis occurs when cytotoxic chemotherapeutic agents cause apoptotic pathways to be initiated and these are often mediated through NFκB signalling (Lawrence, 2009; McQuade *et al.*, 2016). This can lead to the massive upregulation of pro-inflammatory cytokines such as TNF and IL-1β and these can injure the gut leading to mucositis (Sonis *et al.*, 2004). Apoptosis occurs in the GI tract as a result of irinotecan administration, and is probably a factor responsible for chemotherapy-induced diarrhoea which is a common symptom of mucositis (Ikuno *et*

al., 1995; Gibson *et al.*, 2003). 5-FU treatment increases the number of apoptotic cells in the crypts of rats and mice in the colon and small intestine (Pritchard *et al.*, 1998; Logan *et al.*, 2009). NFκB signalling is not the only mechanism by which chemotherapeutic drugs cause apoptosis during the onset of mucositis. For instance, reactive oxygen species are involved in intestinal damage induced by some chemotherapeutic drugs, and as well as activating NFκB signalling reactive oxygen species can activate ceramide synthase which is known to cause apoptosis (Siddique *et al.*, 2012).

1.5 Tyrosine kinase inhibitors

1.5.1 Tyrosine kinase inhibitor-induced gastrointestinal toxicity

Tyrosine kinase inhibitors (TKIs) were developed relatively recently as a form of targeted cancer therapy. The six TKIs which were used in this thesis were gefitinib and erlotinib (figure 1.11), imatinib, dasatinib, nilotinib and bosutinib (figure 1.12). However, there are numerous other TKIs used in cancer therapy. Targeted therapies differ from traditional chemotherapeutic treatments as they are able to discriminate between the rapidly dividing cancer cell and healthy cells which are naturally rapidly dividing. Tyrosine kinases are important modulators of growth in healthy cells. However, mutations affecting these proteins can lead to the increased proliferation and suppression of apoptosis that are characteristic of tumour cells. Tyrosine kinase mutations create protein targets for TKIs, and as tyrosine kinase mutations occur in a wide range of cancers, the targeting of mutations which occur in tyrosine kinases can be an effective way to limit the growth of cancer cells (Arora and Scholar, 2005).

Therapies can target the receptor and non-receptor forms of tyrosine kinases. Receptor tyrosine kinases span the membrane, and are involved in the transduction of signals into the cells from the extracellular environment. Non receptor tyrosine

kinases are not membrane bound and are involved in intracellular signalling processes (Hubbard and Till, 2000). One of the most common adverse side effects of TKI treatments is diarrhoea (Hirsh, 2011). This side effect can lead to drug discontinuation or necessitate a reduction in the dose thus potentially reducing efficacy. The diarrhoea caused by TKIs is mainly of the secretory type, however, the exact mechanisms by which this is caused remain unclear (Loriot *et al.*, 2008).

One important function of the gastrointestinal tract which may be affected by TKIs is the movement of ions to manage the water levels in the luminal environment. This movement is necessary as fluid in the intestinal lumen is important whether there is food in the intestine or not, as it is not sufficient to rely on the presence of food to drive the movement of water into the intestine. Therefore there is active movement of ions into and out of the intestine by the intestinal epithelial cells in order to control the movement of water (McCole and Barrett, 2009). TKIs are thought to affect this movement and cause secretory diarrhoea.

The epidermal growth factor receptor (EGFR) is expressed on the basolateral side of the epithelial cells of the gastrointestinal tract and is important in healing and growth (Uribe and Barrett, 1997). Blocking EGFR signalling is the likely initiating event in EGFR TKI-related diarrhoea (Bowen and M., 2014). EGF signalling inhibition is known to limit the secretion of chloride ions into the lumen of the intestine. The EGFR is activated by G protein coupled receptors through a mechanism involving PI3K (Bertelsen, Barrett and Keely, 2004) (figure 1.11). EGFR inhibitors are commonly used in the treatment of NSCLC. A link between NFκB signalling and resistance to TKI treatment has been found using a cell model of NSCLC. The inhibition of RelA DNA binding was found to enhance the response to the EGFR TKI erlotinib. This indicates that in some cases resistance to TKIs may be due to classical NFκB signalling pathway activity (Blakely *et al.*, 2015).

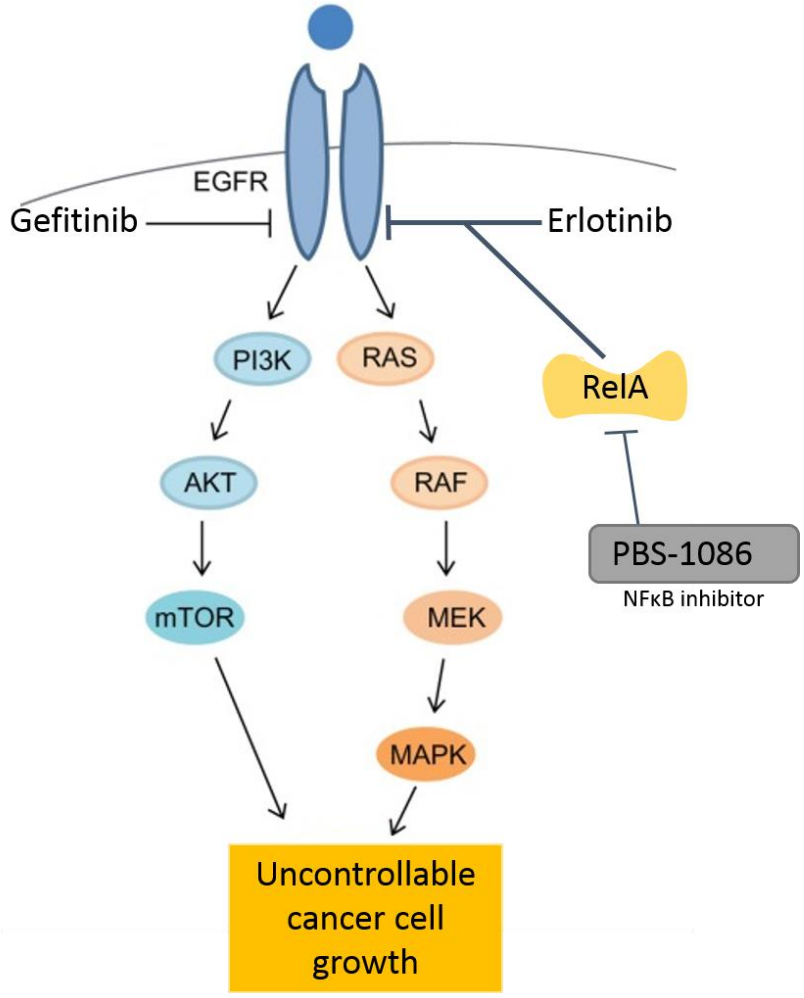

Figure 1.11 Erlotinib and gefitinib both inhibit EGFR. These TKIs are used in treatment of non-small cell lung cancer. The inhibition of EGFR allows the prevention of uncontrollable cancer cell growth. Adapted from Vadakara and Borghaei, 2012.

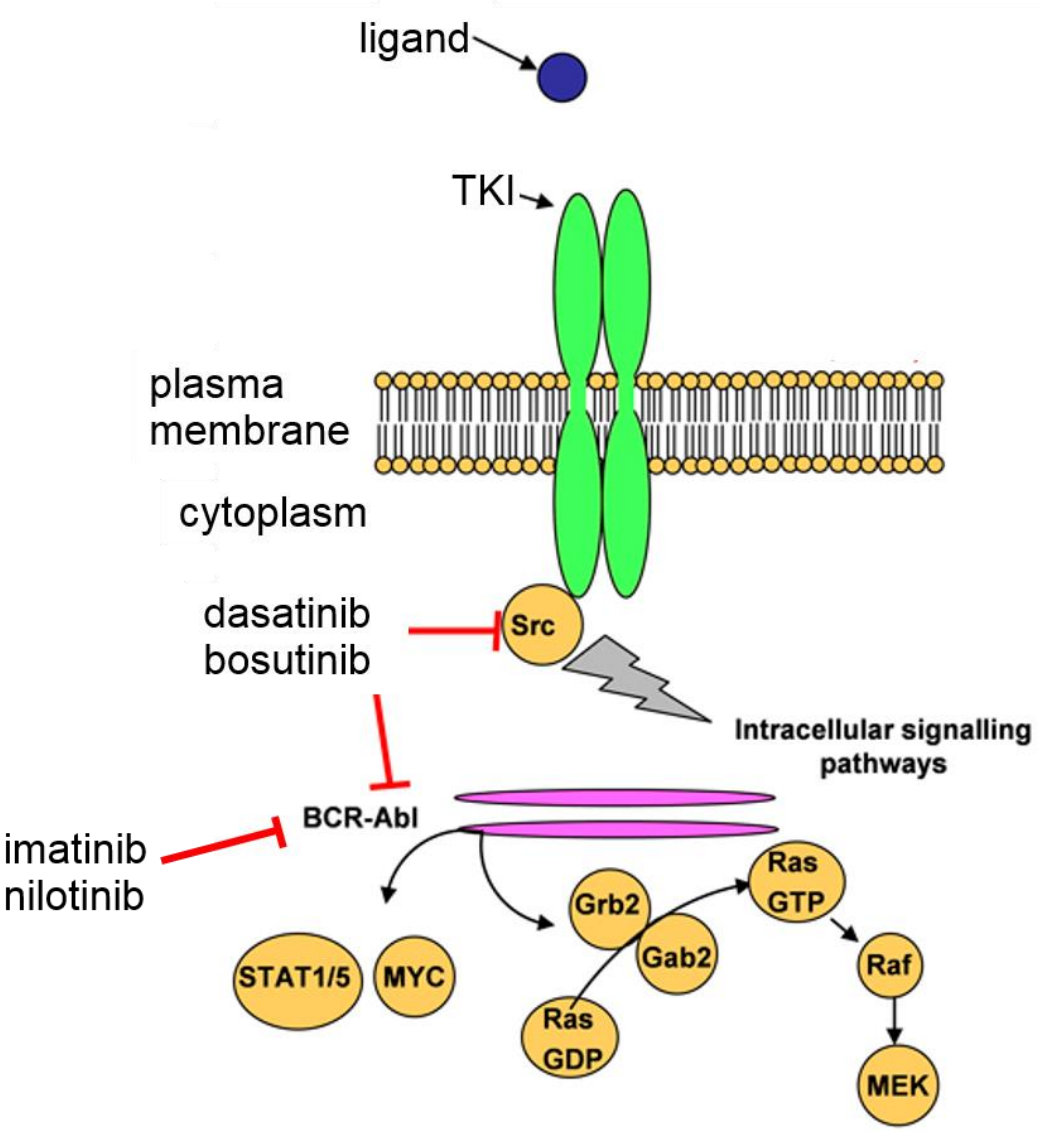

Figure 1.12 Mechanism of action of dasatinib, bosutinib, imatinib and nilotinib. Imatinib was the first TKI developed to target the BCR-ABL mutant protein found in chronic myeloid leukaemia. Both imatinib and nilotinib bind to the inactive conformation of the protein and prevent activation. Dasatinib and bosutinib are dual BCR-ABL and SRC inhibitors, and can bind to and inhibit both proteins. Adapted from Heymann and Rédini, 2013.

1.6 Organoids

1.6.1 Use of intestinal organoids in model development

Traditionally *in vitro* research has been carried out in a predominantly 2D environment. Although results from experiments using traditional cell culture have yielded many important findings, they can be misleading due to the vast difference in cellular environment compared with the *in vivo* environment and due to the lack of an authentic interaction between the cells because of their identical nature. The culture of immortalised lines of cancer cells is often used to investigate physiological processes. However, these 2D cultures are not representative of *in vivo* cells as they are transformed and often far removed genetically from the original cell of origin due to random mutation over time. Assays performed using 2D monolayers of cells also do not allow for the 3D functionality seen in real life systems, where positioning and intercellular signalling play important roles (Simian and Bissell, 2016). The need to better model physiological processes *in vitro*, as well as the movement to reduce laboratory animal use has stimulated interest in alternatives to both 2D cell culture and *in vivo* experimentation. As a result, 3D cell culture systems have been developed. One of the best early examples of this occurred in 1989 when mammary alveoli were cultured on a reconstituted basement membrane matrix. In this breakthrough study it was found that these self-organising groups of cells were representative of *in vivo* breast tissue, and these experiments eventually gave rise to organoid studies (Barcellos-Hoff *et al.*, 1989).

The term ‘organoid’ has come to mean several different things. It is widely accepted that organoids are 3D cultures produced in one of two ways. Firstly, organoids can be cultured from the stem cells of a particular organ to form self-organising structures. Secondly, organoids can be produced by directed differentiation of embryonic stem cells (ESCs) or induced pluripotent stem cells (iPSC), which proliferate and organise

themselves into a structure similar to the origin or intended organ (Fatehullah, Tan and Barker, 2016).

3D cultures of many different tissues have been grown. Different cocktails of growth factors are used in order for the cultures to be expanded into self-organising structures. The organoids are also usually grown on a protein rich gel as a substitute for the extracellular matrix on which the cells would normally grow (Fatehullah, Tan and Barker, 2016).

Organoids have been grown from various parts of the gastrointestinal tract and accessory organs. For instance, liver and pancreas organoids can be grown from adult mouse or human liver stem cells. These organoids come from the same population of progenitor cells. In liver organoid cultures, the cells self-organise into structures resembling the embryonic liver bud and a hepatic ductal compartment. Liver organoids can be grown from the isolation of ducts, however, cultures can also be established using single cells. Pancreatic organoids can be established using a similar method, however, they are only grown using isolated pancreatic ducts. Both liver and pancreas organoids are suitable for genetic manipulation, which allows the introduction of genes of interest into the genome of the organoid (Broutier *et al.*, 2016).

1.6.2 Small intestinal organoids

Small intestinal organoids grown from the crypts of the small intestine were first produced by the Clevers lab (Sato *et al.*, 2009). Their discovery of the Lgr5+ stem cells located at the base of the crypt led to this method being developed (Barker *et al.*, 2007). After discovering that the Lgr5+ stem cells were capable of creating self-organising ‘mini-guts’ *in vivo,* the Clevers group went on to create organoids from the stem cells of the small intestine and colon (Sato *et al.*, 2009; Jung *et al.*, 2011; Sato and Clevers, 2013). The techniques used by Clevers are those which have been

employed in the culture of murine small intestinal organoids in the experiments described in this thesis.

The culturing of murine small-intestinal organoids requires growth factors to stimulate the stem cells to proliferate. When small intestinal crypts are cultured, the essential growth factors are noggin, epidermal growth factor (EGF) and R-Spondin-1. The Noggin protein functions as a bone morphogenic protein (BMP) inhibitor in small intestinal epithelial organoids (Sato *et al.*, 2009). BMP is known to control the proliferation rate of Lgr5+ stem cells, therefore its restriction enables the stem cells to proliferate in the rapid way needed to establish organoid cultures (Qi *et al.*, 2017). EGF is supplemented into the organoid culture, as it plays an essential role in increasing the differentiation and survival of intestinal epithelial cells (Abud, Watson and Heath, 2005). Isolated crypt cultures which are exposed to exogenous WNT form round homogenous cultures (Sato *et al.*, 2011), however when the WNT response is not uniform, the crypt villus architecture of mature organoids develops. This is due to the production of WNT from Paneth cells that reside at the base of the crypt domain (figure 1.13). R-spondin-1 acts as a growth factor for intestinal epithelial cells. It is a canonical WNT agonist which acts in the intestinal tract on LGR5 positive stem cells by stabilising β-catenin, increasing the effect of WNT signalling and allowing them to maintain their stemness. R-spondin-1 has been shown to be essential to maintain the LGR5 positive and actively cycling stem cells in 3D cultures (Kim *et al.*, 2005; de Lau, Snel and Clevers, 2012).

1.6.3 Physiology of intestinal organoids

Organoids which are developed from stem cells of the intestine are known as colonoids if they are cultured from colonic stem cells, or enteroids if they are cultured from small intestinal stem cells (Zachos *et al.*, 2016). The stem cells from the different regions of the small intestine show physiological differences, due to the morphological

differences in these regions. As the stem cells are located in the intestinal crypts, it is the crypts which are isolated in order to culture intestinal organoids through mechanical means.

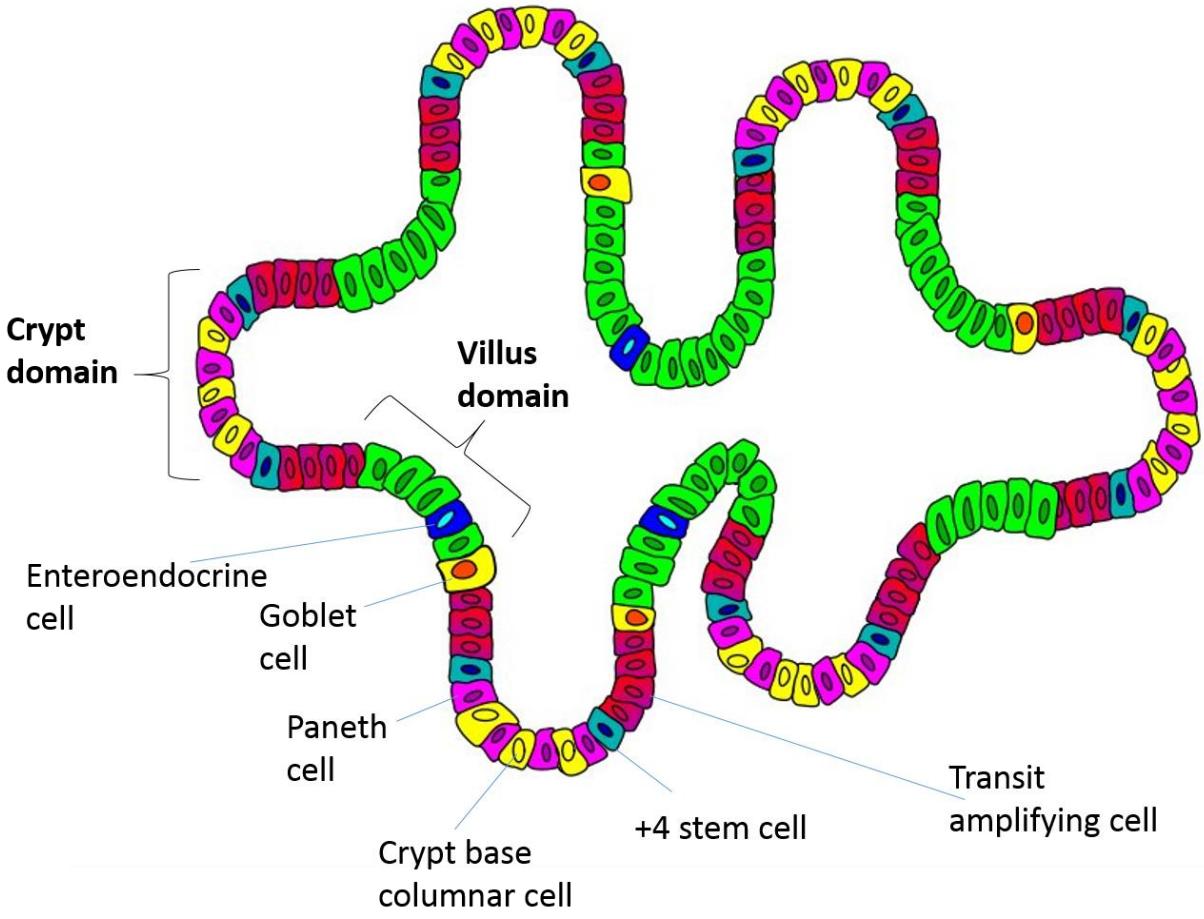

Figure 1.13 Small intestinal organoids are similarly composed to the small intestinal crypts and villi. Indicated on the diagram is the crypt domain, which contains the stem cells and protrudes from the organoid in a bud like form. The villus domain is also indicated, and is found orientated toward the lumen of the organoid, it is therefore into the lumen of the organoid that shed cells will accumulate. This means that the cell shedding process causes a darkening of the centre of the organoid. Cells which are lost basolaterally from the crypt domain are known as blebbing cells, and are often an indication of an increase in cell death in the organoid in response to apoptosis inducing stimuli. The cell types found in the organoid are the same as the cell types found in the small intestinal epithelium, the main cell types are indicated. The absorptive enterocytes are shown in green.

1.6.4 Advantages of 3D organoid studies

Multiple different cell types are found in 3D organoid cultures. The cells in an epithelial cell line monolayer are by definition homogenous and there is no way to use a monolayer to model the complex interactions between cells. Therefore, intercellular signalling is far more relevant to the real life system in a model which has different cell types alongside one another. For example, the intermittent WNT signalling in the intestinal epithelial cells is strong around Paneth cells, which are the origin of the signal, but WNT signalling is absent in other areas. This allows the crypt villus structure to form (Hynds and Giangreco, 2013).

Cells communicate by the exertion of physical force on one another as well as through biochemical and protein signalling pathways, forces which are generated using the focal adhesions between cells as well as the contraction of the cytoskeleton and interactions with the extracellular matrix proteins. This reorganisation allows the cells to effectively push and pull one another. This has shown to be important in the development of 3D structures within the organism, in particular branching morphogenesis (Gjorevski and Nelson, 2010). In addition, it has been shown that mammary cells take cues for their differentiation from mechanical forces. For example, mammary cells which are grown in a more elastic extracellular matrix are more likely to differentiate normally than cells which are grown in a 'stiffer' extracellular environment. This indicates that the extracellular forces which are exerted on breast cells may be linked to the development of breast cancer (Alcaraz *et al.*, 2008). This concept clearly applies to the 3D culture of organoids. When compared to 2D monolayer cultures, the forces these cells undergo share much more similarity with the real life system that they originate from than a homogenous population of cells. The interactions between the cells in 3D are much more realistic compared to a 2D monolayer, and therefore any similar mechanism involving the

exertion of force leading to a change in cell behaviour would be observed in the organoids.

1.6.5 Organoid applications

Organoids have the potential to be used in personalised medicine. This is because they can be grown from a patient's own cells. Not only this, but a very limited amount of tissue is required, meaning that organoids can be grown from patient biopsies and cultured to expand the stocks. Human organoids could therefore be used to test the effects of drugs, examine the effects of genetic editing and the effects of pathogens. Having human tissue available in this way could therefore potentially be very valuable for research into disease (Fatehullah, Tan and Barker, 2016). For example, successful microinjection of organoids was carried out with *S. Typhimurium* in order to investigate how these bacteria invade intestinal cells, how intestinal cells defend against the bacteria and how the different cell types in the intestinal epithelium contribute to the spread of infection (Forbester *et al.*, 2015). Modelling of the process of carcinogenesis has also already been undertaken. Using the incorporation of k-ras mutations, pancreatic and gastric organoids were transformed to a cancerous phenotype (Li *et al.*, 2014). Additionally, Dow and colleagues have used shRNA silencing and restoration of Apc in mice and organoids. Their study used both mice and intestinal organoids to show that Wnt signalling is involved in Apc mutant carcinogenesis, and that Apc is required for continued neoplastic growth, even when p53 and K-ras have been mutated (Dow *et al.*, 2015).

The fundamental morphological changes which occur in response to DNA damaging agents currently need to be studied in animal models before they can be studied in organoids. However, when research reaches the point where organoids are a suitable and validated model for the modelling of the effects of IBD, chemotherapy or TKIs,

intestinal organoids could be used to more efficiently target a wider array of genes which may contribute to disease or interact with the NFκB pathways.

1.7 Aims

1. To investigate the contribution of NFκB signalling pathways during the development of DSS colitis, and the contribution of NFκB signalling in immune and epithelial compartments to the development of this disease.

2. To study the impact that the deletion of individual NFκB subunits has on enteroids treated with chemotherapeutic drugs.

3. To investigate the role that NFκB signalling pathways play in intestinal epithelial cell damage caused by 5-FU and etoposide *in vivo*, and to assess whether these results are comparable with *in vitro* organoid data.

4. To decipher the contribution of individual NFκB subunits in an enteroid model of tyrosine kinase inhibitor related intestinal damage.

2 Materials and methods

2.1 Mice

Male wild-type C57BL/6J mice (Charles River, Margate, Kent) aged 8-24 weeks were acclimatised for at least one week prior to the beginning of experimentation. Transgenic mice were all bred at the University of Liverpool on a C57BL/6J genetic background, including homozygous NFκB1 null (Sha *et al.*, 1995), NFκB2 null (Caamaño *et al.*, 1998) and c-Rel null animals (Köntgen *et al.*, 1995). RelB null mice were bred from heterozygotes on a mixed genetic background mainly comprised of C57BL/6J by Caamaño et al. (1999). The mice were fed standard chow and 12:12 hour light cycles were used. Wherever possible mice were housed in groups of 3 or more; exceptions being in the case of in-fighting in the cage where mice were housed individually.

2.1.1 C-Rel null mice

Electroporation was previously used to introduce the targeting construct into embryonic stem cells; this was used to target amino acids 145-588 in c-Rel and replace them with a PGKNeo cassette (Tumang *et al.*, 1998). The protein was truncated and unable to dimerise, bind to DNA, transport to the nucleus or activate transcription. Normal development was seen in these mice, with normal breeding and lifespan, normal lymphocyte development and haematopoiesis. The mice used were bred from a colony already established at the University of Liverpool. This strain of mice was originally provided by Dr Jorge Caamano from the University of Birmingham.

2.1.2 NFκB1 null mice

NFκB1 null mice were previously generated by the insertion of a 3-Phosphoglycerate kinase (PGK) neo cassette into exon 6 of the NFκB1 gene which lies in the rel homology domain of the protein. This led to non-functional P105 and P50 proteins (the precursor and active versions of NFκB1). The P50 null mice were developmentally normal and developed normal lymphocyte populations, but were defective in clearing intracellular bacteria (Sha *et al.*, 1995). The NFκB1 null mice were bred from a colony kept in the University of Liverpool Biomedical Services unit. This strain of mice was also originally provided by Dr Jorge Caamano from the University of Birmingham.

2.1.3 NFκB2 null mice

NFκB2 null mice were previously produced by inserting a PGK neo cassette into the *NFκB2* gene. This led to the loss of P100 and P52 expression (Caamaño *et al.*, 1998). These mice were also originally provided by Dr Jorge Caamano at the University of Birmingham. The mice used in these studies were bred from the colony maintained at the University of Liverpool.

2.1.4 RelB null mice

RelB null mice were generated by the addition of a pPNSrelB targeting vector to disrupt the *RelB* gene in D3 mouse embryonic fibroblasts. These were injected into blastocysts which were then transplanted into female mice. From these litters, mice which were heterozygous for RelB were obtained. These mice were crossed and the resulting litters contained RelB null mice (Weih *et al.*, 1995). Genotyping was performed by Katie Lloyd at the University of Liverpool. These mice were backcrossed onto a C57BL/6J background for 5 generations by Caamaño et al. (1999), who

provided the original breeding pairs to establish the colony in the Biomedical Services Unit at the University of Liverpool.

2.2 Animal treatments

2.2.1 Induction of DSS colitis

Mice were given DSS (2% w/v M.W = 36,000 – 50,000Da; Catalogue number: 160110; Lot number: 6683K; MP Biomedicals, LLC, UK) in their drinking water from days 0-5, then fresh water was administered from days 5-8. Mice were sacrificed at day 8. Mice were monitored daily for changes in weight and condition; weight was recorded each day and any signs of ill health were noted. Signs of ill health include weight loss, loose stools, blood around the anus, pinched facial features, hunched posture, unkempt fur and unsteadiness. Mice were given wet food in order to encourage feeding and decrease the amount of weight loss.

2.2.2 Irradiation and bone marrow reconstitution

Mice were subjected to whole body γ irradiation in two doses separated by 3 hours starting at 10am. The dose administered on each occasion was 5.5Gy from a ^{137}Caesium source in a rotating closed chamber. Bone marrow was collected from donor mice of either the NFκB2 null or C57BL/6J (wild-type) genotypes. The femur and tibia of the donor mouse was collected and sterilised for 2 minutes in 70% ethanol. The ends of the bones were removed and a needle with PBS was used to flush out the bone marrow. Red blood cell lysis was performed, the cells were quantified and re-suspended at a concentration of 5 million cells/ml. 10^6 donor bone marrow cells were injected into each irradiated mouse by tail vein injection 3 hours following irradiation. Mice were then allowed to recover for 12 weeks with daily monitoring of mouse weights and general condition for at least the first two weeks to monitor for any severe radiation sickness or illness due to being

immunocompromised. Ten C57BL/6J irradiated mice were reconstituted with NFκB2 null bone marrow and 10 were reconstituted with C57BL/6J bone marrow. 10 irradiated NFκB2 null mice were reconstituted with C57BL/6J bone marrow and 10 were reconstituted with NFκB2 null bone marrow.

2.2.3 Murine IP injections with chemotherapeutic drugs

C57BL/6J, c-Rel null, NFκB1 null and NFκB2 null mice were administered chemotherapeutic drugs (5-fluorouracil (5-FU); etoposide). Both chemotherapeutics were administered by a single intraperitoneal injection to n=6 mice per group while tilting the mouse at 45^0 in order to avoid administration into the internal organs. 10mg/kg etoposide (Sigma-Aldrich, E1383) was similarly administered to mice. The mice were treated, left for 4.5 hours and were then culled. 5-FU (Sigma-Aldrich, E1383) was given at 40mg/kg via intraperitoneal injection, the mice were then kept under standard conditions for 24 hours before they were culled.

2.3 Histological techniques and scoring

2.3.1 Tissue collection and preparation for staining

The mice were culled by cervical dislocation or a rising concentration of CO_2. The abdominal cavity was opened with scissors and the small and large intestines were removed. Both were flushed with PBS. A knot was tied at the distal end of the small intestine, and the caecum was left on the colon for orientation purposes. The small and large intestine were fixed in 4% formaldehyde for 24 hours before transfer to 70% ethanol.

After fixation, the small intestine was separated into the proximal, middle and distal sections, and the colon was separated into the distal and proximal sections. The sections were then split into 1cm sections and taped together with loops of 3M micropore tape, the loops were then squeezed in order to form a tight bundle. This

was then cut into small cross sections appropriately sized for embedding, which were placed into histology cassettes (figure 2.1). The cassettes were labelled and placed in 70% ethanol for processing.

Tissue was processed to replace all water with paraffin in a Shandon Hypercentre processor using standard reagents and processing times, then embedded in paraffin blocks. Tissues were embedded vertically in paraffin wax, and 3-5µm transverse sections were placed on APES coated slides for immunohistochemistry or uncoated slides for haematoxylin and eosin staining.

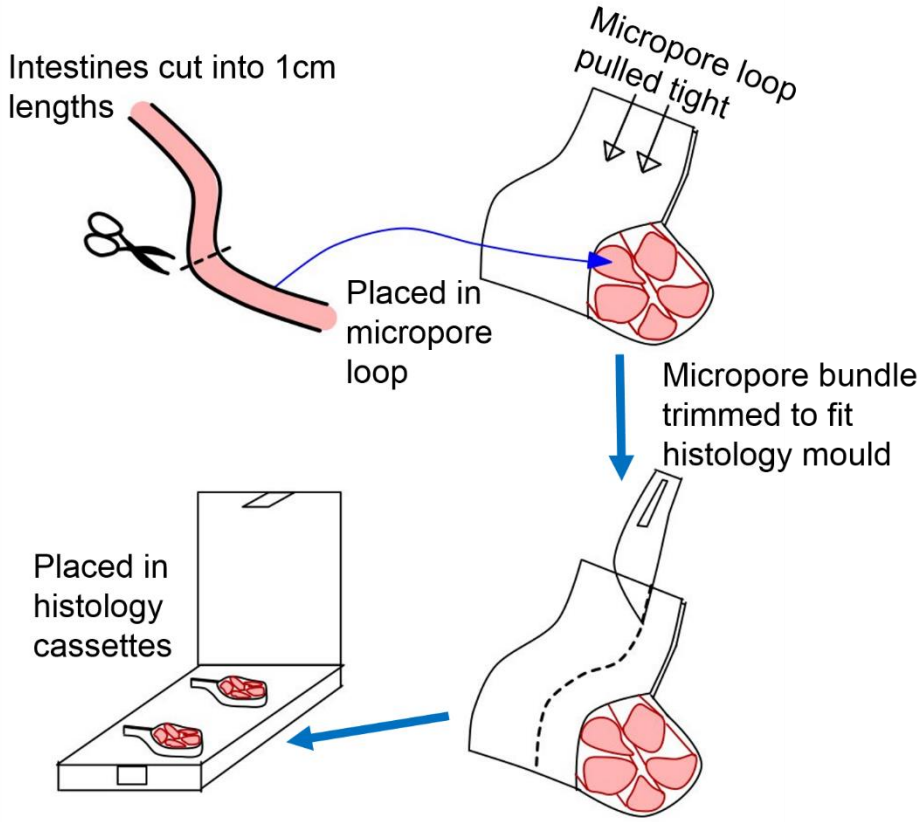

Figure 2.1 Tissue bundling. A loop was made from Micropore tape, the intestines were cut into 1cm lengths and placed into the loop. The Micropore bundle was squeezed tight and 5mm sections were trimmed off. These were placed into the histology cassettes, labelled and placed into 70% ethanol for processing.

2.3.2 Haematoxylin and eosin staining

In order to do standard haematoxylin and eosin (H+E) staining, the tissue was cut into 4µm sections using a microtome, the sections were floated on water and then caught onto glass histology slides. Slides were dried overnight at 37^0C, or for 1 hour at 50^0C. The slides were placed in xylene for 5 minutes, then into a second xylene for 5 minutes. The slides were rehydrated through an increasing concentration of water in ethanol, then placed in haematoxylin for 5 minutes. The slides were placed under running water for 10 minutes to blue the sections, then placed in eosin (Sigma-Aldrich) for 3 minutes. The excess eosin was removed by dipping in 90% ethanol, and the sections were then dehydrated in increasing concentrations of ethanol and placed back in xylene for 5 minutes. The sections were moved to a second xylene for a further 5 minutes, then coverslips were placed on the slides using DPX, a distyrene plasticizer and xylene synthetic resin.

2.3.3 Crypt survival and visual analogue scoring

In order to determine the degree of colitis in mice treated with DSS, 10 circumferences of distal colon were scored per mouse. Using a light microscope to examine haematoxylin and eosin stained sections, the number of healthy crypts in a circumference was counted. A healthy crypt was deemed to have 5 or more cells and mitotic figures; in order to adjust for crypt width, as larger crypts are more likely to appear in a 4µm section than smaller crypts, the diameter of 10 crypts per mouse was measured and the mean diameter value was used to adjust the value according to the size of the crypts. Visual analogue scoring of inflammation from 0 to 4 was also used for each mouse as described by (Cooper *et al.*, 1993).

2.3.4 APES coating slides for immunohistochemistry

In order to produce slides suitable for immunohistochemistry, where a more adhesive and charged slide was required, 3-Aminopropyltriethoxysilane (APES) coatings were applied to the slides. The slide racks were filled with Superfrost glass histology slides (Sigma-Aldrich Z692255-100EA). The slides were placed in four successive glass staining dishes containing 100% acetone, 100% acetone, 2% APES (3-aminopropyltriethoxylsilane) in acetone and distilled water for two minutes each. The slides were then dried at 37^0C overnight before use.

2.3.5 Immunohistochemistry

Slides were placed in xylene for 5 minutes, then into a second xylene for a further 5 minutes to de-wax the sections. The slides were then placed in two changes of 100% ethanol. The slides were then placed into 1% H_2O_2 in methanol to block endogenous peroxidase activity for 12 minutes then through 90% and 70% ethanol baths, and distilled water to rehydrate. Antigen retrieval was carried out by microwaving the sections in 10mM citrate buffer at pH 6 for 20 minutes. The slides were then cooled for 10 minutes and then placed under a dripping tap to cool further for 10 minutes; care was taken to ensure that the sections were not dislodged by the water. Bovine serum albumin (BSA) was used to block non-specific binding, and the primary caspase-3 antibody (R and D systems, AF835 lot CFZ3414111) was applied for 2 hours.

Isotype control rabbit polyclonal IgG (Abcam, ab27472) was used at the same concentration as the primary antibody to detect nonspecific binding. An anti-rabbit HRP labelled polymer from an Envision kit (Abcam, K4002) and a diaminobenzidine (DAB) step was used to visualize the position of the staining. Hematoxylin (Sigma-

Aldrich) staining was then undertaken to counterstain nuclei and then the sections were dehydrated and mounted using DPX mounting media.

2.3.6 Wincrypts scoring

After treatment with etoposide or 5-FU, the distal colons and proximal small intestine of C57BL/6J, c-Rel null, NFκB1 null and NFκB2 null mice were examined after sectioning and H+E staining. Morphological signs of apoptosis and mitosis which can be seen using a light microscope were used to identify cells undergoing each process (figure 2.2). Apoptotic cells were highly eosinophilic and apoptotic bodies were seen as pyknotic nuclei. They also often have a halo effect where the cytoplasm has shrunk leaving an unstained ring around the cell. Mitotic cells had visibly dividing nuclei and separating or visibly condensed chromosomes. 50 hemicrypts were scored per mouse using a code of 1 for a normal cell, 2 for an apoptotic cell and 3 for a mitotic cell. The scoring began at the bottom of the crypt and continued up to either the crypt table or the crypt shoulder in the case of the small intestine. In order to verify that scoring was accurate, intra-scorer verification was used, with the same sections being scored on two separate days by the author and the mitotic and apoptotic index compared (figure 2.3). Inter-scorer verification was also used and another researcher trained in the technique scored several of the same slides for mitotic and apoptotic index comparison (figure 2.4). Using the modified median test no significant differences were found when the distributions were compared.

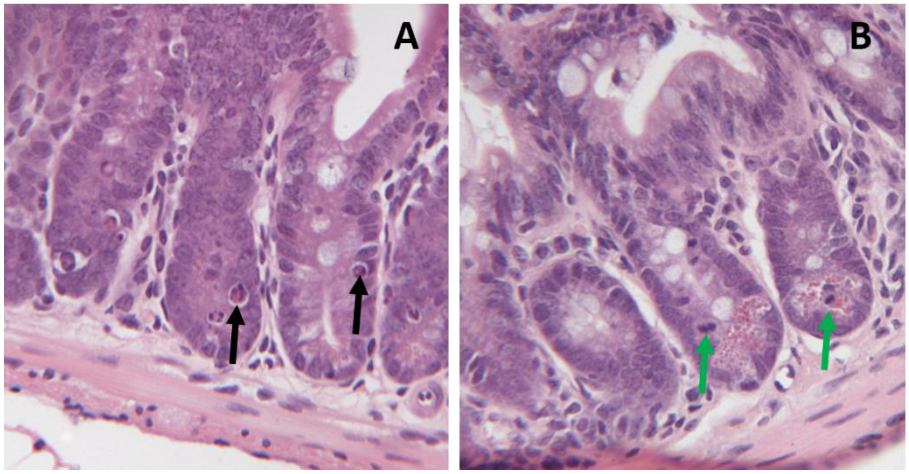

Figure 2.2 Apoptotic and mitotic cells in an H+E stained section. Apoptotic cells and apoptotic bodies are indicated by black arrows (A). Mitotic cells are indicated by green arrows (B).

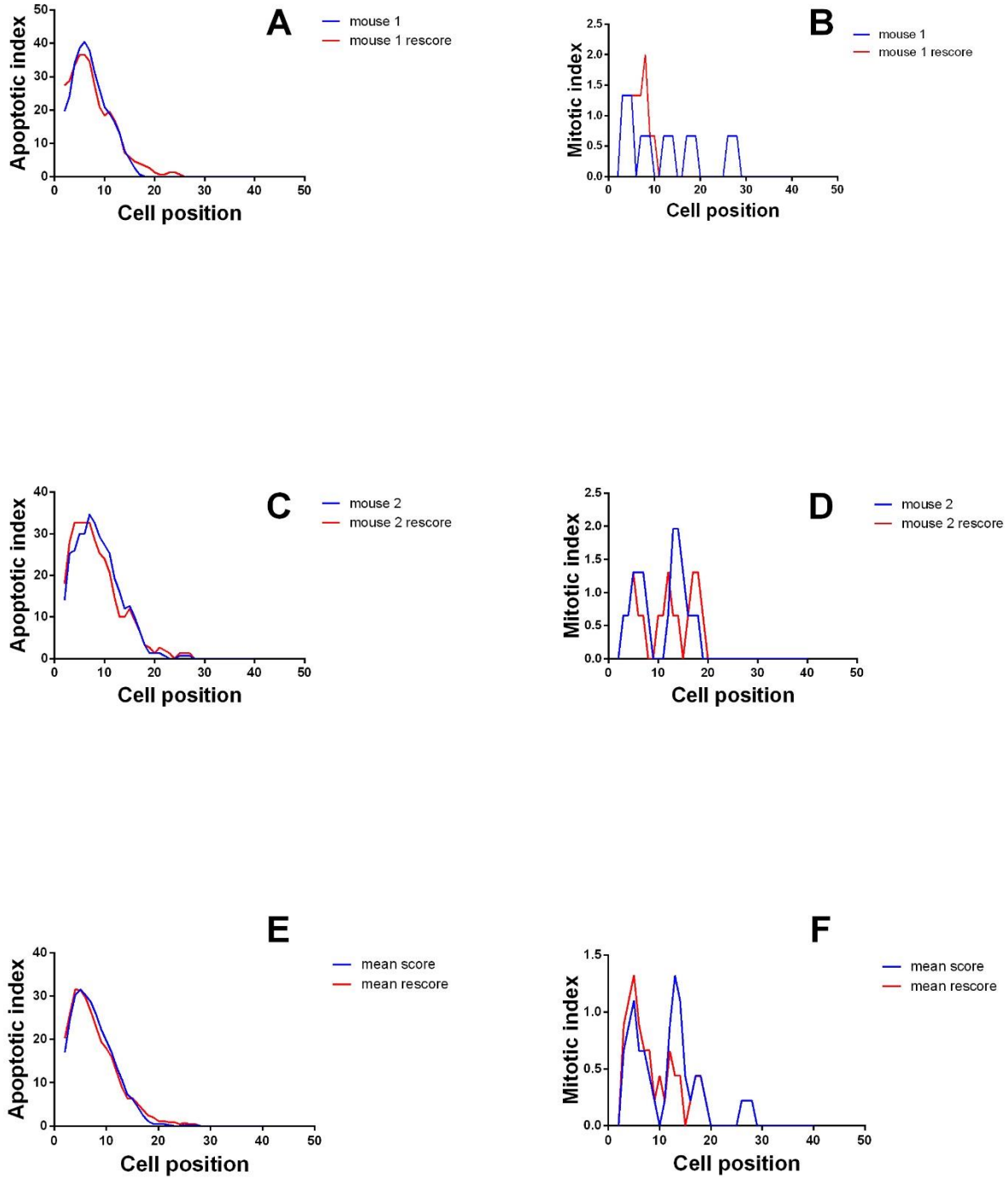

Figure 2.3 Intrascorer variability of apoptosis and mitosis in the small intestine of C57BL/6J male mice 4.5 hours after IP injection of etoposide. Two example mice are shown, the apoptotic index for mouse 1 (A) and the mitotic index for mouse 1 (B) and the apoptotic index for mouse 2 (C) and the mitotic index for mouse 2 (D) are shown. The mean from three mice is also shown for apoptotic index (E) and mitotic index (F). The initial result is shown in blue, and the result of the second score, which was done on a different day is shown in red. No statistically significant differences were reported when the mean score and rescore data were compared (E and F).

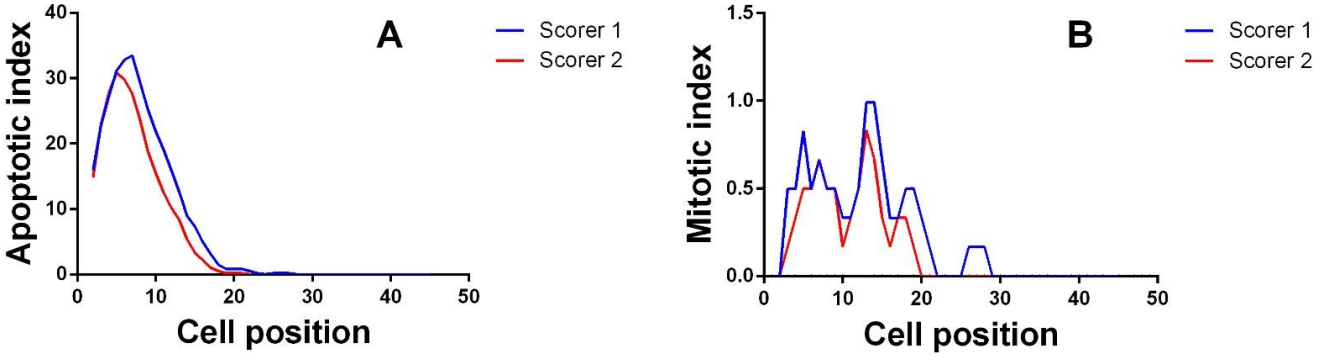

Figure 2.4 Inter-scorer variability of C57BL/6J mice following IP injection of etoposide. Six mice per group. Scorer 1 is the author and in red scorer 2 is another researcher proven to be competent in this technique. The mean apoptotic index (A) and mitotic index (B) from four mice is shown; no statistically significant differences were found using the modified median test.

2.4 RNA extraction and PCR

2.4.1 Mucosal scrapes

To collect the mucosal cells for gene analysis the mouse colon was dissected, flushed with PBS and opened lengthways. It was spread onto a glass microscope slide with the mucosa facing upwards. Another glass slide was used to scrape the mucosa off the muscle layer below leaving only the muscle layer. The mucosa was then placed into an Eppendorf tube, the tube was labelled and placed onto dry ice. In order to investigate the expression of genes in the mucosa during DSS colitis the mucosa was collected from C57BL/6J mice that had been treated with DSS. In order to conduct an NFκB signalling PCR array, 3 mice were culled and the mucosa was collected at day 0, day 5, day 8 and day 11.

2.4.2 RNA extraction

A TissueLyserII instrument (Qiagen) was used with stainless steel balls at a speed of 20Hz to break up the tissue. The mucosa was homogenised for 60 seconds in total, changing the arrangement of the tubes half way through to ensure even homogenisation. RNA was extracted using a Qiagen DNeasy mini kit (Qiagen, cat 74104) according to the manufacturer's guidelines.

2.4.3 Reverse transcription

The quality and quantity of the RNA was assessed using a Nano Drop (Thermo-Scientific Nanodrop 2000c). If the A260/A280 ratios were all greater than 2, this indicated optimal RNA purity. 0.5µg of RNA was reverse transcribed using a RT^2 first strand kit (C-03-superarray, Qiagen, cat no. 330401). 1µl of resulting cDNA was transferred into each 20µl qPCR reaction using RT^2 SYBR green mastermix (Qiagen, cat no.HD08-3) as per the manufacturer's instructions.

2.4.4 Real-time polymerase chain reaction (qPCR)

In order to investigate gene expression a mouse NFκB pathway focused array plate (Qiagen, cat no. PAMM-025Z) was used. The cDNA from each of the three mice was pooled at each time point. 1µl of pooled cDNA was used per reaction on each well of the array plate which contained 84 NFκB target genes and 6 housekeeping genes and analysis was conducted using the comparative delta CT method.

In order to undertake further investigation using RT^2 primer assays, 6 mice per group were culled on day 0 and day 8 of the DSS protocol. A primer set with a validated efficiency of 2 (as long as PCR setup was as per manufacturer's instructions) was used. The gene expression of each of the 6 mice was investigated separately. Genes were investigated using the following primers: *Cox-2* (Qiagen cat no. PPM03647E-200)*, Tnf* (Qiagen cat no. PPMO3113G-200)*, Csf1* (Qiagen, cat no. PPM03116C)*, Ccnd1* (Qiagen cat no. PPM02903F), *Cxcl10* (Qiagen, cat no. PPMO2978E-200), *Bcl2a1a* (Qiagen cat no. PPM03432B-200) and *RelB* (Qiagen cat no. PPM03202D-200). *Gapdh* (Qiagen cat no. PPM02946E-200) was the housekeeping gene used to normalise the data. A Roche LightCycler 480 real time PCR instrument was used to analyse the gene expression in the mucosal scrapes.

Melt curve analysis was used to determine whether only one product was identified in each reaction. A reliable melt curve had a single peak indicating the likelihood of one PCR product. However it must be kept in mind that melt curves with one peak may actually be two peaks which are unresolved and so this is not a fool proof method. Melt curves containing more than one peak were excluded from analysis. Examples are shown in figure 2.5.

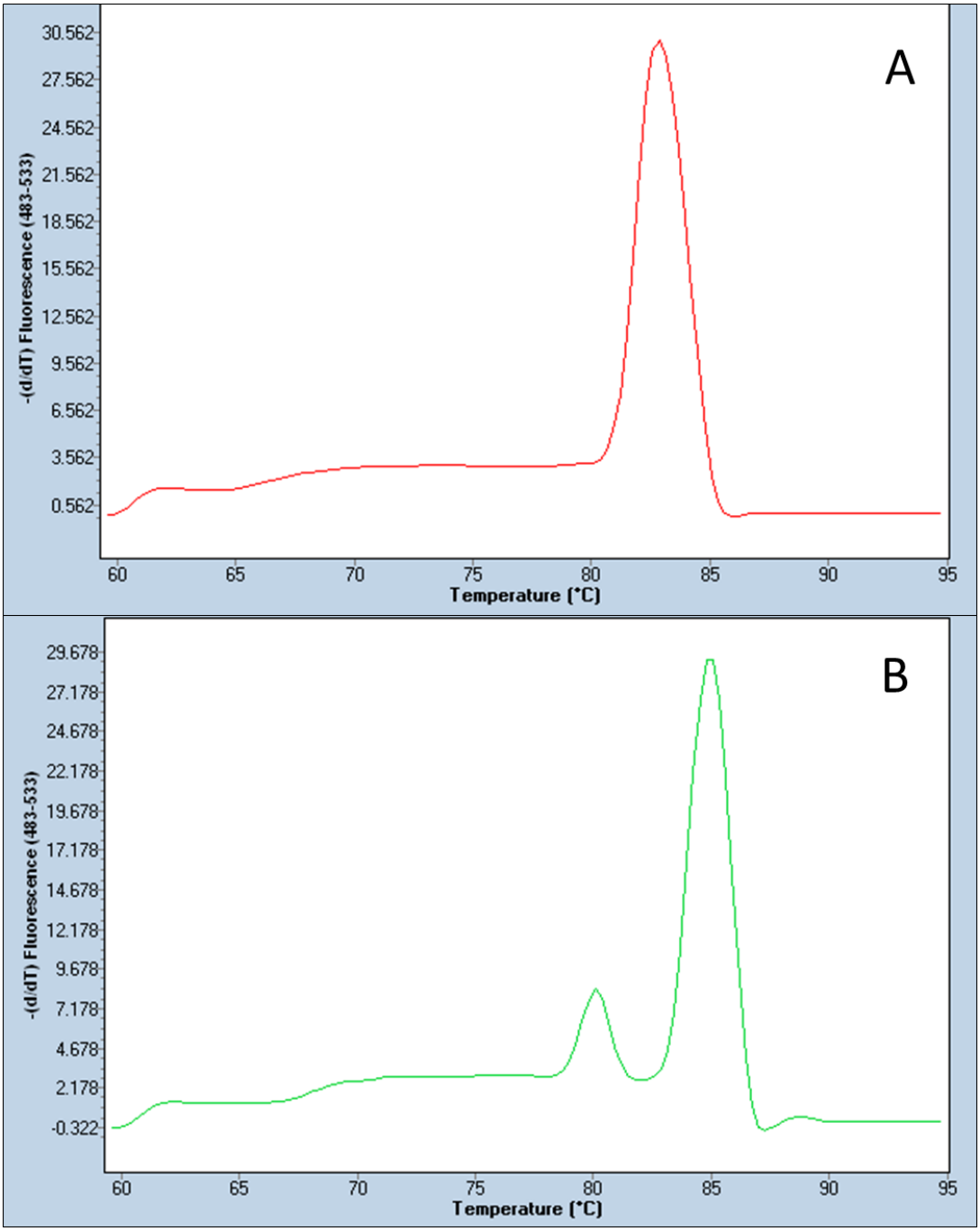

Figure 2.5 An example of a reliable melt curve (A) and an unreliable melt curve (B). The unreliable melt curve has two peaks which indicates that there were two products amplified in the sample. However the reliable melt curve only has one peak which indicates that there was one product formed in the assay. This helps to identify wells for exclusion, it must be noted that what appears to be a single peak may consist of two peaks which are indistinguishable in some cases.

2.5 3D small intestinal organoids

In our lab the small intestinal organoids were grown from the crypts of the proximal small intestine using the method established in the Clevers laboratory. These organoids develop a microvilli brush border on the inward facing cell membranes (Sato *et al.*, 2009), and the supplemental EGF functions to increase the differentiation and proliferation of cells, R-Spondin-1 increases Wnt signalling in the stem cells, maintaining them as stem cells, and Noggin keeps the proliferation of the stem cells to the desired level for culture. Although enteroids are composed of the same cell types as the small intestinal epithelia, the finger like projections of villi do not form although villus domains do. It is thought that in order for villi to form the mesenchymal cells and vasculature must be present (Watson *et al.*, 2014; Zachos *et al.*, 2016). As organoids grow they develop more crypt domains, and the cells which are shed from the villus domains begin to accumulate in the lumen (figure 2.6).

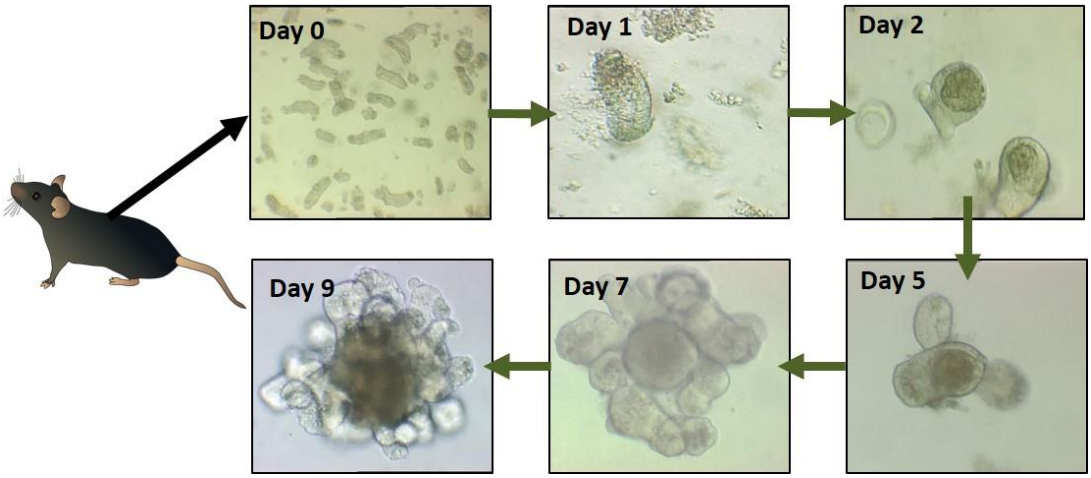

Figure 2.6 In order to establish a small intestinal organoid culture, crypts are isolated from a mouse and embedded in Matrigel with EGF, R-Spondin-1 and Noggin growth factors. The organoids begin to develop bud like crypt domains which protrude outward and cells are shed into the middle of the organoids, indicated by the dark centre of the organoid. Usually the organoids are split every week.

2.5.1 Crypt isolation

Matrigel ® Matrix basement membrane (cat no. 256237) was defrosted on ice before use, and growth factors were added. For proximal small intestinal organoids the growth factors added were recombinant mouse R-spondin-1 (500ng/ml, R+D systems, cat no. 3474-RS), recombinant mouse EGF (50ng/ml, R+D systems, cat no. 2028-EG), and Noggin (100ng/ml, R+D systems cat no. 6997-NG). Frozen pipette tips and ice were used to ensure that Matrigel did not solidify. The proximal 4cm of the small intestine was dissected and flushed with PBS (Sigma-Aldrich), in order to remove its contents. The small intestine was then sliced lengthways in order to expose the mucosa. It was then cut into 1cm sections and washed in ice cold PBS by pipetting up and down in a 30ml universal tube. This was repeated at least 10 times with fresh PBS until the supernatant was clear. 20ml ice-cold chelation buffer (2mM EDTA in PBS) was then added and put on a tube roller mixer at 4^0C for 30 minutes. This was then shaken in the universal tube in order to release the villi into the solution. The chelation buffer was then discarded and 20mls of shaking buffer (43.3mM sucrose and 59.4mM sorbitol in PBS) was then added and shaken by hand for 2 minutes or until the crypts were released into the solution. To confirm that the crypts had been released, the tube was viewed under a microscope. The crypt containing solution was then filtered through a 70µl cell strainer into a 50µl falcon tube kept on ice, washing the filter with approximately 5ml of ice cold shaking buffer. The crypts were then quantified using a 384 well plate to ensure around 500 crypts per well of a 24 well plate were obtained. Sufficient amounts of crypts were then transferred into a 15ml falcon tube, which was placed in a centrifuge. This was then spun down at 200g for 10 minutes, keeping the temperature at 4^0C. The supernatant was then discarded leaving a pellet at the bottom of the falcon tube which consisted of crypts. The pellet was then carefully re-suspended in Matrigel, with 500 crypts per 50µl Matrigel being required. 50µl of the Matrigel was then added to each well of a 24 well plate using a

pipette and frozen pipette tip, and placed in an incubator in order to polymerise the Matrigel for 30-60 minutes. Once the Matrigel was set, 0.5ml minigut culture media was added per well. The minigut culture media was produced by adding 1% L-glutamine, 1ml aliquot of Primocin™ (Invivogen), 10mM HEPES buffer, N2 supplement and a B27 supplement to one bottle of Dulbecco's modified eagles medium nutrient mixture F12 HAM (Sigma D8437). Minigut media was replaced every 4 days.

2.5.2 Splitting organoids

Matrigel was defrosted on ice or on ice overnight in the fridge and growth factors were added (section 1.6.1). A 24 well plate was warmed in an incubator while organoids were prepared for splitting. Organoid media was removed carefully with a pipette in order for the Matrigel to remain undisturbed. 50µl of PBS was pipetted into each Matrigel containing well. Using the pipette tip, the organoids were dislodged and re-suspended by breaking up the Matrigel. The organoids were passed once through an insulin syringe with a 27G needle and into a 15ml falcon tube which was then topped up to 14ml. This was then spun down at 200g for 10 minutes. Taking care not to disturb the pellet, the supernatant was removed along with as much of the residual Matrigel as possible. Using frozen pipette tips, Matrigel with growth factors was added to the pellet and this was re-suspended while gently pipetting up and down. Care was taken not to create air bubbles. 50µl of Matrigel was placed onto each well of the warmed 24 well plate. This was left to polymerase in the incubator for 30 minutes and then 50µl minigut media was added onto each Matrigel containing well of the plate.

2.5.3 Chemotherapeutic drug treatment of organoids

Organoids were treated with etoposide (Sigma-Aldrich, Gillingham, Dorset, UK), irinotecan (Irinotecan solution 20mg/ml, RLBUH NHS trust, Pharmacy department, Liverpool, UK) or 5-Fluorouracil (5-FU; Sigma-Aldrich) at concentrations of 50µM 10µM 5µM and 1µM. All three chemotherapeutic drugs were dissolved in dimethyl sulphoxide (DMSO). The control well contained DMSO of an equivalent concentration to the treatment containing the highest amount of DMSO. Solutions for treatment were made in complete minigut media (media with growth factors added). Two wells per treatment were used, and each well was treated with 500µl of solution. Organoid circularities were measured at day 1 (24 hours) and day 2 (48 hours). The experiments were conducted in duplicate on at least two separate occasions.

2.5.4 Validation of circularity analysis

Circularity is new scoring method which will be discussed further in section 4.2.1. The aim of the technique is to quantify the amount of cell death in an organoid using the link between cell death and increased circularity of organoids. The accuracy of circularity scoring was tested by the author, scoring 10 randomly selected organoids on two separate days in order to check consistency during training in the method (figure 2.7). Inter-scorer variability was also tested with a researcher previously trained in this technique scoring 10 randomly selected organoids which the author also scored in order to check the accuracy of the method (figure 2.8). The organoid circularities were measured before treatment began, for the day 0 time point. 6 organoids per well were photographed and then the circularity was measured by drawing round the organoid using the freehand selection tool in imageJ, using the shape parameters function to measure the circularity and the area. The following formula is used to calculate the circularity, $4\pi(\text{area}) \Big/ \text{perimeter}^2$.

2.5.5 Organoid treatment with tyrosine kinase inhibitors (TKIs)

The TKIs, Erlotinib, Gefitinib, Imatinib, Dasatinib, Bosutinib and Nilotinib were administered to the organoids. Organoids were treated with TKIs at concentrations of 0.01µM, 0.1µM, 1µM and 10µM with a DMSO control. The TKIs were dissolved in DMSO and the concentrations were made fresh in minigut media with growth factors, using a dilution series. Two wells of organoids per treatment were included in each experiment, and the repeat experiments were conducted on 3 separate occasions. Organoid circularities were measured on day 0, day 1 and day 2.

2.5.6 Organoid embedding for histology

The organoids were significantly smaller than the previous intestines that were processed for histology. Therefore, in order to prepare the organoids for histology a different protocol was needed to ensure that the organoids were not lost in the processor during processing. The media was removed from the wells and the Matrigel exposed. The wells were then washed with PBS. 400µl of cell recovery solution (Corning, cat no. 354253) was added to the wells and the 24 well plate was placed onto a shaker to gently mix for 30-45 minutes. 4% paraformaldehyde (Sigma-Aldrich, P6148) was made by diluting the stock 40% solution 1/10 with PBS. The organoids were fixed by gently pipetting them in paraformaldehyde and incubating them at room temperature for 30 minutes. They were then transferred to a 15ml falcon tube and allowed to settle by gravity into an organoid pellet or alternatively they were spun down for 30 seconds at 100g. The supernatant was removed as much as possible without disturbing the organoid pellet. HistoGel (Thermo-Fisher, HG-4000-012) was used to suspend the organoid pellet. The histogel was heated in the microwave at full power for 15 seconds until it became liquid, a sawn off p1000 pipette tip was used to add the Histogel to the organoid pellet, without causing any bubbles to form. The Histogel was then transferred onto a piece of micropore tape and allowed to set. This

was stored in a histology cassette in 70% ethanol until further processing. A Shandon processor was used to replace the water in the organoids with wax overnight using a standard histological protocol containing ethanol and xylene. The organoids were then embedded in paraffin wax blocks for sectioning. For each treatment, before the organoids were fixed, the organoid circularity was measured. Organoid sections were used for caspase-3 staining (section 2.3.5) and H+E staining in order to determine the link between the amount of apoptosis and the circularity of the organoids.

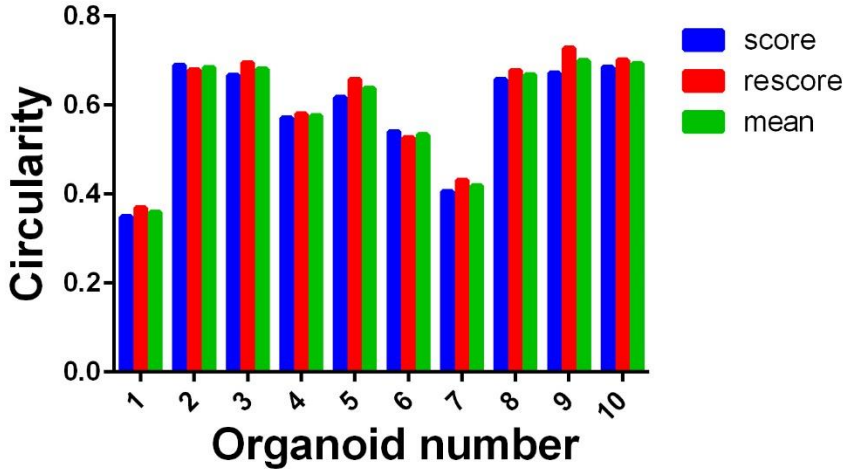

Figure 2.7 Intra-scorer variability when organoids were scored and then rescored on a different day. 10 C57BL/6J organoids were chosen at random. The initial score is shown in blue, the rescore is shown in red and the mean score is shown in green.

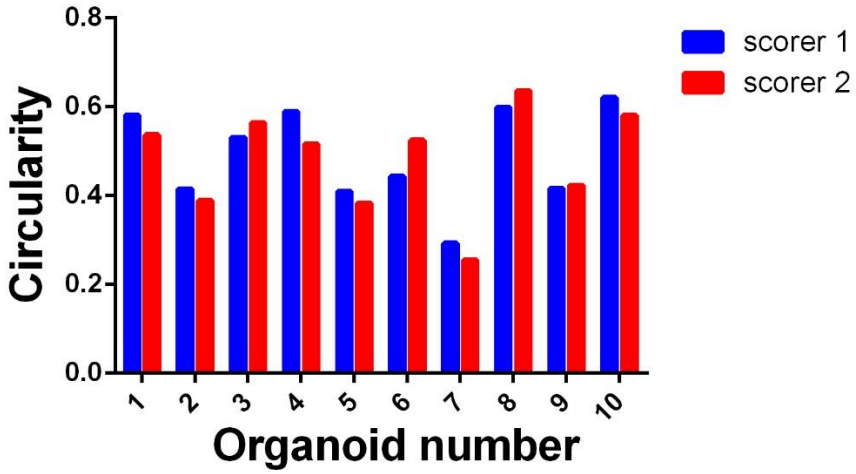

Figure 2.8 Inter-scorer variability when organoids were scored and then rescored by another individual trained in the scoring technique. Scorer 1 is the researcher and scorer 2 is the researched previously proven to be competent in the technique. 10 organoids were randomly chosen.

2.6 Statistics

Statistics were performed using windows GraphPad Prism version 6 software. In order to find differences between datasets, the data were first tested for normality. If data were found to be normally distributed one way analysis of variance (ANOVA) was used when one variable was tested and two way ANOVA was used when there were two variables present. If data were not normally distributed then Kruskal Wallis ANOVA with multiple comparisons was used. Post-hoc tests were selected using GraphPad Prism guidelines based on suitability and depending upon whether the data were compared to a control or all means were compared to each other (http://www.graphpad.com/guides/prism/6/user-guide). The modified median test (Potten, Owen and Roberts, 1990) was used to test for significant differences between the cell positions when the apoptotic and mitotic index were scored on histological sections of small intestinal and colonic tissue. Statistically significant differences between datasets were considered to be present when a P value of less than 0.05 was found. Data are described in the format mean ± standard deviation in all cases.

3 Mechanisms by which NFκB2 signalling may modulate colitis susceptibility

3.1 Introduction

NFκB signalling pathways have a well-established role in regulating inflammation in the colon (Lawrence, 2009). In particular the classical NFκB activation pathway is a key up-regulator of pro-inflammatory cytokines (TNF-α, IFN-γ, IL-6, IL-1 etc.) which are excessively expressed in the intestinal mucosa of patients with IBD (Atreya *et al*., 2008). However the classical NFκB activation pathway has been shown to have both pro and anti-inflammatory functions (Lawrence, 2009). Pro-inflammatory functions of the classical NFκB activation pathway occur in epithelial cells of the intestinal mucosa. In particular the RelA subunit has been shown to be upregulated in the inflamed gut of inflammatory bowel disease (IBD) patients (Neurath *et al.*, 1996) and is directly involved in the disruption of the epithelial barrier of the intestine by TNF-induced injury (Al-Sadi *et al.*, 2016; Ye and Sun, 2017). The anti-inflammatory effect of the classical NFκB activation pathway has also been well documented. In one study in which the transactivation domain of the NFκB1 subunit was deleted from the genome, it was found that the constantly active NFκB1 dimers functioned to inhibit inflammation by repressing NFκB target genes (Kang *et al.*, 1992; Bohuslav *et al.*, 1998). Additionally NFκB1 knockout mice which were also heterozygous for *RelA* have also been found to be more susceptible to *Helicobacter hepaticus* induced colitis (Erdman *et al.*, 2001). The classical NFκB activation pathway can also have an anti-inflammatory effect through the immune compartment. Apoptosis is involved in the resolution of inflammation as it is the method of elimination of immune cells. Classical NFκB signalling activates apoptotic pathways in neutrophils and without classical NFκB signalling the resolution of the inflammatory response has been shown to be delayed (Lawrence *et al.*, 2001; Greten *et al.*, 2007).

Like classical NFκB activation pathway signalling, alternative NFκB signalling has also been shown to be involved in the pathogenesis of inflammatory bowel disease. The alternative NFκB activation pathway is subject to much tighter control than the classical pathway and is activated by different kinases (chapter 1.3.3). Signalling can be activated by factors such as TNF family cytokines, receptor activator of kappa B ligand (RANKL and TNFSF11), B cell activation factors and CD40 ligands (Senftleben *et al.*, 2001; Dejardin *et al.*, 2002; Novack *et al.*, 2003; Bonizzi *et al.*, 2004). In the healthy gut the alternative NFκB activation pathway is involved in normal lymphoid function. The loss of either RelB or NFκB2, transcription factors which function in the alternative NFκB activation pathway, leads to the loss of germinal centre B cells and plasma cells (De Silva *et al.*, 2016). Tertiary lymphoid structures (TLS) are an interesting inflammatory phenomenon seen in IBD and other autoimmune diseases (AIDs) such as rheumatoid arthritis (McNamee and Rivera-Nieves, 2016). They appear as organised structures which form in areas of inflammation from clusters of immune cells. Although they are not organs, and are not encapsulated like other lymphoid structures, they do contain active germinal centres (McNamee *et al.*, 2013). TLSs have been observed in IBD in humans, in mouse models of IBD and specifically in DSS induced colitis (Buettner and Lochner, 2016; Olivier *et al.*, 2016).

DSS induced colitis is a well-established murine model of IBD. DSS addition to the drinking water results in a chemically induced form of colitis which causes disruption of the epithelium and an increased inflammatory infiltrate in the murine mucosa. DSS treated mice lose weight and often suffer from diarrhoea and haematochezia (Melgar, Karlsson and Michaëlsson, 2005). The DSS model of colitis most closely resembles ulcerative colitis as it only affects the distal colon and generates a Th2 inflammatory response in C57BL/6J wild-type mice. It has been suggested that the DSS molecule disrupts the epithelial monolayer and causes the luminal contents of the colon to come into contact with the underlying tissue (Chassaing *et al.*, 2014).

Autoimmune diseases (AIDs) are known to share characteristics and susceptibility loci with one another. IBD and rheumatoid arthritis are two such diseases, and interestingly one of the extra-intestinal effects of IBD is an inflammatory arthritis (Arvikar and Fisher, 2011; Richard-Miceli and Criswell, 2012). The alternative NFκB activation pathway has also been shown to be involved in murine models of rheumatoid arthritis. Mice which lack NIK, a key alternative pathway activating kinase, were resistant to experimental inflammatory arthritis. The mice were resistant to both a lymphocyte mediated model of arthritis, and a spontaneous genetic form of arthritis (Aya *et al.*, 2005). In human disease the alternative NFκB activation pathway has been shown to be involved in the formation of TLSs (Noort *et al.*, 2015). Of particular interest it was found that NIK, NFκB2 and RelB were significantly upregulated in tissues containing TLSs.

NFκB2 has also been shown to be present in the colonic mucosa of ulcerative colitis patients (Andresen *et al.*, 2005) and previously published data from our lab has shown that NFκB2 null mice were less susceptible to DSS colitis than C57BL/6J wild-type mice. They were shown to have significantly less body weight loss at day 6 following DSS treatment, retained a largely normal colonic epithelial appearance and only showed a slight inflammatory infiltrate with no oedema. C-Rel null and NFκB1 null mice were also shown to have a non-significant increase in disease severity relative to C57BL/6J when administered 2% DSS. The colon was shortened with a completely disrupted epithelial cell layer and submucosal oedema was observed in the distal region of the colon (Burkitt *et al.*, 2015)

Therefore in the following studies our focus has been on the alternative NFκB activation pathway. RelB null mice were found to be unsuitable for the experiment due to their stunted growth and low survival rates which would potentially result in an altered DSS load (Weih *et al.*, 1995). RelA null mice have an embryonic lethal phenotype at day 15/16 of gestation (Beg *et al.*, 1995) and therefore were also

unavailable for use in this study. The previous DSS study in our lab using NFκB knockout mice was terminated at day 6 due to a higher than expected level of disease in some genotypes. As the peak weight loss following DSS occurs on day 8, which correlates to the most severe level of disease it was decided to end our study on day 8, or day 11 in order to collect data from the time of most severe disease. The following studies aim to build upon the previous work in our lab in order to unravel the mechanism by which NFκB2 null mice are protected from developing DSS induced colitis.

3.2 Results

3.2.1 Dextran sulphate sodium (DSS) induced colitis in wild-type C57BL/6J mice

Colitis was induced by the administration of DSS in the drinking water to 12 C57BL/6J male mice. In our specific pathogen free (SPF) animal facility 2% DSS has previously been found to be the most appropriate dose in wild-type mice, resulting in mice losing ~10% of their initial body weight. Mice were therefore given DSS at 2% w/v in their drinking water for 5 days, they were then administered water until they were culled. The mice were weighed daily and monitored throughout the experiment for changes in their stool consistency. Three mice were culled at each time point (day 0, 5, 8 and 11 from the start of DSS administration) and histological sections were examined from the distal colon (figure 3.1).

The 12 mice in total in the control group which were given water, showed a small increase in body weight from the beginning to the end of the experiment. At day 5 they had gained 0.6±1% of their starting body weight, at day 8 they had gained 2.2±1.8% and at day 11 they had gained 4.1±3.3% (figure 3.2). When DSS colitis was induced in C57BL/6J mice, weight loss and inflammation began around day 5. Histology of the distal colon demonstrated that the most severe inflammation occurred

at day 8, and that there was a significant disruption of the epithelium and a large amount of inflammatory infiltrate; histology of the time course is shown in figure 3.1. At day 11 the colon appeared to recover following epithelial cell regeneration, with evidence of several mitotic figures and a reduced inflammatory infiltrate. Mice also regained some of the weight they had lost at this time point. The mean weight loss observed when mice were given 2% DSS was 1.3±2.4% at day 5, 13.4±6% at day 8 and 7.7±6.4% at day 11 (figure 3.2). When area under the curve and statistical analysis were conducted, the DSS treated mouse weight profile was found to be significantly reduced when compared to the untreated control group ($P<0.0001$; figure 3.3). Additionally when the datasets were compared using a suitable statistical test at individual time points the mice given DSS were found to have lost significantly more weight than the controls at day 6 ($P=0.0004$), day 7 ($P<0.0001$), day 8 ($P<0.0001$), day 9 ($P<0.0001$), day 10 ($P<0.0001$) and day 11 ($P<0.0001$).

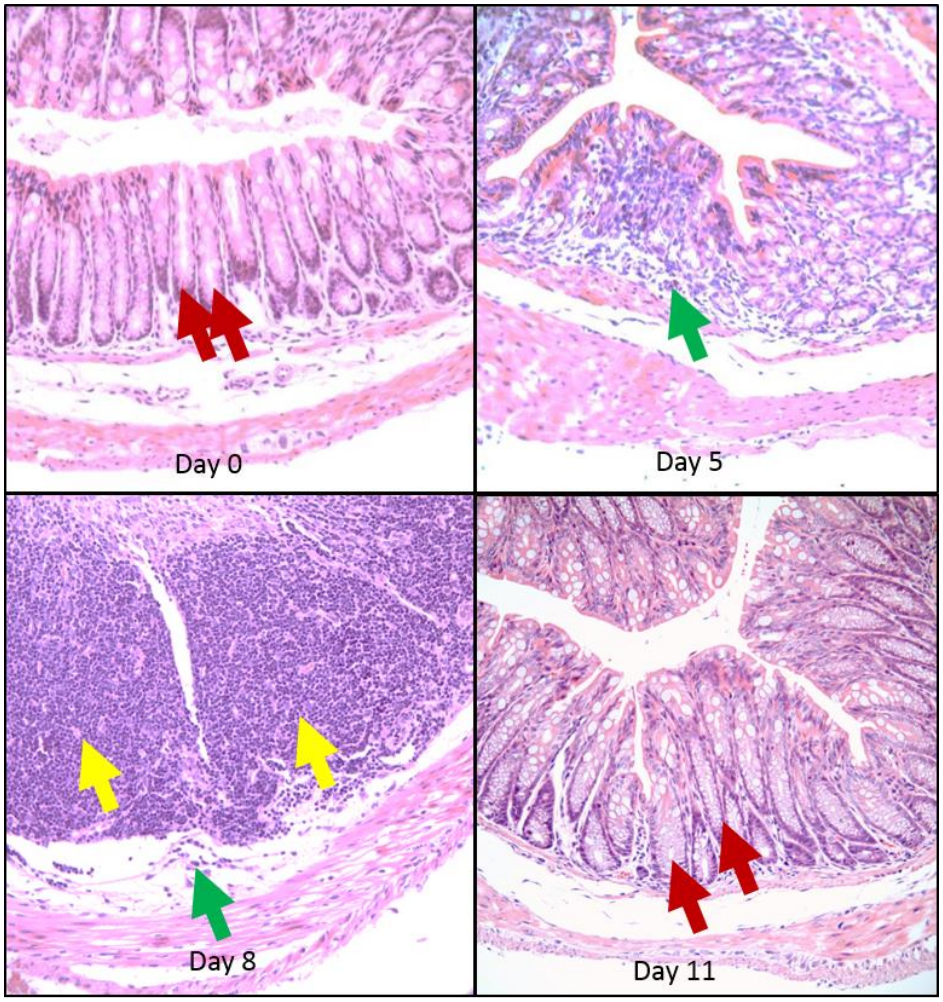

Figure 3.1 Histological examination of the colon of C57BL/6J mice at day 0 (untreated), day 5, day 8 and day 11 following 2% DSS. Figure shows the distal colon 20X magnified. Red arrows indicate crypts. Yellow arrows indicate areas of disrupted crypts and green arrows indicate the inflammatory infiltrate.

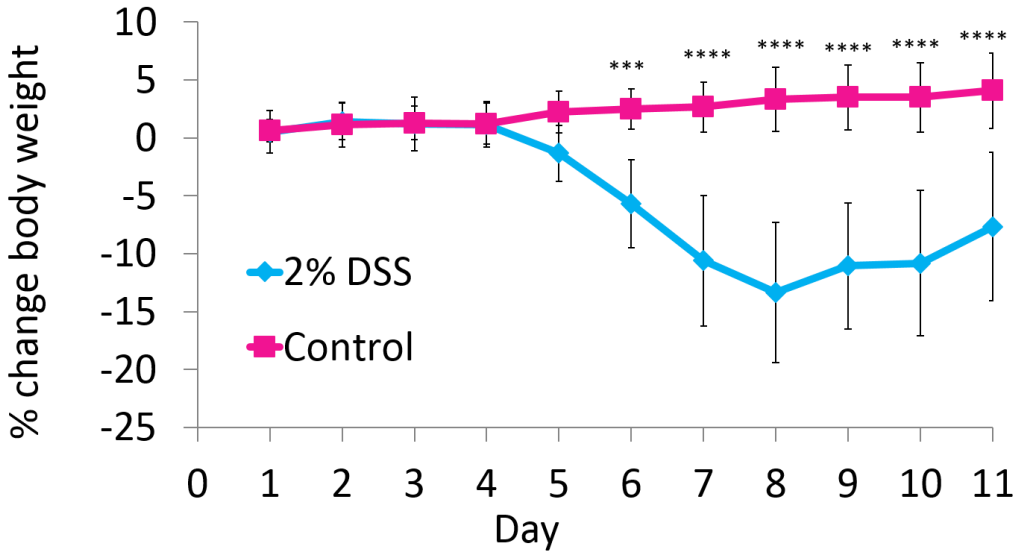

Figure 3.2 Percentage weight change observed over the course of DSS induced colitis in C57BL/6J mice. 2% DSS was given in drinking water and mice were sacrificed on day 11. Control mice (pink) were on water throughout. DSS mice (blue) were given DSS for 5 days, then water for a further 6 days. N=9 and N=6 for DSS and control respectively. Data shown as mean +/- standard error of the mean. ****=P<0.0001 ***=P<0.001. One way ANOVA and Dunnett's multiple comparisons used.

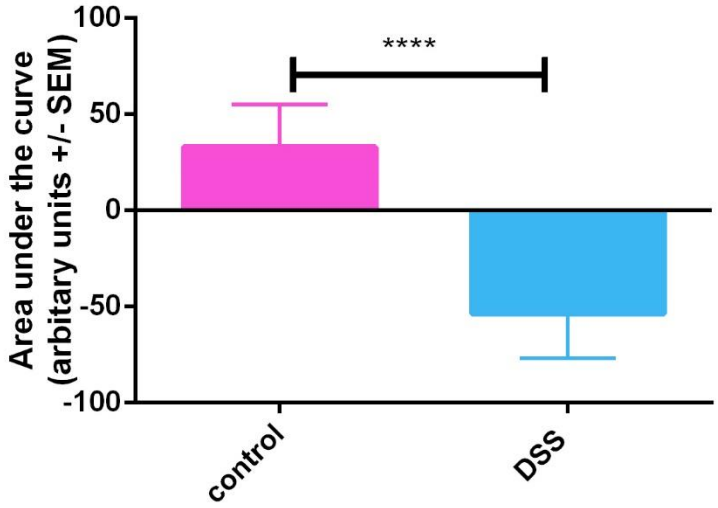

Figure 3.3 Area under the curve analysis for percentage weight change over the course of colitis of C57Bl/6J mice given DSS colitis and control mice. In pink is shown the control data and in blue is shown the data from DSS treated mice. Data shown as mean area under the curve +/- standard error of the mean. **** p<0.0001 (t-test).

3.2.2 NFκB2 null mice were resistant to weight loss induced by DSS

Male mice aged at 10-12 weeks were used, with ten mice per genotype. C57BL/6J, NFκB2 null, NFκB1 null and c-Rel null mice were administered 2% DSS in their drinking water for 5 days and were then given fresh water for a further 3 days (day 8). The mice were all culled on day 8 of the study in order to gather information from the point at which the induced colitis was shown in section 1.2.1 to be most severe. Mice were monitored for changes in weight and monitored for diarrhoea and blood around the anus or in the stool. Two animals from the NFκB1 null mouse group were culled due to ill health before the end of the experiment and one was found dead in the cage despite regular monitoring. One animal in the C57BL/6J group was also culled prematurely due to ill health. Weights were recorded daily and the data are shown in figure 3.4 as the total percentage of the mouse initial body weight. On days 7 and 8 of the experiment the NFκB2 null mice had only lost 4.5±4.47% and 5.5±6.31% of their body weight respectively, and none developed diarrhoea or haematochezia at any time during the study. In contrast the C57BL/6J null mice had lost 13.8±3.37% and 15.6±3.42% on days 7 and 8 respectively with all animals showing evidence of diarrhoea or haematochezia. C-Rel null mice lost 15.6±4.56% and 20.4±4.55% with 7 mice developing diarrhoea or haematochezia, and NFκB1 null mice lost 15.1±4.47% and 18.4±2.90% of their body weight on days 7 and 8 respectively with all 7 animals developing diarrhoea or haematochezia during the study. When area under the curve analysis was carried out, it was found that there was a significant difference between the NFκB2 null mice and the C57BL/6J ($P=0.046$) mice, but no significance differences were found between c-Rel null and NFκB1 null mice when compared to the C57BL/6J mice (figure 3.5).The different genotypes of untreated mice appeared very similar in size, weight and appearance. Untreated NFκB2 null mice were however found to be slightly larger than C57BL/6J mice ($P=0.0003$; Figure 3.6). The

load of DSS will be lower in a larger mouse; this may be partially responsible for the reduced disease seen in the NFκB2 null mice when compared to the C57BL/6J mice.

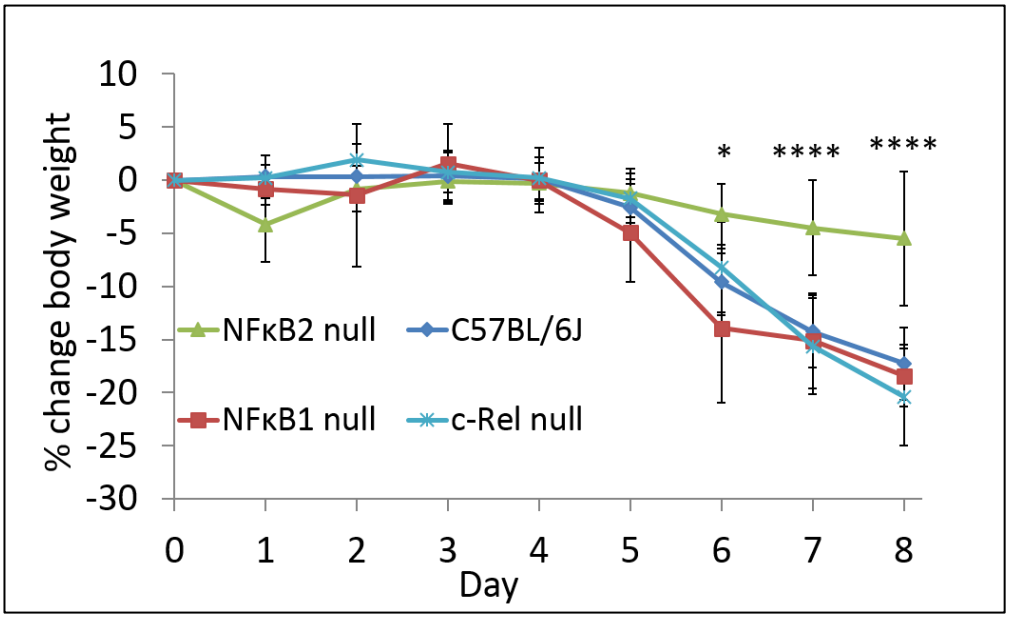

Figure 3.4 Percentage weight change from day 0 to day 8 of DSS induced colitis**.** Mice were given DSS in drinking water for 5 days and culled on day 8. NFκB2 null (green), C57BL/6J (dark blue), NFκB1 null (red) and c-Rel null (turquoise). Data presented as mean +/- standard error of the mean. N=9 for C57BL/6J, N=7 for NFκB1 null, N=10 for c-Rel null and NFκB2 null. Statistical significance between NFκB2 null group and C57BL/6J group represented on the graph by *=P<0.05 and ****=P<0.0001. NS between the C57BL/6J group and c-Rel null or NFκB1 null. One-way ANOVA and Dunnett's multiple comparisons test used.

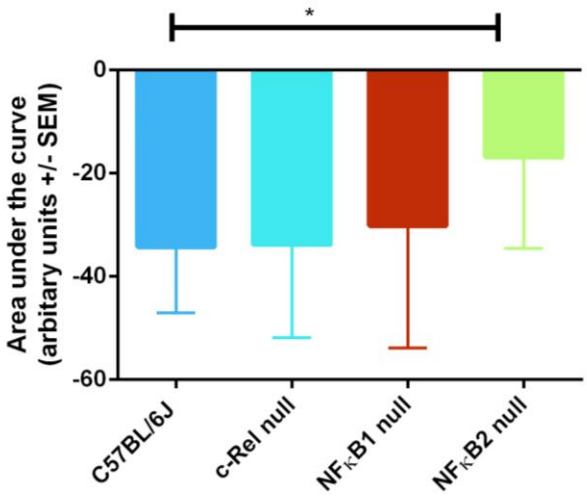

Figure 3.5 Area under the curve analysis of weight monitoring data from knockout mice given DSS. Mice were given DSS for 5 days and culled on day 8. The mice were culled on day 8. C57BL/6J (blue), c-Rel null (turquoise), NFκB1 null (red) and NFκB2 null (green). Statistical significance shown as *=P<0.05. One-way ANOVA and Dunnett's multiple comparisons test used.

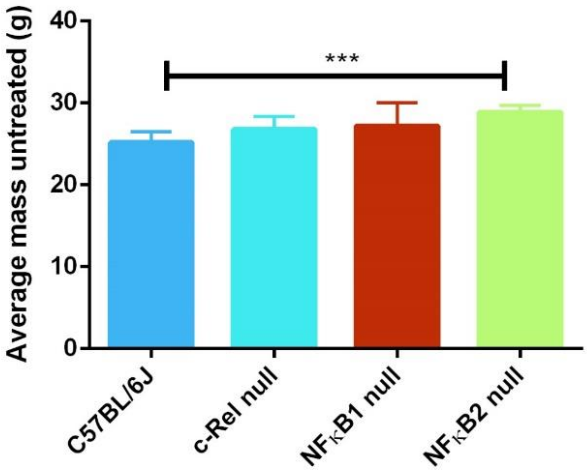

Figure 3.6 Weights of mice (N=10 per group) at baseline. Data taken from day 0 of DSS study. C57BL/6J (blue), c-Rel null (turquoise), NFκB1 null (red), and NFκB2 null green) are shown. Significant difference between C57BL/6J and NFκB2 null mouse P=0.003. ***=P<0.001. One-way ANOVA and Dunnett's multiple comparisons test used.

3.2.3 After DSS treatment NFκB2 null mice had significantly more surviving crypts than wild-type whereas c-Rel null mice had significantly less

A crypt survival assay was performed on day 8 in order to provide an indication of the extent of epithelial damage in the distal colon of DSS treated C57BL/6J, NFκB2 null, NFκB1 null and c-Rel null mice (figure 3.7A). The number of crypts were counted in 10 circumferences of distal colon per mouse. A crypt was counted if it had 5 or more cells and mitotic figures. Ten crypt widths were also measured per mouse, in order to adjust the value taking into account crypt size (Potten *et al.*, 1981). We also used visual scoring to further assess the colitis-associated inflammation for each mouse in the study (figure 3.8). The histological slide from the distal colon of each mouse was examined. A score from 0 to 4 was assigned as described by Cooper and colleagues (Cooper *et al.*, 1993). This allowed us to verify conclusions made using the weight monitoring data (section 1.3.2), and was necessary as weight change can be affected by variables other than the severity of DSS colitis such as increased stress due to handling, or an unrelated illness. Crypt number at baseline allowed us to control for any differences between genotypes which may affect the final result. However at baseline the wild-type C57BL/6J (144.5±21.7), c-Rel null (133.8±8.9), NFκB1 null (138.0±9.7) and NFκB2 null (145.0±24.4) mice had similar numbers of colonic crypts per circumference with no significant differences between them (figure 3.7B). Crypt survival in C57BL/6J mice decreased significantly following DSS administration ($P<0.0001$) from 144.5±21.7 to 71.9±23.3 at day 8, with a mean inflammation score of 3±1. Following DSS, NFκB2 null mice had significantly more surviving crypts (134.4±24.4) than C57BL/6J at day 8 ($P=0.0007$) and a mean inflammation score of 1.5±1.1 which was significantly lower than C57BL/6J ($P=0.009$). In NFκB2 null mice, the level of crypt survival after DSS treatment was not statistically different to the baseline level ($P=0.8$). The NFκB1 null mice had a similar level of crypt survival to the C57BL/6J mice at 55.3±50.7 after DSS administration. Additionally they had a mean

inflammation score of 3±1 which was identical to the C57BL/6J mice. The c-Rel null mice had a significantly lower number of surviving crypts compared to C57BL/6J after DSS treatment at 21.1±15.1 (P=0.0031; Figure 3.7B). They had a mean inflammation score of 3.4±1 which was statistically no different from DSS treated C57BL/6J mice. The NFκB1 null mice result may however be unrepresentative as during the study 2 of these mice were culled prematurely due to severe illness and 1 was found dead in the cage. Had these mice been culled at day 8 they would likely have exhibited extremely severe colitis and shown a significantly lower crypt survival than C57BL/6J at day 8.

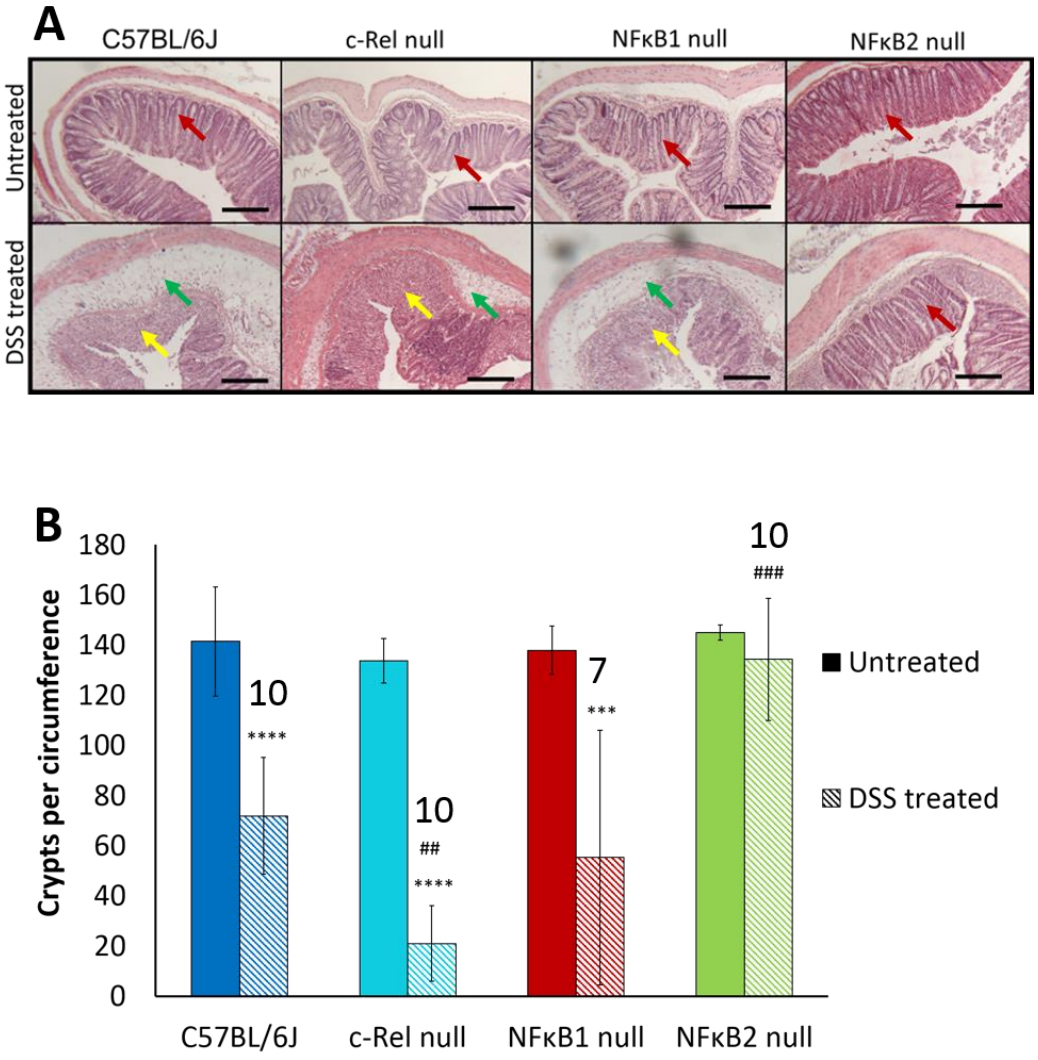

Figure 3.7 (A) H+E stained sections of C57BL/6J, c-Rel null, NFκB1 null and NFκB2 null colonic crypts following 2% DSS treatment. Red arrows indicate intact crypts, green arrows indicate the inflammatory infiltrate and yellow arrows indicate disrupted epithelium. **(B)** Crypt survival in mice at day 8 (striped) and day 0 (block colour) of DSS colitis. C57BL/6J (blue), c-Rel null (turquoise), NFκB1 null (red) and NFκB2 null (green) are shown. Untreated mice N=6 per group. C57BL/6J, c-Rel null and NFκB2 null N=10, NFκB1 null N=7, animal survival numbers are displayed above bars. Two way ANOVA and Dunnett's post hoc test used: Statistical significance between the untreated and DSS treated groups within the genotypes are shown by ****=P<0.0001 and ***=P<0.001. Significant differences between the DSS treated C57BL/6J mice and the DSS treated knockout mice are shown by ##=P<0.01 and ###=P<0.001.

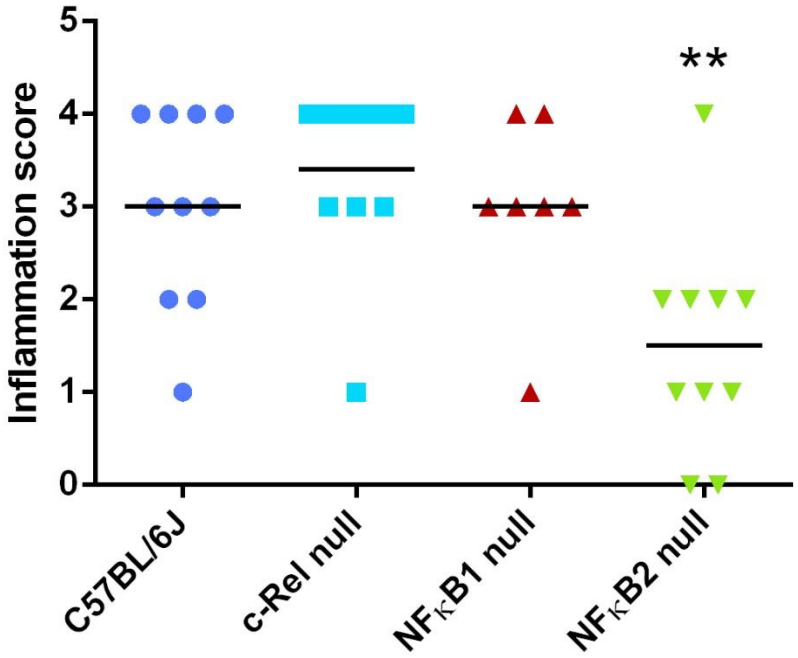

Figure 3.8 Inflammation score after DSS treatment for each genotype of mouse. Horizontal line at the mean. C57BL/6J, c-Rel null and NFκB2 null N=10, NFκB1 null N=7. Differences between datasets calculated using one way ANOVA and Dunnett's post hoc test. **=P<0.01 compared to C57BL/6J.

3.2.4 NFκB regulated gene expression during the onset of DSS colitis and recovery

In order to investigate the expression of genes that were regulated by NFκB during colitis, an NFκB target gene array was used. This array included 84 genes thought to be involved in NFκB mediated pathways (PCR array Qiagen mouse NFκB target genes PAMM-025Z). The samples were collected from C57BL/6J mice at day 0, day 5, day 8 and day 11 following 2% DSS colitis induction and recovery. Mucosal scrapes were taken from the colon of the mice after culling the mouse, removing the colon and opening the colon longitudinally. The colon was then placed on a glass slide and the mucosa was scraped off using another slide. These samples were collected in Eppendorf tubes and immediately frozen using dry ice, and the samples were stored in a -80°C freezer until use. The RNA was extracted and the samples were reverse transcribed. The PCR array was then carried out using pooled cDNA from 3 mice. The complete protocol is described in chapter 2.1.12, 2.1.13, 2.1.14.

3.2.5 The ΔΔCT method was used to calculate the fold change from CT values

The **ΔΔCT** method was used to calculate the amount of target gene present. All genes were normalised to the control housekeeping gene *Gapdh.* Expression is presented in comparison to a baseline expression, either day 0 in figures 3.9 and 3.10 or C57BL/6J wild-type mice in figures 3.10 and 3.11. **ΔΔCT** calculations were conducted as follows.

Gapdh was used as a reference gene to normalise the expression for each sample. CT is the CT value given for the gene, reference CT is the value for *Gapdh* for that particular sample.

ΔCT = CT- reference CT

The baseline level was either the day 0 untreated group or the C57BL/6J wild-type group. The mean average of the baseline group was used to calibrate all values including the baseline group itself in order to generate values from the control group which can undergo statistical analysis and show the variation in data.

ΔΔCT=targetCT- baselineCT

Fold change relative to the control group and normalised to *Gapdh* was calculated by the following:

Fold change = $2^{-\Delta\Delta CT}$

Using fold regulation, when a gene increases in expression the value will be above 1. However, when a gene decreases in expression the value will be expressed as a decimal. As the genes which we are investigating are those which show an up-regulation during colitis, fold change was chosen in order to display the data graphically.

3.2.6 Several pro inflammatory genes were up-regulated at the transcript level in C67BL/6J colonic mucosal scrapes during DSS induced colitis

An NFκB target gene array showed that several pro-inflammatory genes were up-regulated by 2 fold or more during DSS colitis. These were *Adm, Bcla1a, C3, Ccl12m Ccl22, Ccl5, Ccr5, Cd40, Cd74, Cd80, Csf1, Csf2rb, Csf3, Cxd1, Cxcl10, Cxcl3, Cxcl9, F3, Fas, FasL, Icam1, Ifng, Il12B, Il1a, Il1b, Il1r2, Il1rn, Il2ra, Mmp9, Myc, Nqo1, Plau, Ptgs2(Cox-2), Rel, Sele, Selp, Stat1, Tnf, Tnfrsf1bm.* There were also several genes that were down regulated by 2 fold or more, these were *Agt, Cd83, Ifnb1, Il15, Il2, Il4, Il6, Ins2, Ltb, Mapk26, Mitf1, Nr4a2, Relb, Snap25, Trp53.* All genes shown to be up-regulated are listed with fold regulation in table 1. A list of all genes

tested with descriptions is included in appendix 1. Several genes were upregulated at day 5, with further upregulation at day 8 followed by partial restitution by day 11. Day 8 was the point at which the most dramatic gene expression change occurred (figure 3.9B) and this correlated with the time at which the most severe clinical and histological manifestations of disease were also observed in DSS treated mice.

	day 5	day 8	day 11
Adm	3.605	5.579	4.6589
Agt	0.429277	0.127626	0.366019
Akt1	0.85859	1.1647	1.1567
Aldh3a2	0.673627	0.65066	1
Bcl2a1a	5.9794	30.2738	10.7779
Bcl2l1	1.0425	1.2311	1.4241
Birc2	0.602918	0.74744	0.972668
Birc3	1.3472	1.2834	1.5369
C3	2.4116	16.2234	4.9588
C4a	0.790014	1.9453	1.2658
Ccl12	2.0562	3.6553	1.4241
Ccl22	2.5847	0.712048	1.1892
Ccl5	0.895015	11.8762	2.639
Ccnd1	1.3013	1.7053	1.5263
Ccr5	1.6818	30.4844	9.5137
Cd40	1.3287	9.8492	5.579
Cd74	0.907523	2.2038	2.1886
Cd80	1.7291	20.2521	7.5685
Cd83	0.170756	0.267946	0.435275
Cdkn1a	0.939496	1.2924	1.454
Cfb	1.2311	1.257	1.4641
Csf1	0.655179	6.3643	3.5064
Csf2	0.602918	1.8532	0.673627
Csf2rb	5.0982	64.8934	19.6983
Csf3	0.602918	62.2499	5.2054
Cxcl1	13.0864	115.3601	13.0864
Cxcl10	4.6589	39.1245	12.2101
Cxcl3	11.4716	424.6116	56.8859
Cxcl9	2.6208	9.8492	6.9163
Egfr	1.3566	1.1251	1.8277
Egr2	1.9862	1.4641	1.8661
F3	2.1435	2.4623	2.5847
F8	0.602918	0.447507	0.673627
Fas	1.5692	1.5157	2.0994
Fasl	0.986193	1.8277	2.7702
Gadd45b	1.2142	1.3287	0.939496
Icam1	2.0849	17.1484	6.6346
Ifnb1	0.602918	0.447507	0.673627
Ifng	0.602918	19.0273	2.1886
Il12b	0.602918	2.6759	0.673627
Il15	0.348687	0.32533	0.806647
Il1a	2.4284	122.7858	19.6983
Il1b	18.6357	744.4339	155.4169

	day 5	day 8	day 11
Il1r2	5.2054	105.4197	20.8215
Il1rn	5.5022	3.605	3.0314
Il2	0.602918	0.447507	0.673627
Il2ra	0.566444	7.4643	4.5315
Il4	0.602918	0.447507	0.673627
Il6	2.2658	254.2317	5.9381
Ins2	0.602918	0.447507	0.673627
Irf1	1.6702	1.3104	1.879
Lta	0.737137	0.5	1.3287
Ltb	0.332171	0.582377	1.0943
Map2k6	0.384216	0.281262	0.554785
Mitf	0.348687	0.624181	0.702198
Mmp9	2.9282	97.6806	45.2548
Myc	0.397772	0.411794	0.510517
Myd88	1.3472	1.5263	1.3013
Ncoa3	0.901226	0.959233	1.1487
Nfkb1	0.801089	0.901226	1.0867
Nfkb2	0.78456	0.773754	1.0867
Nfkbia	1.4142	1.5476	1.3195
Nqo1	0.659761	9.0005	0.965904
Nr4a2	0.295247	0.353557	0.607091
Pdgfb	0.757863	1.0353	1.5369
Plau	3.4822	40.2244	11.7942
Ptgs2	6.8685	210.8393	25.1067
Rel	2.2658	4.3772	3.3173
Rela	1.0867	1.0644	1.1975
Relb	0.757863	0.476327	0.570386
Sele	0.602918	4.7899	3.1383
Selp	1.6472	60.5477	21.4068
Snap25	0.952653	0.426312	0.395023
Sod2	0.712048	1.0281	0.817929
Stat1	1.6133	1.8532	2.2815
Stat3	1.6586	1.4142	1.8661
Stat5b	0.539607	0.558628	0.77918
Tnf	8.5742	9.6465	6.6807
Tnfrsf1b	2.7702	5.9794	3.0105
Tnfsf10	1.9862	0.926612	1.3287
Traf2	0.829325	0.901226	1.0425
Trp53	0.381563	0.668986	0.74744
Vcam1	1.0353	5.579	6.6346
Xiap	1.5583	1.0644	1.6472

Table 3.1 NFκB target gene expression during DSS-induced colitis induction and recovery in C57BL/6J mice. mRNA from mucosal scrapes of colon was reverse transcribed to produce cDNA. Fold change is shown on this chart with decimal reciprocals of negative numbers representing down regulation. All values are compared to day 0. Up-regulated genes are highlighted in green and down-regulated genes are highlighted in red.

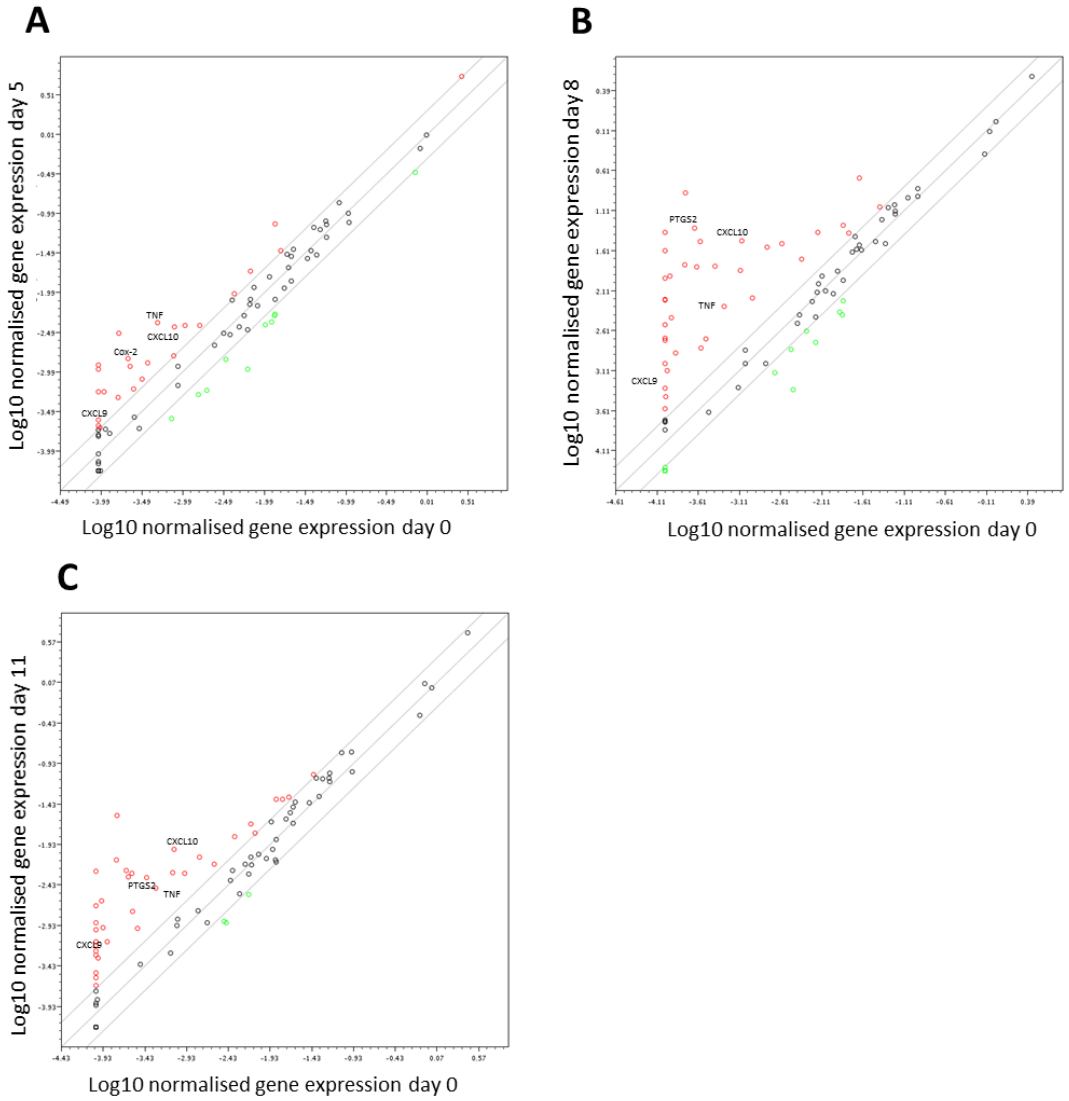

Figure 3.10 NFκB target gene array data. (A) Day 5 vs. day 0 gene expression (B) Day 8 vs day 0 gene expression (C) day 11 vs day 0 gene expression. Upregulated genes shown in red, downregulated genes shown in green.

5 genes were selected for further investigation, in order to determine whether the expression of that mRNA was likely to be a contributing factor to disease progression. Upregulated genes were selected as these make the most attractive targets, due to the fact that they can be pharmacologically inhibited.

Tnf was selected as this cytokine increases the inflammatory response and also plays a role in activating the NFκB signalling pathway (Hamilton, 2008). In the PCR array *Tnf* was found to have positive fold changes of 8.6, 9.6 and 6.7 at days 5, 8 and 11 respectively. *Cox-2* was selected as this gene functions as a pro-inflammatory prostaglandin which is known to be involved in the inflammatory response (Wang and Dubois, 2010). *Cox-2* showed positive fold changes of 6.9, 210 and 25.1 on days 5, 8 and 11 respectively. As these genes are known to be upregulated in inflammation this adds validity to the study.

Cxcl9 and *Cxcl10* were selected for investigation as they showed up-regulation throughout the course of colitis and these genes are both involved in chemotaxis and T cell homing and activation (Rosenblum *et al.*, 2010). In the PCR array *Cxcl9* had a positive fold change of 2.6 at day 5, 9.8 at day 8 and 6.9 at day 11. *Cxcl10* has a positive fold change of 2.6 at day 5, 9.8 at day 8 and 6.9 at day 11. Finally *Csf-1* was selected as this gene is involved in the activation of myeloid cells (Garcia *et al.*, 2016). Loss of a single *Csf1* receptor allele in male mice has been shown to protect them from DSS colitis (Huynh *et al.*, 2013), and blockage of *Csf1* has been shown to protect mice from DSS colitis with a trend towards a lowering of the amount of pro-inflammatory cytokines (Marshall *et al.*, 2007). *Csf1* showed a positive fold change of 6.4 at day 8 and 3.5 at day 11 in the PCR array. The fold changes of these genes during colitis induction and recovery are shown graphically in figure 3.10.

Array data was generated from pooled DNA from 3 mice. It was therefore necessary to confirm the results using PCR primer assays using samples generated from

individual mice in order to perform statistical analysis on the data. Six C57BL/6J mice were treated with 2% DSS following the standard DSS dosing regime and were culled on day 0, day 5, day 8 and day 11. Significant changes was found at day 8 in *Cox-2, Csf1* and *Tnf* with positive fold changes of 25±29 (P=0.004), 6.6±7.48 (P=0.0104) and 71.5±29 (p=0.004) respectively. The abundances of *Cxcl10* and *Cxcl9* in individual mice also supported the array data with a trend to increased expression at day 8 compared to untreated animals. However, these were not found to be statistically significant due to animal-animal variation. Gene expression data from PCR primer assays for *Cxcl9, Cxcl10, Tnf, Cox-2* and *Csf1* are shown in figure 3.11.

Untreated NFκB2 null mouse gene expression was next compared to untreated C57BL/6J wild-type mice. No significant differences at baseline were found and the data are shown in figure 3.12. Fold regulation of *Cxcl10* day 0 was 1 ±0.7 and day 8 was 0.8±0.1, *Cxcl9* on day 0 was 1±0.8 and day 8 was 1±0, *Cox-2* on day 0 was 1±0.5 and day 8 was 1±0.2, *Tnf* on day 0 was 1±0.5 and day was 8 0.9±0. *RelB* expression was also investigated and it was found to be significantly lower in NFκB2 null mice than in C57BL/6J wild-type at baseline.

The expression of the same 5 genes were investigated in NFκB2 null mice by PCR assay. None of these genes were significantly up-regulated at day 8 following the DSS dosing regimen when compared to day 0 data. The gene expressions were close to the expression levels at baseline with *Cxcl10* on day 0 at 1±0.7 and day 8 at 0.8±0.1, *Cxcl9* on day 0 at 1±0.8 and day 8 at 1±0, *Cox-2* on day 0 at 1±0.5 and day 8 1±0.2, *Tnf* on day 0 1±0.5 and day 8 0.9±0.1. These data for the fold regulations of *Cxcl9, Cxcl10, Tnf, Cox-2* and *Csf1* are shown in graphical form in figure 3.13.

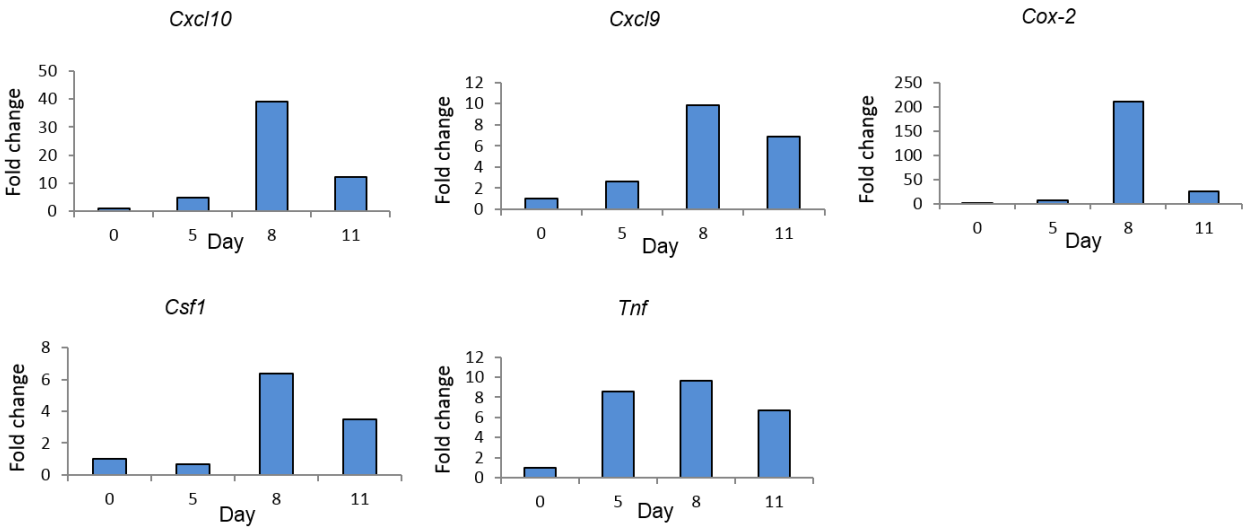

Figure 3.11 Gene expression from NFκB target gene array. C57BL/6J colonic mucosal scrapes at day 5, 8 and 11 compared to day 0 following DSS induced colitis. C57BL/6J mice aged 10-12 weeks. cDNA extracted from mucosal scrapes taken from the colon. cDNA pooled from 3 mice.

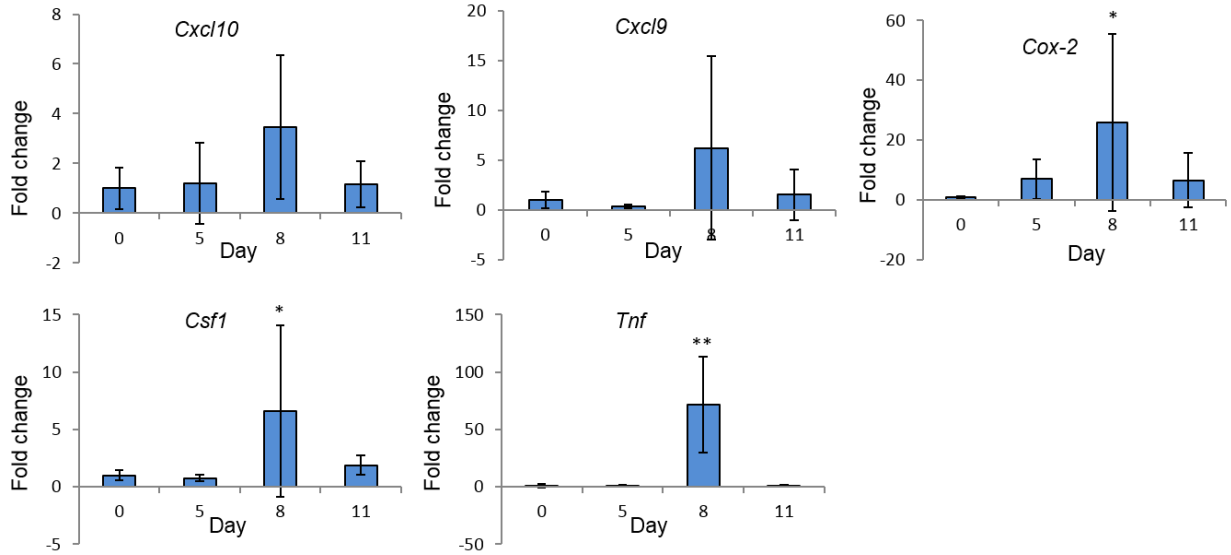

Figure 3.12 Gene expression from PCR assay in C57BL/6J wild-type colonic mucosal scrapes at day 5, 8 and 11 compared to day 0 following DSS induced colitis. Data shown as mean +/- standard deviation. C57BL/6J mice aged 10-12 weeks. DNA extracted from mucosal scrapes taken from the colon. 6 mice in each group. *=P<0.05 **=P<0.01.

3.2.7 Pro-inflammatory genes which were up-regulated in C57BL/6J wild-type mice were not up-regulated in NFκB2 null mice

After DSS administration at day 8 of the protocol the C57BL/6J wild-type mice showed more severe inflammation and disease than NFκB2 null mice. All five genes which were initially selected for investigation were included in the analysis including *Cxcl9* and *Cxcl10*. Although these two genes did not show statistically significant increases in expression at day 8 they appeared to show a strong trend toward up-regulation and were up-regulated in the array. When the levels of expression of *Cxcl9, Cxcl10, Cox-2, Csf1* and *Tnf* were investigated it was found that all five genes showed significantly lower levels of expression in NFκB2 null mice than wild-type. If gene expression in C57BL/6J mice on day 8 was set to a value of one, the NFκB2 null day 8 values compared to this were as follows. *Cox-2* was 0.09±0.1 (P=0.037), *Csf1* was 0.21±0.28 (P=0.037), *Cxcl9* was 0.12±0.16 (P=0.037), *Cxcl10* was 0.0056±0.0057 (P=0.0036) and *Tnf* was 0.22±0.034 (P=0.0037). These data are shown in figure 3.14.

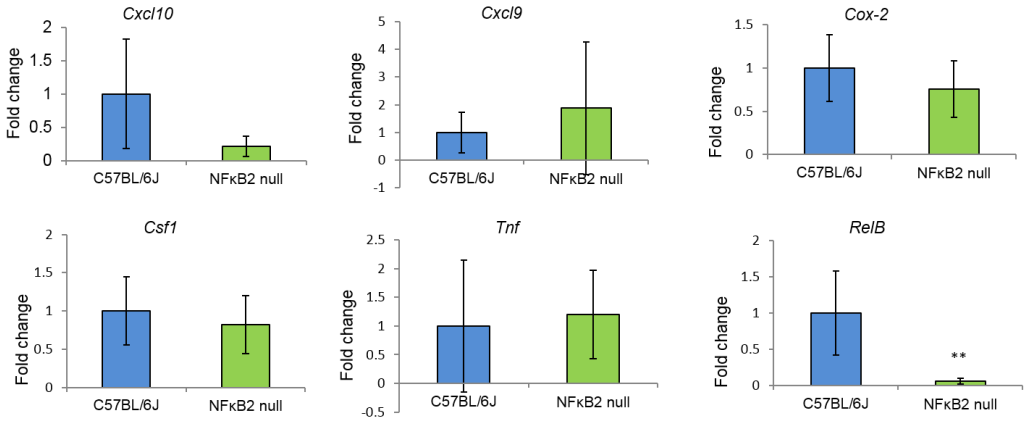

Figure 3.13 Gene expression in NFκB2 null mice at day 0 compared to C57BL/6J wild-type mice at day 0 of DSS induced colitis. Data shown as mean +/- standard deviation. NFκB2 null mice on a C57BL/6J background were used. DNA extracted from mucosal scrapes taken from the colon. 6 mice per group.

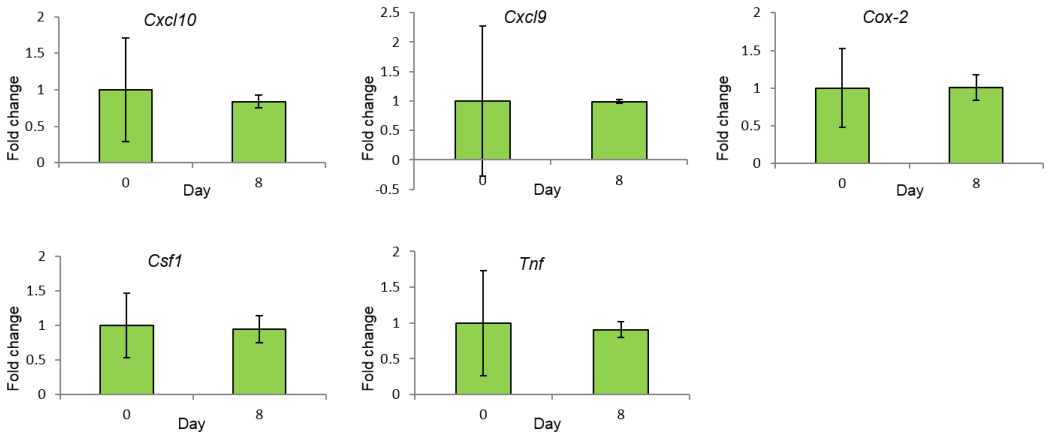

Figure 3.14 Gene expression in NFκB2 null mice at day 8 compared to day 0 of DSS study. Data shown as mean +/- standard deviation. NFκB2 null mice on a C57BL/6J background were used. Mice given DSS for 5 days followed by 3 days of water. DNA extracted from mucosal scrapes taken from the colon. 6 mice in each group.

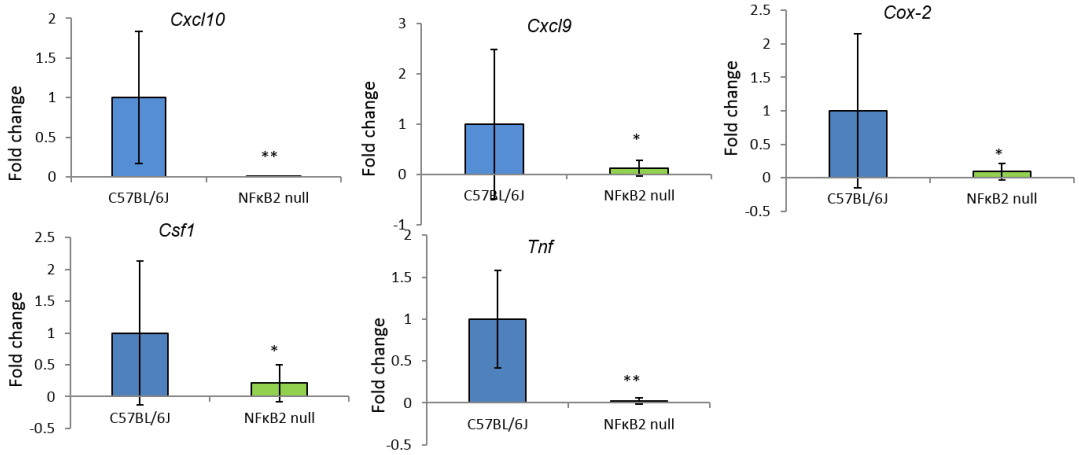

Figure 3.15 Gene expression in NFκB2 null colonic mucosa at day 8 compared to C57Bl/6J wild-type mice at day 8 of DSS induced colitis. Data shown as mean +/- standard deviation. NFκB2 null mice were on a C57BL/6J background used. Mice were given DSS for 5 days followed by 3 days of water. DNA extracted from mucosal scrapes taken from the colon. 6 mice per group.

	CXCL10	CXCL9	COX-2	CSF-1	TNF
Function	**Attractant for T lymphocytes**	**Attractant for T lymphocytes**	**Pro-inflammatory prostaglandin**	**Activator of myeloid cells**	**Pro-inflammatory response cytokine**
C57BL/6J Day 0 vs day 8	↔	↔	↑	↑	↑
NFκB2 null Day 0 (vs C57BL/6J)	↔	↔	↔	↔	↔
NFκB2 null Day 0 vs day 8	↔	↔	↔	↔	↔
NFκB2 null Day 8 (vs C57BL/6J)	↓	↓	↓	↓	↓

Table 3.2. Summary of gene expression data from PCR experiments. ↓ represents a decrease in gene expression, ↑ represents an increase in gene expression and ↔ represents little or no change in gene expression.

3.2.8 Generation of a murine bone marrow reconstitution protocol

Previous investigations described in section 3.2.2 and 3.2.3. suggested that NFκB2 is important in regulating the murine response to DSS induced colitis. However these studies in a global knockout mouse were unable to determine which cell types were important in determining this altered phenotypic response. We therefore wanted to generate bone marrow chimeras to determine the importance of NFκB2 in immune or other mucosal cell types in regulating DSS colitis susceptibility. We first generated a protocol to quantify the percentage of bone marrow reconstitution using reporter mice. This involved lethal irradiation of 6 C57BL/6J mice in order to destroy their bone marrow. The mice were then administered bone marrow from a donor tdTomato mouse via intravenous tail vein injection. Mice were then left to recover for 12 weeks. After this period of recovery, mice were either left untreated (N=3) or were given DSS for 5 days followed by water for a further 3 days (N=3) and were then culled.

H+E sections of the distal colon were taken to confirm the induction of colitis. Mice were also weighed throughout the study. After 12 weeks the femurs were harvested

and flushed out in order to quantify tdTomato positive and negative cell populations by flow cytometry. Bone marrow from a C57B/6J mouse was used as a negative control. The bone marrow of the mice which had been reconstituted, when viewed under a fluorescent microscope, mostly showed red fluorescence (figure 3.16). Flow cytometry was used to validate the reconstitution protocol further.

The flow cytometry data showed that the bone marrow from the reconstituted mice was 98.1±0.7% reconstituted (figure 3.17). The 6 mice were found to be reconstituted by 97.9%, 97.2%, 99%, 99%, 98.2% and 97.5%. The negative control mouse had 6% fluorescence, indicating that there is only a low baseline level of fluorescence. It was therefore concluded that the reconstitution protocol had been successful.

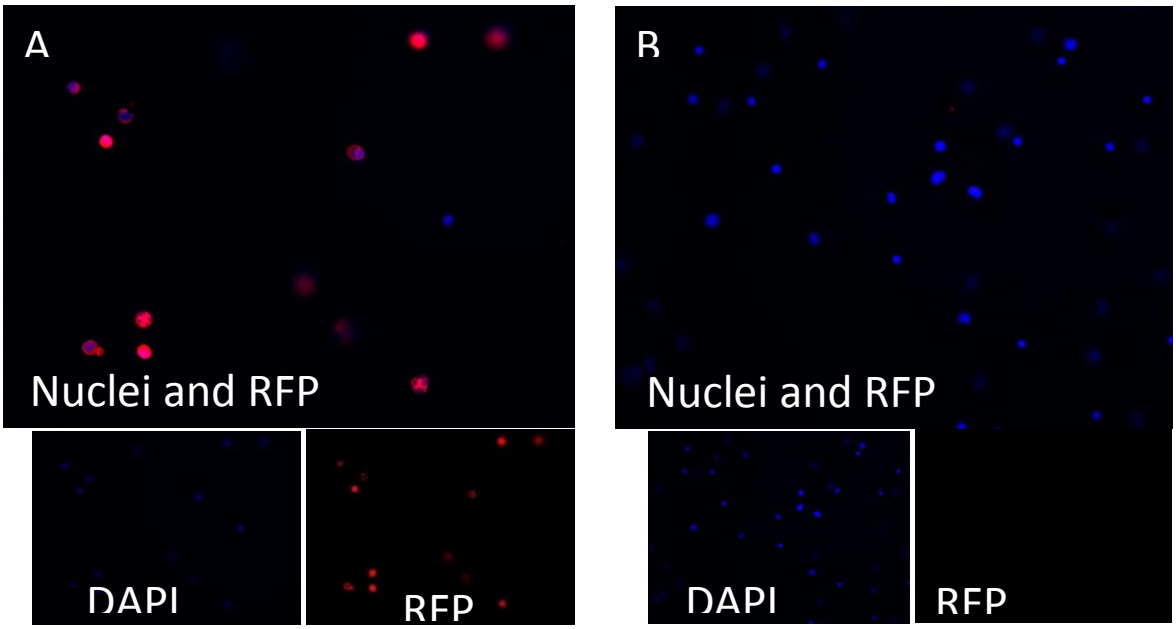

Figure 3.16 Bone marrow from a mouse reconstituted with bone marrow from a tdTomato mouse compared to bone marrow from a wild-type mouse. Panel A shows bone marrow from the reconstituted mouse and panel B shows the bone marrow from an untreated mouse.

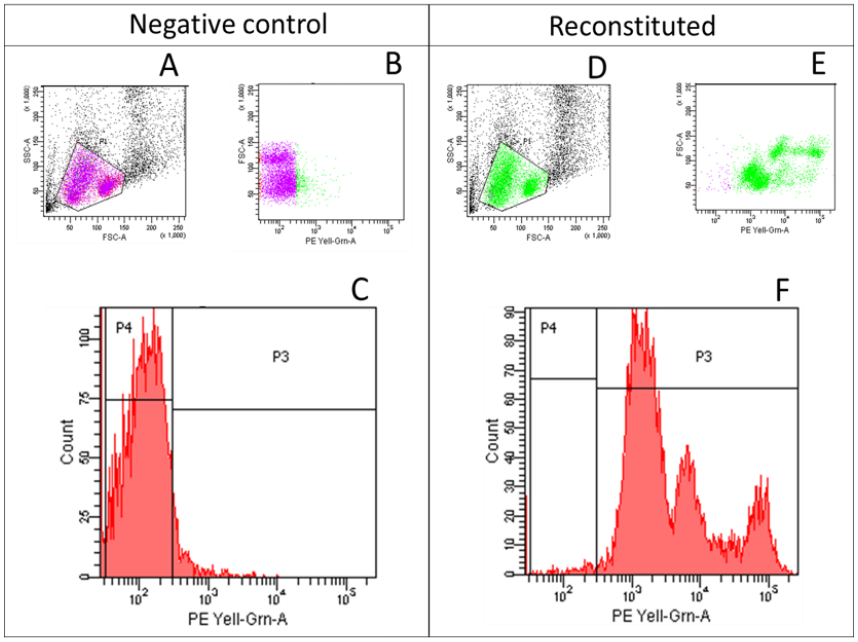

G

	% cells fluorescent
Mouse 1	97.9
Mouse 2	97.2
Mouse 3	99
Mouse 4	99
Mouse 5	98.2
Mouse 6	97.5
Control	6

Figure 3.17 FACS analysis of mice reconstituted with bone marrow from tdTomato mice. Panels A and D show how the cell populations that were selected. In this analysis we selected two populations of immune cells. In B and E the purple population of cells represents those which were not fluorescent and green represents the cells which were fluorescent. C and F represent the total cell count (y axis) which exceeds the fluorescence threshold and is therefore included in the cell count. The threshold is positioned on the X axis between 10^2 and 10^3. Example data from one of the reconstituted mice is shown. G displays the data for the individual mice, with the % of the selected cell population. Bone marrow from a mouse reconstituted with bone marrow from a tdTomato mouse have an average FACS percentage of fluorescing cells of 98.1±0.7% (N=6). Bone marrow from negative control mouse had 6% fluorescence.

3.2.9 NFκB2 regulated susceptibility to DSS colitis in the colonic mucosa

As bone marrow reconstitution was adequately achieved following the protocol established in section 2.1.6, we conducted the same reconstitution protocol in groups of either C57BL/6J or NFκB2 null mice. We used bone marrow derived from either C57BL/6J or NFκB2 null mice. Following reconstitution mice were either left untreated or were administered DSS in their drinking water to induce colitis. Representative histological sections of the mice at day 8 of the DSS study are shown in figure 3.18.

Weight monitoring data were used to investigate the colitis that the mice experienced throughout the course of the experiment (figure 3.19). Area under the curve analysis data are shown in figure 3.20 and were used to determine if there were statistically significant differences in weight loss between groups. As anticipated and in keeping with previous similar experiments, this analysis revealed that there was a significant decrease in the amount of weight lost by NFκB2 null mice compared to C57BL/6J mice ($P=0.0051$). Controls for the experiment were mice that had been reconstituted with bone marrow of their own genotype, in order to control for any effects on the response to colitis that the irradiation and reconstitution may have had. C57BL/6J (C57BL/6J) denotes a C57BL/6J mouse which had been reconstituted with bone marrow from a C57BL/6J mouse. Similarly NFκB2 null (NFκB2 null) denotes an NFκB2 null mouse which had been reconstituted with bone marrow from an NFκB2 null mouse. C57BL/6J (NFκB2 null) denotes a C57BL/6J mouse which had been reconstituted with NFκB2 null bone marrow and NFκB2 null (C57BL/6J) represents an NFκB2 null mouse which had been reconstituted with C57BL/6J bone marrow.

C57BL/6J (NFκB2 null) mice lost significantly less weight than C57BL/6J (C57BL/6J) mice ($P=0.046$) and showed a similar amount of weight loss to NFκB2 null (NFκB2 null) animals, with area under the curve analysis revealing no significant difference. This suggests that there is a protective effect when NFκB2 is deleted from the immune

compartment which is not due to the effects of full body irradiation. Additionally this suggests that although DSS load may have had an impact on the degree of the colitis, NFκB2 null mice are genetically protected from colitis in addition to being larger. NFκB2 null (C57BL/6J) mice and NFκB2 null (NFκB2 null) mice were not significantly different from one another in terms of weight loss. This suggests that the presence of NFκB2 in the immune compartment does not appear to have an impact on the response to DSS colitis.

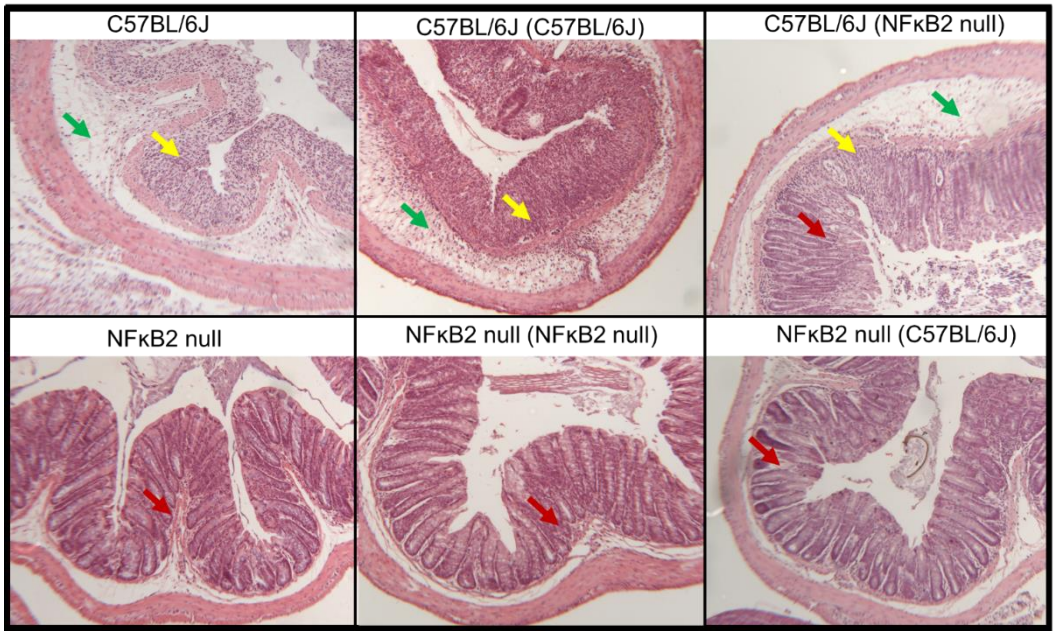

Figure 3.18 Histological sections stained with H+E at day 8 of DSS study. Red arrows indicate intact crypts. Green arrows indicate inflammatory infiltrate and yellow arrows indicate the disrupted epithelium. Untreated and reconstituted C57BL/6J mice are shown on the top row. Untreated and reconstituted NFκB2 null are shown on the bottom row.

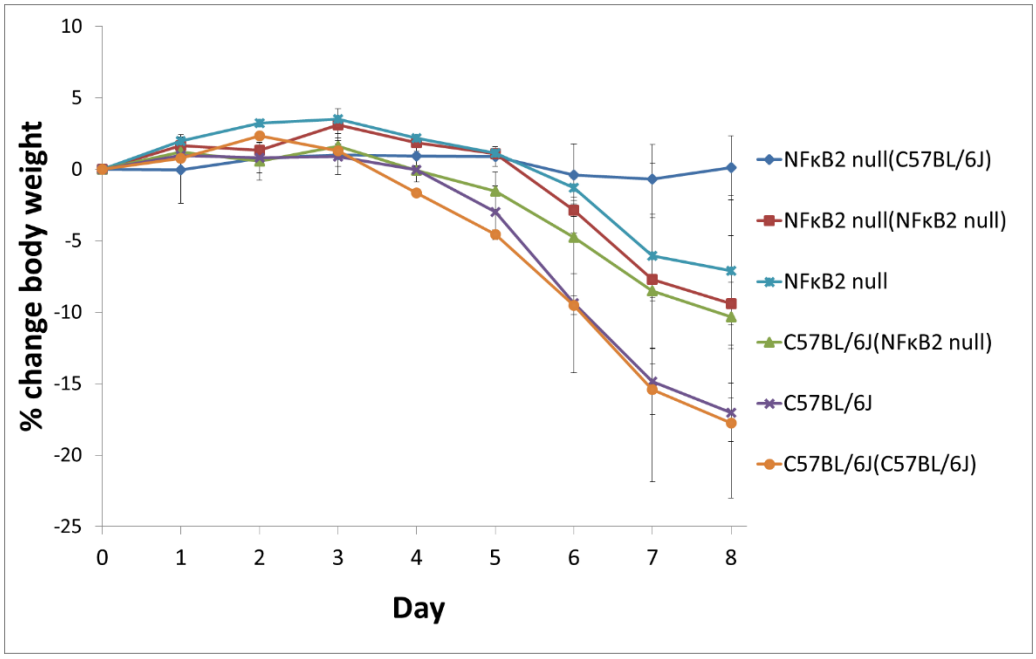

Figure 3.19 Weight monitoring data for mice in bone marrow reconstitution and DSS study. Mean average whole body weight data shown as mean ± standard deviation. Mice denoted as 'genotype (genotype of bone marrow)'. Wild type mice: C57BL/6J (Purple), C57BL/6J (C57BL/6J) (orange), C57BL/6J (NFκB2 null) (green). NFκB2 null mice: NFκB2 null (turquoise), NFκB2 null (NFκB2 null) (red), and NFκB2 null (C57BL/6J) (blue). 10 mice per group.

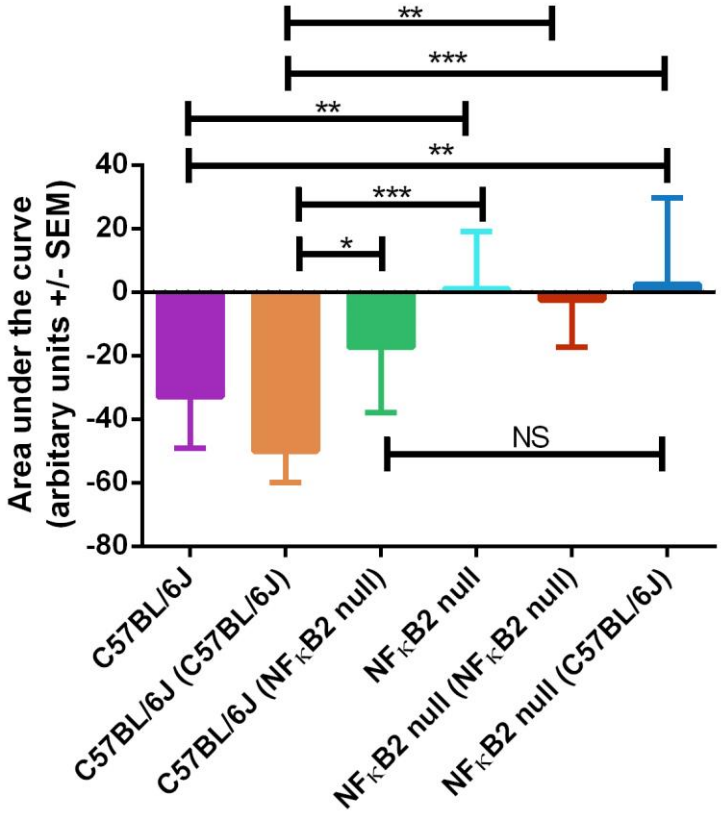

Figure 3.20 Area under the curve analysis of weight monitoring data from bone marrow reconstitution experiments. Area under the curve compared using Dunn's multiple comparisons. *=P<0.05 **=P<0.01 ***=P<0.001

3.2.10 NFκB2 functions to increase the effects of DSS in both the immune and mucosal populations of the mouse

Bone marrow reconstitution was undertaken using C57BL/6J mice and NFκB2 null mice. Crypt survival assays (figure 3.21) and histological inflammation scoring (figure 3.22) were performed as described in section 1.3.2 using mice from day 8 of the DSS protocol in order to quantify the degree of colitis. As expected, compared to C57BL/6J (69±27) a significant increase in crypt survival (suggesting the presence of less severe colitis) was seen in NFκB2 null mice (117±29; P=0.0119). NFκB2 null (NFκB2 null) mice had a crypt survival of 106±24 and this was not statistically significantly different to either NFκB2 null or C57BL/6J crypt survival. C57BL/6J (C57BL/6J) mice had a crypt survival of 73±27, with significantly fewer surviving crypts than in NFκB2 null mice (P=0.0359), as well as being similar to C57BL/6J mice. NFκB2 null (NFκB2 null) and C57BL/6J (C57BL/6J) mice did not show statistically significantly different levels of crypt survival from one another although the inflammation score for C57BL/6J (C57BL/6J) mice was significantly lower than for NFκB2 null (NFκB2 null) (P<0.0001). NFκB2 null (C57BL/6J) mice had a crypt survival of 128.2±10.6 which was significantly higher than C57BL/6J (C57BL/6J) crypt survival (P=0.0037), and a significantly lower inflammation score (P<0.0001) but the value was similar to NFκB2 null (NFκB2 null) crypt survival. C57BL/6J (NFκB2 null) mice had a crypt survival of 87±44.6 and did not show significant differences in crypt survival compared to either C57BL/6J (C57BL/6J) or NFκB2 null (NFκB2 null) mice, although they did have a significantly higher inflammation score than NFκB2 null (NFκB2 null) mice (P=0.03). However there was significantly more crypt survival in NFκB2 null (C57BL/6J) than C57BL/6J (NFκB2 null) mice (P=0.0419).

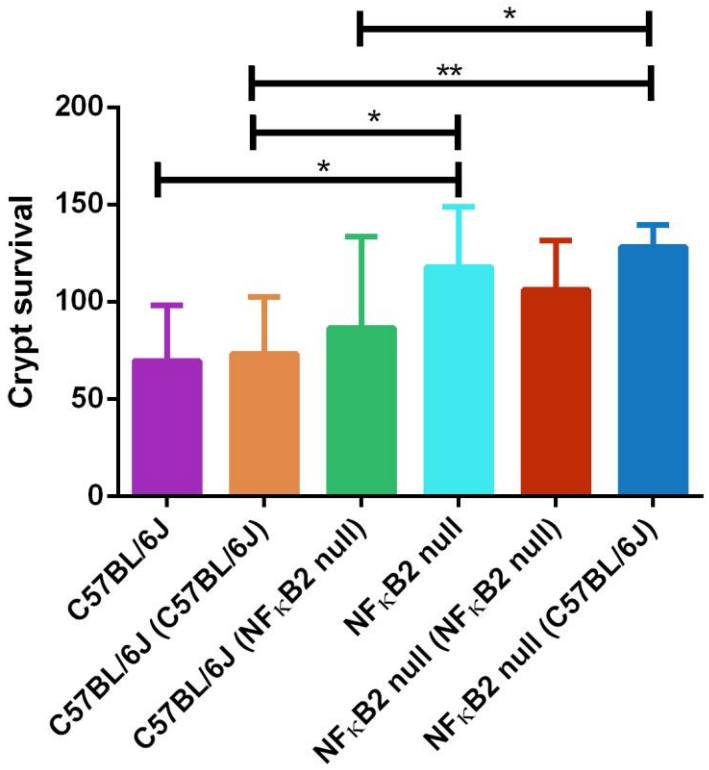

Figure 3.21 Crypt survival at day 8 for irradiated mice reconstituted with bone marrow from C57BL/6J mouse or NFκB2 null mouse. Data shown as mean of average crypts per circumference per mouse with standard deviation shown on error bars. Male mice aged 10-12 weeks. DSS given to the mice for 5 days then water for a further 3 days. 10 mice per group. *=P<0.05, **=P<0.01

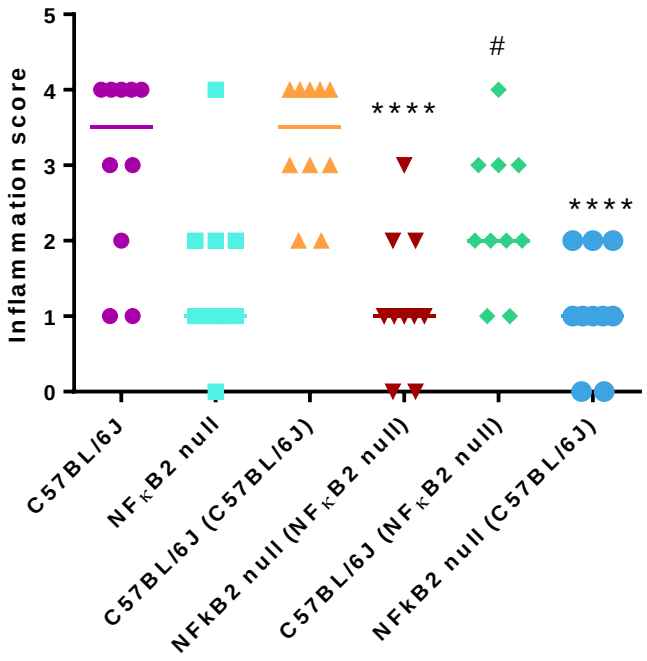

Figure 3.22 Histological inflammation score for each of the bone marrow reconstituted genotypes. Median shown by horizontal line. Differences tested using one way ANOVA. ****p<0.0001 comparison with C57BL/6J (C57BL/6J). #P<0.001, compared with NFκB2 null (NFκB2 null).

3.3 Discussion

In this chapter, the protective effect of NFκB2 deletion against DSS colitis has been examined, as well as the potential downstream genes involved and the contribution of the immune system. The DSS colitis model was first described in 1990 (Okayasu *et al.*, 1990)**.** This model is popular due to the ease of administration of the DSS in the drinking water and the low risk of mortality compared to other models of colitis (Melgar *et al.*, 2008). DSS colitis causes body weight loss, blood in the stool and around the anus, diarrhoea, colonic inflammation and histological changes (Melgar, Karlsson and Michaëlsson, 2005). Clinical signs of colitis in DSS treated mice are similar to those observed in humans with inflammatory bowel disease (IBD). Humans present with weight loss, diarrhoea and sometimes rectal bleeding similarly to the mice in this DSS study. Morphological changes consistent with colitis were also apparent in the distal colon. Taken together, these observations confirmed that DSS colitis was successfully induced in the animals and that the selected time points were suitable for assessment of colitis induction and recovery in further gene expression studies.

Previous work in our lab found that NFκB2 null mice were relatively resistant to DSS/AOM treatment (Burkitt *et al.*, 2015). Therefore the resistance to DSS colitis alone that we observed in NFκB2 null mice was not unexpected. The difference in weight between C57BL/6J wild-type mice was significant although NFκB2 null mice were also slightly heavier. This means that care in interpreting the results must be taken as the difference in colitis susceptibility could be at least partly due to a lower DSS load in the mice with the larger mass. The C57BL/6J mice also varied in size and some were larger than others, but we did not see a dramatic decrease in colitis in heavier C57BL/6J mice in a similar way to that observed in NFκB2 null mice. Therefore it is assumed that although the increased weight of untreated NFκB2 null

mice is not ideal, the impact of this parameter on our overall results is likely to be minimal.

Signalling via the alternative NFκB activation pathway is controlled by the processing of the precursor NFκB2 protein p100 into the active form P52. RelB does not function as a homodimer, so alternative NFκB pathway signalling is controlled by either heterodimers containing NFκB2 and RelB or homodimers of NFκB2. Because P52 does not have the ability to activate transcription, the NFκB2:RelB dimer is the transcriptionally active dimer functioning in the alternative NFκB activation pathway (Dejardin, 2006). NFκB2 also forms transcriptionally active dimers with c-Rel and RelA, members of the classical NFκB activation pathway. These dimers are active in the NFκB hybrid pathway as they contain elements of both pathways (Dejardin, 2006). C-Rel null mice developed more severe DSS induced colitis than C57BL/6J mice according to crypt survival data. In these mice the NFκB2:c-Rel dimer cannot form. It is therefore less likely that the lack of NFκB2:c-Rel dimers is responsible for the resistance of NFκB2 null mice to colitis. Dimerisation of NFκB2 and NFκB1 would form a transcriptionally inactive complex, so this is unlikely to be a key cause of the aggravation of colitis by NFκB2. The RelA embryonic lethal phenotype means that we were unable to use RelA null mice for a DSS study. RelA and NFκB2 would form a transcriptionally active complex. Therefore RelA:NFκB2 and NFκB2:RelB dimers may be involved in the exacerbation of colitis, which suggests that either the alternative NFκB activation pathway or the NFκB:RelA dimer is involved in aggravation of inflammation and colitis (Melgar, Karlsson and Michaëlsson, 2005).

In gene expression data (summarised in table 3.2), certain genes that are expressed in the murine colonic mucosa were measured before, during and after DSS colitis induction in both wild-type and NFκB2 null mice. One gene investigated was *Cox-2*, as it is known to be expressed in the human colon during ulcerative colitis (Wang and Dubois, 2010), in the murine colon during DSS colitis (Fukata *et al.*, 2006) and to be

overexpressed in the Il-10 null mouse model of colitis (Shattuck-Brandt *et al.*, 2000). Although the upregulation of *Cox-2* allowed us to validate the gene expression data, by studying a gene which has been shown to be upregulated in other studies, *Cox-2* is unlikely to be linked to the protection of NFκB2 null mice against DSS induced colitis. Although Cox-2 deficient mice experience worse DSS induced colitis which indicates that the protein has a protective effect (Morteau *et al.*, 2000), *Cox-2* was found to be down-regulated in NFκB2 null mice, making it unlikely that this protein is involved in the amelioration of colitis observed in this genotype. Additionally, epithelial cell specific deletion of *Cox-2* has been shown to have no effect upon the severity of DSS colitis (Ishikawa, Oshima and Herschman, 2011), whereas in our data the deletion of epithelial NFκB2 has a significant protective result against DSS colitis.

One gene which may contribute to the progression of DSS colitis is *Csf1.* This gene was shown to be up-regulated during DSS colitis in wild-type mice. However no up-regulation was seen in NFκB2 null mice. Additionally, previous studies have shown that mice which are deficient in CSF1 or its receptor are protected from developing DSS colitis (Marshall *et al.*, 2007). The downstream effect of NFκB2 upon DSS colitis in C57BL/6J mice may involve CSF1. As *Csf1* null mice also have reduced up-regulation in pro-inflammatory cytokines, the blockage of *Csf1* likely leads to reductions in the expression of other cytokines. Using a neutralising anti-*Csf1* antibody, Marshall *et al.* (2007) showed that *Csf1* is involved in exacerbating inflammation in BALB/C mice with significantly less inflammation in the colon, as well as a decrease in the inflammatory infiltrate (Marshall *et al.*, 2007). The Csf1 protein is found circulating in the blood and is expressed on cell surfaces (Dai *et al.*, 2002). A lack of Csf1 on the surface of the epithelial cells of the colon could therefore potentially account for some of the reduced inflammation seen in NFκB2 null mice. It is also possible that circulating cells having deficiency in *Csf1* may cause the protective effect seen in C57BL/6J (NFκB2 null) mice. Additionally *Csf-1* is involved

in the control of macrophages; it is therefore possible that NFκB2 null mice experience less severe colitis due to the lack of Csf-1 controlled macrophages (Hamilton, 2008). Another gene investigated was TNF. TNF was up-regulated during the course of colitis, and was down-regulated in NFκB2 null mice compared to C57BL/6J mice. This cytokine is expressed in the mucosa during colitis and is actually dependant on CSF1 (Garcia *et al.*, 2016). It is therefore possible that one mechanism of DSS induction is via NFκB2 activation of *Csf1*, and *Csf1* activation of *Tnf*.

Cxcl10 is an attractant for T lymphocytes (Taub *et al.*, 1993), therefore the down-regulation of this protein in NFκB2 null mice may contribute to the protection from DSS colitis seen in NFκB2 null mice, particularly if this involves impaired formation of tertiary lymphoid structures (section 3.1). Although development of DSS colitis does not strictly require T lymphocytes in SCID mice, T cells will become involved in mouse strains which have normal immune systems (Chassaing *et al.*, 2014). CXCL10 and its receptor have been found to be overexpressed in human IBD biopsies, and colonic epithelial cells express CXCL10 in both UC and CD patients. The authors of this work concluded that the overexpression of CXCL10 in UC and CD patients occurs in both the immune compartment and the mucosal compartment (Ostvik *et al.*, 2013). The gene expression data from NFκB2 null vs C57BL/6J mice indicated that *Cxcl10* is down-regulated in the colonic mucosa of NFκB2 null mice. There was no significant up-regulation of this protein in C57BL/6J mice at day 8 of DSS compared to day 11. However the overall level at day 0 was not significantly different between C57BL/6J mice and NFκB2 null mice. This means that the C57BL/6J mice do not express more of the protein all the time. The difference lies only in the expression of the protein during DSS colitis. This indicates that there may be control of *Cxcl10* expression by NFκB2 or the alternative NFκB activation pathway. Another member of the cxc cytokine family, *Cxcl9,* has been proven to be up-regulated during DSS colitis (Ito *et al.*, 2006). Interferon gamma is a regulator of *Cxcl9* expression and this signalling

functions during Crohn's disease (Ito *et al.*, 2006) although the DSS model more closely resembles ulcerative colitis. Interferon gamma has been shown previously in our lab to be down-regulated in NFκB2 null mice compared to C57BL/6J wild-type mice during DSS colitis (Hanedi, 2013). *Cxcl9* is therefore also a possible candidate gene for contributing to the exacerbation of colitis in wild-type mice.

Bone marrow reconstitution studies employed full body irradiation of mice in order to destroy the bone marrow followed by tail vein injection of bone marrow from a donor mouse. This was successfully validated using tdTomato mice as bone marrow donors followed by subsequent examination of the bone marrow of C57BL/6J recipient mice by fluorescence microscopy. We can therefore be confident that the C57BL/6J and NFκB2 null mice used in the reconstitution study were successfully reconstituted with donor bone marrow.

We cannot exclude that irradiation and reconstitution may have influenced some of our bone marrow reconstitution results as we found no statistically significant differences between the C57BL/6J (C57BL/6J) mice and NFκB2 null (NFκB2 null) mice following DSS in the crypt survival assay. However NFκB2 null (C57BL/6J) mice were still protected from developing DSS induced colitis despite having C57BL/6J bone marrow. These mice showed a similar level of protection from DSS colitis as NFκB2 null mice. This suggests that NFκB2 predominantly functions in the epithelial compartment to exacerbate colitis. In both the crypt survival assay and the weight monitoring area under the curve analysis, NFκB2 null (C57BL/6J) mice were found to have significantly more crypt survival than C57BL/6J (C57BL/6J) mice and to show no significant difference compared to NFκB2 null (NFκB2 null) mice. C57BL/6J (NFκB2 null) mice had a crypt survival value between the two controls of C57BL/6J (C57BL/6J) and NFκB2 null (NFκB2 null) without showing a significant difference to either. One conclusion that could be drawn from this result is that these mice have partial protection derived from their NFκB2 null immune compartment. Therefore,

although the immune system being NFκB2 null appears to have a protective role in C57BL/6J mice, the introduction of a C57BL/6J immune system does not appear to convey susceptibility to DSS colitis upon NFκB2 null mice. In fact NFκB2 null mice which were reconstituted with C57BL/6J bone marrow appeared to be even less susceptible to colitis than NFκB2 null, with the weight monitoring data showing hardly any weight loss throughout the experiment. The overall conclusions from the data are that both the epithelial and the immune systems appear to contribute to DSS colitis, and that as the deletion of NFκB2 from the immune system partially protected the mice from developing DSS colitis, the lower DSS load experienced by the larger NFκB2 null mice is not responsible.

PCR assays were completed using the cDNA obtained from mucosal scrapes. This technique was used to investigate gene expression changes during the course of colitis and also in NFκB2 null mice compared with the wild-type. Although this technique only collects cells from the mucosa, the immune cells present in an inflamed mucosa will mean that in some cases a mucosa containing many immune cells would be compared to a mucosa containing few immune cells. However, our later findings in the irradiation and bone marrow reconstitution study suggested that the epithelial compartment probably has more of an impact on the degree of colitis than the immune compartment due to the increased protection against colitis seen in NFκB2 null mice with a C57BL/6J immune compartment. So although this technique is not ideal if the genes involved in colitis are mostly expressed in the mucosal compartment, and these are related to NFκB2 as we suspect, then the data would still be of interest. However use of a cell sorting technique to specifically isolate epithelial cells for testing would be useful in future experiments of this type.

4 The role of NFκB family members in regulating the enteroid response to chemotherapeutic drugs

4.1 Introduction

An important distinction between cancerous cells and normal cells is the abnormally rapid proliferation seen in cancer cells. Cancer treatments are often used to target rapidly proliferating cancer cells by disrupting the process of cell division. One consequence of this is that the rapidly dividing cells of the normal small intestine are often also affected by cancer treatments (Umar, 2010). This can lead to severe adverse effects which mean that continuation of treatment is not possible (Boussios *et al.*, 2012). The prevention of cytotoxicity to normal intestinal cells would therefore be extremely useful to patients to improve the safety and efficiency of their treatment. In this chapter experiments using murine small intestinal organoids, also known as enteroids (see section 1.6.2), were performed to investigate the direct effects of chemotherapeutic drugs on normal small intestinal epithelial cells.

Chemotherapy can cause mucositis, which in turn leads to diarrhoea, nausea and even death. Therefore, determining how chemotherapeutic drugs cause mucositis would allow treatments to target the cause more effectively (Pico, Avila-Garavito and Naccache, 1998). This would in turn lead to patients potentially tolerating higher doses of chemotherapy, and the continuation of treatments which would otherwise have to be halted due to their severe adverse effects. Mucositis occurs in the gut when chemotherapeutic agents cause a high rate of apoptosis in intestinal epithelial cells. These cells are affected due to the high rate of proliferation which occurs in the normal gut. It is commonly observed as the formation of ulcerative lesions in the gastrointestinal tract (section 1.4) - the mechanisms by which mucositis occurs are

however still unclear. However, it is well known that mucositis involves intestinal epithelial cell apoptosis (Keefe *et al.*, 2000).

As members of the NFκB family of transcription factors are known to regulate the responses of the intestine to inflammation and DNA damaging agents (Burkitt *et al.*, 2015), we hypothesised that they may additionally regulate the intestinal response to chemotherapeutic drugs. Therefore, NFκB subunit knockout mice were used to investigate whether there were any differences in the response to chemotherapeutic drugs. NFκB1 null, NFκB2 null, RelB null and c-Rel null mice were used, and wild-type C57BL/6J mice used as the control.

The drugs used were the chemotherapeutic agents etoposide, irinotecan and 5-fluorouracil (5-FU). Etoposide is a topoisomerase II poison (Montecucco and Biamonti, 2007). Topoisomerases use ATP to relax DNA supercoils which occur when the DNA double helix becomes too tightly coiled and forms a problematic secondary coil. Etoposide works by stopping topoisomerase II from being able to reattach the ligated DNA strands. Etoposide mediated cell death in neuroblastoma cells has been shown to be mediated by signalling via the classical NFκB activation pathway (Galenkamp *et al.*, 2015).

Irinotecan is a chemotherapeutic drug originally isolated from a Chinese/Tibetan ornamental tree (Rothenberg, 2001). Like etoposide it is also a topoisomerase inhibitor however it inhibits the topoisomerase I enzyme and is used to treat colon cancer (Yu *et al.*, 2005). Irinotecan is known to frequently cause mucositis in patients and irinotecan related mucositis predominantly manifests as diarrhoea (Bleiberg and Cvitkovic, 1996). Crypt apoptosis has been shown to be a prominent feature of the gut in rats treated with irinotecan, where NFκB activation by TNFα has also been shown to occur and tissue damage coincided with the location of NFκB subunit P65 expression (Bowen et al. 2006).

5-FU is a thymidylate synthase inhibitor used in the treatment of several different cancers including colorectal and breast cancer (Longley, Harkin and Johnston, 2003). The main mechanism of 5-FU induced cancer cell death is via DNA strand breaks, which triggers the DNA damage response. Similarly to irinotecan TNFα has been shown to be upregulated in the murine intestinal mucosa after 5-FU treatment, indicating an inflammatory response. Murine villi were also found to be shorter and smaller with narrower crypts in response to 5-FU treatment (Soares *et al.*, 2008). Interestingly probiotics have been shown to reduce the mucosal damage inflicted by 5-FU indicating a role for the microbiome in regulating the severity of 5-FU induced mucositis(Yeung *et al.*, 2015). Research into the effect of deletion of NFκB1 on the ability of 5-FU to inhibit colon cancer cell growth has shown that NFκB1 up-regulation is involved in resistance to the drug (Feistle *et al.*, 2012). RelA has also been shown to be upregulated in 5-FU resistant colon cancer cell lines (Körber *et al.*, 2016). This suggests that the canonical NFκB activation pathway may be involved in the resistance of cancer cells to 5-FU.

RelA (P65) and NFκB1 are already known to be activated by DNA damage (Zhou *et al.*, 1999). The alternative NFκB pathway members, RelB and NFκB2 and the classical pathway member c-Rel have all been implicated in resistance to apoptosis induced by DNA damage caused by ionising radiation (Sun *et al.*, 2007; Holley *et al.*, 2010; Lambros *et al.*, 2015). We therefore wanted to determine whether the genetic deletion of individual NFκB family proteins in small intestinal enteroids would alter the cell death response to chemotherapeutic drugs.

4.2 Results

4.2.1 Validation of circularity scoring method in enteroids

Circularity as a method of investigating cell death in enteroids has been previously investigated in our lab following TNF treatment (Jones and Duckworth unpublished). Circularity differences between organoids are demonstrated in figure 4.2. Standard light microscopy images of enteroids were taken and ImageJ was used to determine how circular enteroid circumferences became post treatment. It was found that an increase in cell death (measured by active caspase-3 immunohistochemistry) correlated with an increase in enteroid circularity. Here, validation of the circularity scoring method was undertaken to determine whether increased apoptotic cell death was also associated with an increase in the circularity of enteroids following treatment with etoposide and 5-FU. This was conducted in order to verify that the increase in circularity of enteroids was not specific to TNF treatment, as previously observed (Jones and Duckworth, unpublished). As etoposide and irinotecan are both topoisomerase inhibitors this validation was only done using etoposide. 5-FU treatment was also used for validation.

In order to validate whether an increase in cell death caused an increase in circularity, both circularity and apoptosis were measured in enteroids that had been treated with 50µM etoposide or 50µM 5-FU for up to 24 hours in order to provide some organoids with variable degrees of cell death. Apoptosis was measured using active caspase-3 immunohistochemistry (figure 4.1A) and H+E staining (figure 4.1B). This enabled the identification of apoptotic cells by two separate methods. The total number of cells in each 4µm section was counted, and the number of apoptotic cells was counted using the counter plug in on image J. Six enteroids were examined per time point.

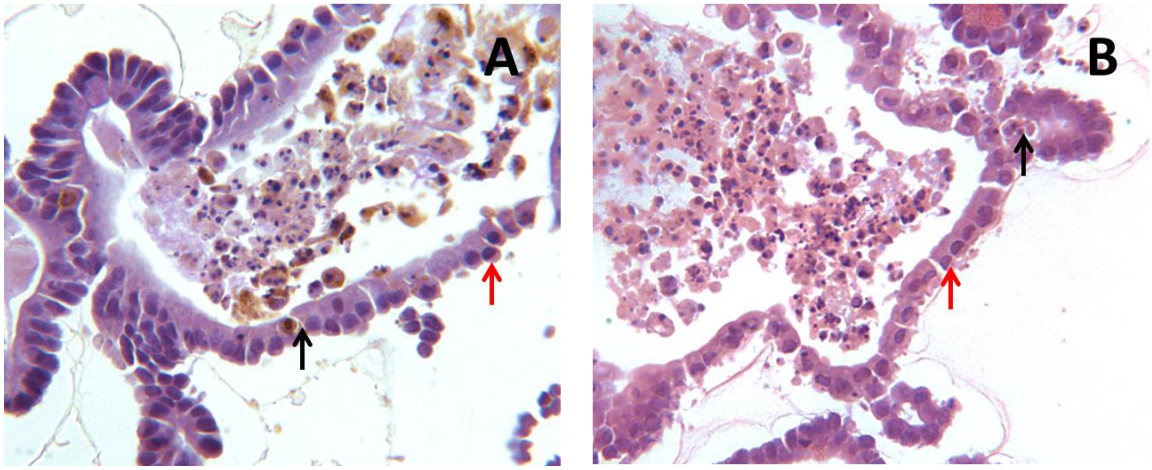

Figure 4.1 Four micron sections of paraffin embedded enteroids showing both methods of detection of the amount of apoptosis. Panel A shows an active caspase-3 stained enteroid and B shows an H+E stained section. Normal cells are indicated with red arrows and apoptotic cells are indicated with black arrows. In order to calculate the amount of apoptosis in an embedded enteroid the total number of live epithelial cells of the enteroid appearing in the 4µm section was counted, and then the total number of apoptotic cells in continuity with the epithelium was counted and the percentage was calculated.

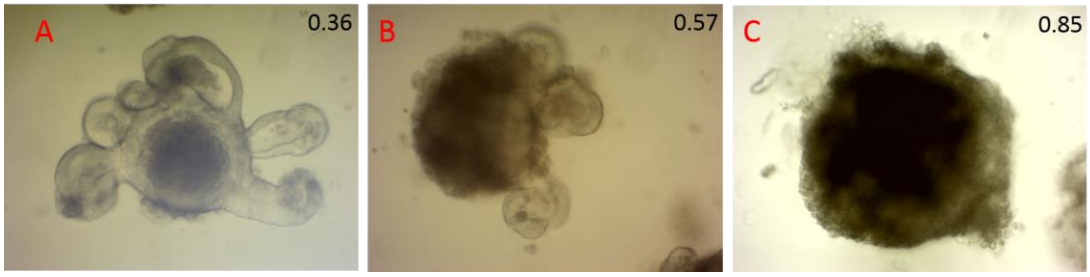

Figure 4.2. Illustration of circularity method. Circularity score shown in top right hand corner. Healthy enteroid (A), organoid with increased cell death (B), organoid with completely disrupted phenotype (C).

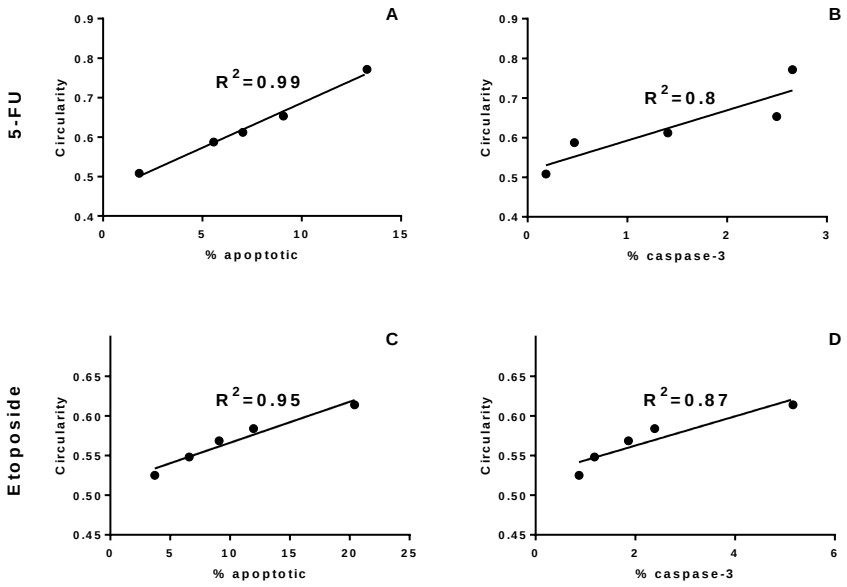

Figure 4.3 Validation data for enteroids treated with 50µM 5-FU (A and B) and 50µM etoposide (C and D) at various time points up to 24 hours. Graphs A and C show the correlation between the number of epithelial cells which showed apoptotic morphology (x-axis) and the mean average circularity (y-axis). Graphs B and D show the correlation between the number of epithelial cells which were positive for active caspase-3 (x-axis) and the average circularity (y-axis). The circularity and apoptosis of 6 enteroids were measured per time point. R^2 values are shown on the graph.

The relationship between apoptosis and circularity was strong in enteroids treated with 5-FU and etoposide. The R^2 values were all above 0.8 which indicates that there is a very strong linear relationship between the apoptosis measurement and circularity assessment (figure 4.3). Additionally this indicates that the likelihood that circularity is a reliable measure of the amount of apoptosis in this system is high. These results support the hypothesis that there is a correlation between circularity and the amount of cell death in enteroids.

4.2.2 Chemotherapeutic drugs caused a rapid initiation of enteroid cell blebbing and apoptosis

Epithelial cell blebbing and shedding in enteroids takes place both into the lumen and the outside of the enteroid. Epithelial cell shedding into the enteroid lumen can only be seen using light microscopy as a 'darkening' of the lumen as it fills up with dead cells. However the blebbing of apoptotic cells onto the outside of the enteroid can be more readily observed. In order to investigate the effect of etoposide, 5-FU and irinotecan on enteroids, early time point images were taken at 0, 4, 8, 16 and 24 hours and representative examples are shown in figure 4.4. These revealed that the initial responses to the chemotherapeutic drugs involved apoptotic cells being expelled from the epithelium onto the outside of the enteroid. These cells were subsequently detached from the enteroid into the surrounding matrix and media.

When C57BL/6J enteroids were treated with 10µM etoposide, the first sign of this epithelial cell blebbing occurred around 16 hours after the start of treatment (figure 4.4D). From this point epithelial cells then began to rapidly accumulate on the outside of the enteroid, indicating abundant pathological cell apoptosis and blebbing. When the C57BL/6J enteroids were exposed to etoposide for 24 hours, many of them showed a disrupted enteroid phenotype which consisted of several dead cells and the lack of an intact epithelium (figure 4.4E). In 5-FU treated enteroids cell blebbing also began at around 16 hours (figure 4.4J). However this blebbing did not appear to happen in as large amounts as with etoposide. This indicates that the onset of the cytotoxic effect of 5-FU was less intense after 16 hours than in etoposide treated enteroids. The majority of the enteroids had intact epithelia at 24 hours after 10µM 5-FU treatment. Irinotecan was the final chemotherapeutic drug used to treat C57BL/6J enteroids. These enteroids began to shed cells onto the outside of the enteroid at around 24 hours (figure 4.4O). The enteroids retained an intact epithelium and did not develop a disrupted phenotype at the same dose and time point observed

following the other tested drugs. This indicates that at this dose irinotecan was the least potent of the three chemotherapeutics at inducing direct enteroid cytotoxicity.

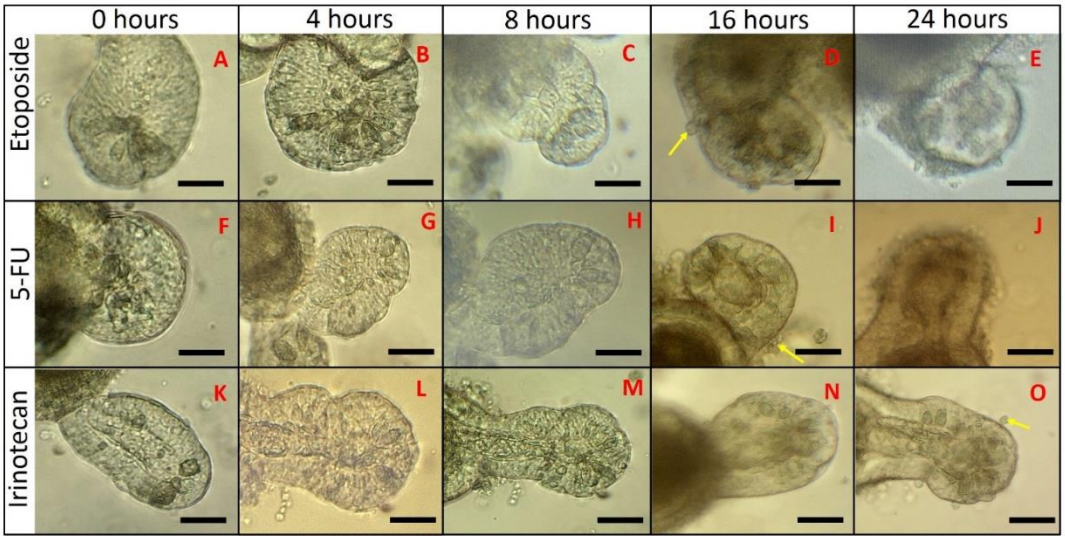

Figure 4.4 Early time point images of enteroids treated with 10μM etoposide (A to E) 10μM 5-FU (F to J) and 10μM Irinotecan (K to O). Pictures were taken at 0 hours, 4 hours, 8 hours, 16 hours and 24 hours. The first observed blebbing epithelial cells are indicated by yellow arrows. Cells began to bleb after around 16 hours for Etoposide and 24 hours for 5-FU. Scale bar 20μm.

4.2.3 Treatment of NFκB-null enteroids with chemotherapeutic agents

Chemotherapeutic drugs were next administered to enteroids derived from C57BL/6J, NFκB1 null, c-Rel null, RelB null and NFκB2 null mice. These enteroids were passaged at least once, and were treated with the chemotherapeutic drugs 3 days after passaging, once they had obtained a suitable size, due to the fact that in the first few days of growth enteroids are round with no crypt domains protruding (section

1.6.3). Their circularity was measured using imageJ shape descriptors using the formula $4\pi(\text{area})/\text{perimeter}^2$.

The enteroids were treated with etoposide, 5-FU and irinotecan. Representative enteroids are shown for each genotype at the highest treatment concentration (50μM) in figure 4.5 (etoposide), figure 4.7 (5-FU) and figure 4.9 (irinotecan).

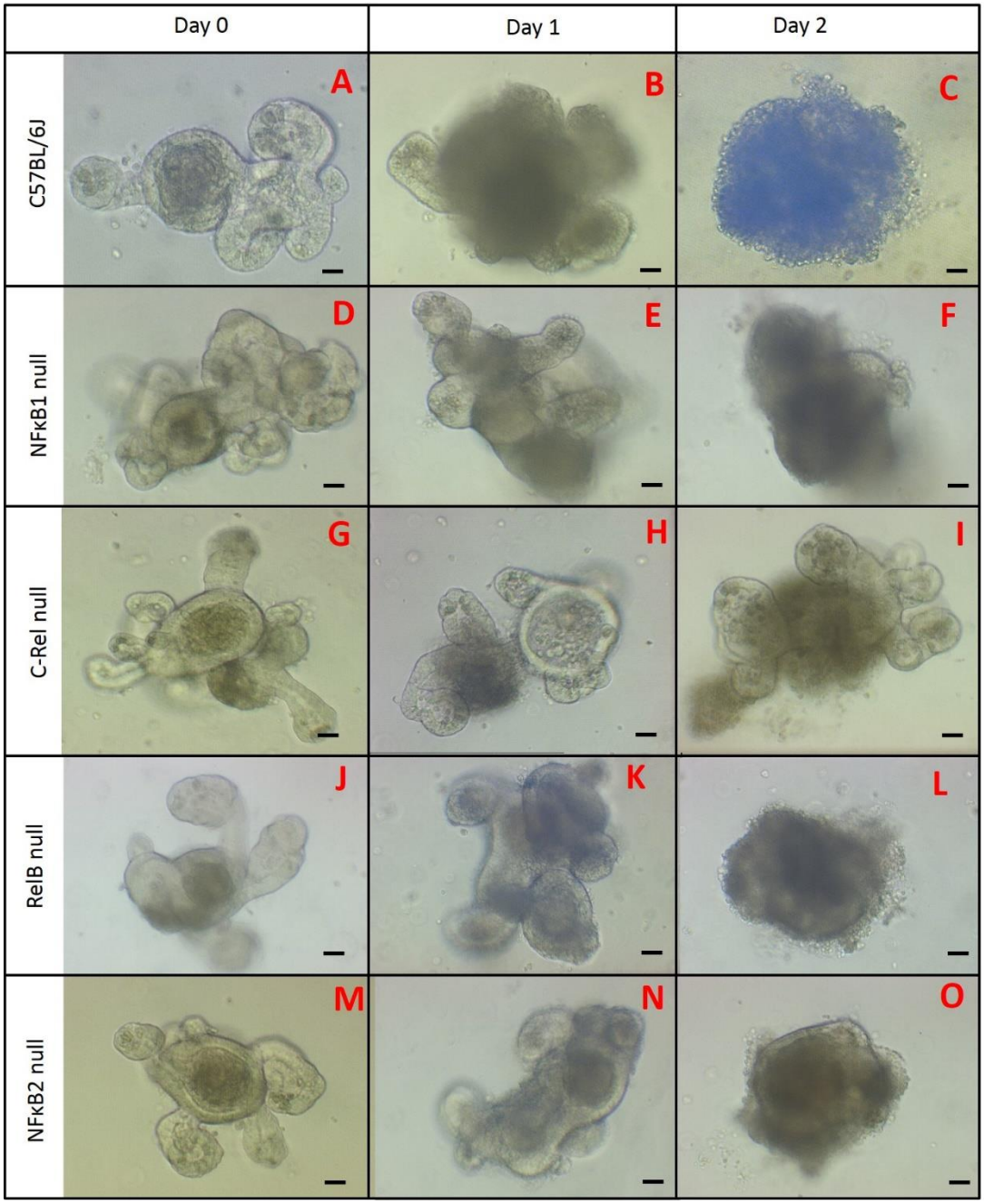

Figure 4.5 Enteroids treated with 50µM etoposide showed signs of increased cell death from day 0 to day 2. C57BL/6J (A to C), NFκB1 null (D to F), c-Rel null (G to I), RelB null (J to L) and NFκB2 null (M to O). Representative enteroid shown for each time point. Scale bars 20µM.

4.2.4 Etoposide caused cell death in C57BL/6J enteroids

C57BL/6J enteroids were treated with etoposide at 1µM, 5µM, 10µM and 50µM concentrations with a DMSO control containing an equivalent volume of DMSO (figure

4.6). The control enteroids showed no significant differences in circularities on day 0 (0.44±0.038), day 1 (0.43±0.007) and day 2 (0.43±0.051) suggesting that baseline circularity values were stable. When treated with 1μM and 5μM etoposide there were also no significant differences in circularity between day 0, day 1 and day 2. However 10μM etoposide caused enteroid circularity to increase significantly from 0.43±0.011 on day 0 to 0.53±0.032 on day 1 ($P=0.034$) and 0.61±0.088 on day 2 ($P=0.0001$). 50μM etoposide similarly caused the circularity to increase significantly from 0.44±0.035 on day 0 to 0.60±0.088 on day 1 ($P=0.0003$). Circularity rose further to 0.71±0.058 on day 2, which was significant compared to both day 0 ($P<0.0001$) and day 1 ($P=0.021$). This suggests that significant amounts of apoptosis were present 48hrs following 10-50μM etoposide treatment of C57BL/6J enteroids.

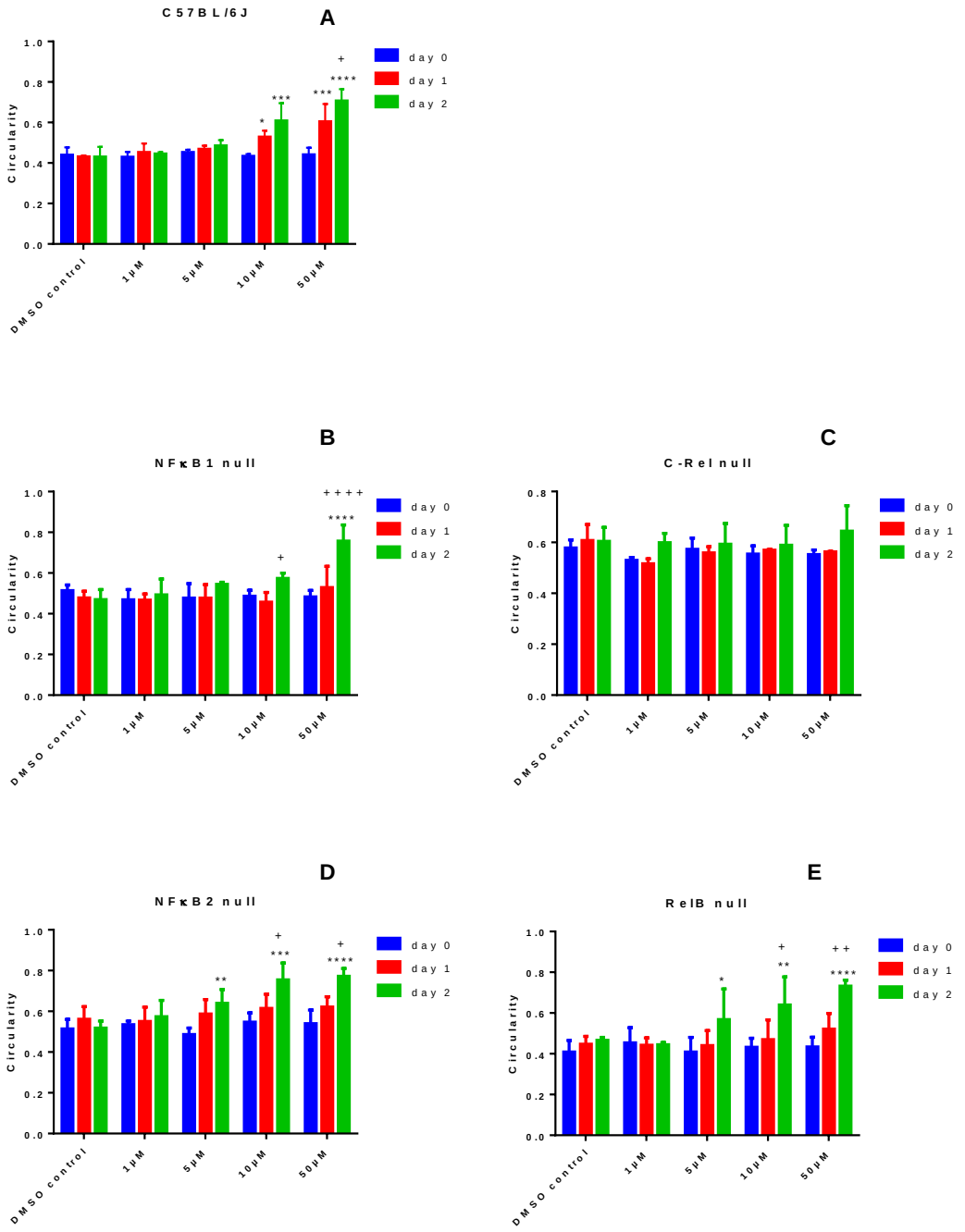

Figure 4.6 Etoposide treatment of C57BL/6J (A), NFκB1 null (B), c-Rel null (C), NFκB2 null (D) and RelB null (E) enteroids. Enteroids were treated with DMSO, 1μM, 5μM, 10μM or 50μM etoposide over 2 days. Circularity measurements were taken at day 0, day 1 and day 2 (48 hours). Six enteroids were measured per well, and two wells of each treatment were measured per experiment. The experiments were carried out in triplicate. Average circularity from N=3 is shown with standard deviations. * represents significance compared to day 0, and + represents significance compared to day 1. P values are as follows *=P<0.05 **=P<0.01 ***=P<0.001 ****=P<0.0001. +=P<0.05 ++=P<0.01 ++++=P<0.0001.

4.2.5 Etoposide was less effective at causing cell death in NFκB1 null enteroids

There were no significant difference in circularity between day 0 (0.51±0.027), day 1 (0.48±0.033) and day 2 (0.47±0.050) in control NFκB1 null enteroids suggesting that baseline circularity values were stable. NFκB1 null enteroids treated with 1μM etoposide showed a slight non-significant increase in circularity from 0.469±0.050 at day 0, to 0.467±0.030 on day 1 and 0.49±0.077 on day 2. When enteroids were treated with 5μM etoposide the day 0 (0.48±0.07) and day 1 (0.48 0.07) circularities remained the same, with an increase in circularity only being observed at day 2 (0.54±0.010). However this was not found to be statistically significant. Enteroids treated with 10μM etoposide showed a significant increase in circularity from day 0 to day 2 (0.57±0.026; P=0.037). Similarly NFκB1 null enteroids treated with 50μM etoposide showed a significant increase in circularity from day 0 to day 2 (0.76±0.079; P<0.0001). As NFκB1 null enteroids did not show a significant increase in circularity by day 1 following 10μM etoposide treatment, we conclude that etoposide had less of an effect on them compared with wild-type C57BL/6J enteroids. It was also noted that visually these enteroids remained mostly normal in appearance with intact epithelia at day 1 (figure 4.5D to F). After this there was a rapid increase in cell death and deterioration of the epithelial layers by day 2.

4.2.6 C-Rel deletion protected enteroids from etoposide induced cell death

There were no significant increases in circularity between day 0 (0.58±0.031), day 1 (0.61±0.063) and day 2 (0.60±0.055) in DMSO treated control c-Rel null enteroids. There were also no significant changes in circularity following treatment with any of the concentrations of etoposide at any time point. This indicates that the c-Rel protein may be involved in regulating the initiation of etoposide induced cell death. Although no significance was found at any concentration, there did appear to be a pattern of

increase at the two highest concentrations which indicates that c-Rel deletion does not give complete protection from the effects of etoposide. The large standard deviations seen at day 2 however indicate that some enteroids were very much affected by etoposide whereas others were not. This may indicate that slight differences in the position in the distal small intestine have an impact on the cell death that occurs despite the lack of c-Rel. Additionally this may indicate that some stem cell clones are sensitive whereas others are not. The appearance of the c-Rel null enteroids did indicate that there was an increase in cell death and epithelial cell blebbing (figure 4.5 G to I), with a darkening of the centre of the enteroids indicating that the lumen contained increased numbers of dead cells. However there were no difference between these and untreated c-Rel null enteroids at the same time point.

4.2.7 NFκB2 deficiency resulted in lower concentrations of etoposide being needed to cause a significant increase in cell death

In DMSO treated control NFκB2 null enteroids no significant differences were seen in circularity between day 0 (0.51±0.046), day 1 (0.56±0.062) and day 2 (0.52±0.034). NFκB2 null enteroids treated with 1μM etoposide also showed no significant differences increases in circularity. There was a significant increase in circularity seen in enteroids treated with 5μM etoposide from a day 0 circularity of 0.49±0.032 to a day 2 circularity of 0.64±0.067 (P=0.0085), although there was no significant difference between day 0 and day 1 (0.59±0.071) or day 1 and day 2. Enteroids treated with 10μM etoposide showed no significant change in circularity between day 0 (0.55±0.045) and day 1 (0.61±0.069). The day 2 circularity was however significantly higher than both day 0 (P=0.0004) and day 1 (P=0.017) with a circularity of 0.755±0.082. Enteroids treated with 50μM etoposide again did not show a significant increase between day 0 (0.54±0.007) and day 1, but did show a significant increase in circularity between day 0 and day 2 at 0.77±0.038 (P<0.0001) and day 1 and day 2 (P=0.010). The NFκB2 null enteroids were more sensitive to the lower

concentrations of etoposide than the C57BL/6J enteroids, but they appeared to take longer to respond to 10µM and 50µM concentrations of etoposide. This was also observed on examination of the enteroids with many of them appearing normal after the first day of treatment, with the sudden onset of a disrupted phenotype apparent by day 2 (figure 4.5 M to O).

4.2.8 Etoposide treatment was more effective at causing cell death in RelB null enteroids than in C57BL/6J enteroids

RelB null enteroids again showed no significant differences between the circularity of untreated controls between day 0 (0.41±0.057), day 1 (0.45±0.038) and day 2 (0.47±0.015). Following 1µM etoposide there was also no significant change in circularity between day 0 (0.45±0.074), day 1 (0.44±0.036) and day 2 (0.45±0.010). However, RelB enteroids were affected by a lower concentration of etoposide than C57BL/6J enteroids, with significant increases in circularity being seen following 5µM treatment similarly to NFκB2 null enteroids. Although the RelB null enteroids showed no significant difference from day 0 (0.41±0.072) to day 1 (0.44±0.073), there was a significant increase from day 0 to day 2 (0.57±0.15; P=0.034) when treated with 5µM etoposide. There was no significant difference between day 1 and day 2. RelB null enteroids treated with 10µM etoposide had a circularity of 0.43±0.045 on day 0 and 0.47±0.096 on day 1, which increased significantly to 0.64±0.14 on day 2 (P=0.0052 compared to day 0 and P=0.024 compared to day 1), as was the case in NFκB2 null enteroids. RelB null enteroids treated with 50µM etoposide had circularity measurements at day 0 of 0.43±0.047 and day 1 of 0.52±0.077 with no significant difference. The day 2 circularity of 0.73±0.029 was however significantly increased compared to both day 0 (P<0.0001) and day 1 (P=0.0045) which was again similar to the results observed in NFκB2 null enteroids. Phenotypic changes in RelB null enteroids treated with 50µM etoposide were very pronounced (figure 4.5J to L), with the loss of the lumen and disruptions of epithelial layers being apparent in all

enteroids by day 2, although not many enteroids showed this disrupted appearance on day 1. RelB null enteroids therefore appeared to be more sensitive to a lower concentration of etoposide (5µM), but took a longer time to react to the drug at 10µm and 50µM.

4.2.9 5-FU treatment caused increased circularity of C57BL/6J enteroids

We wanted to determine whether similar responses were observed in enteroids that had been treated with other chemotherapy agents. There were no significant differences in circularity at day 0 (0.41±0.043), day 1 (0.37±0.058) and day 2 (0.42±0.056) in untreated wild-type C57BL/6J enteroids. There were also no significant differences seen when C57BL/6J enteroids were treated with 1µM 5-FU between day 0 (0.38±0.038) and day 1 (0.44±0.029); the slight increase in circularity observed on day 2 (0.41±0.038) was also not significant. There were also no significant differences seen between enteroids following treatment with 5µM 5-FU. There was however a significant increase in circularity following 10µM 5-FU with circularities of 0.39±0.036 on day 0 and 0.60±0.11 on day 2 ($P=0.0007$). A significant increase in circularity was also found in enteroids treated with 50µM 5-FU between day 0 (0.43±0.059) and day 1 (0.57±0.12; $P=0.030$) and between day 0 and day 2 (0.69±0.077; $P<0.0001$). As there was no significant difference between day 1 and day 2 following the highest concentration treatment, it is likely that this result was due to a rapid increase in circularity. This was also indicated by the morphological changes observed in the enteroids with enteroids beginning to appear disrupted at 24 hours after beginning to display blebbed cells at 16 hours, and showing significant cell death at 24 hours (figure 4.7A to C).

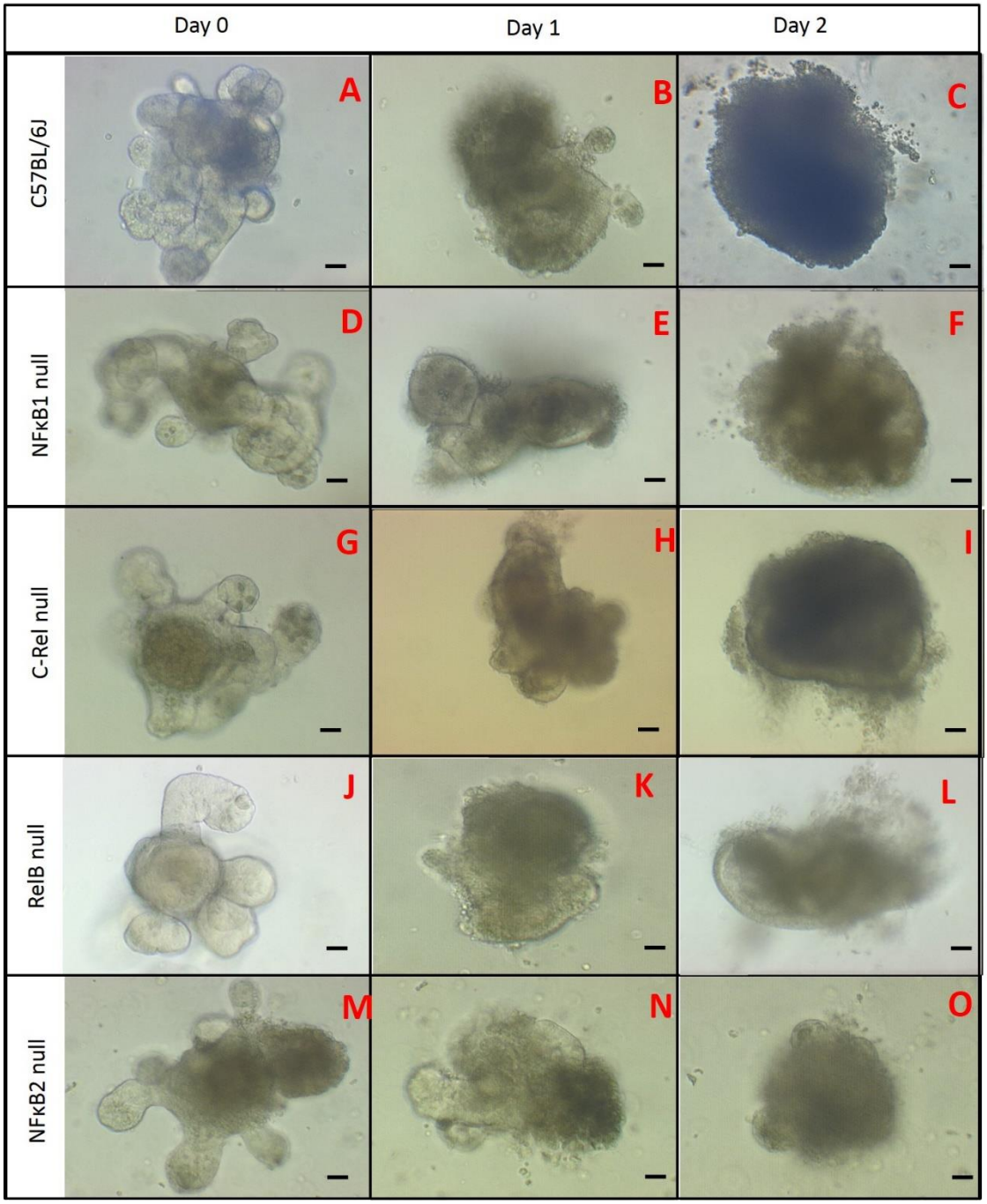

Figure 4.7 Enteroids were treated with 50µM 5-FU from day 0 to day 2. C57BL/6J (A to C), NFκB1 null (D to F), c-Rel null (G to I), RelB null (J to L) and NFκB2 null (M to O). Representative enteroids are shown. Scale bar 20µM.

4.2.10 NFκB1 null enteroids responded similarly to C57BL/6J enteroids following treatment with 5-FU

The NFκB1 null untreated control enteroids showed similar circularities on day 0 (0.50±0.017), day 1 (0.46±0.035) and day 2 (0.51±0.013). No significant difference in circularity was found between day 0, day 1 and day 2 when enteroids were treated with 1μM or 5μM 5-FU. 10μM 5-FU treated NFκB1 null enteroids began to round up resulting in circularity values of 0.56±0.078 at day 1, which increased significantly to 0.69±0.049 on day 2 (P=0.0163). Enteroids treated with 50μM 5-FU also showed significant increases in circularity to 0.63±0.065 at day 1 and 0.76±0.042 on day 2. The NFκB1 null enteroids showed similar increases in circularity as C57BL/6J enteroids following treatment with the two highest concentrations of 5-FU. The time point of these morphological changes was different however, with C57BL/6J enteroids responding at a later time point. This may mean that the response to 5-FU was delayed compared with the C57BL/6J enteroids. Examination of the morphology of the enteroids indicated that there were increased numbers of shed cells accumulating in the lumen of C57BL/6J enteroids by day 1, however the epithelia of these enteroids were largely still intact (figure 4.8B). The vast majority of enteroids regardless of genotype (C57BL/6J or NFκB1 null) demonstrated a disrupted phenotype by day 2 (figure 4.8F).

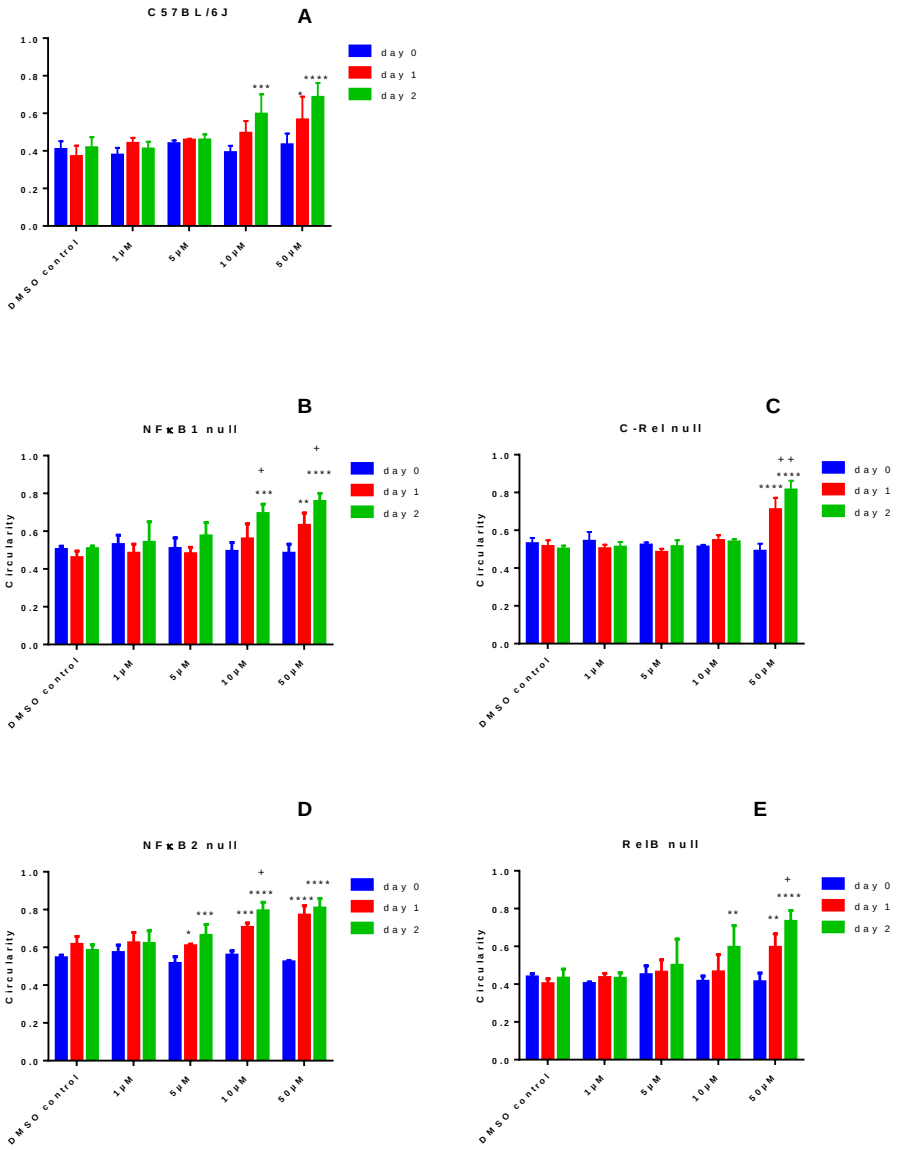

Figure 4.8 5-FU treatment caused increased circularity in C57BL/6J, NFκB1 null, RelB null and NFκB2 null and c-Rel null enteroids. Enteroids were treated with DMSO only, 1μM, 5μM, 10μM or 50μM 5-FU over 2 days. Circularity measurements were taken at day 0 (0 hours), day 1 (24 hours) and day 2 (48 hours). Six enteroids were measured per well, and two wells of each treatment were measured per experiment. The experiments were carried out in triplicate. Average circularity from N=3 is shown with standard deviations. * represents significance compared to day 0, and + represents significance compared to day 1. P values are as follows *=P<0.05 **=P<0.01 ***=P<0.001 ****=P<0.0001. +=P<0.05 ++=P<0.01.

4.2.11 C-Rel null enteroids were less sensitive to 5-FU than C57BL/6J enteroids

The circularity of DMSO treated c-Rel null enteroids remained very similar between day 0 (0.53±0.030), day 1 (0.51±0.033) and day 2 (0.50±0.017). There were no significant differences in the circularity of c-Rel null enteroids treated with 1μM 5-FU with slight decreases seen in mean circularity from day 0 (0.54±0.050) to day 1 (0.50±0.021) and day 2 (0.51±0.027) as with wild-type enteroids. There were also no significant differences in the circularity of c-Rel null enteroids treated with 5μM 5-FU when comparing day 0 (0.52±0.014), day 1 (0.48±0.018) and day 2 (0.51±0.034). In contrast to C57BL/6J enteroids however there were no significant increases in the circularity of 10μM 5-FU treated c-Rel null enteroids from day 0 (0.51±0.011) to day 1 (0.55±0.027) or day 2 (0.54±0.014). There was a significant increase in circularity following 50μM 5-FU from day 0 (0.49±0.039) to day 1 (0.71±0.063; $P<0.0001$), followed by a significant increase from day 1 to day 2 (0.81±0.048; $P=0.0016$). The c-Rel null enteroids showed the typical darkening of the lumen which indicates a build-up of dead cells (figure 4.7H) and the vast majority demonstrated evidence of a disrupted phenotype as shown in figure 4.7I by day 2. C-rel null enteroids were therefore less sensitive to 5-FU induced cell death as they were not significantly affected by any but the highest concentration (50μM) of this drug.

4.2.12 NFκB2 null enteroids were more sensitive to 5-FU than C57BL/6J enteroids

DMSO treated control NFκB2 enteroids showed no significant differences between day 0 (0.55±0.013), day 1 (0.616±0.042) and day 2 (0.58±0.031). There were also no significant differences between day 0 (0.57±0.040), day 1 (0.62±0.055) and day 2 (0.62±0.067) following 1μM 5-FU. In enteroids treated with 5μM 5-FU, significant increases were found in circularity between day 0 (0.52±0.035) and day 1 (0.61±0.008; $P=0.02$). This was in contrast to C57BL/6J enteroids which were not

affected by this concentration of 5-FU. There was a significant increase between day 0 at 0.47±0.021 and day 1 at 0.71±0.023 (P=0.0003), and between day 1 and day 2 at 0.79±0.045 (P=0.034) in NFκB2 null enteroids treated with 10μM 5-FU. Enteroids treated with the highest concentration of 5-FU (50μM) were found to show a significant difference in circularity between day 0 at 0.52±0.005 and day 1 at 0.77±0.049 (P<0.0001). However no difference was found between day 1 and day 2 at 0.81±0.050 (P=0.50). This indicates that at the highest concentration of 5-FU tested the enteroids reached their peak circularity very quickly, with the disrupted phenotype becoming predominant at day 1 (figure 4.7N).

4.2.13 RelB null enteroids had a similar response to 5-FU as C57BL/6J enteroids

RelB enteroids treated with DMSO again showed no difference in circularity between day 0 (0.44±0.017), day 1 (0.40±0.025) and day 2 (0.43±0.048). RelB null enteroids treated with 1μM 5-FU also showed no significant differences in circularity between these days. RelB null enteroids treated with 5μM 5-FU showed a slight increase in circularity to 0.46±0.065 and 0.50±0.138 on days 1 and 2 respectively. However no significant differences were found at this concentration. Enteroids treated with 10μM 5-FU did however show statistically significant increases in circularity between day 0 (0.42±0.027) and day 2 (0.60±0.12; P=0.0052). Representative RelB null enteroids for each time point are shown in figure 4.7J to L. The enteroids began to lose their epithelial integrity at day 1 and contained large numbers of dead cells, evidenced by the darkened lumen. The enteroids were almost all completely disrupted by day 2, although some enteroids remained highly circular and still showed evidence of intact epithelia (figure 4.7L).

4.2.14 Irinotecan caused increased cell death in C57BL/6J enteroids

DMSO treated control C57BL/6J enteroids had a day 0 circularity of 0.44±0.034, a day 1 circularity of 0.44±0.013 and a day 2 circularity of 0.49±0.064. No significant changes in circularity were found between days in DMSO treated controls. C57BL/6J enteroids treated with 1μM or 5μM irinotecan showed no significant difference in circularity over 2 days of treatment. However, enteroids treated with 10μM irinotecan showed a significant increase in circularity between day 0 and day 2 (P=0.0004). As expected, the highest concentration of irinotecan caused the most significant increase in enteroid circularity. When treated with 50μM irinotecan, C57BL/6J enteroids showed a significant increase in circularity to 0.61±0.082 at day 1 (P=0.0007) and 0.72±0.048 at day 2 (P<0.0001; figure 4.10A). The phenotypical changes seen at the highest concentration are shown by representative enteroids in figure 4.9A to C. It is evident that the majority of enteroids had developed a disrupted phenotype by day 1, with very few enteroids being observed with intact epithelia.

4.2.15 Irinotecan was less effective at causing cell death in NFκB1 null enteroids

NFκB1 null DMSO treated control enteroids did not show any difference in circularity between day 0 (0.50±0.044), day 1 (0.50±0.27) and day 2 (0.49±0.055). There were also no differences seen in 1μM irinotecan treated NFκB1 null enteroids between day 0 (0.52±0.053), day 1 (0.52±0.042) or day 2 (0.47±0.019). There were also no differences seen in enteroids treated with 5μM between days 0 (0.53±0.031), 1 (0.51±0.069) and 2 (0.50±0.043). Unlike the C57BL/6J enteroids, no significant increases in circularity were observed following 10μM irinotecan treatment. Circularity remained relatively constant between day 0 at 0.53±0.051, day 1 at 0.51±0.037 and day 2 at 0.51±0.025. Enteroids treated with 50μM irinotecan however showed significant increases in circularity between day 1 at 0.56±0.054 and day 2 at 0.665±0.095 (P=0.038) but not between day 0 (0.49±0.017) and day 1 (figure 4.9B).

This suggests that irinotecan was slow to cause cell death even at the highest concentration tested, as it only began to induce morphological changes around day 1. Even at the highest concentration many of the enteroids still maintained epithelial cell layer integrity (figure 4.9F) with some crypt buds remaining. This was in contrast to the C57BL/6J enteroids which were completely disrupted and highly circular at this timepoint.

4.2.16 Irinotecan was more effective at causing cell death in c-Rel null enteroids

C-Rel null DMSO treated control enteroids began with a day 0 circularity of 0.58±0.032 which increased slightly at day 1 to 0.65±0.009, and decreased again at day 2 to 0.59 0.035. No significant differences were found when the circularity data were compared. When treated with 1µM irinotecan, c-Rel null enteroids showed no statistically significant differences in circularity over the course of the experiment. Enteroids treated with 5µM irinotecan had an initial baseline circularity of 0.56±0.078, which increased slightly to 0.62±0.042 at day 1 and significantly increased to 0.72±0.041 at day 2 ($P=0.020$). This was in contrast to the C57BL/6J enteroids. Although the C57BL/6J enteroids showed a pattern of increased circularity following both 1µM and 5µM treatments, with irinotecan these differences were not statistically significant. 10µM irinotecan treated c-Rel null enteroids began with a circularity of 0.56±0.029 which increased to 0.62±0.034 at day 1, however no statistical significance was found although there was a significant increase in circularity from day 1 to day 2 (0.74±0.0105; $P=0.012$). 50µM irinotecan treated c-Rel null enteroids had an initial circularity of 0.55±0.10 which increased to 0.61±0.032 at day 1 and again to 0.81±0.057 at day 2. However, statistical significance was only found between day 1 and day 2 ($P<0.0001$), indicating a potentially slower response to irinotecan even though the c-Rel null enteroids were more sensitive at lower concentrations when compared with C57BL/6J enteroids (figure 4.10C).

Morphological changes observed in c-Rel null enteroids when treated with 50μM irinotecan are shown in figure 4.9G to I. Most of the c-Rel null enteroids at day 1 had a darkened lumen indicating the presence of several dead shed cells, but otherwise a relatively normal phenotype was maintained with many enteroid buds still being evident (figure 4.9H). However at day 2 of the irinotecan treatment the enteroids mostly showed a disrupted phenotype (figure 4.9I).

4.2.17 Irinotecan was less effective at causing cell death in NFκB2 null enteroids than C57BL/6J enteroids

In the DMSO treated NFκB2 null enteroids the initial circularity at day 0 was 0.59±0.075, at day 1 it was 0.595±0.082 and at day 2 it was 0.63±0.087. When treated with 1μM or 5μM irinotecan NFκB2 null enteroids showed no significant differences in circularity at any time point tested. When treated with 10μM irinotecan the NFκB2 enteroids had an initial circularity of 0.54±0.035, which increased to 0.69±0.079 on day 1 and to 0.77±0.11 on day and this was statistically significant (P=0.010; figure 4.10D). The pattern of increased circularity with each of the treatments is evident from the graph. The large standard deviation seen may indicate that there was variation between the sensitivity of the enteroids, perhaps due to slight differences in sensitivity due to the position in the proximal small intestine or intestinal stem cell population. At the highest concentration of irinotecan the majority of NFκB2 null enteroids looked relatively normal at day 1 (figure 4.9N), however some enteroids displayed the disrupted phenotype at this stage. By day 2 NFκB2 null enteroids all displayed the disrupted phenotype (figure 4.9O).

4.2.18 Irinotecan was less effective at causing cell death in RelB null enteroids compared with C57BL/6J

DMSO control treated RelB null enteroid circularity stayed consistent over the 3 days of treatment, with day 0 at 0.45±0.035, day 1 at 0.45±0.074 and day 2 at 0.48±0.037. In RelB null enteroids treated with either 1µM or 5µM irinotecan there was no significant change in circularity over the time course of the experiment from 0-2 days. In contrast to circularity changes following 10µM irinotecan in C57BL/6J enteroids, 10µM irinotecan did not cause any significant changes in RelB null enteroid circularity between day 0 (0.44±0.098), day 1 (0.46±0.083) and day 2 (0.50±0.070). A significant increase in circularity was however observed between day 0 and day 2 in RelB null enteroids treated with 50µM irinotecan. The enteroids began with a circularity of 0.43±0.090, the day 1 circularity was 0.49±0.054 which then increased at day 2 to 0.67±0.060. These enteroids were particularly resistant to apoptosis as unlike other genotypes there was no obvious pattern of increase in circularity from day to day. When treated with the highest concentration of irinotecan, the morphology of RelB null enteroids was relatively normal at day 1 (figure 4.9K), however they did become highly disrupted at day 2 (figure 4.9L).

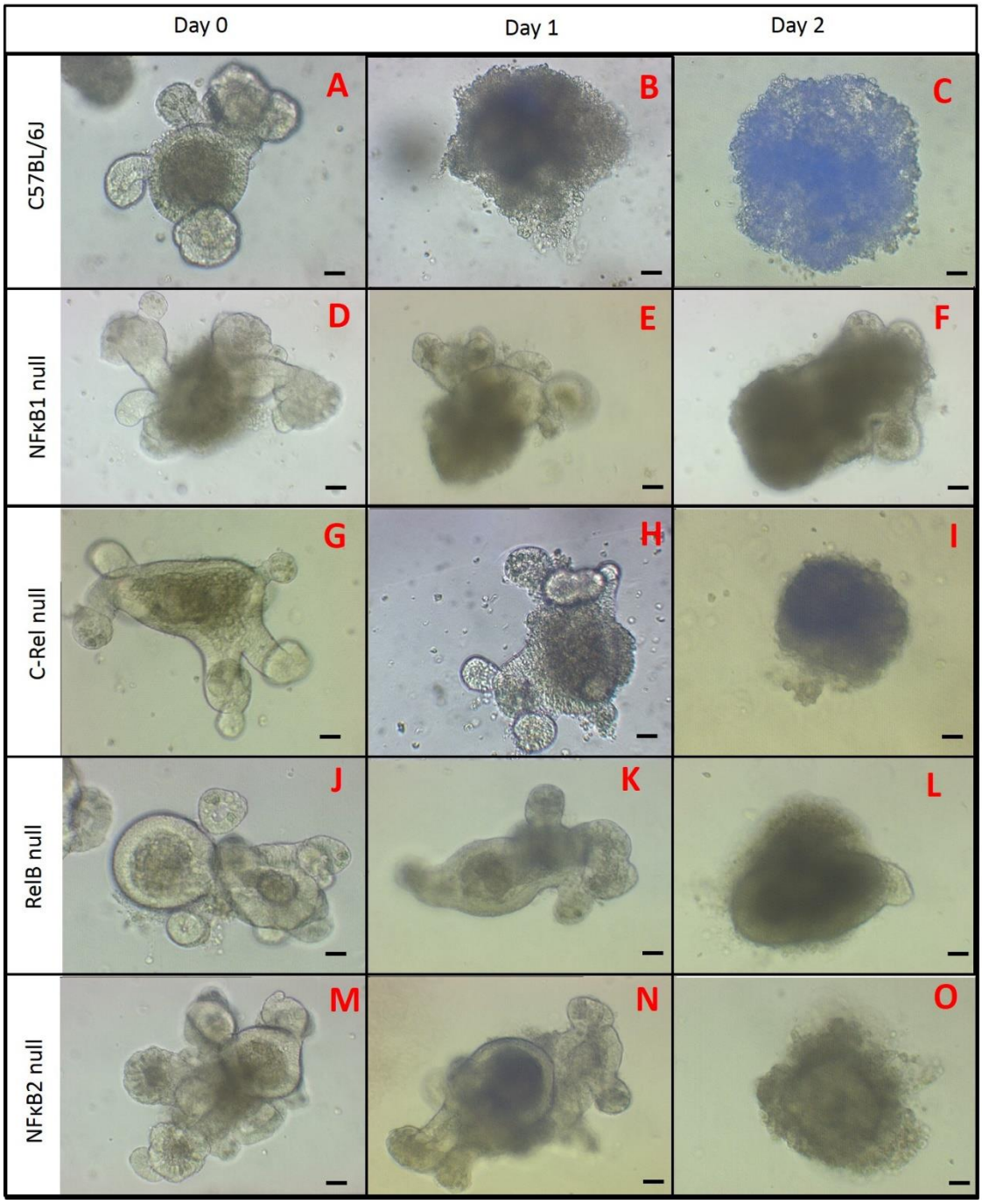

Figure 4.9 Enteroids treated with 50µM irinotecan showed signs of increased cell death. Enteroids are shown from day 0, day 1 and day 2. C57BL/6J (A to C), NFκB1 null (D to F), c-Rel null (G to I), RelB null (J to L), NFκB2 null (M to O) were treated. Scale bar 20µm.

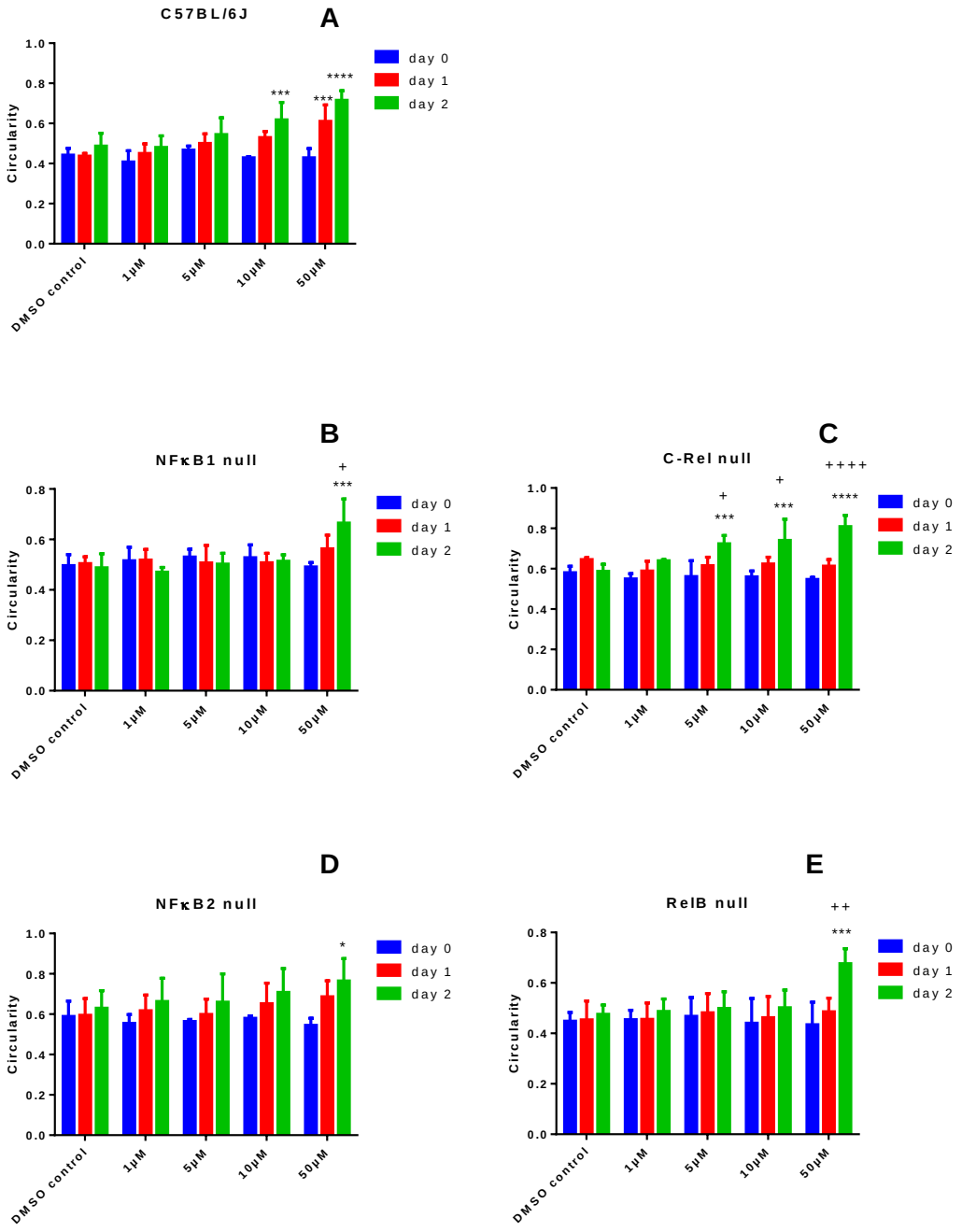

Figure 4.10 Irinotecan caused increased circularity in C57BL/6J, NFκB1 null, RelB null, NFκB2 null and c-Rel null enteroids. Enteroids were treated with DMSO only, 1µM, 5µM, 10µM or 50µM irinotecan over 2 days. Circularity measurements were taken at day 0(0 hours) day 1 (24 hours) and day 2 (48 hours). Six enteroids were measured per well, and two wells of each treatment were measured per experiment. The experiments were carried out in triplicate. Average circularity from N=3 is shown with standard deviations. * represents significance compared to day 0, and + represents significance compared to day 1. P values are as follows *=P<0.05 ***=P<0.001 ****=P<0.0001. +=P<0.05 ++=P<0.01 ++++=P<0.0001.

Etoposide		5-FU		Irinotecan	
Genotype	**apoptosis**	**Genotype**	**apoptosis**	**Genotype**	**apoptosis**
C57BL/6J	↑↑	C57BL/6J	↑↑	C57BL/6J	↑↑
NFκB1	↑	NFκB1	↑↑	NFκB1	↑
NFκB2	↑↑↑	NFκB2	↑↑↑	NFκB2	↑
C-Rel	↔	C-Rel	↑	C-Rel	↑↑↑
RelB	↑↑↑	RelB	↑↑	RelB	↑

Table 4.1 Summary of organoid circularity data. Arrows indicate the degree of increase in circularity induced by each treatment and each genotype. ↔ represents little or no change in circularity, ↑ represents increase in circularity.

4.3 Discussion

The circularity method of measuring enteroid cell death in response to cytotoxic stimuli successfully demonstrated a positive correlation between the percentage of morphologically apoptotic cells and the circularity of the enteroids and between the percentage of active caspase-3 positive cells and the circularity of the enteroids. The R^2 correlation values were above 0.8 for both etoposide and 5-FU in both the apoptotic morphological and caspase-3 validations which indicates a strong relationship between apoptosis and circularity (section 4.2.1).

The chemotherapeutic drugs etoposide, 5-FU and irinotecan were all effective in causing increased apoptosis in C57BL/6J small intestinal enteroids. By the end of the treatment with the highest concentration (50µM) of these chemotherapeutic drugs a disrupted enteroid phenotype was always observed. Irinotecan and 5-FU had less of an effect on the enteroids than etoposide at the same concentration. The increase in circularity was significant at day 1 in the 10µM etoposide treated enteroids but only on day 2 for the irinotecan and 5-FU treated enteroids. A summary of the data is provided in table 4.1.

The various NFκB subunit knockout enteroids showed some interesting differences in susceptibility to chemotherapeutic drug induced cell death. In particular c-Rel

appeared to be involved in regulating the onset of pathological cell blebbing and apoptosis from the outer surface of the enteroids as c-Rel null enteroids were resistant to damage when treated with etoposide and 5-FU. In contrast c-Rel null enteroids were more sensitive to irinotecan, and showed increased amounts of cell death compared to C57BL/6J enteroids following this treatment. The resistance of c-Rel null mice to chemotherapeutic drug induced small intestinal apoptosis is therefore not a universal phenomenon and appears to differ between the topoisomerase I inhibitor irinotecan, and the topoisomerase II inhibitor etoposide.

C-Rel and NFκB1 are both NFκB subunits which function in the classical activation pathway. However the reduced susceptibility to chemotherapy induced cell death seen in the c-Rel null enteroids was not seen in NFκB1 null enteroids. Although the NFκB1 null enteroids were slightly less susceptible to etoposide induced cell death than the C57BL/6J null enteroids, they showed no differences in susceptibility compared to C57BL/6J enteroids when treated with 5-FU and were slightly less susceptible to irinotecan induced apoptosis. This indicates that the effects seen in c-Rel null enteroids are not simply due to disruption of the classical NFκB activation pathway. Generalisations about classical pathway effects may be an oversimplification in the case of this study and it can be concluded that the effects seen in c-Rel null mice were probably not due to NFκB1:c-Rel dimer activity.

The loss of c-Rel has been linked to increased cell survival after treatment with DNA damaging agents in previous studies in our lab, with c-Rel null mice showing persistent colonic mitosis and resistance to apoptosis when subjected to gamma radiation. Additionally when treated with AOM/DSS these mice were found to develop more tumours and these were found to have more cell proliferation and less apoptosis than those observed in wild-type animals (Burkitt *et al.*, 2015). This indicates a resistance to DNA damage induced apoptosis and cessation of proliferation in both cancerous lesions and the healthy GI tract.

C-Rel has been linked to both pro and anti-apoptotic signalling pathways in HeLa cells (Bernard *et al.*, 2002), and has also been reported to have both pro-apoptotic and anti-apoptotic functions in a tissue specific manner. Additionally, the downregulation of RelA in colon cancer cells has been linked to an increased sensitivity to irinotecan, indicating an anti-apoptotic effect of classical NFκB pathway dimers (Guo *et al.*, 2004). The inhibition of the NFκB pathway by targeting of IKK has also been shown to enhance the action of irinotecan and the irinotecan active metabolite SN-38 (Lagadec *et al.*, 2008). However, further in-depth investigations of classical pathway NF-κB signalling are warranted as these data contrast NFκB1 null enteroid studies presented here that suggest that NFκB1 null enteroids do not show increased cell death in response to irinotecan.

Additionally, as the enteroids were composed of only epithelial cells from the proximal small intestine a more likely explanation for this difference involves the mechanism of action of irinotecan. For instance, the different sensitivities of the c-Rel null enteroids to etoposide and 5-FU compared to irinotecan may be because etoposide and 5-FU induce cell death via a p53 dependant mechanism (section 4.1) and there is evidence to suggest that irinotecan induces cell death via bax and bak in the gastrointestinal tract (Bowen *et al.*, 2007). C-rel has been shown to interact with p53, and crosstalk has been observed between the two in diffuse large cell B-lymphoma (Li *et al.*, 2015). Therefore the presence of c-Rel could influence the response to p53 dependent cell death stimuli such as etoposide or 5-FU differently to the p53 independent stimulus irinotecan. C-Rel null HeLa cells have also been shown to exhibit decreased amounts of the anti-apoptotic proteins bcl-2 and bcl-xl (Slotta *et al.*, 2017). As irinotecan induces apoptosis via the activation of bak and bax, the imbalance in the BCL family proteins may be responsible for irinotecan-induced cell death in c-Rel null enteroids as there may be less inhibition of bak and bax signalling by bcl-2 and bcl-xl. Further studies are needed to determine whether these are the mechanisms responsible for

differences in susceptibility of c-Rel null enteroids to apoptosis induced by different chemotherapeutic agents.

Enteroids derived from both alternative NFκB activation pathway genetic knockouts (NFκB2 null and RelB null), were more sensitive to etoposide treatment than C57BL/6J enteroids, and NFκB2 null enteroids were also more sensitive to the effects of 5-FU. This indicates a protective effect for the alternative NFκB activation pathway, contrary to the protective effect of NFκB2 null epithelia seen in chapter 3. In support of this, NFκB2 has also been found to contribute towards chemotherapy resistance when it is overexpressed in etoposide treated prostate cancer cells (Nadiminty *et al.*, 2006).

The microbiome has been shown to have a significant contribution to irinotecan related mucositis, with irinotecan related diarrhoea being found to correlate with an increase in β-glucuronidase-producing bacteria such as *E. coli* in rats (Stringer et al. 2009a). Similarly, 5-FU has also been shown to have an effect on the microflora of the gut, and this may in turn contribute to 5-FU induced mucositis (Stringer et al. 2009b). Interestingly a recent study has found that the cytotoxicity of some chemotherapeutic drugs including etoposide against cancer cell lines can be decreased by the presence of common tumour associated bacteria (Lehouritis *et al.*, 2015). A co-culture model involving bacteria and enteroids would allow us to improve upon these experiments without needing to undertake *in vivo* experiments. This might create a more realistic model of the interactions between these drugs and the small intestine. Many studies using gastrointestinal enteroids and bacteria have already been conducted (Hill and Spence, 2017). Studies using microinjection techniques in order to introduce bacteria into the enteroid lumen may be an interesting way to continue these studies.

As the enteroid model employed in this chapter includes epithelial cells only, it is important to be aware that this model of intestinal cell damage does not include any effects of drugs upon hematopoietic or mesenchymal cells. C-Rel deletion protected enteroids from damage induced by 5-FU and etoposide, but not against irinotecan. In the next chapter we have therefore investigated the effects of two of these drugs, etoposide and 5-FU upon apoptosis induction in the murine small intestine and colon *in vivo*.

5 The role of NFκB subunits in regulating etoposide and 5-FU induced apoptosis and mitosis in murine small intestinal and colonic crypts

5.1 Introduction

The crypts of the small intestine and the colon are particularly vulnerable to the DNA damaging effects of chemotherapeutic drugs due to the high rate of proliferation observed in the normal gastrointestinal tract. The gastrointestinal damage induced by chemotherapy is known as mucositis and is one of the most severe and potentially life threatening side effects of cancer treatment (Sonis, 2004). Mucositis occurs when DNA damaging agents such as 5-FU cause an increase in apoptosis in the small intestine and colon. The chemotherapeutic drugs induce DNA damage in the rapidly proliferating stem cells of the crypt, and this leads to cell death in the proliferative zone of the crypt and resultant villus blunting, enhanced epithelial permeability and increased inflammation that may further enhance pathology in a positive feedback loop (Yu, 2013).

5-fluorouracil (5-FU) is a frequently used chemotherapeutic treatment (Longley, Harkin and Johnston, 2003) which induces apoptosis in cancer cells through the inhibition of thymidylate synthase and the incorporation of fluorinated pyrimidines into RNA (Houghton, Houghton and Wooten, 1979). Animal studies have shown that 5-FU causes villus shortening, reduced cellularity and subsequent mucositis through enterocyte cell apoptosis (Soares *et al.*, 2008). Off target effects in the gastrointestinal tract are known to be mostly independent of thymidine synthase, but dependent on p53 (Pritchard *et al.*, 1997). The primary location of 5-FU induced apoptosis in the small intestine is the transit amplifying cell zone. However, in the colon the stem cells found at the base of the crypt are found to be the most susceptible to 5-FU-induced apoptosis (Pritchard *et al.*, 1997).

Etoposide is another commonly used chemotherapeutic drug which functions as a topoisomerase inhibitor. This drug functions to poison the topoII cleavage complex and prevents double stranded DNA breaks from re-ligating. Re-ligation can occur when the topoII enzyme removes the inevitable entanglement and supercoils which form due to the double helical nature of the DNA strand (Montecucco, Zanetta and Biamonti, 2015). Similarly to 5-FU, etoposide induced apoptosis is dependent on p53, which is activated by Nemo-like kinase (NLK) as a result of the etoposide related DNA damage response (Zhang *et al.*, 2014).

As with 5-FU, one of the off target effects of etoposide is the death of the rapidly cycling cells of the intestinal tract. These off-target effects in the small intestine result in villus shortening, crypt atrophy and compromised epithelial integrity. Apoptosis appears to occur by the same mechanism as seen in etoposide mediated tumour cell death. In both tumour and healthy cells, etoposide causes cell death via the formation of double stranded DNA breaks which the cells are then unable to repair. Interestingly, recent research has shown that mice which are fasted before etoposide administration are more able to repair the DNA damage and are therefore less susceptible to etoposide related gastrointestinal mucositis (Tinkum *et al.*, 2015).

NFκB family members are known to upregulate both pro and anti-apoptotic cytokines in a tissue specific manner (Barkett & Gilmore, 1999). It is therefore warranted to explore whether NFκB subunits regulate the severity of intestinal mucositis. The NFκB family of transcription factors have also been suggested to be a link between inflammation and cancer, and the classical NFκB activation pathway is known to contribute to carcinogenesis in inflammation related cancer, and can be directly activated by the inflammasome as the inflammasome is known to phosphorylate IκBs which inhibit the IKK complex (Kasza, 2013; Lin and Zhang, 2017).

There is evidence to suggest that NFκB plays a role in chemotherapy induced apoptosis of tumour cells. NFκB is known to be activated in response to chemotherapy and the classical pathway subunit P65 has been shown to be upregulated in the small intestine 2 days following administration of 5-FU in mice (Chang *et al.*, 2012). Inhibition of classical NFκB signalling is also known to sensitise CML cell lines to etoposide induced apoptosis. Additionally the stabilisation of IκBα led to P50 and P65 homodimers and heterodimers being retained in an inactive form in the cytoplasm which caused an increase in etoposide related apoptosis (Morotti *et al.*, 2006). Similarly, inhibition of the classical NFκB pathway using an IκB super-repressor is known to increase the amount of apoptosis caused by 5-FU in colon cancer cells (Voboril *et al.*, 2004). From this evidence, it seems highly plausible that NFκB is involved in regulating the response of the gut to chemotherapeutic drug induced damage.

Previous studies in our lab have found that NFκB1 and NFκB2 are involved in regulating epithelial cell apoptosis at the villus tip (Williams *et al.*, 2013). NFκB1 null mice have also been shown to have longer colonic crypts than wild-type animals (Inan *et al.*, 2000), which suggests that they have a higher rate of proliferation to account for this. We therefore hypothesised that 5-FU and etoposide may have altered effects in mice which are deficient in specific NFκB subunits.

Previous studies in our lab have indicated that there are differences in the intestinal apoptotic response of NFκB knockout mice to DNA damaging stimuli. 24 hours after administration of azoxymethane (AOM), NFκB2 null mice were found to have more colonic epithelial apoptosis than C57BL/6J mice and c-Rel null mice were found to have a decreased amount of colonic epithelial apoptosis. Additionally, when c-Rel null mice were subjected to γ irradiation, they also exhibited less colonic apoptosis compared with C57BL/6J mice, indicating involvement of the classical NFκB pathway in the response to DNA damaging stimuli (Burkitt *et al.*, 2015).

We therefore set out to investigate whether the response to the chemotherapeutic drugs 5-FU and etoposide in the small intestinal and colonic crypts was different in various NFκB knockout mice. Due to resource and time constraints irinotecan was not investigated *in vivo* at this time. Results presented in the previous chapter suggested that c-Rel null enteroids were resistant to cell death induced by etoposide and 5-FU, and that NFκB2 null enteroids showed an increased sensitivity to these drugs. Some resistance to etoposide was also found in NFκB1 null enteroids (chapter 4). The distal colon and proximal small intestine were chosen for analysis in this study as these are the areas of both organs previously shown to be most susceptible to the administration of DNA damaging agents. The aim of this chapter was therefore to investigate the actions of 5-FU and etoposide on the intestinal epithelia of NFκB knockout mice *in vivo*.

5.2 Results

5.2.1 Crypt length in the colon and small intestine was consistent between untreated NFκB null mice

We initially set out to determine whether there were any baseline differences in small intestinal and colonic crypt architecture before challenging mice with chemotherapeutic agents. We therefore assessed baseline crypt length in each transgenic strain of mouse compared against their wild-type (WT) counterparts C57BL/6J. Mean crypt length was measured by cell number in 6 untreated mice per genotype (C57BL/6J, NFκB1 null, NFκB2 null, c-Rel null). The C57BL/6J small intestinal crypt length was 20.88±1.78 cells, in c-Rel null mice it was 21.38±0.7 cells, in NFκB1 null mice it was 20.63±1.05 cells and in NFκB2 null mice it was 18.82±1.63 cells. No significant differences were found between the control C57BL/6J and the knockout groups using one way ANOVA. In the colon the mean C57BL/6J crypt length was 19.54±0.89 cells, c-Rel null colonic crypts had 18.70±1.38 cells, NFκB1 null

colonic crypts had 21.85±1.86 cells and in NFκB2 null colonic crypts had 21.76±19.51 cells (figure 5.1). In contrast to previous studies that showed NFκB1 null animals had longer crypts, no significant differences were found between the C57BL/6J mice and the knockout mice in either the proximal small intestine or distal colon. Representative images are shown of small intestinal crypts (figure 5.2A to D) and colonic crypts (figure 5.3A to D).

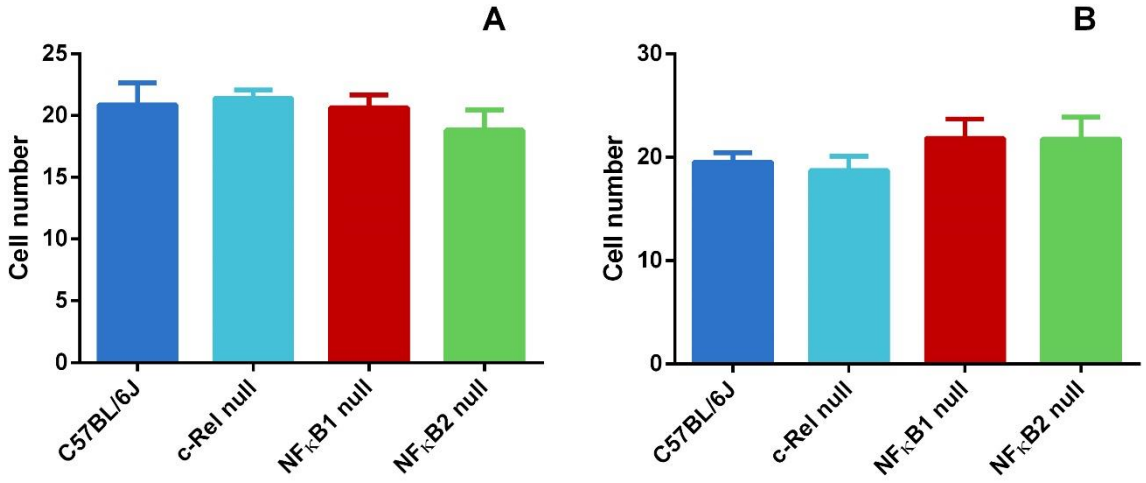

Figure 5.1 The length of small intestinal and colonic crypts in untreated mice. A shows small intestinal crypts and B shows colonic crypts. The number of cells per crypt was counted. C57BL/6J, c-Rel null, NFκB1 null and NFκB2 null mice are shown. N=6 mice per group. One way ANOVA and Dunnett's multiple comparisons performed on data.

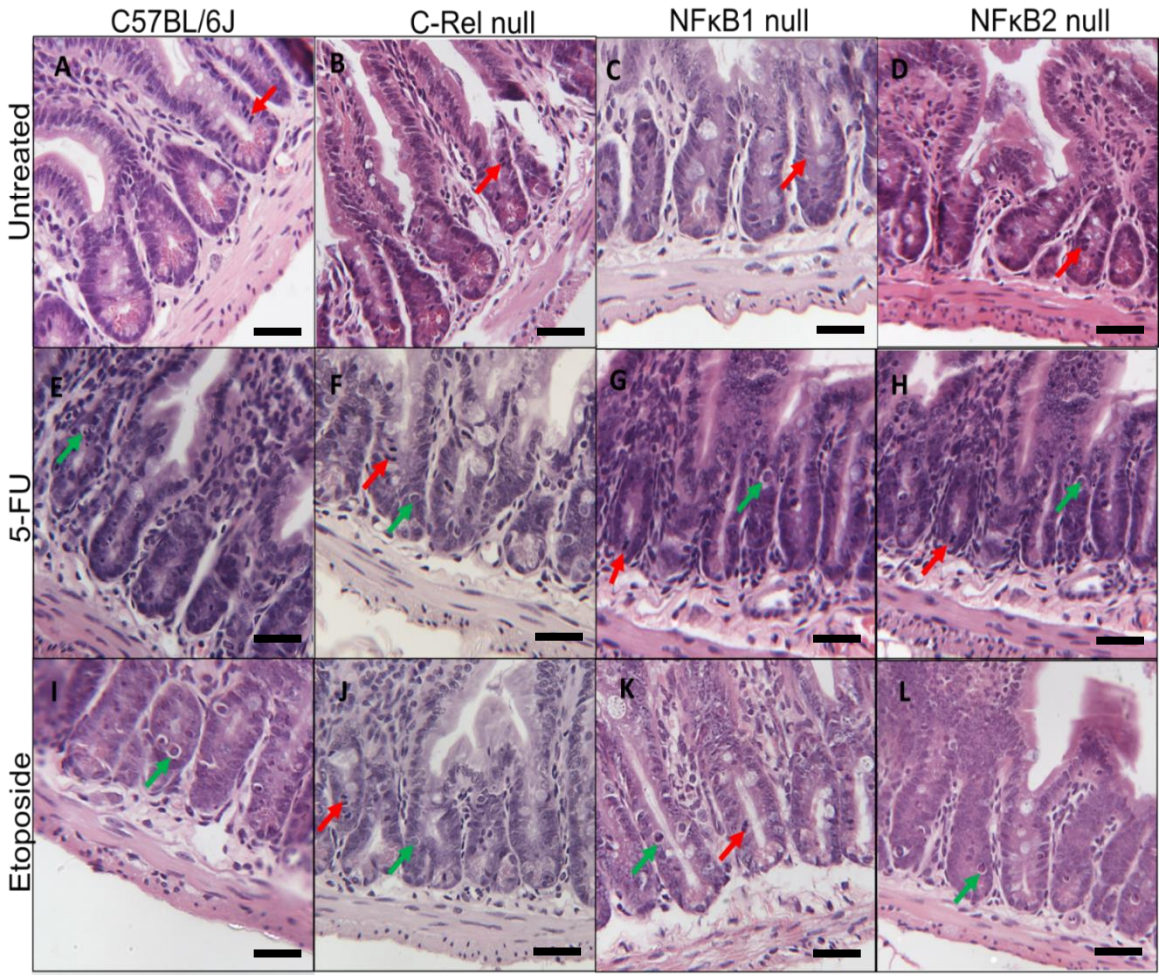

Figure 5.2 Chemotherapeutic agents cause an increase in the amount of apoptosis in the small intestinal crypts. H+E stained small intestinal crypts from C57BL/6J, c-Rel null, NFκB1 null and NFκB2 null mice which were untreated, treated with 5-FU for 24 hours or treated with etoposide for 4.5 hours. Crypts were stained with H+E in order to identify apoptotic and mitotic cells. A to D show the untreated small intestine, E to H show the small intestine from mice treated with 5-FU for 24 hours, and I to L show the mice treated with etoposide for 6 hours. Red arrows show mitotic cells, green arrows show apoptotic cells.

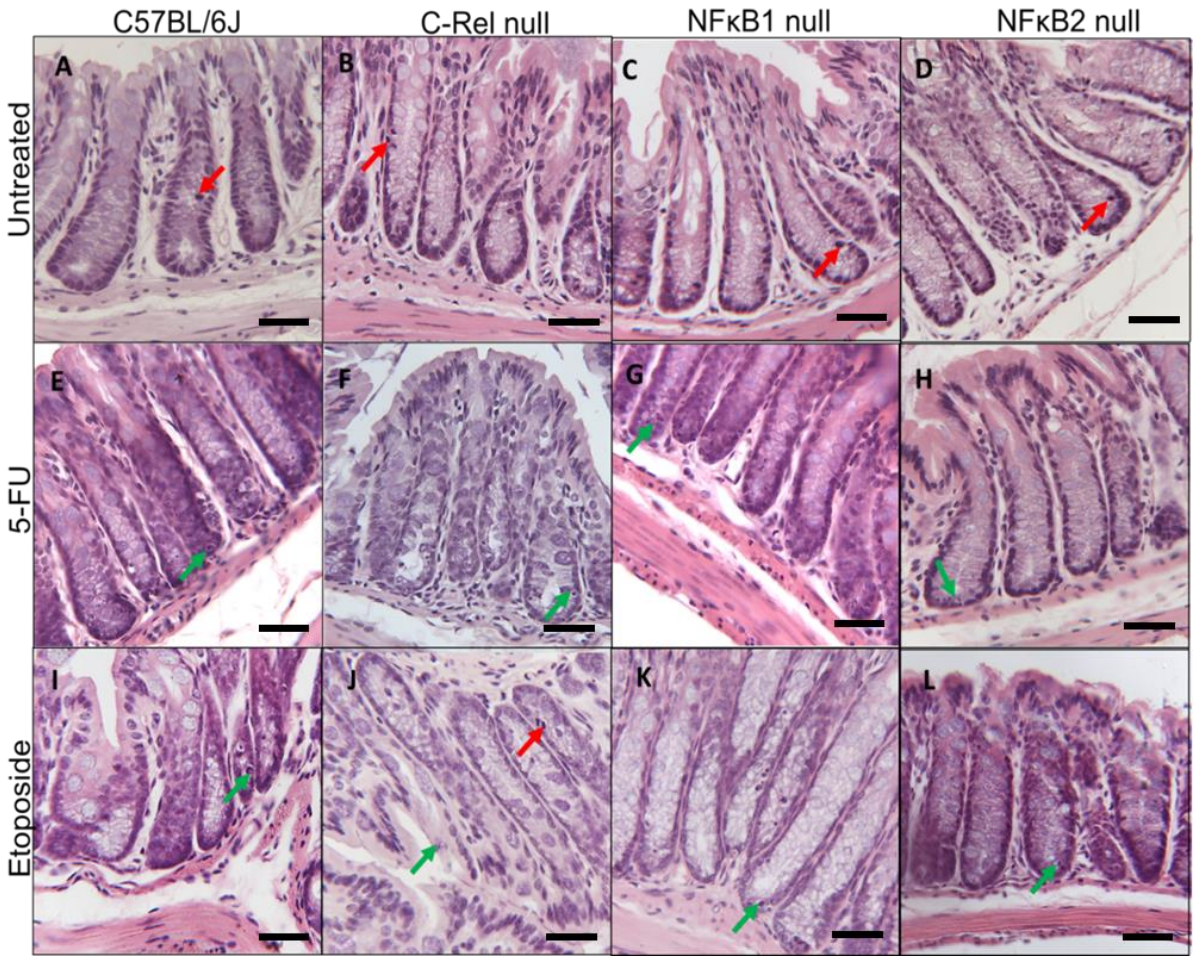

Figure 5.3 5-FU and etoposide treated colon showing the increase in apoptosis caused by the administration of these chemotherapeutic drugs. Representative images shown at x40 magnification. Bright field microscopy used to capture images. Standard H+E staining technique used. Red arrows indicate mitotic cells, green arrows indicate apoptotic bodies and apoptotic cells. A to D represents the untreated genotypes, E to H represents the 5-FU treated mice and I to L represents the etoposide treated mice (C57BL/6, c-Rel null, NFκB1 null, NFκB2 null from left to right).

5.2.2 NFκB1 null and NFκB2 null small intestinal crypts showed increased baseline proliferation

We assessed the baseline amount of mitosis in the small intestine of all genotypes to control for any differences when investigating the proliferation level in chemotherapeutic drug treated mice. In the small intestinal crypts of C57BL/6J mice there was a peak in mitosis at cell position 8 with a mitotic index at this cell position of 4.44%. C-Rel null small intestinal crypts showed maximal mitosis at cell position 10 with a peak mitotic index of 7.89% and there were peak mitotic indices of 7.67% at cell position 7 in NFκB1 null crypts and 8.78% at cell position 10 in NFκB2 null crypts. A significantly higher mitotic index was found between cell position 3 and 18 in the c-Rel null small intestinal crypts compared to C57BL/6J, and in the NFκB2 null mice significant increases were observed at cell positions 10 to 15 (figure 5.4A). The percentage of total cells that were mitotic in C57BL/6J small intestinal crypts was 2.44±0.94%, in c-Rel null crypts it was 3.52±0.58%, in NFκB1 null crypts it was 3.82±1.15% and in NFκB2 null crypts it was 4.49±1.06%. NFκB1 and NFκB2 null small intestinal crypts were both found to have significantly more mitosis than C57BL/6J crypts (NFκB1 P=0.045, NFκB2 P=0.0059) (figure 5.4C). Representative images of small intestinal crypts from untreated C57BL/6J and all transgenic strains of mice are shown in figure 5.2A to D.

5.2.3 No differences in baseline apoptosis were observed in the small intestine of NFκB knockout mice

Maximal amounts of apoptosis in the small intestinal crypts of untreated C57BL/6J mice were observed at cell position 5 with a peak apoptotic index of 2.33%. c-Rel null crypts also showed maximal apoptosis at cell position 5 with a peak apoptotic index of 3.22%. In NFκB2 null small intestinal crypts peak apoptosis occurred at cell position 6 with an apoptotic index of 3.33% and in NFκB1 null crypts, the peak amount of apoptosis was at cell positions 4 and 5 with an apoptotic index of 2.11%. The

apoptotic index of this genotype was found to be significantly higher than the C57BL/6J between cell positions 7 and 14 by modified median test (figure 5.4B). The mean percentage of apoptotic cells in C57BL/6J mice was 1.09±0.73%, in c-Rel null mice it was 1.65±0.79%, in NFκB1 null mice it was 1.12±0.70% and in NFκB2 null mice it was 1.79±0.58% (figure 5.4D). No significant differences were found between these datasets, suggesting that there were no major differences in baseline apoptosis between any strains of mice tested in the small intestine.

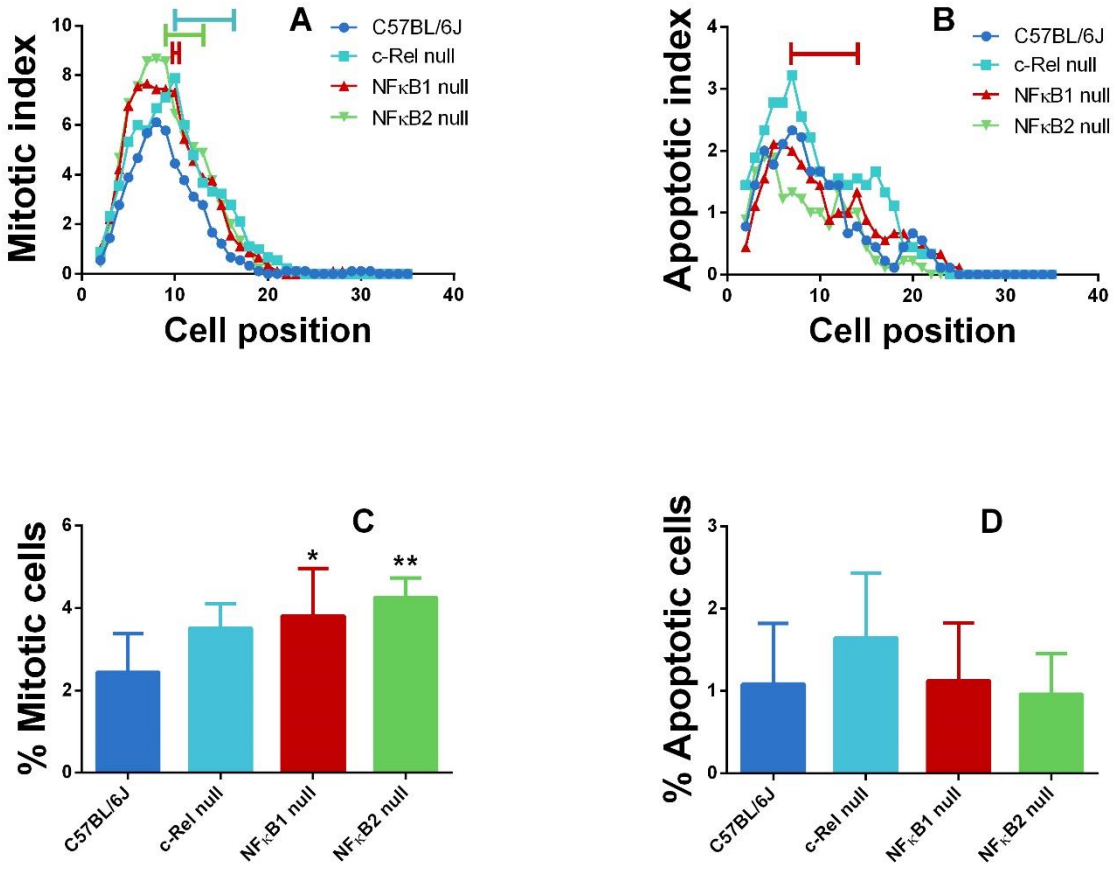

Figure 5.4 Mitosis and apoptosis detected in the small intestinal crypts of NFκB knockout mice. The position and amount of mitotic and apoptotic cells were measured in small intestinal crypts. Graph A shows the mitotic index, B shows the apoptotic index, C shows quantification of the cells undergoing mitosis and D shows quantification of number of cells undergoing apoptosis. C57BL/6J (Blue), c-Rel null (turquoise), NFκB1 null (red) and NFκB2 null (green) are shown (N=3). Turquoise line represents a significant difference between the c-Rel null mitotic index and the C57BL/6J mitotic index when modified median test was performed. Green line represents significant difference between the NFκB2 null crypts mitotic index and the C57BL/6J and the red line represents significant difference between the NFκB1 null crypts and the C57BL/6J apoptotic index. C and D were compared by one way ANOVA and Dunnett's multiple comparisons *=P<0.05 **=P<0.01

5.2.4 The baseline amount of mitosis was lower in NFκB2 null colonic crypts compared with control C57BL/6J mice

As we showed significant increases in baseline mitosis in NFκB1 and NFκB2 small intestine, we wanted to assess the same parameter in the colon of these mice. The mitotic index data indicated a decreased amount of mitosis in NFκB2 null crypts with significantly decreased mitotic index between cell positions 5 and 15 when compared to C57BL/6J animals. Peaks in mitosis were seen at cell position 5 in C57BL/6J mice with a peak mitotic index of 6.67%, in c-Rel null mice maximal mitosis was observed at cell position 6 with a peak mitotic index of 7.22%. There was a peak in mitotic index in NFκB1 null mice at cell position 5 with a mitotic index of 6.44% and in NFκB2 null this occurred at cell position 5 with a peak mitotic index of 3.87% (figure 5.5A). The percentage of the total cells which were undergoing mitosis was also found to be significantly less in NFκB2 null colonic crypts compared to C57BL/6J. C57BL/6J distal colonic crypts were found to have 2.58±0.89% mitotic cells, c-Rel null crypts were found to have 2.763±0.50% mitotic cells, NFκB1 null crypts were found to have 2.98±0.94% mitotic cells whereas NFκB2 null crypts were significantly lower at 1.28±0.29% (figure 5.5C). This suggests that rates of mitosis and therefore proliferation are reduced in the distal colonic crypts of NFκB2 null mice. Representative images of untreated colonic crypts are shown in figure 5.4 (A to D).

5.2.5 Apoptosis in the colonic crypts was elevated in NFκB1 null and NFκB2 null colonic crypts when compared to C57BL/6J

As we had shown that there were no significant differences between baseline levels of apoptosis in the small intestine, we wanted to test whether this was also the case in the colon of the NFκB knockout mice. Very little colonic apoptosis was observed at baseline in any strain of mice investigated. However peaks in apoptotic index were seen in C57BL/6J colonic crypts at cell position 4 with a apoptotic index of 1.67%, c-Rel null mice showed maximal apoptosis at cell position 5 with an apoptotic index of

1.33%, NFκB1 null colonic crypts showed maximal apoptosis at cell position 7 with an apoptotic index of 1.78% and NFκB2 null mice demonstrated maximal apoptosis at cell position 3 and 4 with an apoptotic index of 2.40%. When the data were assessed using the modified median test, it was found that there was a significant increase compared to C57BL/6J crypts in the NFκB2 null colonic crypts between cell positions 5 and 10 and in the NFκB1 null crypts between cell positions 9 and 10 (figure 5.5B). The percentage of total cells which were apoptotic in untreated C57BL/6J crypts was 0.47±0.23%, in c-Rel null there were 0.54±0.36% apoptotic cells, in NFκB1 null there were 0.77±0.35% and in NFκB2 null there were 0.80±0.57% apoptotic cells (figure 5.5D).This suggests that NFκB1 null and NFκB2 null mice may have slightly increased colonic epithelial apoptosis at baseline compared to C57BL/6J mice.

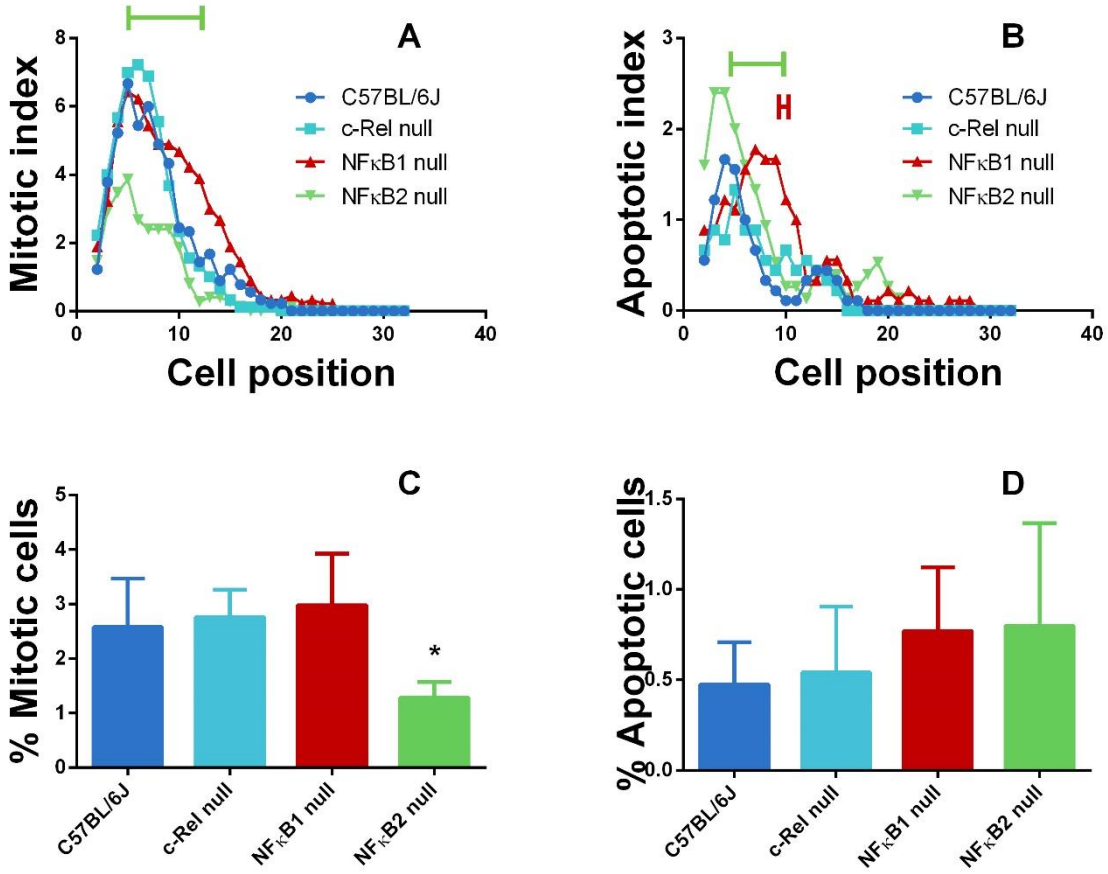

Figure 5.5 Mitosis and apoptosis in colonic crypts of untreated NFκB knockout mice. quantified using Wincrypts software. Graph A shows the mitotic index, B shows the apoptotic index, C shows quantification of the total number of mitotic cells and D shows quantification of number of cells undergoing apoptosis. C57BL/6J (blue), c-Rel null (turquoise), NFκB1 null (red) and NFκB2 null (purple) are shown (N=4). A and B show that there were significant differences in the amount of mitosis/apoptosis at the particular cell positions covered, green line indicates the difference between the NFκB2 and the C57BL/6J, red line indicates the difference between the NFκB1 null crypts and C57BL/6J. Cell positional analysis was assessed by modified median test. Mean mitotic/apoptotic index was assessed by 1-way ANOVA and Dunnett's multiple comparisons. Graph C and D *=P<0.05.

5.2.6 C-Rel null mice showed persistent mitosis in distal small intestinal crypts when treated with 5-FU

5-FU was administered to mice at a dose of 40mg/kg for 24 hours. This dose and time point has been shown to induce maximal intestinal epithelial apoptosis in mice (Pritchard *et al.*, 1997). The peak mitosis in the small intestinal crypts of C57BL/6J mice occurred at cell position 4 with a mitotic index of 2%. The peak mitotic index in c-Rel null mouse small intestine occurred at cell position 7 with a mitotic index of 5.73%, at this cell position the C57BL/6J, NFκB1 null, and NFκB2 null mouse small intestines all showed a mitotic index of 1% (figure 5.6A). When a modified median statistical test was used to analyse the data there was no significant difference found between c-Rel null and C57BL/6J mice. However, there were significantly more mitotic cells in total suggesting that mitosis was more persistent in c-Rel null animals. The C57BL/6J mice had a mean of 0.22±0.06% cells in mitosis and the c-Rel null mice had a significantly higher percentage of total mitotic cells at 1.64±1.68% ($P=0.025$; figure 5.6C). There were no significant differences between the C57BL/6J small intestinal crypts compared to NFκB1 null (0.14±0.10%) and NFκB2 null (0.18±0.15%). When compared to baseline untreated mitosis, there was significant suppression of total mitotic cells in C57BL/6J crypts after 5-FU treatment ($P<0.0001$). The knockout mice also all showed significant decreases in mitosis when treated with 5-FU (c-Rel null $P=0.0001$, NFκB1 null $P<0.0001$, NFκB2 null $P<0.0001$) However mitosis in c-Rel null mice persisted whereas mitosis was almost completely suppressed in other WT and transgenic mouse strains (figure 5.8A). Representative H+E images are shown in figure 5.2E to H.

5.2.7 Amounts of apoptosis in the small intestine were decreased in c-Rel null mice compared to C57BL/6J, NFκB1 null and NFκB2 null mice in response to 5-FU

5-FU treatment of C57BL/6J mice showed a significant increase in the amount of small intestinal epithelial apoptosis compared with untreated crypts ($P<0.0001$; figure 5.6B). A similar significant increase was also seen in the NFκB1 null ($P<0.0001$) crypts and the NFκB2 null ($P<0.0001$) crypts following 5-FU administration. However no significant difference in small intestinal crypt apoptosis was found between the c-Rel null untreated mice and the 5-FU treated mice ($P=0.41$; figure 5.8C).

The peak amount of apoptosis in C57BL/6J small intestinal crypts was found at cell position 5 at 20.10% (figure 5.6B). C-Rel null mice had a significantly lower peak apoptotic index, with a peak of 5.7% at cell position 7, and when modified median tests were conducted the c-Rel null crypts were found to have significantly less apoptosis between cell positions 2 and 23. NFκB2 null mice showed a peak in apoptosis around cell position 4 at 16.2%, and the modified median test showed that there was a significantly lower apoptotic index compared to wild-type mice from cell position 6 to 13. There were no significant differences found in NFκB1 null small intestinal apoptotic index when compared to C57BL/6J mice. When the overall amounts of apoptotic cells were compared, C57BL/6J mice were found to have 11.30±2.60% of total cells undergoing apoptosis in small intestinal crypts. C-Rel null mice had 3.31±2.68% apoptosis which was significantly less than the C57BL/6J crypts ($P<0.0001$). NFκB1 null crypts (11.43±1.85%) and NFκB2 null crypts (9.43±1.73%) did not show any significant differences in the amount of apoptosis compared with C57BL/6J mice (figure 5.6D). H+E images of representative crypts are shown in figure 5.2E to H.

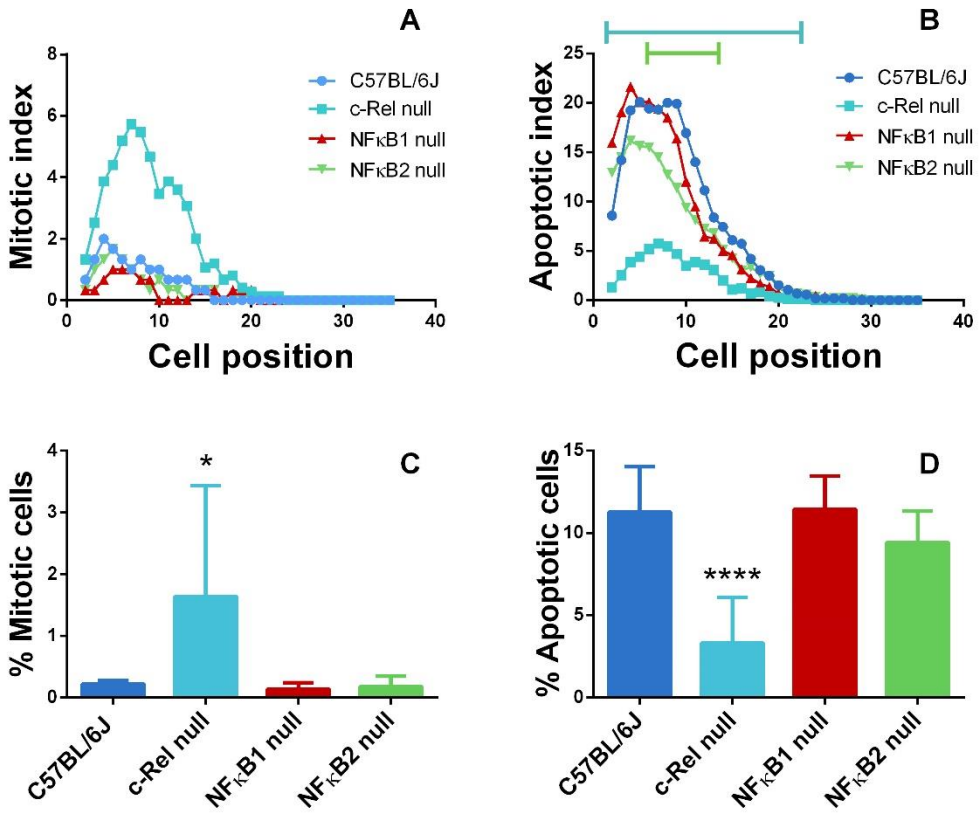

Figure 5.6 Small intestinal apoptosis and mitosis in 5-FU treated mice. C-Rel null mice appeared to be relatively resistant to the suppression of mitosis and the increased apoptosis caused by 5-FU in the small intestine. Mice were treated with 40mg/kg 5-FU for 24 hours. The amount of mitosis and apoptosis in small intestinal crypts was measured in C57BL/6J (blue), c-Rel null (turquoise), NFκB1 null (red) and NFκB2 null (green) mice. The mitotic index represents the percentage of cells at the particular position that are mitotic (A) and apoptotic (B). The percentage of overall cells that were mitotic (C) or apoptotic (D) are also shown. Statistics A and B modified median test vs C57BL/6: turquoise line represents c-rel significance between cell positions 2 and 23, green line represents NFκB2 significance between cell positions 6 and 13. Statistics C and D: one way ANOVA and Dunnett's multiple comparisons vs C57BL/6J *=P<0.05 ****=P<0.0001. NFκB1null and NFκB2 null N=6. C-Rel null N=8 and C57BL/6J N=9.

5.2.8 Persistent mitosis was observed in colon of 5-FU treated c-Rel null mice

Very little mitosis was detected in the colon of mice treated with 5-FU regardless of strain (figure 5.7A and C). The peak mitosis in C57BL/6J colonic crypts was just 0.11% at cell positions 3 to 5. The peak colonic mitotic index in NFκB1 null mice was also 0.11% and in NFκB2 null mice it was 0.13%. However the peak mitotic index in c-Rel null crypts was 1.4% at cell position 5. When modified median tests were performed it was found that there was a significant increase in mitosis in c-Rel null when compared to C57BL/6J mice between cell positions 4-10. The overall percentage of mitotic cells was very low for C57BL/6J mouse colon at 0.04±0.09% mitotic cells. The c-Rel null mouse colon however had a mean of 0.15±0.1% mitotic cells, the NFκB1 null mouse colon had a mean of 0.00025±0.00056% and the NFκB2 null mouse colon had a mean percentage mitosis of 0.0031±0.0045%. None of these strains showed any significant differences compared to the C57BL/6J percentage of mitotic cells. Although it appeared that c-Rel null mice were protected to some extent from the suppression of colonic mitosis caused by 5-FU in C57BL/6J wild-type mice, there was still a significant decrease in mitosis when compared to untreated c-Rel null tissues ($P<0.0001$; Figure 5.8C). Therefore, a similar phenotype was observed in c-Rel null colon to that observed in small intestine (see 5.2.6) although the response was less marked in this tissue.

5.2.9 Colonic apoptosis in response to 5-FU treatment was similar across all strains of mice

As differences had been found in the small intestine, we wanted to assess whether there were any differences in colonic apoptosis in response to 5-FU across the genotypes. No significant differences were however found when the C57BL/6J, c-Rel null, NFκB1 null, NFκB2 null colonic crypt apoptotic indices following 5-FU administration were compared (figure 5.7B). The mean amount of total apoptosis in

colonic crypts from 5-FU treated C57BL/6J (11.13±3.13%), c-Rel null (12.71±6.84%), NFκB1 null (10.14±2.07%) and NFκB2 null (10.84±1.87%) mice was not found to be significantly different (figure 5.7D). As previously shown (section 5.2.3), the percentage of cells in apoptosis at baseline was also similar for all strains of mice. Additionally after treatment with 5-FU the increase in apoptosis observed in colonic crypts when compared to untreated crypts from the same strain was significant in C57BL/6J ($p<0.0001$), C-Rel null ($P<0.0001$), NFκB1 null ($P<0.0001$) and NFκB2 null mice ($P<0.0001$). It can therefore be concluded that NFκB null mouse colons do not have an altered apoptotic response to 5-FU when compared with wild-type (C57BL/6J) mice. When the total apoptotic number data were compared to the baseline levels for each genotype all the strains had a P value of <0.0001 (figure 5.8B).

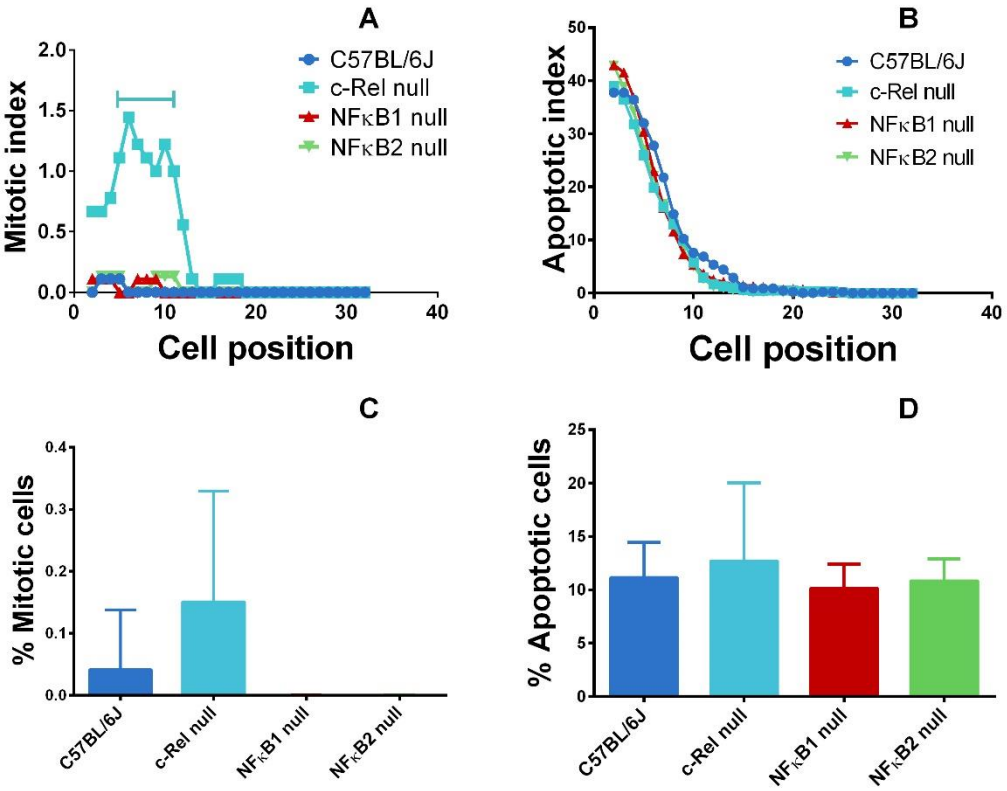

Figure 5.7 Colonic apoptosis and mitosis in 5-FU treated NFκB knockout and wild-type mice. Mice were treated with 5-FU 40mg/kg for 24 hours. The amount of mitosis and apoptosis in the colonic crypts was measured in C57BL/6J (blue), c-Rel null (red), NFκB1 null (green) and NFκB2 null (purple) mice. The mitotic index represents the percentage cells at each particular cell position that are mitotic (A) and the apoptotic index represents the percentage cells at each position which are apoptotic (B). The percentage of overall cells that were mitotic (C) or apoptotic (D) are shown. Statistics: *=Modified median found difference from C57BL/6J. N=6. One way ANOVA and Dunnett's multiple comparisons used.

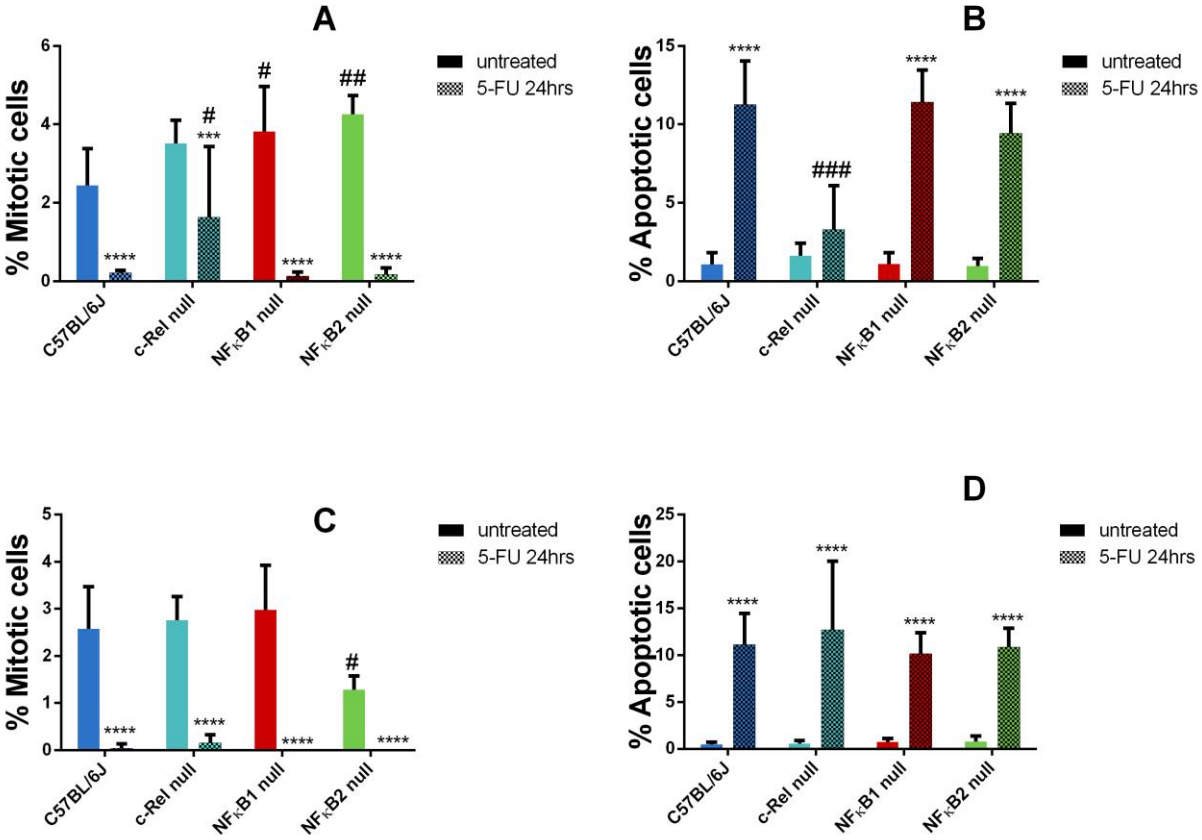

Figure 5.8 Comparison of 5-FU treated and untreated small intestinal and colonic apoptosis and mitosis, in wild-type and NFκB null mice. Small intestinal mitosis (A), small intestinal apoptosis (B), colonic mitosis (C) and colonic apoptosis (D) 24 hours after 40mg/kg 5-FU treatment compared to the untreated control for C57BL/6J (N=9), c-Rel null (N=8), NFκB1 null (N=6) and NFκB2 null mice (N=6). Two way ANOVA and Tukey post hoc statistical test used. Significant differences when compared to untreated of the same genotype represented by ***=P<0.001 and ****=P<0.0001. Significant differences when compared to the C57BL/6J data from the same time point represented by #=P<0.05, ##=P<0.01 and ####=P<0.0001

5.2.10 Etoposide suppressed small intestinal mitosis

As we showed altered susceptibility to GI damage induced by 5-FU, we wanted to determine whether this difference was unique to this drug or was present following treatment with another chemotherapeutic agent, namely etoposide. Etoposide was administered at 10mg/kg by IP injection and mice were culled after 4.5 hours. When comparing the etoposide treated small intestinal crypts to the untreated small intestinal crypts it was found that there was a significant decrease in mitosis in all genotypes (figure 5.11A).

When modified median statistical tests were used to compare the mitotic index data (figure 5.9A), no significant differences were found between C57BL/6J, c-Rel null, NFκB1 null and NFκB2 null murine small intestinal crypts following etoposide treatment. The C57BL/6J small intestinal crypts contained 0.19±0.19% mitotic cells; this measurement was found to be slightly higher in c-Rel null crypts at 0.61±0.67% however this difference was not statistically significant. In the crypts of NFκB1 null mice 0.11±0.10% of cells were found to be mitotic while 0.11±0.061% were mitotic in NFκB2 null crypts. Mitosis in NFκB1 and NFκB2 null small intestinal crypts after etoposide administration was also not found to be statistically significant compared to C57BL/6J crypts (figure 5.9C).

5.2.11 c-Rel null mice were relatively resistant to etoposide induced small intestinal apoptosis

As well as mitosis we also investigated whether there was any altered susceptibility to apoptosis in the small intestinal crypts of etoposide treated mice. There were significantly fewer apoptotic cells in c-Rel null crypts (6.15±2.59%) than wild-type (14.19±1.35%) following etoposide. No significant differences were found between C57BL/6J crypts and NFκB1 null (11.84±3.23%) or NFκB2 null (12.00±4.05%) crypts

(figure 5.9D). Small intestinal apoptosis however increased significantly in all genotypes following etoposide treatment compared to untreated mice of the same genotype (figure 5.11B).

The apoptotic index data indicated that there was a significantly lower apoptotic index in c-Rel null small intestinal crypts when compared to C57BL/6J crypts from cell position 2 to 28 following etoposide treatment (figure 5.9B). Additionally NFκB1 null crypts were found to have significantly less apoptosis than C57BL/6J from cell position 12 to 19 following etoposide injection.

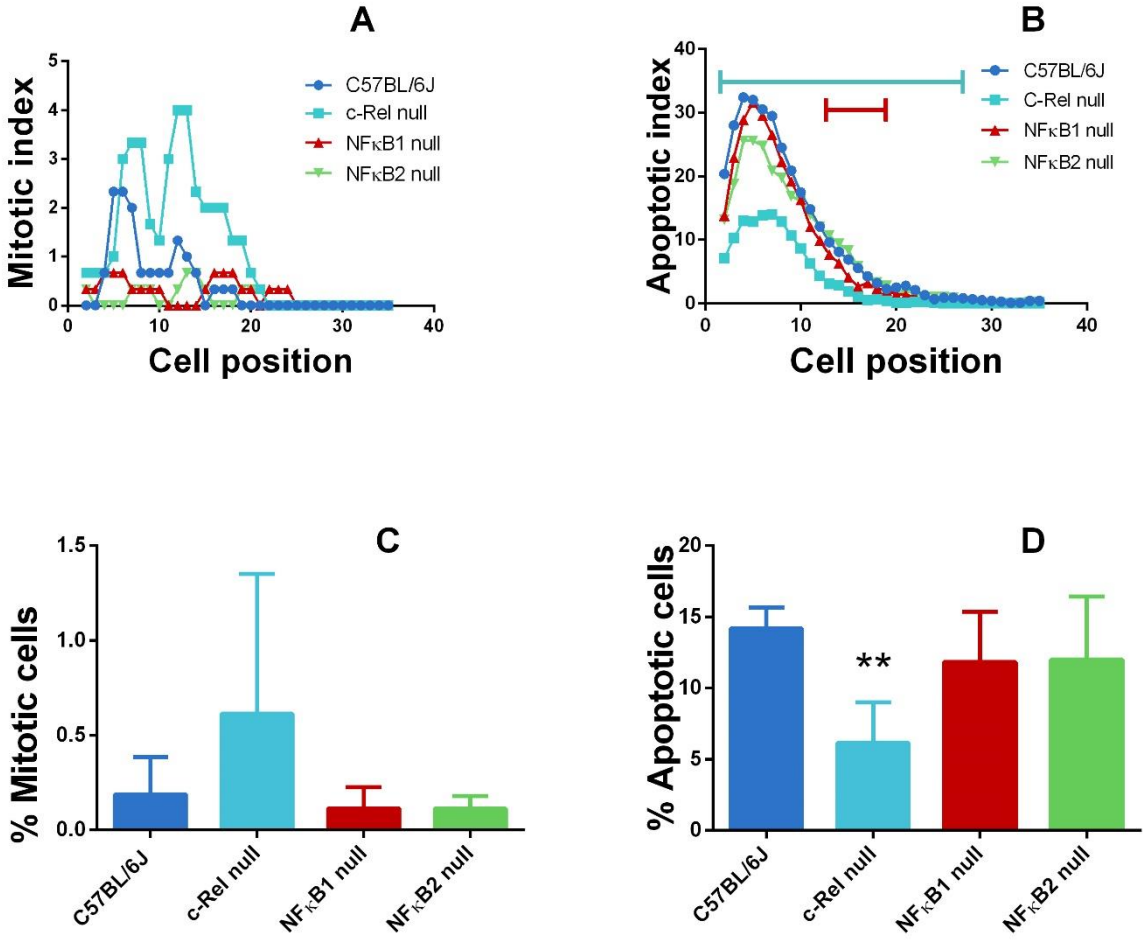

Figure 5.9 Small intestinal apoptosis and mitosis in etoposide treated wild-type and NFκB null mice. Mice were treated with etoposide over 4.5 hours. The amount of mitosis and apoptosis in the small intestinal crypts was measured in C57BL/6J (blue), c-Rel null (turquoise), NFκB1 null (red) and NFκB2 null (green) mice (N=6 for all groups). The mitotic index represents the percentage cells at each particular cell position that are mitotic (A) and the apoptotic index represents the percentage cells at each position which are apoptotic (B). The percentage of overall cells that were mitotic (C) or apoptotic (D) are also shown. Statistics: modified median test (A and B) with horizontal lines in corresponding colours and over the relevant cell positions to represent significant differences found from C57BL/6J. One way ANOVA and Dunnett's post hoc test used (C and D) **=P<0.01.

5.2.12 c-Rel null mice showed persistent colonic crypt mitosis following etoposide treatment

As differences were found using 5-FU, we also wanted investigate whether there was any difference in the effect of etoposide on mitosis in the colonic crypts in our transgenic mice. The percentage of total cells undergoing mitosis in the C57BL/6J colon treated with etoposide was 0.056±0.067%, this was increased in c-Rel null colons following etoposide treatment with a percentage of total cells undergoing mitosis of 0.42±0.30% which was found to be significantly higher (P=0.0060). In NFκB1 null (0.026±0.059%) and NFκB2 null (0.040±0.058) colonic crypts it was found that there were similar amounts of mitosis to C57BL/6J wild-type colon following etoposide. The overall percentage of total cells undergoing mitosis dropped in the etoposide treated colonic crypts when compared with the untreated control in the C57BL/6J (P<0.0001), c-Rel null (P<0.0001) NFκB1 null P<0.0001) and NFκB2 null mice (P<0.0001; figure 5.11C). The amount of mitosis decreased to a similar value to that seen in the 5-FU treated mice in all the genotypes, with no significant differences between the percentage of total mitotic cells being observed in the C57BL/6J (P=0.99), c-Rel null (P=0.46), NFκB1 null (P=0.99) and NFκB2 null (P=0.98) colonic crypts (Figure 5.10A and C).

5.2.13 Etoposide treated c-Rel null mice showed reduced colonic apoptosis

We investigated the amount of apoptosis in the colonic crypts of the wild-type and transgenic mice after etoposide treatment. C57BL/6J colonic crypts contained 7.52±1.09% apoptotic cells. There were significantly fewer apoptotic cells in the c-Rel null mice after etoposide treatment (P=0.0040). There were however no significant differences between the NFκB1 null crypts at 5.45±1.83% and the NFκB2 null crypts

at 8.22±3.13%. The apoptotic index was found to be lower in the etoposide treated c-Rel null colonic crypts compared to the etoposide treated C57BL/6J colonic crypts over cell positions 1 to 25. in the NFκB2 null colonic crypts it was found to be lower over cell positions 16 to 18 as well as in the NFκB1 null colonic crypts over cell positions 3 to 15 (figure 5.10B). The amount of apoptosis in the distal colonic crypts treated with etoposide when compared with the untreated control was found to be significantly increased in all genotypes except for c-Rel null mice (figure 5.11D). These data suggest that c-Rel deletion protects against the induction of colonic apoptosis by etoposide.

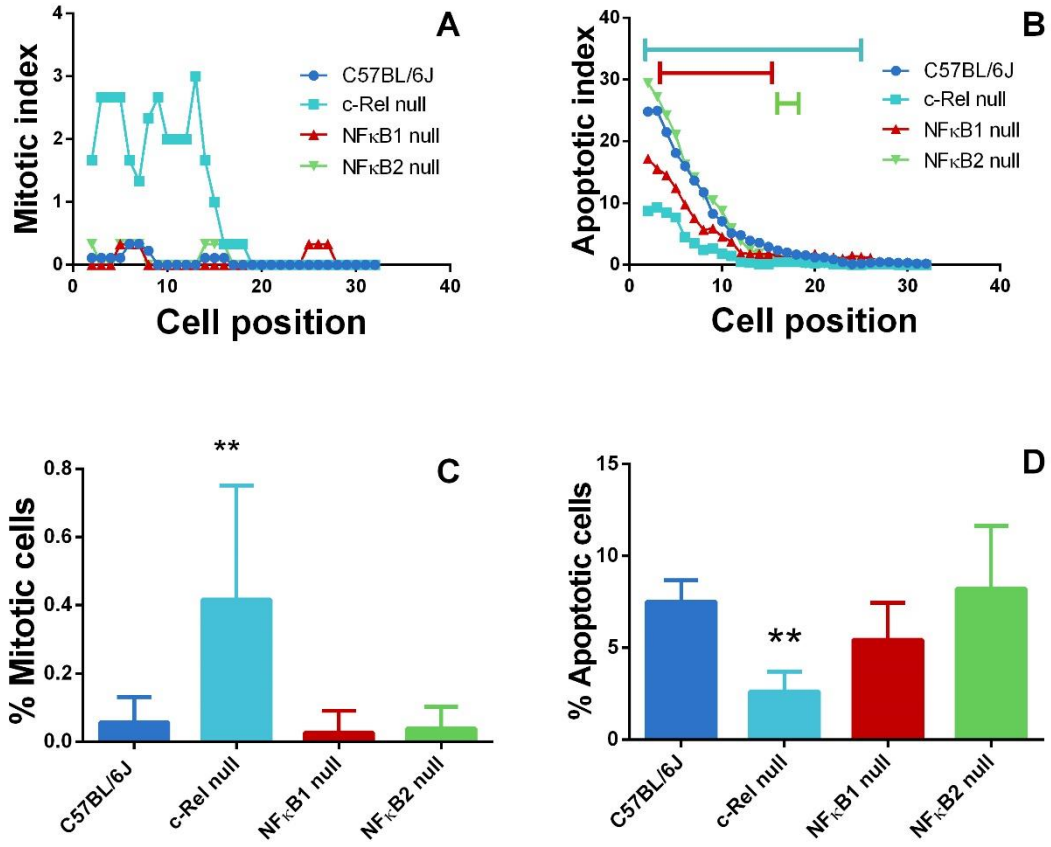

Figure 5.10 Colonic apoptosis and mitosis in etoposide treated wild-type and NFκB null mice. Mice were treated with etoposide over 4.5 hours. The amount of mitosis and apoptosis in the colonic crypts was measured in C57BL/6J (blue), c-Rel null (turquoise), NFκB1 null (red) and NFκB2 null (green) mice. The mitotic index represents the percentage of cells at the particular position that are mitotic (A) and apoptotic (B). The percentage of overall cells that were mitotic (C) or apoptotic (D) are also shown. N=6 for all groups. Statistics calculated using modified median test for panel A and B with coloured horizontal line representing significance. One way ANOVA and Dunnett's multiple comparison used to test for statistical differences in panel C and D. **=P<0.05.

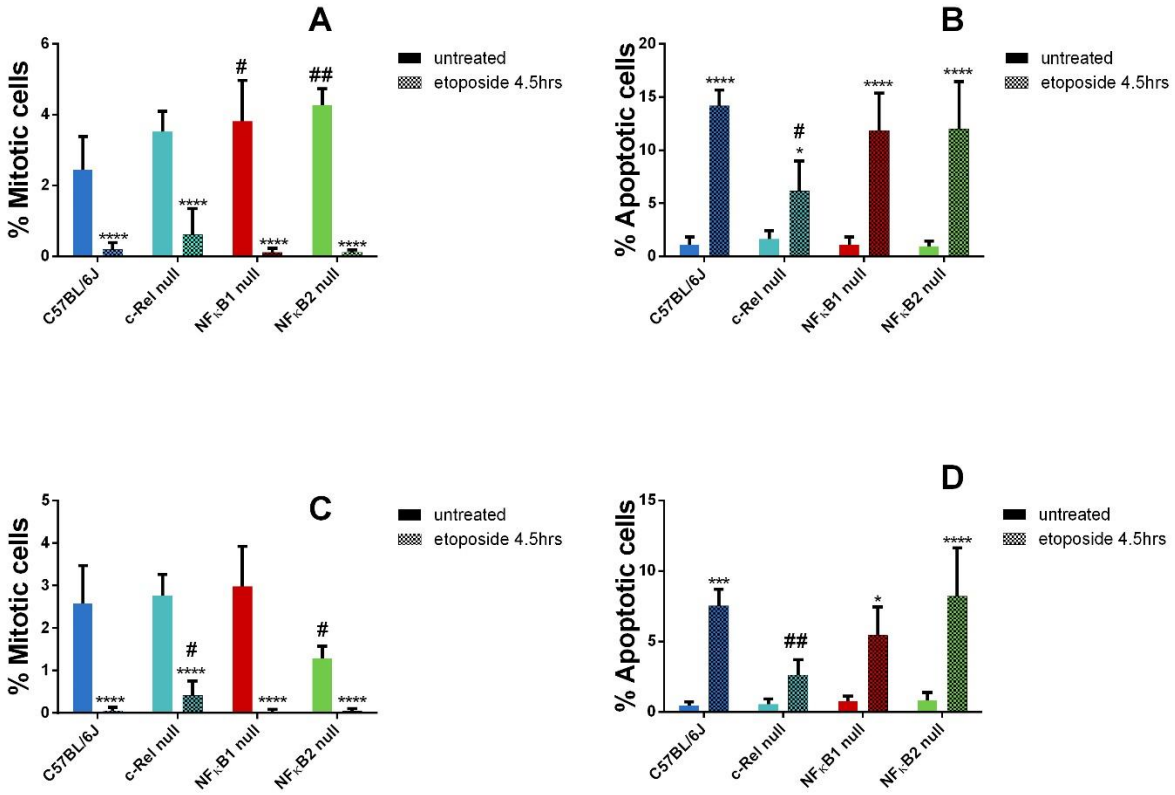

Figure 5.11 Comparison of untreated and etoposide treated small intestinal and colonic apoptosis and mitosis in etoposide treated wild-type and NFκB null mice. Small intestinal mitosis (A), small intestinal apoptosis (B), colonic mitosis (C) and colonic apoptosis (D) in 10mg/kg etoposide treated mice after 4.5 hours. C57BL/6J (N=9), c-Rel null (N=8), NFκB1 null (N=6) and NFκB2 null mice (N=6). Two way ANOVA and Tukey's multiple comparison statistical test used. * used to represent statistical significance when comparing to untreated data from the same genotype, *=P<0.05, ***=P<0.001 and****=P<0.0001. # used to represent statistical significant when comparing to the C57BL/6J data from the same time point, #=P<0.05, ##=P<0.01.

5.3 Discussion

The C57BL/6J responses described in this chapter following 5-FU and etoposide treatment were similar to previous observations in this strain of wild-type mice. P53 dependent DNA damage induced by etoposide is seen to occur primarily in the stem cells of the small intestine and the colon (Potten, Wilson and Booth, 1997). Additionally the amounts of apoptosis and mitosis in both the colon and small intestine were found to be similar to those described previously in our lab (Duckworth, Clyde and Pritchard, 2012). 5-FU induced apoptosis was seen in the early transit amplifying cells of the small intestine, and this was previously described by the Potten group (Pritchard *et al.*, 1997). The 5-FU treated C57BL/6J apoptotic index peaked further up the small intestinal crypt axis than that seen in etoposide treated C57BL/6J mice. This corresponds with the difference in location of the transit amplifying cells and the stem cells of the small intestine.

The expression of NFκB family members appears to differentially regulate small intestinal and colonic apoptosis and mitosis in response to the two chemotherapeutic drugs 5-FU and etoposide. The most interesting finding was that the c-Rel null mice were resistant to apoptosis caused by both of these drugs, as well as displaying persistent mitosis following treatment. This contrasted with the almost complete suppression of cell proliferation observed in wild-type mice following drug administration. In terms of the response to etoposide and 5-FU by c-Rel null tissues, the *in vivo* data also correlated with the enteroid study results presented in Chapter 4. C-Rel null small intestinal enteroids were found to be resistant to cell death induced by etoposide when this was measured as an increase in enteroid circularity (Chapter 4.2.6). Similarly, the c-Rel null mice showed significantly less apoptosis in the small intestine after treatment with etoposide when compared to the C57BL/6J mice. Additionally in the colon, apoptosis in c-Rel colonic crypts remained at a similar

amount to that observed in untreated tissue. Resistance to cell death was also found in c-Rel null enteroids when treated with 5-FU. *In vivo,* we detected significantly fewer apoptotic cells in the small intestine when compared to C57BL/6J after treatment with 5-FU. Mitosis in c-Rel null mice was observed in higher amounts than in C57BL/6J mice after the mice had been treated with 5-FU in both the small intestine and colon. C-Rel null mice were also found to be resistant to 5-FU induced colonic apoptosis, with significantly less apoptosis being observed over a large area of the crypt compared to wild-type colon. Overall these results suggest that the enteroid model of the gut is reliable for assessing the response of the gut to these DNA damaging stimuli.

The results found were also in agreement with previous data reporting the consequences of treating NFκB null mice with azoxymethane, a DNA damaging chemical used to induce colonic carcinoma (Burkitt *et al.*, 2015). In this study, c-Rel null colonic adenomas in mice were found to contain less apoptotic cells and more mitotic cells than wild-type tumours. It was suggested the c-Rel null mice may retain damaged cells in the epithelium, which is why they are more prone than the wild-type C57BL/6J mice to developing colonic tumours. C-Rel null mice were also reported to be protected from the consequences of 12Gy γ radiation and had significantly more colonic epithelial mitosis following treatment with 1Gy γ radiation. This is in direct agreement with the findings in this chapter and indicates that the intestines of c-Rel null mice appear to be protected from the apoptosis that is induced by a variety of DNA damaging agents.

However, in contrast to the results presented here, it has also been shown that c-Rel is involved in enhanced epithelial proliferation due to interactions between the protein ΔNp63α and c-Rel. Nuclear accumulation of c-Rel increased proliferation and maintained it in the presence of growth arresting signals. (King *et al.*, 2008). Additionally ΔNp63α has been found to be co-expressed with c-Rel in head and neck

cancers, in which it appears that c-Rel acts to increase proliferation and suppress apoptosis (Lu *et al.*, 2011). There is evidence to suggest that c-Rel is also involved in breast cancer, as active c-Rel was previously found to be present at very high levels in the nuclei of 20 out of 23 tested human breast tumours (Sovak *et al.*, 1997). There are several reports which suggest the overexpression of c-Rel in breast tissue leads to an increased likelihood of the development of breast tumours in mice (Romieu-Mourez *et al.*, 2003). C-Rel acting to increase proliferation in cancer is in contrast with our findings, and NFκB signalling is known to be pro- or anti-apoptotic in a tissue specific manner.

From this study we suggest that c-Rel has a pro-apoptotic effect in the gastrointestinal tract in response to DNA damaging stimuli. This function in response to chemotherapeutics such as etoposide and 5-FU could potentially be exploited in the treatment of cancer. Drug therapy to increase the amount of active c-Rel in cancer cells may also be useful. However, although the suppression of c-Rel in the gastrointestinal tract appears to suppress mucositis, a possible consequence of this is that c-Rel suppression may lead to intestinal epithelial cells harbouring harmful mutations.

C-Rel deletion was found to protect against chemotherapeutic drug induced damage in both mice and enteroids. As enteroids are comprised solely of epithelial cells this suggests that their resistance is an epithelially mediated effect. This indicates that the protective effect against mucositis may be achieved by targeted suppression of c-Rel in gastrointestinal epithelia. As the suppression of c-Rel was previously shown to increase proliferation and decrease mitosis in colonic adenocarcinoma, it is unlikely that suppression of c-Rel would be useful in GI cancer.

The inhibition of c-Rel DNA binding activity using the small molecule inhibitor IT-603 has been successfully undertaken in a mouse study of graft versus host disease

(Shono et al., 2014). Using an inhibitor specific to c-Rel in order to increase the anti-tumour activity of chemotherapeutic drugs therefore has potential in the treatment of human disease, particularly if a highly specific inhibitor could be used alongside chemotherapy.

6 The effect of tyrosine kinase inhibitors on small intestinal enteroids

6.1 Introduction

Tyrosine kinases are activated by ligand binding which triggers dimerisation and the subsequent phosphorylation of tyrosine residues on target proteins (Paul and Mukhopadhyay, 2004). Protein tyrosine kinase receptors are normally tightly controlled, however constitutive activation of tyrosine kinases is known to occur in some cancers (Paul and Mukhopadhyay, 2004). Mutations in protein tyrosine kinase receptors form a large group of known oncogenes (Blume-Jensen and Hunter, 2001). As a result of this, tyrosine kinase inhibitors (TKIs) are sometimes used in cancer treatment. TKIs target cancer specific molecules and signalling pathways, have a high specificity towards cancer cells and work by competitive ATP inhibition (Arora and Scholar, 2005). These treatments allow cancer patients to avoid some of the nonspecific cytotoxicity associated with conventional chemotherapy (Arora and Scholar, 2005). TKIs are administered to patients to treat a wide variety of malignancies, and although these therapies are more specific to molecular targets involved in cancer growth and progression than conventional chemotherapy, off target effects are often seen. GI toxicity is one of these effects and often occurs in the form of diarrhoea (Ranson, 2004; Arora and Scholar, 2005).

Chronic myeloid leukaemia (CML) treatment has been revolutionised by the use of TKIs (Pasic and Lipton, 2017). CML is a disease which affects around 1 person per 100,000 per year (Apperley, 2015). CML results in a rapid increase in the number of granulocytic cells and is fatal if left untreated (Pasic and Lipton, 2017). CML is characterised by the presence of the Philadelphia chromosome which causes the constitutively active BCR-ABL tyrosine kinase to be produced (Deininger, Buchdunger and Druker, 2005; Ren, 2005). The BCR-ABL tyrosine kinase is derived

from the C-ABL protein which is a tyrosine kinase involved in the cell cycle as well as response to DNA damage and growth factor signalling (Kharbanda *et al.*, 1995). BCR-ABL is an abnormal and constituently active derivative of C-ABL (Konopka, Watanabe and Witte, 1984). This tyrosine kinase is produced by the fusion of chromosome 22 at the *BCR* housekeeping gene and chromosome 9 at the *ABL* gene (Rowley, 1973; Groffen *et al.*, 1984; Kurzrock, Gutterman and Talpaz, 1988)

6.1.1 BCR-ABL inhibitor TKIs

The most established TKI used to treat CML is imatinib. This drug was discovered in 1996 and is usually used in the early stages of the disease. It functions by inhibiting BCR-ABL along with the other receptors C-KIT and PDGFR (Druker *et al.*, 1996; Buchdunger *et al.*, 2000). Imatinib has made a huge impact on the lives of CML patients. Before the discovery of imatinib the treatment for CML involved drugs including interferon-α (IFN-α) with ara-C and chemotherapy, and the 5 year survival rate was only 52% (Allan, Richards and Shepherd, 1995). The adverse effects seen were severe and included fever, a flu-like syndrome, neurologic symptoms, psychiatric disorder, hepatic events, diarrhoea, nausea, vomiting and skin rash. These drugs are still used in patients who cannot tolerate TKIs, or in countries where patients do not have access to publicly funded healthcare and cannot afford the more expensive TKI treatments (Chen *et al.*, 2011). The IRIS clinical trial, one of the best known imatinib clinical trials, demonstrated a >3 log fold reduction of the BCR-ABL transcript in patients treated with imatinib, with a 6 year follow up in 2009 showing that only 5% of deaths that occurred during the following 6 years were due to CML (Hochhaus *et al.*, 2009). This was a huge improvement from previous therapeutic outcomes. However the treatment is not without its pitfalls. Gastrointestinal toxicity makes up 26% of the known side effects of imatinib (Gambacorti-Passerini *et al.*, 2011). Nausea and diarrhoea are common side effects of imatinib therapy, and it is thought that the inhibition of KIT, which is involved in the regulation of intestinal

motility, or the irritant effects of the compound may cause these side effects (Deininger *et al.*, 2003). The inability of some patients to continue taking imatinib therapy has prompted the development of other TKIs which can be used in CML patients who are resistant or fail to respond to imatinib (Baccarani *et al.*, 2009).

Nilotinib is a newly developed TKI which is now also used to treat Philadelphia chromosome positive CML (Hochhaus *et al.*, 2015). It has been shown to be 20 times more effective than imatinib against BCR-ABL expressing cells (O'Hare *et al.*, 2005). It is very similar to imatinib, as it also inhibits the tyrosine kinases C-Kit and PDGFR (Weisberg *et al.*, 2005). Nilotinib has been shown to be effective in treating newly diagnosed CML patients in the ENESTnd study (Kantarjian *et al.*, 2011). With a dose of 300mg Nilotonib twice daily, 26% of patients showed undetectable levels of BCR-ABL transcripts, compared to 10% of patients on a 400mg once daily dose of imatinib. Gastrointestinal side effects include nausea and diarrhoea, with 9% of imatinib resistant patients suffering from diarrhoea and 10% suffering from nausea (le Coutre *et al.*, 2008).

Another newly developed tyrosine kinase inhibitor is dasatinib. This drug is a second generation TKI and is used in cases where imatinib is unsuitable. It is a dual inhibitor of both C-ABL and SRC tyrosine kinases and it has been shown to be 335 times more effective at inhibiting C-ABL than imatinib (O'Hare *et al.*, 2005). Gastrointestinal side effects of dasatinib are common, with 31% of patients reported to experience diarrhoea, 22% reported to experience nausea and 13% reported to experience vomiting. A mouse model of CML in which the mice express BCR-ABL has been used to investigate the adverse effects of the drug, however the only gastrointestinal effect seen in the study was an infiltration of granulocytes into the small intestinal mucosa (Schubert *et al.*, 2017).

Bosutinib is another second generation TKI which also functions as a dual BCR-ABL and SRC inhibitor. It has been found to be more potent than imatinib in inhibiting BCR-ABL in CML cell lines (Puttini *et al.*, 2006). Recent trials appeared to show that bosutinib was a more effective treatment with 41% of patients achieving less than 0.1% *Bcr-Abl* transcript at 12 months compared with imatinib at 27% (Cortes *et al.*, 2011). With bosutinib clinical trials still ongoing (https://clinicaltrials.gov/ct2/show/NCT02130557) it remains to be seen whether bosutinib will be used as a frontline treatment for CML. Diarrhoea is the most common side effect associated with bosutinib, with 82% of patients being affected. Nausea and vomiting are also very commonly reported adverse effects (Kantarjian *et al.*, 2014).

6.1.2 Epidermal growth factor receptor tyrosine kinase inhibitors

Another class of TKIs are the epidermal growth factor receptor (EGFR) TKIs. The first to be developed were erlotinib and gefitinib. These were initially developed to treat non-small cell lung cancer (NSCLC) (Shepherd *et al.*, 2005; Thatcher *et al.*, 2005), and have been found to be especially effective in patients with EGFR mutations (Soria *et al.*, 2012). Non-small cell lung cancer is the most common form of lung cancer and activating mutations of EGFR are found in 17% of patients with NSCLC and in 67% of those patients who had never smoked (Rosell *et al.*, 2009; Soria *et al.*, 2012).

Erlotinib is also used to treat metastatic pancreatic cancer (Belani, 2010), and gefitinib is also in phase 2 clinical trials for oesophageal cancer (Belkhiri and El-Rifai, 2015). Gefitinib and erlotinib are both reversible TKIs, as opposed to irreversible inhibitors such as afatinib (Belani, 2010). In non-small cell lung cancer, gefitinib and erlotinib cause significant and similar levels of gastrointestinal side effects including diarrhoea, nausea and vomiting (Burotto et al., 2015). Gefitinib was reported to cause diarrhoea in 35%, nausea in 20% and vomiting in 15% of patients in a clinical trial of 723

previously treated NSCLC patients. The adverse events seen in the clinical trials were recorded using the grading system of the Common Terminology Criteria for Adverse Events (available at evs.nci.nih.gov). The severity of the adverse events was mainly grade 1 and 2 with only 2.5% of patients reporting grade 3 or 4 diarrhoea and less than 1% reporting grade 3 or 4 nausea or vomiting (Kim et al., 2008). Erlotinib was found to cause diarrhoea in 55%, nausea in 40% and vomiting in 25% of patients in a clinical trial of 727 previously treated NSCLC patients. Adverse effects at grade 3 and above appear to be slightly worst for erlotinib with 5% for diarrhoea, 3% for nausea and 3% for vomiting (Shepherd et al., 2005). Atrophy of the small intestine is seen in mice treated with both gefitinib and erlotinib. Gefitinib has been found to reduce the small intestinal surface area and cause villus atrophy and reduction in the length of crypts (Hare et al., 2007). Apoptotic events in the middle and distal murine small intestine were also found to be significantly increased by an erlotinib. This was accompanied by a reduction of villus height and a decrease in the surface area of the small intestinal mucosa (Rasmussen et al., 2010).

6.1.3 Adverse effects of tyrosine kinase inhibitors

TKIs are therapies that are recommended to continue indefinitely (Baccarani *et al.*, 2009). Therefore reducing side effects is of particular relevance as any side effect will have a large impact on patients. Negative effects of all TKIs includes gastrointestinal complications such as vomiting and diarrhoea. Some of these side effects lead to the discontinuation of treatments due to their severity. Diarrhoea is listed as a side effect for all the TKIs which were studied in this chapter. According to Cancer Research UK the likelihoods of patients developing diarrhoea as a side effect are as follows for the BCR-ABL targeting TKIs: Nilotinib 1 in 10 people, imatinib 1 in 3 people, dasatinib 3 in 10 people and bosutinib 8 in 10 people (www.cancerresearchuk.org). For the EGFR targeting TKIs the likelihoods of developing diarrhoea are as follows: erlotinib 1 in 2 people, gefitinib 1 in 2 people (www.cancerresearchuk.org).

Pharmacological management of TKI related diarrhoea is usually restricted to loperamide. This medication is effective in managing TKI related diarrhoea, however it does not target the underlying off target mechanisms of the TKI related diarrhoea (Hirsh, 2011).

6.1.4 Organoids as a model for testing tyrosine kinase inhibitors

Immortalised GI cancer cell lines are not ideal for testing drugs as they are much hardier and do not represent normal physiology. Additionally, normal intestinal cells cultured as 2D monolayers under standard culture techniques do not survive long enough to allow drug testing to take place, as they die due to an attachment induced form of cell death known as anoikis (Grossmann et al., 1998). Enteroids are an emerging *in vitro* model and may provide insights into the workings of the gut, due to being relatively easy to grow and genetically manipulate, they also have a similar cellular composition to the *in vivo* gut (Merker, Weitz and Stange, 2016). Therefore using enteroids we were able to investigate whether the TKIs caused intestinal epithelial cell death and whether this could be a potential mechanism for the gastrointestinal side effects of TKIs seen in patients.

Previously when cell death inducing stimuli including 5-FU and etoposide in chapter 4 were applied to enteroids, phenotypic changes occurred. The enteroids became more circular and the crypt domains became less pronounced. As enteroids underwent more and more cell death, the epithelial barrier and the lumen of the enteroid became compromised and eventually enteroids became disrupted.

NFκB signalling has previously been shown to be active in CML. The canonical pathway is active in uncontrolled proliferation and resistance to apoptosis is seen in cells which have uncontrolled ABL signalling. Blocking the canonical NFκB signalling pathway has also been shown to sensitise BCR-ABL leukaemia cells to imatinib and dasatinib (Hsieh and Van Etten, 2014). NFκB2 signalling has previously been shown

to regulate intestinal epithelial cell shedding and apoptosis after both LPS and TNF treatment, with NFκB2 null mice having a 20% reduction in villus shortening and negligible amounts of cell shedding when compared to similarly treated control animals (Williams *et al.*, 2013).

TKIs have been investigated locally in the Department of Molecular and Clinical Pharmacology at the University of Liverpool and are known to have GI side effects. We wanted to determine the response of wild-type enteroids to TKI treatment and the influence of NF-κB modulation on the response to TKI-induced phenotypic changes. In this study, the mechanisms by which TKIs induce cell death in intestinal epithelial cells was investigated and the morphologies of enteroids treated with different TKIs were assessed. Differences between NFκB2 deficient enteroids and C57BL/6J enteroids were also investigated to determine whether this gene potentially regulates susceptibility to developing TKI-induced diarrhoea.

6.2 Results

Untreated NFκB2 null enteroids did not show any phenotypic differences when compared with untreated C57BL/6J enteroids. Additionally untreated C57BL/6J enteroids were shown to have no statistically significant differences in circularity compared to NFκB2 null enteroids at days 0, 1 and 2 (figures 6.6 and 6.10).

6.2.1 Dasatinib, bosutinib, erlotinib and gefitinib caused pathological cell blebbing in small intestinal enteroids

In order to investigate the morphology of enteroids at early time points, small intestinal enteroids were administered 10μM gefitinib, erlotinib, dasatinib, bosutinib and nilotinib. Enteroids were monitored at 0, 4, 8, 16 and 24 hours post addition of TKI (figure 6.1 & 6.2). The earliest indication of increased cell death in enteroids was the discharge of cells from the surface of the enteroid, a process termed blebbing. Increased cell blebbing or shedding can be a sign of disease or the presence of a

cytotoxic stimuli (Williams et al., 2013). Increased cell death and expulsion of the cells from the outside of the enteroids was observed when enteroids were treated with dasatinib, bosutinib, erlotinib and gefitinib (figure 6.2) but not imatinib or nilotinib (figure 6.1).

6.2.2 Dasatinib caused the earliest pathological cell shedding at 4 hours post treatment

Increased cell blebbing was seen in dasatinib treated enteroids (figure 6.2A to E). The enteroids began to extrude increased numbers of cells around 4 hours post dasatinib treatment. This was the earliest occurrence of pathological cell shedding observed in this study. The rate of apoptotic cells being extruded continued until 24 hours post dasatinib treatment, where the epithelial integrity of most of the enteroids was impaired and the vast majority of them had the disrupted phenotype typical of a dead enteroid (figure 6.2E).

6.2.3 Bosutinib caused small intestinal cell blebbing from 16 hours

The initial reaction of enteroids to bosutinib administration is shown in figure 6.1 (A to E). Bosutinib treatment caused a small amount of pathological cell blebbing on some enteroid crypt domains around 16 hours post treatment (Figure 6.1D) and were shed from the epithelial monolayer. However, enteroids did not have a disrupted phenotype 24 hours post bosutinib treatment (Figure 6.1E), and some did not appear to have increased cell blebbing at all. This may indicate that there is an initial increase in cell death which the enteroid is able to recover from, and that some enteroids are resistant to cell death induced by bosutinib.

6.2.4 Erlotinib caused pathological cell blebbing beginning at 16 hours post treatment

Enteroids treated with erlotinib for 24 hours (figure 6.2F to J) began to show signs of pathological cell blebbing after around 16 hours (Figure 6.2I) and this continued up

until 24 hours post treatment where many enteroids showed the beginnings of a disrupted phenotype and many contained large clumps of dead cells.

6.2.5 Gefitinib caused a rapid onset of cell shedding from 16 hours post treatment

Enteroids treated with gefitinib (figure 6.2K to O) began to extrude more cells from the outside of the crypt domain at around 16 hours post gefitinib administration (figure 6.2N). The outside of enteroids treated with gefitinib was covered with dead cells 24 hours post gefitinib treatment with loss of epithelial integrity seen in most enteroids. Most of the enteroids had a disrupted phenotype.

6.2.6 Imatinib and nilotinib did not cause pathological cell blebbing in enteroids at up to 24 hours after treatment

There was no difference in the appearance of untreated enteroids and enteroids treated with 10μM imatinib or nilotinib for 24 hours. The effects of imatinib treatment from 0 hours to 24 hours are shown in figure 6.1 F to J, and of nilotinib treatment are shown from figure 6.1 K to O. This suggests that the mechanisms of induction of diarrhoea may be different between bosutinib, imatinib and nilotinib.

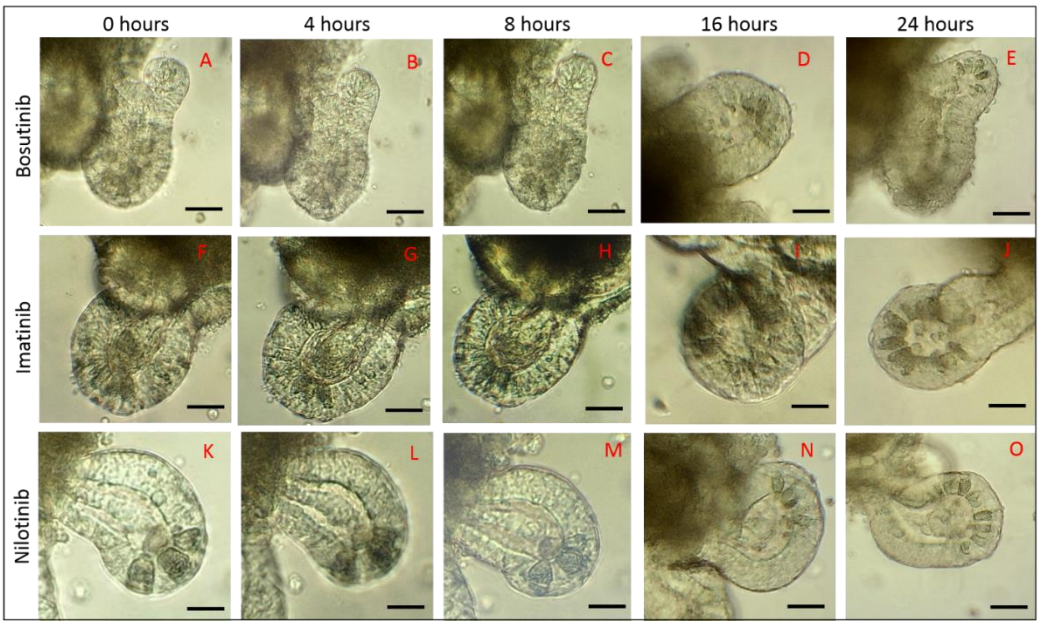

Figure 6.1 Phenotypical changes in C57BL/6J enteroids treated with 10µM imatinib (A to E), bosutinib (F to J) and nilotinib (K to O) over 24 hours. Increased cell blebbing was observed in enteroids treated with bosutinib, beginning at 8 hours (H) and increasing at 16 (I) and 24 hours (J). No increased cell shedding was seen following imatinib or nilotinib. X20 objective bright field microscopy used to take images. Representative enteroid shown. Enteroids used between 2 and 5 passages. Scale bar 20µm.

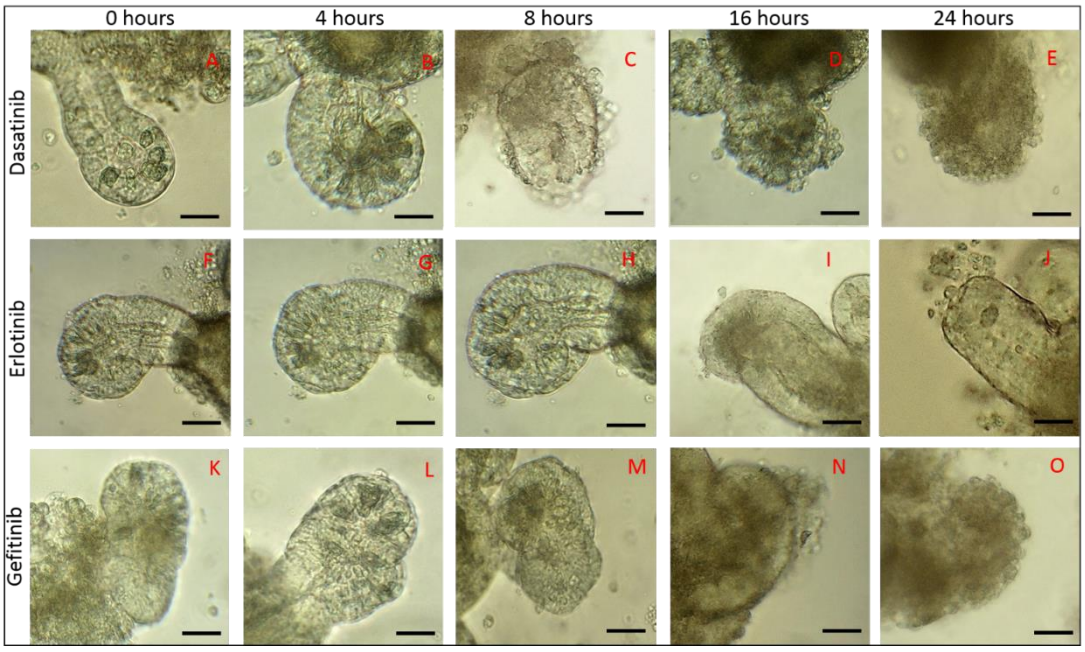

Figure 6.2 Phenotypical changes in C57BL/6J enteroids treated with 10µM dasatinib (A-E), erlotinib (F-J) and gefitinib (K-O) over 24 hours. Increased shedding was observed following dasatinib from 8 hours (C), erlotinib and gefitinib from 16 hours (D and N respectively). X20 objective bright field microscopy used to take images. Representative enteroid shown. Enteroids used between 2 and 5 passages.

6.2.7 C57BL/6J and NFκB2 null small intestinal enteroids had similar baseline growth dynamics

Both C57BL/6J and NFκB2 null mice were used in order to determine whether the NFκB2 protein, previously shown to be involved in regulating intestinal epithelial cell shedding (Williams et al., 2013) and intestinal crypt apoptosis (Burkitt *et al.*, 2015) *in vivo,* is involved in regulating TKI induced enteroid cell death.

To assess this enteroids of both C57BL/6J wild-type and NFκB2 null genotype were treated with tyrosine kinase inhibitors. Gefitinib, erlotinib, dasatinib, imatinib, bosutinib and nilotinib were administered to enteroids at 0.01μM 0.1μM 1μM and 10 μM concentrations for 3 days. Controls for each day of treatment were treated with an equivalent volume of DMSO. Two wells per treatment were conducted per experiment, and each experiment was repeated three times. There were no baseline differences in growth dynamics/morphology between C57BL/6J and NFκB2 null enteroids (figure 6.6 and 6.10).

6.2.8 Imatinib, bosutinib and nilotinib caused no significant increase in C57BL/6J or NFκB2 null enteroid circularity

C57BL/6J enteroids treated with bosutinib (figure 6.3 A to C), imatinib (figure 6.3 D to F) and nilotinib (figure 6.3 G to I) did not show any morphological signs of cell death from day 0 to day 2. Surprisingly the increased cell blebbing seen in some bosutinib treated enteroids (section 6.2.3) did not lead to a disrupted enteroid phenotype, and the enteroids appeared to recover from the initial increase in cell death. Similar responses were observed in NFκB2 null enteroids, with no morphological changes observed following treatment with bosutinib (figure 6.4 A to C), imatinib (figure 6.4 D to F) and nilotinib (figure 6.4 G to I) at 10μM concentration.

There was no significant increase from the circularity of day 0 to day 1 or day 2 for imatinib, bosutinib or nilotinib in C57BL/6J or NFκB2 null mice following any of the

TKI treatments (figure 6.5). C57BL/6J enteroids treated with imatinib showed a modest but significant decrease in circularity at day 2 compared to day 0 at the concentrations of 0.1μM (P=0.035) and 10μM (P=0.0042; figure 6.5A). This suggests that imatinib had no major effect on epithelial apoptosis, blebbing or shedding.

Nilotinib at 0.01μM caused a significant decrease in circularity from day 0 to day 1 in NFκB2 null enteroids (P=0.0031; figure 6.5D). Additionally, a significant decrease in NFκB2 null enteroid circularity compared with C57BL/6J occurred at day 2 of 0.01μM nilotinib treatment (figure 6.6). As enteroids grow they have crypt domains extending further from the lumen causing a larger perimeter compared to area and therefore a decrease in circularity. There were no significant differences observed between the circularity of the untreated enteroids from day 0, 1 and 2. This indicates that there was little or no increase in cell death and shedding caused by these TKIs.

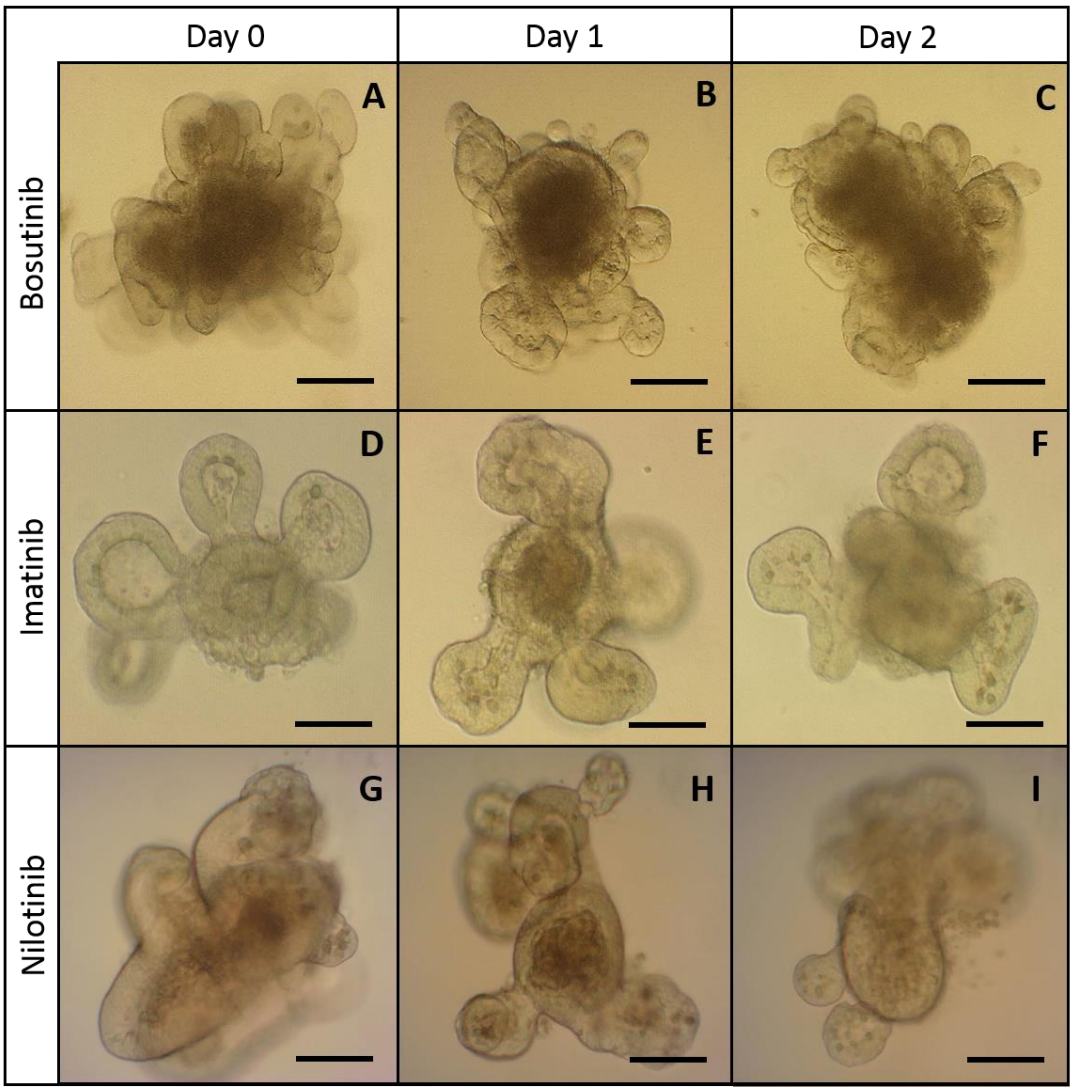

Figure 6.3 C57BL/6J enteroids treated with 10µM bosutinib (A to C) imatinib (D to F) and nilotinib (G to I). Enteroids shown at 0 hours, 24 hours and 48 hours. None of the enteroids showed any phenotypic changes when treated with the TKIs. Representative enteroids are shown. Enteroids of between 3 and 6 passages were used. Scale bar 50µm.

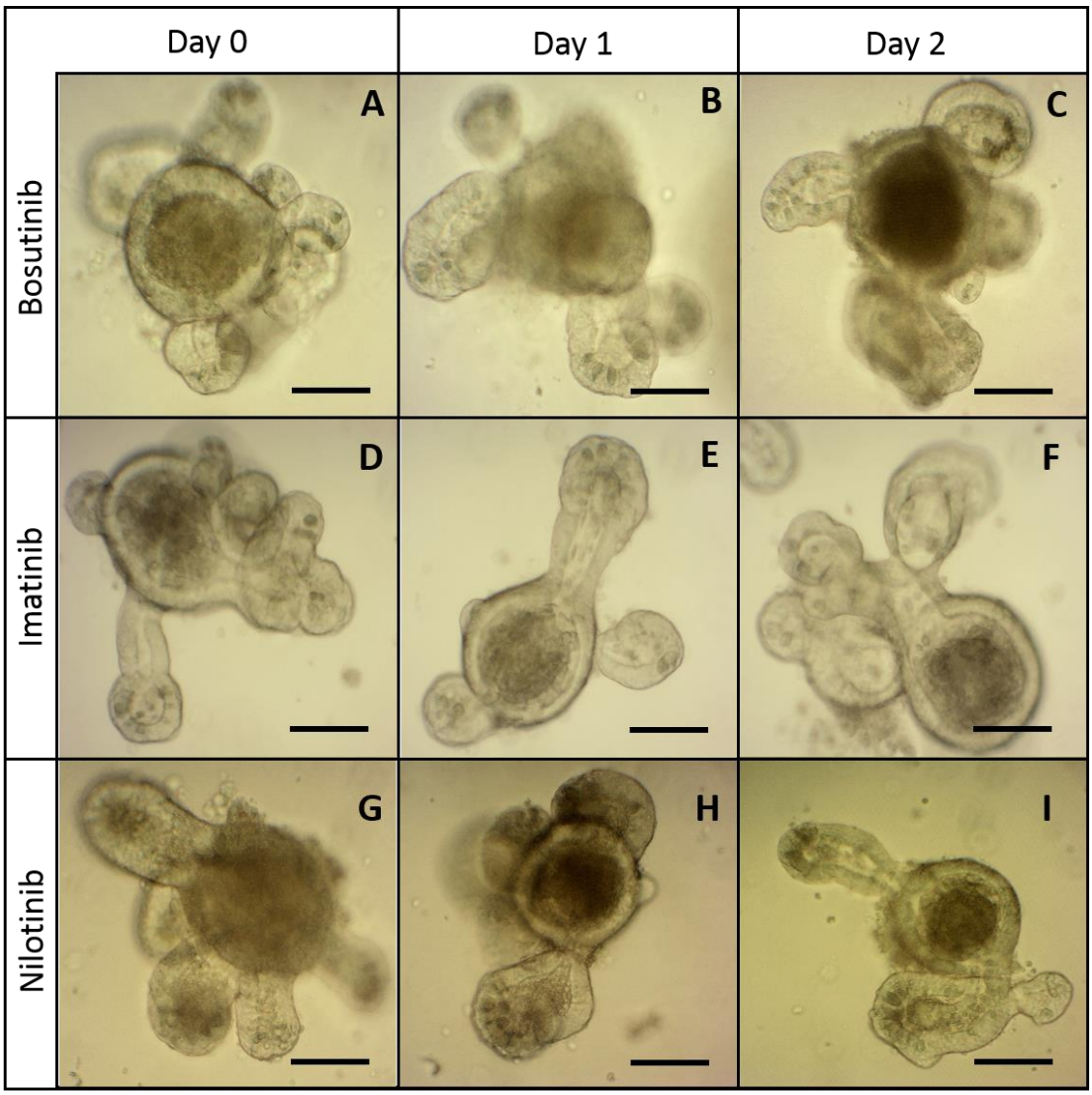

Figure 6.4 NFκB2 null enteroids treated with 10µM bosutinib (A to C) imatinib (D to F) and nilotinib (G to I). Enteroids shown at 0 hours, 24 hours and 48 hours. None of the enteroids showed any phenotypical changes when treated with the TKIs. Representative enteroids are shown. Enteroids of between 3 and 6 passages were used. Scale bar 50µm.

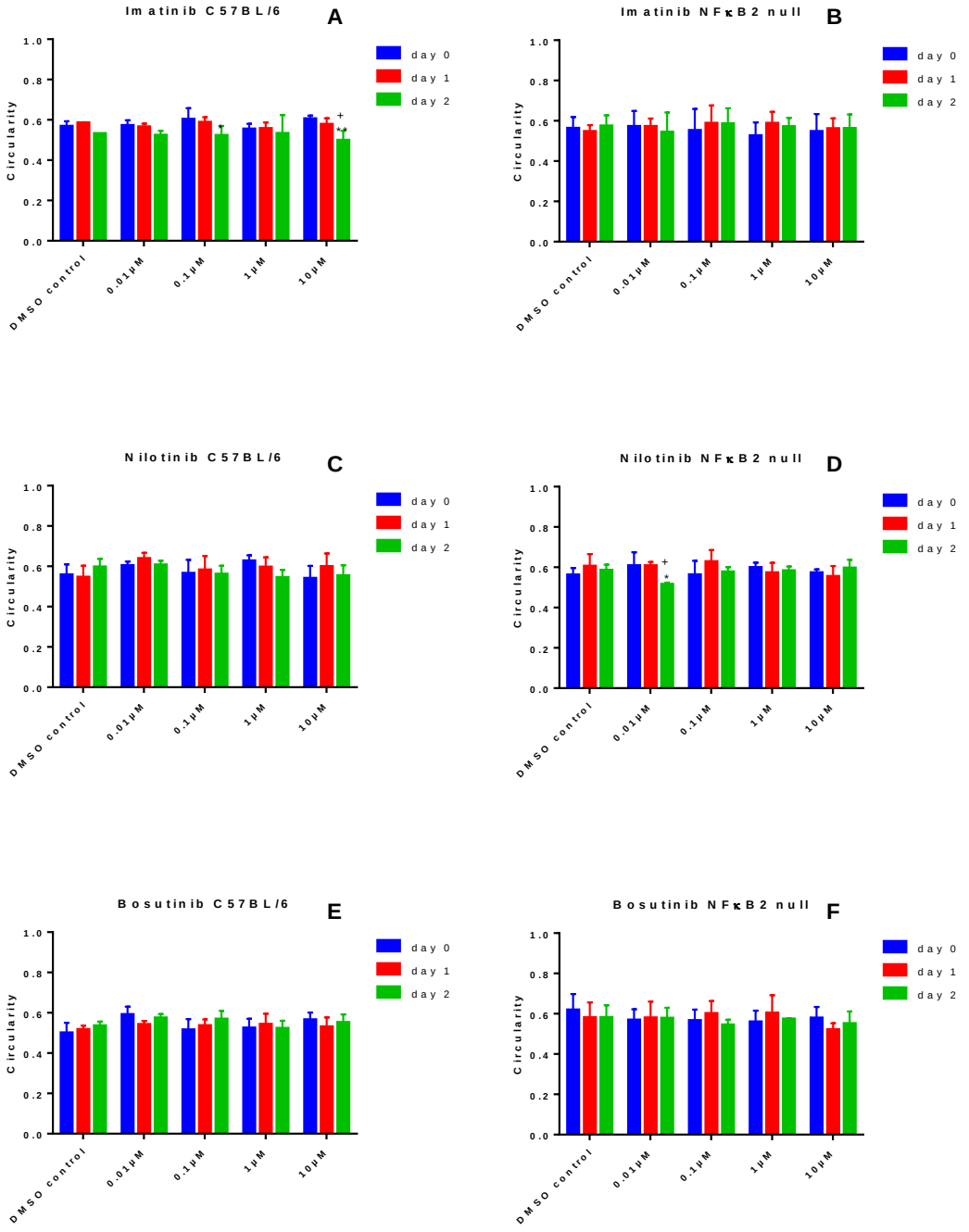

Figure 6.5 Circularity values for C57BL/6J enteroids treated with 0.01μM, 0.1μM, 1μM and 10μM, imatinib (A), nilotinib (C) and bosutinib (E) and NFκB2 null enteroids treated with 0.01μM, 0.1μM, 1μM and 10μM imatinib (B) nilotinib (D) and bosutinib (F). Circularity measurements were taken at day 0 (blue), day 1 (red) and day 2 (green). 2-Way ANOVA and Tukey's multiple comparison used for statistical analysis. * represents statistical differences compared to day 0 value. *=P<0.05. + represents statistical differences compared to day 1 value +=P<0.05. Enteroids of between 2 and 7 passages were used. N=3 (3 experimental replicates) and n=2 (2 technical replicates per experiment).

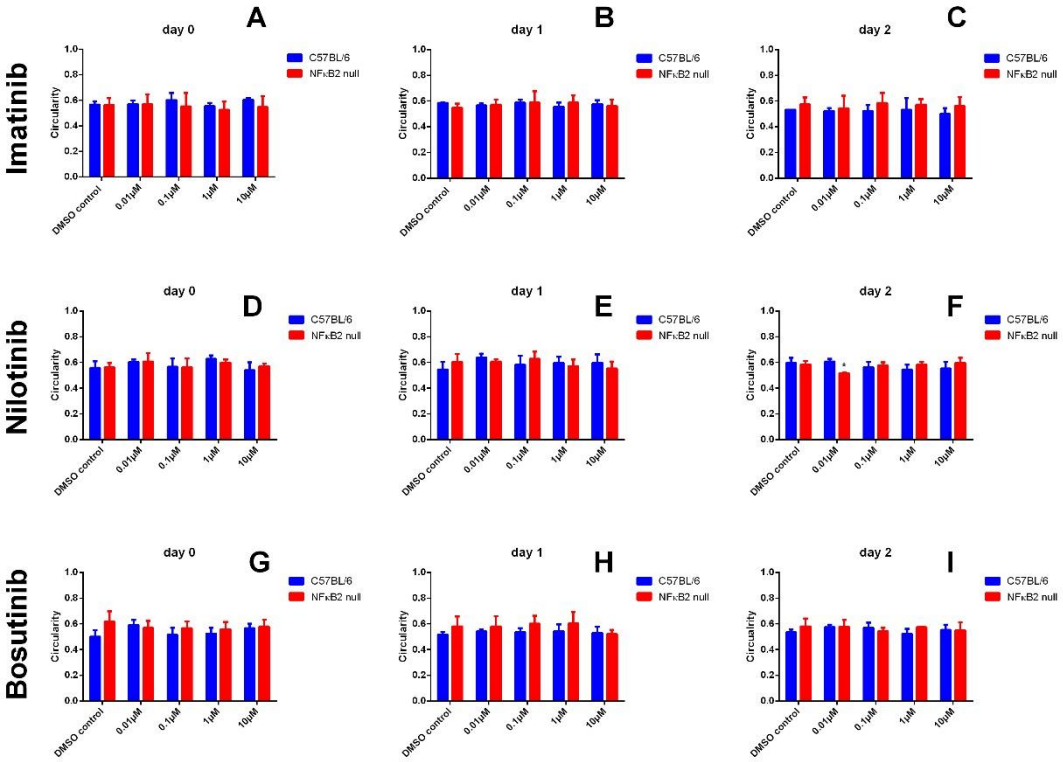

Figure 6.6 Circularity values for C57BL/6J (blue) compared with NFκB2 null (red) enteroids treated with 0.01μM, 0.1μM, 1μM and 10μM of imatinib (A-C),nilotinib (D-F) and bosutinib (G-I). Enteroids compared on day 0, day 1 and day 2. 2-Way ANOVA and Tukey's multiple comparison used for statistical analysis. * represents statistical differences compared to day 0 value. *=P<0.05. Enteroids of between 2 and 6 passages used. N=3 (3 experimental replicates) and n=2 (2 technical replicates per experiment).

6.2.9 Gefitinib increased circularity of both C57BL/6J and NFκB2 null enteroids

C57BL/6J enteroids treated with gefitinib underwent rapid increases in cell death (Figure 6.7 D to E). At the highest concentration of gefitinib, the majority of C57BL/6J enteroids had a disrupted phenotype by day 1 of treatment (figure 6.7E). A similar effect was seen in NFκB2 null enteroids administered the same treatment (figure 6.8 D to E).

C57BL/6J and NFκB2 null enteroids were not affected by 0.01μM of gefitinib, as shown by the absence of any significant increase in circularity between day 0, day 1 and day 2 (figure 6.9 A and B respectively). C57BL/6J enteroids treated with 1μM of gefitinib showed a significant increase (P=0.0066) in circularity of 0.56 to 0.68 from day 0 to day 1. An additional increase in circularity was observed at day 2 post gefitinib treatment with a circularity of 0.79, which was significant when compared to day 0 (P<0.0001) and day 1(P=0.0066). NFκB2 null enteroids treated with 1μM gefitinib had a mean average circularity of 0.5302 on day 0, this increased to 0.73 at day 1 and 0.76 at day 2. Both day 1 (P<0.0001) and day 2 (P<0.0001) circularities were found to be statistically significantly increased when compared to the untreated controls. C57BL/6J enteroids treated with 10μM gefitinib had a circularity of 0.58 at day 0 which increased significantly at day 1 to 0.78 (P<0.0001) and on day 2 to 0.808 (P.0.001). NFκB2 null enteroids treated with 10μM gefitinib had a mean circularity of 0.56 at day 0, which increased to 0.81 at day 1 (P<0.0001) and 0.84 at day 2 (P<0.0001). When the C57BL/6J and NFκB2 null enteroid datasets were compared, no significant differences were found between any of the groups at day 0, day 1 or day 2 (figure 6.10 A, B and C respectively). This suggests that gefitinib does not modulate enteroid cell death via NFκB2 signalling.

6.2.10 Erlotinib-induced enteroid apoptosis was regulated by NFκB2 signalling

C57BL/6J enteroids treated with 10μM erlotinib had a disrupted phenotype by day 1 post treatment and all enteroids in this group exhibited a disrupted phenotype by day 2 (Figure 6.7 G to J). NFκB2 null enteroids showed a blunted response to erlotinib treatment with most enteroids showing a normal phenotype at day 1, but many were disrupted by day 2 (figure 6.8 G to I). No significant differences compared to the control were seen in enteroids of either genotype treated with erlotinib concentrations of 0.01μM or 0.1μM erlotinib (figures 6.9C and 6.9D). In C57BL/6J enteroids treated with 1μM erlotinib, the circularity increased from 0.50 at day 0 to 0.60 at day 1 to 0.65 at day 2 (figure 6.9A). A significant increase was seen between day 0 and day 1 ($P=0.0065$) and between day 0 and day 2 ($P=0.0001$). In NFκB2 null enteroids treated with 1μM erlotinib, there were no significant differences in circularity on day 1 or 2 compared to day 0. This indicates that the NFκB2 null enteroids required the highest concentration of 10μM and the longest exposure time of 48 hours to demonstrate significant cell death.

When the response to erlotinib of C57BL/6J and NFκB2 null enteroids was compared, it was found that at day 1 there was significantly lower circularity in NFκB2 null enteroids at 10μM compared with C57BL/6J (figure 6.10E), and at day 2 there was significantly lower circularity in NFκB2 null enteroids compared with C57BL/6J at 1μM (figure 6.10F). Erlotinib had induced cell death in the C57BL/6J enteroids by day 1 at 10μM and by day 2 at 1μM, but these treatments did not result in rounding in the NFκB2 null enteroids, suggesting that deletion of NFκB2 signalling specifically in intestinal epithelial cells confers resistance against erlotinib induced cells death and potentially the GI side effects of erlotinib therapy.

6.2.11 Dasatinib caused cell death and the disrupted phenotype more rapidly in C57BL/6J compared with NFκB2 null enteroids

Examination of phenotypical changes in C57BL/6J (figure 6.7A to C) and NFκB2 null enteroids (figure 6.8A to C) revealed no differences in response to 10μM dasatinib treatment. The C57BL/6J and NFκB2 null enteroids treated with 0.01μM and 0.1μM dasatinib showed no significant changes from day 0 to day 1 and 2 (figure 6.9E and F respectively). There were no differences between the untreated DMSO controls for day 0, 1 and 2 for either genotype. The C57BL/6J enteroids treated with 1μM dasatinib showed increases in circularity from day 0 (0.54) to day 1 (0.65; P=0.0014) and retained the same level of circularity through day 2 (0.65; P=0.0013). NFκB2 null enteroids treated with 1μM dasatinib began at day 0 with a mean circularity of 0.55 which increased to 0.69 at day 1 (P<0.0001) and 0.67 at day 2 (P<0.0001).

C57BL/6J enteroids treated with 10μM dasatinib began with a mean circularity of 0.56 which then rose to 0.75 at day 1 and 0.76 at day 2. There was significant change between day 0 and day 1 (P<0.0001), and day 0 and day 2 (P<0.0001).

When treated with 10μM dasatinib the NFκB2 null enteroids initially had a mean circularity of 0.54 at day 0. The circularity increased significantly at day 1 to 0.76, and at day 2 increased again to 0.83.

Comparison of C57BL/6J and NFκB2 null enteroids revealed no significant differences between day 0 and day 1 enteroids at any of the concentrations of dasatinib tested (figure 6.10 G and H). However at day 2 significant differences were found between the 0.01μM and 10μM concentrations of dasatinib (figure 6.10I). When treated with 10μM dasatinib, NFκB2 null enteroids were significantly more circular (P=0.049) than C57BL/6J. The increase in circularity between each of the days may indicate that the drug causes a slower cell death in the NFκB2 null enteroids as there is more time for the enteroids to become circular, as opposed to being dead at day 1

and the circularity not changing as seen in C57BL/6J enteroids. Alternatively this may indicate that NFκB2 null enteroids are more sensitive to dasatinib when compared with C57BL/6J enteroids.

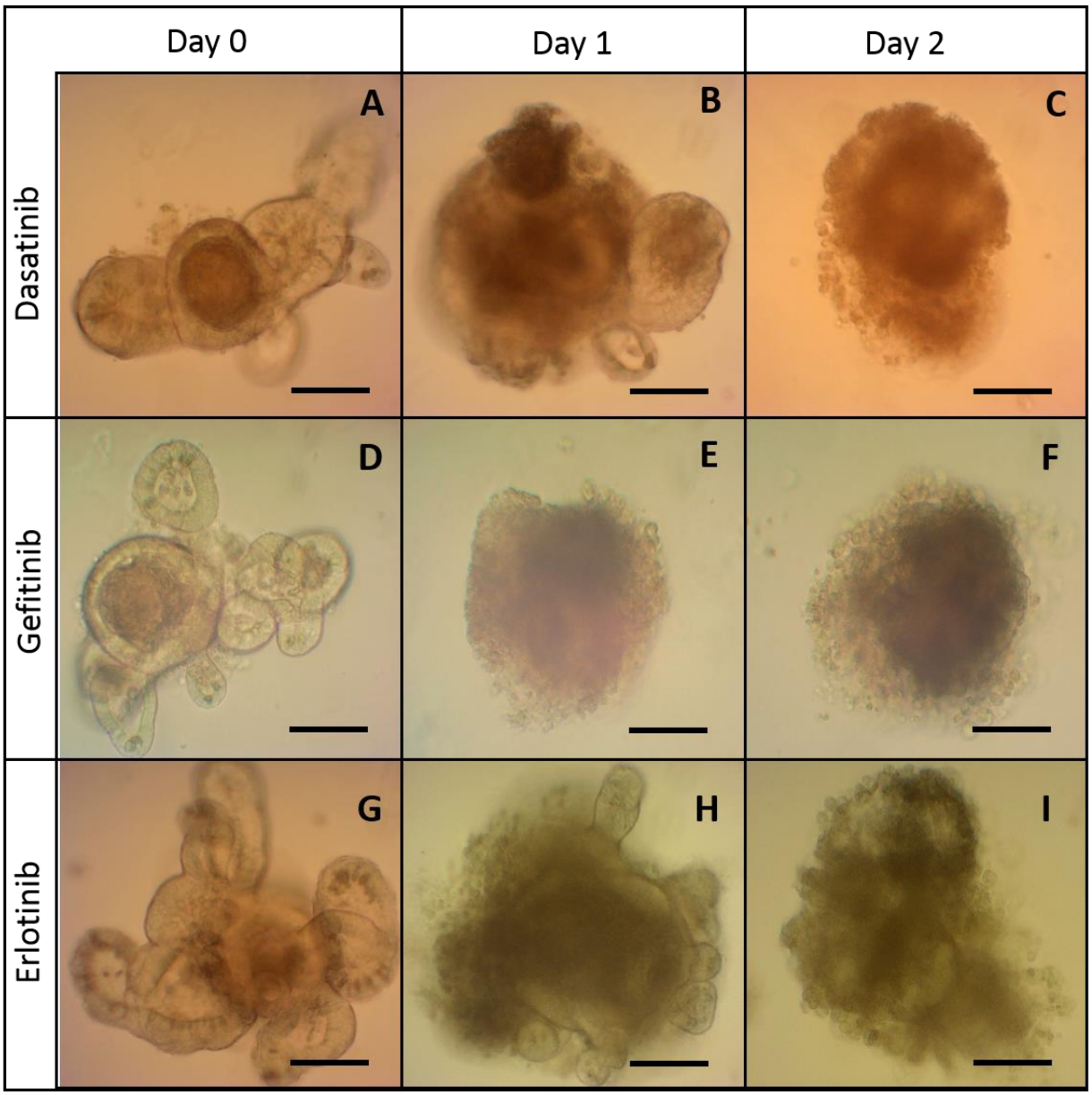

Figure 6.7 C57BL/6J enteroids treated with 10μM dasatinib (A to C), gefitinib (D to F) and erlotinib (G to I). Enteroids shown at 0 hours, 24 hours and 48 hours. A disrupted enteroid phenotype was seen in dasatinib treated enteroids by day 2(C), in gefitinib treated enteroids at day 1(E) and in erlotinib treated enteroids at day 2 (I). Representative enteroids are shown. Enteroids of between 2 and 7 passages used. Scale bar 50μm.

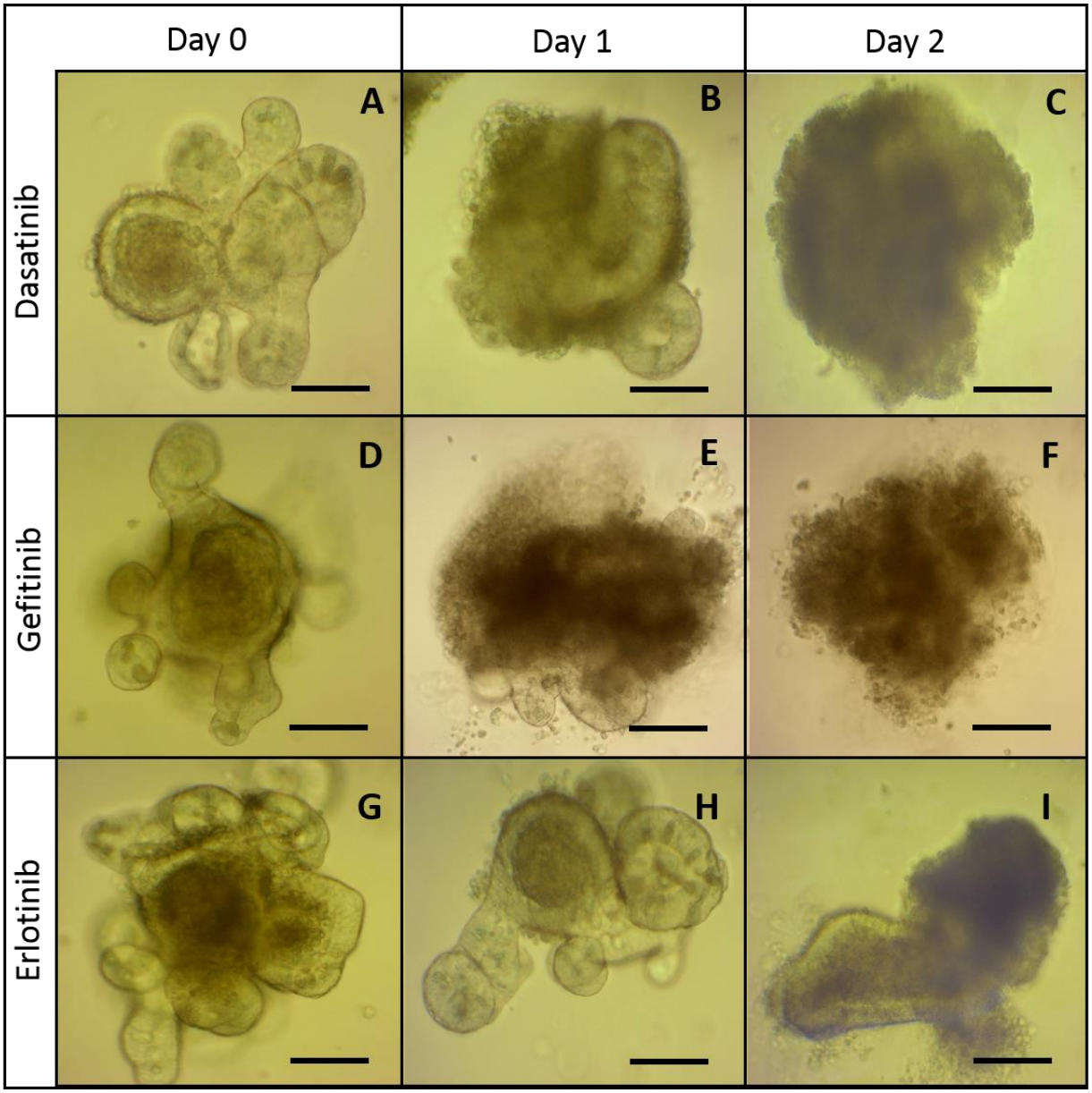

Figure 6.8 NFκB2 null enteroids treated with 10μM dasatinib (A to C), gefitinib (D to F) and erlotinib (G to I). Enteroids shown at 0 hours, 24 hours and 48 hours. A disrupted enteroid phenotype was seen in dasatinib treated enteroids by day 2(C), in gefitinib treated enteroids at day 2(F) and in erlotinib the majority were disrupted by day 2 (I). Representative enteroid shown. Enteroids of between 2 and 7 passages were used. 50μm scale bar.

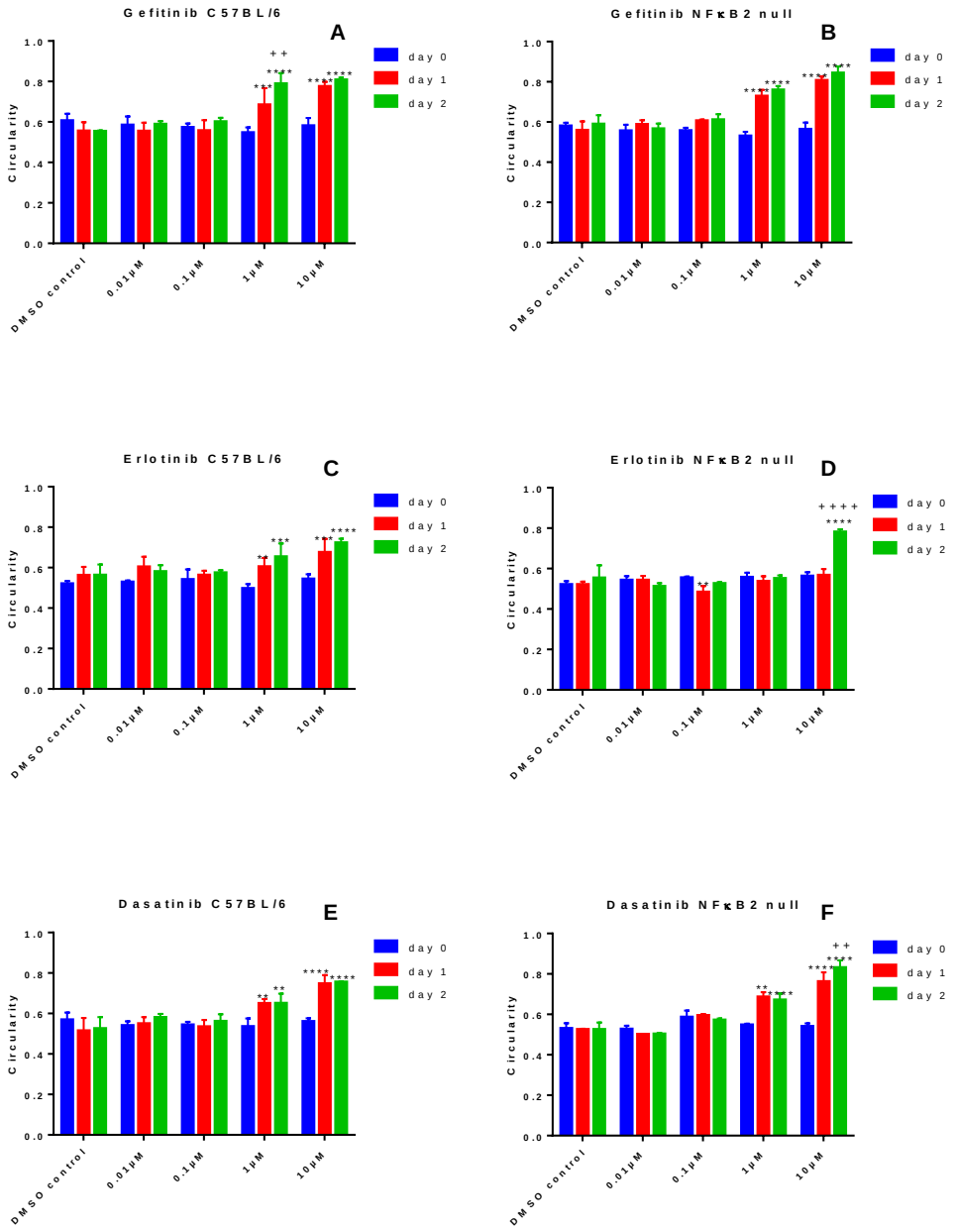

Figure 6.9 Circularity values for C57BL/6J enteroids treated with 0.01µM, 0.1µM, 1µM and10µM gefitinib (A), erlotinib (C) and dasatinib (E) and NFκB2 null enteroids treated with 0.01µM, 0.1µM, 1µM and 10µM gefitinib (B) erlotinib (D) and dasatinib (F). Circularity measurements were taken at day 0 (blue), day 1 (red) and day 2 (green). 2-Way ANOVA and Tukey's multiple comparison used for statistical analysis. * represents statistical differences compared to day 0 value. *=P<0.05, **=P<0.01, ***=P<0.001, ****=P<0.0001. + represents statistical differences compared to day 1 value ++=P<0.05, ++++=P<0.0001. Enteroids of between 2 and 7 passages used. N=3 (3 experimental replicates) and n=2 (2 technical replicates per experiment).

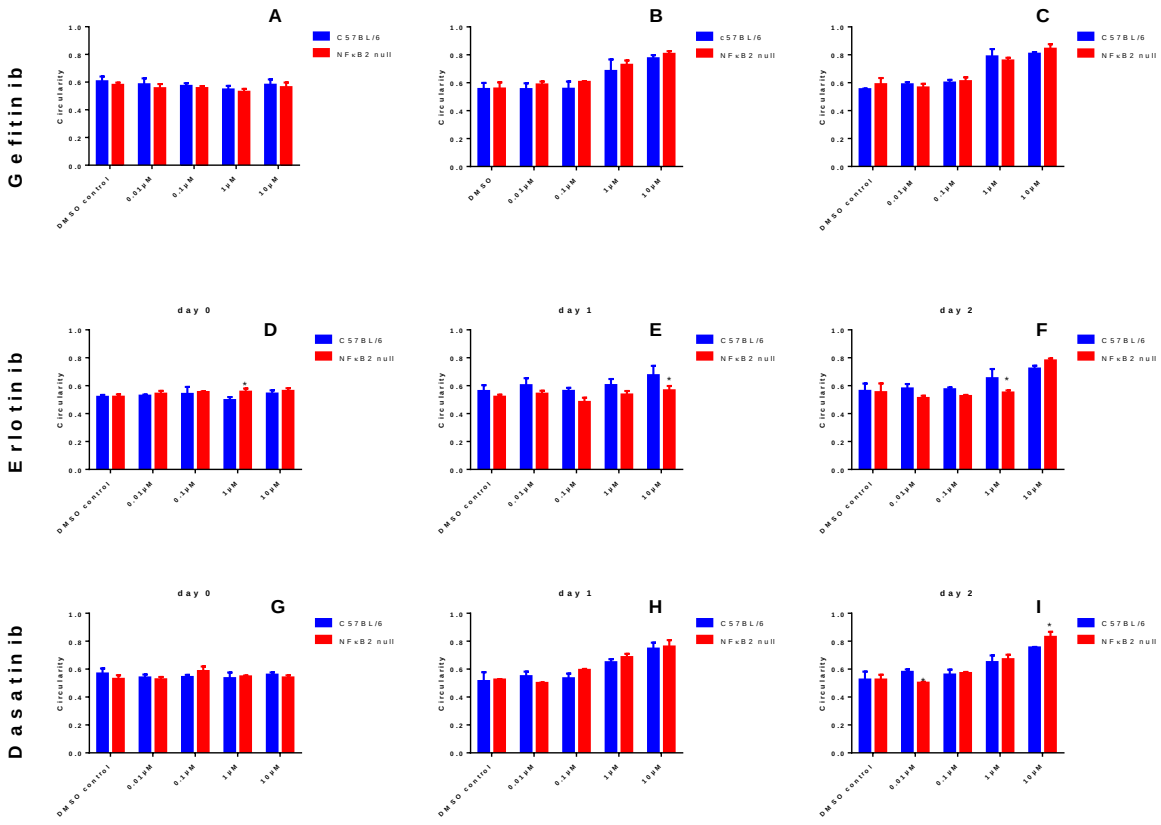

Figure 6.10 Circularity values for C57BL/6J (blue) compared with NFκB2 null (red) enteroids treated with 0.01µM, 0.1µM, 1µM and 10µM of gefitinib (A-C), erlotinib (D-F) and dasatinib (G-I). Enteroids compared on day 0, day 1 and day 2. 2-Way ANOVA used for statistical analysis. * represents statistical differences compared to day 0 value. *=P<0.05. Enteroids of between 2 and 7 passages used. N=3 (3 experimental replicates) and n=2(2 technical replicates per experiment).

Name	Targets	Used for	Apoptosis in C57BL/6J	Apoptosis in NFκB2 null
Imatinib	BCR-ABL	CML	↔	↔
Nilotinib	BCR-ABL	CML	↔	↔
Dasatinib	BCR-ABL, SRC	CML	↑↑	↑↑
Bosutinib	BCR-ABL, SRC	CML	↔	↔
Gefitinib	EGFR	NSCLC	↑↑	↑↑
Erlotinib	EGFR	NSCLC	↑↑	↑

Table 6.1. Summary of TKIs and their effects on C57BL/6J and NFκB2 null organoids. ↔ represents little or no change in circularity, ↑ represents increase in circularity.

6.3 Discussion

Imatinib, nilotinib and bosutinib did not cause any significant increase in cell death in organoids of either C57BL/6J or NFκB2 null phenotype whereas, dasatinib, gefitinib and erlotinib induced cell death in both genotypes (table 3). Imatinib, dasatinib, bosutinib and nilotinib are used to treat chronic myeloid leukaemia by targeting BCR-ABL. However off target and unwanted gastrointestinal side effects are often reported by patients. Dasatinib however was the only BCR-ABL targeting tyrosine kinase inhibitor to cause significant increases in circularity in murine enteroids, although bosutinib also caused a noticeable increase in cell blebbing at early time points. Both bosutinib and dasatinib are dual BCR-ABL and SRC inhibitors (Boschelli et al., 2001; Keller, Schafhausen and Brummendorf, 2009). It is therefore likely that wild-type ABL inhibition does not induce cell death in enteroids, as imatinib and nilotinib inhibit ABL but did not cause any effects on the enteroids. Therefore SRC inhibition may account for the increased cell death induced by dasatinib and bosutinib. SRC is known to modulate several oncogenic signalling pathways including EGFR, HER2/neu, FGFR and VEGF (Lombardo et al., 2004). SRC is also known to inhibit cell death by inhibiting the intrinsic apoptosis pathway by accelerating the degradation of BIK, a tumour suppressor which is involved in the initiation of apoptosis (Lopez et al., 2012).

One of the most frequent adverse effects to be observed when EGFR inhibitor TKIs are used in cancer treatment is diarrhoea. This can lead to the decreasing of dose or even ceasing treatment in patients, and may cause a significant decrease in a patient's quality of life (Ito *et al.*, 2006; Hirsh, 2011). In addition, diarrhoea can become significantly worse in patients who require chemotherapy alongside TKI treatment (P. Chen et al., 2011). Hypotheses about how TKIs targeting EGFR cause diarrhoea vary; for example it has been suggested that an alteration of chloride absorption in the intestine due to the blockage of the negative regulation of chloride by EGF causes

diarrhoea (Uribe et al., 1996; Loriot et al., 2008). Considering the increase in apoptosis observed in this enteroid model, a more likely explanation is that these drugs cause direct damage to the mucosa as a result of the inhibition of proliferative signalling of EGFR (Berlanga-Acosta et al., 2001; Loriot et al., 2008). EGFR has been shown to be involved in the response to DNA damaging agents. For example EGFR defective mice have been found to be more susceptible to DSS induced colitis, and EGF null mice have been shown to have increased severity of lesions in the duodenum in response to cyteamine (Egger et al., 2000; Troyer et al., 2001). It has been previously shown that erlotinib administration in mice caused damage to the small intestinal and colonic mucosa by increased apoptosis, which was most pronounced in the distal small intestine (Rasmussen et al., 2010). The same researchers also showed that gefitinib caused intestinal damage and villus atrophy in the small intestine, in particular the proximal region (Hare et al., 2007). Gefitinib and erlotinib both caused cell death in enteroids. Both of these are EGFR inhibitors, and as EGFR has been shown to inhibit cell shedding in ileal enteroids and in zebrafish small intestine (Miguel et al., 2017), it is likely that this inhibition is the cause of the enteroid death.

The mechanism of action of EGFR inhibitor damage to small intestinal enteroids has not been directly investigated in this study. However gefitinib has been shown to increase apoptosis in bladder cancer cells by the blockage of EGFR. This leads to a reduction of the usual inhibition of extrinsic apoptosis (Shrader et al., 2007). This form of cell death has been shown to occur via death receptor 5 (DR5) and the extrinsic apoptotic pathway in non-small cell lung cancer cells (Yan et al., 2015) and gastrointestinal epithelial cells have also been shown to have increased apoptosis in response to an antagonistic monoclonal antibody to DR5 in ileal crypt basal columnar cells (Finnberg et al., 2016). Therefore decreased inhibition of the extrinsic apoptotic pathway is a possible mechanism for the cell death observed in enteroids due to

gefitinib. Further evidence for this is seen in the decreased response of NFκB2 null enteroids treated with erlotinib compared to wild-type. Signalling via NFκB2 has been shown to favour apoptosis and cell shedding when LPS and TNF were used to induce cell death in NFκB2 null mice (Williams et al., 2013) via the extrinsic apoptotic pathway. Therefore EGFR inhibitors may be causing cell death through blocking the anti-apoptotic effects of EGFR signalling, and NFκB2 null mice may be protected from this as the lack of NFκB2 caused a reduction in extrinsic apoptotic signalling (Yamaoka et al., 2008).

An interesting consequence of NFκB2 deficiency would likely be increased amounts of RELB available for heterodimer formation with other NFκB subunits. Research into multiple myeloma (Roy et al., 2016) indicated that the lack of P100 (the pre-proteolysis form of NFκB2) in MEF (mouse embryonic fibroblast) cells caused increased numbers of RELB:P50 dimers to form. This group also showed that these dimers could confer resistance to TNF mediated apoptosis in MEFs (Roy et al., 2016). It is possible that if this dimer is present in the NFκB2 deficient murine gut, it may explain the resistance of NFκB2 null mouse epithelia to apoptosis, and the NFκB2 null mouse derived enteroid resistance to apoptosis induced by erlotinib. This dimer may therefore represent a possibility for future investigation into how to reduce damage induced by pro-apoptotic NFκB2 signalling.

Gefitinib treated enteroids did not show any differences in the amount of cell death between C57BL/6J and NFκB2 null genotypes. However, gefitinib and erlotinib may not have the same properties, as demonstrated in studies where they were shown to damage different regions of the mouse small intestine more severely (Hare et al., 2007; Rasmussen et al., 2010), with gefitinib inducing peak intestinal damage in the proximal small intestine and erlotinib causing more apoptosis and villus atrophy in the distal small intestine. Therefore it may be that the proximally derived enteroids used in our study were overly sensitive to gefitinib - this may explain the lack of a difference

between the responses of C57BL/6J and NFκB2 null enteroids. Such a strong response may have masked any differences between the C57BL/6J and NFκB2 null enteroids. In light of this it may be beneficial to repeat the gefitinib study using distal enteroids instead.

The increase in cell blebbing caused by dasatinib could also be partly explained by an increased activation of the extrinsic apoptotic pathway. SRC kinases act upstream of EGFR signalling pathways (Lombardo et al., 2004), therefore this may be a cause of the cell death. However as SRC is also known to suppress cell death via the intrinsic pathway of apoptosis (Lopez et al., 2012), this seems a more obvious explanation for cell death. NFκB2 null enteroids did take longer to develop a disrupted phenotype than C57BL/6J enteroids, indicating some resistance. Therefore it is possible that there is a similar RELB:P50 dimer effect in the dasatinib treated enteroids alongside the direct SRC effects.

The results presented in this chapter indicate that there is a link between mechanisms of cell death caused by erlotinib and the NFκB2 protein, with NFκB2 deficiency resulting in definite protective effects. Further investigation is now needed to determine why this difference was not seen in gefitinib treated enteroids, as we expected a similar result. Future studies using an NFκB2 null mouse model of erlotinib administration could also be performed to see if this effect occurs *in vivo*. If NFκB2 null mice experience less diarrhoea and intestinal damage when erlotinib is administered, this would further suggest that the diarrhoea is caused by cell death via the extrinsic apoptotic pathway to which NFκB2 contributes.

7 General discussion

NFκB signalling is involved in regulating the proliferation and homeostasis of the intestinal epithelium as well as a large number of other physiological functions (Gilmore, 2006; Perkins and Gilmore, 2006). The classical NFκB signalling pathway has been extensively studied, and consequently much is known about the function of its main subunit RelA. The RelA:NFκB1(P50) dimer is the most abundant dimer in classical NFκB signalling (Oeckinghaus and Ghosh, 2009). RelA is known to be essential for the normal proliferation of intestinal epithelial cells, the protection of epithelial cells during inflammation and the recovery of epithelia from the damage caused by inflammation (Steinbrecher *et al.*, 2008). Deletion of NEMO, a key classical signalling kinase, causes spontaneous colitis and excessive amounts of intestinal apoptosis (Nenci *et al.*, 2007). As well as functioning in normal intestinal epithelia, classical NFκB pathway signalling is known to control the expression of cytokines, chemokines and adhesion molecules, and plays a key role in the inflammatory response in the gut (Wullaert, Bonnet and Pasparakis, 2011). RelA is highly active in IBD patients, and corticosteroids have been shown to strongly inhibit its expression (Schreiber, Nikolaus and Hampe, 1998). NFκB signalling has also been shown to be active in mouse models of colitis (Soler *et al.*, 1999), and inhibition of classical NFκB pathway signalling is known to ameliorate colitis in IL10 null mice (Davé *et al.*, 2007), in DSS-induced colitis and in TNBS-induced colitis (Shibata *et al.*, 2007). As well as its role in regulating inflammation, NFκB signalling also plays a key role in regulating the response to DNA damaging agents. For instance, classical NFκB pathway signalling is known to block apoptosis in epithelial cells, and its inhibition causes increased apoptosis in the murine intestinal epithelium in response to ionising radiation (Egan *et al.*, 2004; Wang *et al.*, 2004). However, despite several key studies exploring the importance of the classical NFκB signalling pathway in the normal and damaged intestine, the role of the alternative NFκB signalling pathway has not been

as extensively studied. Active NFκB2 signalling has been observed in human ulcerative colitis (Andresen *et al.*, 2005) and NFκB2 deletion in mice has been shown in this thesis (chapter 3.3.2) and in prior studies to reduce susceptibility to DSS-induced colitis (Burkitt *et al.,* 2015). Additionally in our lab, the small intestinal epithelial cells of NFκB2 null mice have been found to be less susceptible to lipopolysaccharide (LPS)-induced apoptosis (Williams *et al.*, 2013). We therefore wanted to investigate whether NFκB2 null mice showed altered susceptibilities to other forms of GI damage. Therefore, the aim of this thesis was to investigate the roles of various NFκB subunits in regulating the GI damage caused by various agents and to investigate to what extent these effects were mediated by intestinal epithelial cells.

7.1 Main findings

7.1.1 NFκB2 subunit deletion ameliorates colitis and this effect is mediated by both the immune and epithelial compartments

Previous work in our lab found that NFκB2 null mice were less susceptible to DSS-induced colitis (Burkitt *et al.*, 2015). In this thesis it was also found that NFκB2 null mice developed a reduced severity of DSS-induced colitis, with reduced inflammation in the distal colon and very little noticeable change in the overall health of treated mice. Conversely c-Rel null mice were statistically significantly more susceptible to DSS-induced colitis than their wild-type counterparts; a trend that was also observed by Burkitt *et al.* 2015, however, this initial study did not reach statistical significance (Burkitt *et al.* 2015). There is a correlation between our observation of altered susceptibility to DSS-induced colitis in c-Rel null mice with findings in human IBD as the *c-Rel* gene homolog, *REL,* has been shown to be at high risk of harmful mutation in patients with both Crohn's disease and ulcerative colitis (Franke *et al.*, 2010; McGovern *et al.*, 2010).

We wanted to address whether altered susceptibility to DSS-induced colitis was a consequence of perturbed NFκB signalling exclusively in the immune or epithelial cell compartments. Investigation using bone marrow reconstitution to introduce the hematopoietic cells of either C57BL/6J or NFκB2 null mice into both C57BL/6J and NFκB2 null recipient mice indicated that colitis susceptibility was mediated by signalling in both the immune compartment and the epithelial compartment, suggesting that both cell populations are important for regulating the epithelial cell response to damage caused by DSS. In addition, during DSS-induced colitis the alternative NFκB signalling pathway functions in haematopoietic and epithelial cells to increase severity of colitis. These data are supported by previous findings by Hollenbach and colleagues who found that a significant downregulation of alternative NFκB pathway signalling induced by a MAPK inhibitor ameliorated DSS-induced colitis in mice (Hollenbach *et al.*, 2004). Another interesting study whose findings mirrored ours was conducted using *Nlrp12* null mice. These mice demonstrated an exacerbation of DSS-induced colitis mediated by alternative NFκB signalling in both the hematopoietic and non-hematopoietic compartments (Allen *et al.*, 2012).

A whole host of pro-inflammatory factors are undoubtedly activated by alternative NFκB pathway signalling during DSS-induced colitis (McDaniel *et al.*, 2016), and it is clear from our results that the tightly controlled alternative NFκB signalling pathway influences the outcome of DSS administration. On a molecular level we showed that *Tnf, Cox-2, Cxcl9, Cxcl10* and *Csf1* were upregulated in the colonic mucosa of DSS treated C57BL/6J mice, but were not upregulated in NFκB2 null mice*. Cox-2* and *Tnf* are known to be upregulated during inflammation, and their upregulation in our study added validation and confidence to the results. Csf1 is known to be responsible for the activation of macrophages and increasing inflammation in BALB/C mice (Marshall *et al.*, 2007), and is also known to cause the upregulation of *Tnf. Cxcl10* is overexpressed in the mucosa of UC patients (Ostvik *et al.*, 2013).

7.1.2 C-Rel deletion protects enteroids from 5-FU and etoposide induced cell death

Intestinal mucositis is a serious unwanted side effect of chemotherapy and is caused by the action of chemotherapeutic agents on the rapidly proliferating epithelial cells of the gut. In order to investigate whether NFκB subunit deletion has protective effects in chemotherapy related GI damage, enteroids were treated with 5-FU, etoposide and irinotecan. The enteroids consisted solely of epithelial cells and therefore this investigation focussed on the effects of chemotherapy on the gut epithelia in isolation. Before enteroids were used to investigate the intestinal epithelial cell specific effects of these chemotherapeutic agents, we needed a method by which to measure morphology and cell death. Enteroids have previously been observed to become more circular in response to cytotoxic stimuli (Jones and Duckworth, unpublished) with the disappearance of protruding crypt domains. The circularity of enteroids can be measured using the 'counter' plug in on image J using light microscope images of enteroids *in vitro*. Methods were also developed to embed enteroids in Histogel and section them to perform H+E staining and immunohistochemistry (IHC). We found that there was a positive linear correlation between the amounts of morphologically apoptotic and active caspase-3 positive cells seen in H+E and IHC stained sections of enteroids, and the circularity of these enteroids, suggesting that circularity is a good indicator of active caspase-3 activity.

Unlike the protectivity conferred by NFκB2 deletion during DSS-induced GI damage *in vivo* (section 3.2.2-3.2.3), NFκB2 null enteroids were found to be more sensitive to etoposide and 5-FU induced cell damage. Additionally, RelB null organoids were more sensitive to etoposide, indicating that the alternative NFκB signalling pathway may function to protect the intestinal mucosa from these DNA damaging stimuli. However, similarly to the DSS-induced colitis data, both RelB and NFκB2 null enteroids were found to be resistant to irinotecan induced cell death indicating a

protection conferred by a lack of alternative NFκB pathway signalling. The c-Rel null organoids were also found to be resistant to 5-FU and etoposide induced cell death. Targeting the c-Rel subunit in the intestinal epithelium may therefore reduce the severity of intestinal mucositis and is worth investigating this as an adjuvant to 5-FU chemotherapy. NFκB1 null organoids were resistant to etoposide induced cell death although they responded similarly to C57BL/6J organoids when treated with 5-FU.

Irinotecan had varying effects on the classical NFκB pathway knockout enteroids, with a protective effect seen in NFκB1 null enteroids and an increased amount of cell death seen in c-Rel null enteroids. Although NFκB signalling can be broadly categorised into two pathways, the classical and alternative pathways, it is important to be mindful that although these groupings are useful, there is crossover between the pathways and sometimes the subunits which belong to the same pathway can have conflicting roles.

7.1.3 *In vivo* deletion of c-Rel protects intestinal epithelial cells from 5-FU induced apoptosis

In order to further investigate the effect of NFκB deletion and to validate whether enteroid models are a reliable representation of *in vivo* signalling, we treated mice with 5-FU and etoposide. Previous evidence from γ irradiation studies conducted in our lab suggested that c-Rel null mice may be protected from the consequences of DNA damage, as less γ-radiation-induced crypt loss and a reduction in DNA damage response was seen in the intestines of c-Rel null mice (Burkitt *et al.*, 2015).

In the current study c-Rel null mice showed persistent mitosis in the colon following etoposide and in both the colon and small intestine following 5-FU. The mice also showed significantly less apoptosis when treated with etoposide in both the small intestine and colon, and a decreased amount of 5-FU-induced small intestinal apoptosis when compared to C57BL/6J mice. This is in agreement with our enteroid

data (section 4.2.11), and indicates that the enteroid model is a suitable model for testing the toxicity of these chemotherapeutic agents. The targeted inhibition of c-Rel in the GI tract may be a strategy that could be employed in order to reduce mucositis caused by etoposide or 5-FU. Additionally, this approach may also apply to other chemotherapeutic agents and these could be identified using the enteroid model. Conversely, the inhibition of c-Rel in the intestinal mucosa may cause the retention of DNA damage in the small intestinal mucosa. This could increase the number of carcinogenic mutations being retained in the epithelium and increase the chances of cancer developing. Previous studies in our lab have shown that c-Rel null mice are more susceptible to azoxymethane (AOM)-DSS-induced carcinogenesis (Burkitt *et al.*, 2015). AOM and DSS treated mice had more tumours of a larger size than wild-type mice administered the same treatments. This was further supported by another study undertaken in our lab which indicated that c-Rel null mice were resistant to *H. felis*-induced gastric apoptosis, but then later developed cancerous lesions indicating that the c-Rel null mice are afflicted with DNA damage in the cells, but the DNA damage response less readily causes apoptosis compared with wild-type mice administered the same treatment (Burkitt *et al.*, 2013).

7.1.4 The effect of TKIs on small intestinal organoids

TKIs are another type of cancer therapy that often cause severe adverse GI effects such as diarrhoea. Mechanisms of TKI-induced diarrhoea are currently poorly understood. Enteroids were treated with a selection of TKIs in order to determine whether they would cause intestinal epithelial cell death by direct mechanisms. It was found that the EGFR inhibitors erlotinib and gefitinib and the dual ABL/SRC inhibitor dasatinib caused significant cell death in C57BL/6J organoids whereas imatinib, nilotinib and bosutinib did not. Although bosutinib did cause some blebbing at early time points, this did not translate into significant changes in the organoid circularity. Gastrointestinal side effects including diarrhoea, vomiting and nausea have been

documented for all of these TKIs. It can therefore be hypothesised that the GI side effects seen in patients treated with erlotinib, gefitinib and dasatinib are at least partly due to direct effects on intestinal epithelial cells. NFκB2 null mice were used to investigate the contribution of the NFκB2 subunit to intestinal epithelial cell damage. We found that NFκB2 deletion caused a protective effect against cell death in organoids treated with erlotinib. Therefore, the GI specific targeting of NFκB2 in patients treated with erlotinib could potentially relieve GI adverse events and allow an increased dosage of the drug in patients whose GI side effects are dose limiting.

7.2 Implications for the field of organoid studies

Studies using enteroids are cost effective and quick compared to *in vivo* research and are a rapidly growing field (Fatehullah, Tan and Barker, 2016). Enteroids can be expanded and cultured for long periods of time and the sacrifice of only one mouse per enteroid line is required, in contrast to the many mice which would be used in *in vivo* studies. Additionally, mice which are unhealthy due to genetic alteration are not as extensively required. For instance, only one RelB null mouse would be required to establish an enteroid line as opposed to the dozens of RelB null mice that would be required for an *in vivo* study. This additionally allows compliance with the replacement and reduction portions of the 3Rs guidelines (NC3Rs, 2017) and with the principles of humane experimental technique first set out by Russell and Burch (Tannenbaum and Bennett, 2015).

Our studies have indicated that enteroids are a suitable model for testing the direct effects of GI damaging agents on intestinal epithelial cells. This is indicated by similarities between the data generated using enteroids and the results generated *in vivo* in mouse models when c-Rel null mice and enteroids were treated with etoposide and 5-FU. The idea that organoids can mimic epithelial cell effects required further

study, however our data show promise that organoids may be useful for drug testing, and investigations into the mechanism of epithelial cell damage.

7.3 Limitations of the studies presented

The models used in this study were all derived from animal tissues and cells. Although the animal models used are useful, they are not perfect models of human disease. Mice were housed in a newly built specific pathogen free unit and were therefore exposed to minimal environmental bacteria, which may have affected their commensal bacteria population. Additionally, although mucosal scrapes are an accepted technique used to investigate gene expression in the intestinal mucosa, the inflamed mucosa contained many immune cells as well as epithelial cells. Therefore, comparing the inflamed mucosa to the healthy mucosa to determine mechanisms by which NFκB2 null mice were resistant to DSS-induced colitis resulted in the comparison of different cell populations between C57BL/6J and NFκB2-null mice. Data from day 8 post DSS treatment in particular resulted in a large increase in gene expression of several genes compared to day 0, which is likely to be due to the different populations of cells. Future studies should consider single cell sequencing or laser capture/FACS isolation of specific cell populations followed by expression analysis.

Although enteroids are vastly superior for modelling normal intestinal epithelia than 2D monocultures of malignant intestinal cells, they are still subject to limitations. For example, they do not represent the microenvironment of the cells *in vivo* as they lack the protective mucus of the GI tract which houses the commensal bacteria of the gut (section 1.1.5). Although the current enteroid technique involves culturing only the epithelia, the microbiota play a crucial role in the response of the gut to many damaging stimuli, and as enteroids lack their own commensal bacteria, they do not recapitulate any of the bacterial-epithelial cell interactions seen *in vivo*. Matrigel is

used as a substitute basement membrane for the enteroids to grow within, and is a uniform and rigid material. In order to address this issue, experimentation with alternative basement membranes will be necessary in the future.

The apoptotic scoring methods presented in this thesis relied on morphological signs of apoptosis which can often lead to an underestimation of the total amount of apoptosis (Jerome, Vallan and Jaggi, 2000). Comparisons between H+E, caspase-3 staining and TUNEL assays have been made and the TUNEL assay is thought to detect more apoptosis (Marshman *et al.*, 2001). Therefore investigation into alternative methods of apoptosis detection may allow us to improve the accuracy of the experiments by detecting and identifying currently undetectable increases or decreases in apoptosis.

7.4 Future plans

Improvements of the enteroid model are needed in order to more closely mimic the commensal bacteria that are present in the native microenvironment and the mechanical forces that occur *in vivo*. Human enteroid studies will however allow us to investigate human disease processes using human cells in an unprecedented way. Human organoid cultures have already been established from human small intestinal and colonic tissue by the Clevers group (Sato et al., 2011) as well as in our lab. Additionally, the development of microinjection protocols which involve the injection of bacteria into the central lumen of organoids may allow us to develop a GI toxicity model which includes the commensal bacteria. The application of bacteria to organoids has already been successfully undertaken in studies investigating probiotics and IBD (Tsilingiri et al., 2012), and adaptation of this established protocol in our own lab may allow us to avoid excessive optimisation of the protocol. It would therefore be an ideal continuation of these studies to develop a human organoid model with physiologically relevant bacteria, in order to more accurately mimic the

environment of the gut. In studies using human organoids it would however be necessary to directly delete NFκB subunits from the organoids. Therefore a gene editing system would be required. One such system which could be used is the clustered regularly interspersed short palindromic repeats (CRISPR)/Cas9 system. CRISPR/Cas9 technology takes advantage of the bacterial defence system in order to allow gene editing (Driehuis and Clevers, 2017). In future studies, this system could allow us to continue our enteroid studies using human enteroids which have NFκB subunit deletions in order to determine whether the effects seen in mouse enteroids are also seen in human enteroids. In particular, we could use this system to alter the c-Rel status in human enteroids in order to determine whether this causes the protective effects seen against etoposide and 5-FU seen in mouse enteroids. This gene editing system has already been shown to be suitable for human and mouse organoids (Schwank *et al.*, 2013). Targeting c-Rel in order to increase the dose of chemotherapy that can be administered may allow an increase in the dose of the drug while limiting the GI side effects. We tested etoposide and 5-FU and found that c-Rel deletion was protective in both cases. These chemotherapeutic drugs both cause apoptosis via p53 dependant mechanisms, therefore other chemotherapeutic agents which cause apoptosis via p53 would also be interesting targets for further study.

Although most studies indicate that NFκB signalling is activated by the DNA damage response, it is unclear whether NFκB also has a role in the initiation of the DNA damage response. The reduced apoptosis observed in response to DNA damaging agents seen in c-Rel null organoids and mice suggests that c-Rel deletion may prevent the DNA damage response from occurring. Investigations into this could benefit from PCR assays to determine the activation of key DNA damage response genes, in c-Rel null and wild type tissue. The absence of activated members of the ATR pathway would indicate that c-Rel deletion is responsible for the dampening of the DNA damage response and therefore the NFκB pathways function prior to the

DNA damage response as well as after. Proteomics may also be a useful tool in order to investigate which NFκB subunits are altered at the protein level following treatment with DNA damaging agents, compared with untreated tissue. Additionally, investigation into whether inhibition or stimulation of identified components from the proteomic analysis alters the DNA damage seen by the same agent would be useful. This could reveal whether NFκB subunit activation or inhibition is a cause or consequence of the DNA damage response.

7.5 Overall conclusions

NFκB2 is clearly involved in regulating the severity of DSS colitis in C57BL/6J mice. The damage to the intestine caused by the administration of DSS is mediated by both the mucosal and hematopoietic cells. One possible mechanism by which NFκB2 might cause inflammation is via the upregulation of *Csf1, Cxcl10 and Cxcl9*. These proteins may therefore be useful targets in future studies and also possible targets for future studies into DSS colitis. Targeting of NFκB2 in the GI epithelium is therefore potentially a novel treatment for IBD.

The deletion of c-Rel from epithelia has been shown to protect both mouse colon and small intestine *in vivo* as well as enteroids *in vitro* from apoptosis induced by etoposide and 5-FU. Persistent mitosis was also observed in both of these models. Therefore, the targeting of c-Rel in the small intestinal epithelium may be a novel treatment for mucositis caused by some chemotherapeutic agents.

NFκB2 deletion in enteroids has also been shown to confer protection against the effects of erlotinib. If this is a direct effect on the intestinal epithelium, the diarrhoea caused by erlotinib may be ameliorated by targeting NFκB2 in the intestinal mucosa.

In conclusion therefore, NFκB subunits are promising targets for improving the management of IBD and chemotherapy-induced intestinal mucositis.

8 Appendix

Appendix 1.

Symbol	Description
Adm	Adrenomedullin
Agt	Angiostensinogen
Akt1	Thymoma viral proto-oncogene 1
Aldh3a2	Aldehyde dehydrogenase family 3, subfamily A2
Bcl2a1a	B-cell leukemia/lymphoma 2 related protein A1a
Bcl2l1	Bcl2-like 1
Birc2	Baculoviral IAP repeat-containing 2
Birc3	Baculoviral IAP repeat-containing 3
C3	Complement component 3
C4a	Complement component 4A (Rodgers blood group)
Ccl12	Chemokine (C-C motif) ligand 12
Ccl22	Chemokine (C-C motif) ligand 22
Ccl5	Chemokine (C-C motif) ligand 5
Ccnd1	Cyclin D1
Ccr5	Chemokine (C-C motif) receptor 5
Cd40	CD40 antigen
Cd74	CD74 antigen (invariant polypeptide of major histocompatibility complex, class II antigen-associated)
Cd80	CD80 antigen
Cd83	CD83 antigen
Cdkn1a	Cyclin-dependent kinase inhibitor 1A (P21)
Cfb	Complement factor B
Csf1	Colony stimulating factor 1 (macrophage)
Csf2	Colony stimulating factor 2 (granulocyte-macrophage)
Csf2rb	Colony stimulating factor 2 receptor, beta, low-affinity (granulocyte-macrophage)
Csf3	Colony stimulating factor 3 (granulocyte)
Cxcl1	Chemokine (C-X-C motif) ligand 1
Cxcl10	Chemokine (C-X-C motif) ligand 10
Cxcl3	Chemokine (C-X-C motif) ligand 3
Cxcl9	Chemokine (C-X-C motif) ligand 9
Egfr	Epidermal growth factor receptor
Egr2	Early growth response 2
F3	Coagulation factor III
F8	Coagulation factor VIII
Fas	Fas (TNF receptor superfamily member 6)
Fasl	Fas ligand (TNF superfamily, member 6)
Gadd45b	Growth arrest and DNA-damage-inducible 45 beta
Icam1	Intercellular adhesion molecule 1

Ifnb1	Interferon beta 1, fibroblast
Ifng	Interferon gamma
Il12b	Interleukin 12B
Il15	Interleukin 15
Il1a	Interleukin 1 alpha
Il1b	Interleukin 1 beta
Il1r2	Interleukin 1 receptor, type II
Il1rn	Interleukin 1 receptor antagonist
Il2	Interleukin 2
Il2ra	Interleukin 2 receptor, alpha chain
Il4	Interleukin 4
Il6	Interleukin 6
Ins2	Insulin II
Irf1	Interferon regulatory factor 1
Lta	Lymphotoxin A
Ltb	Lymphotoxin B
Map2k6	Mitogen-activated protein kinase 6
Mitf	Microphthalmia-associated transcription factor
Mmp9	Matrix metallopeptidase 9
Myc	Myelocytomatosis oncogene
Myd88	Myeloid differentiation primary response gene 88
Ncoa3	Nuclear receptor coactivator 3
Nfkb1	Nuclear factor of kappa light polypeptide gene enhancer in B-cells 1, p105
Nfkb2	Nuclear factor of kappa light polypeptide gene enhancer in B-cells 2, p49/p100
Nfkbia	Nuclear factor of kappa light polypeptide gene enhancer in B-cells inhibitor, alpha
Nqo1	NAD(P)H dehydrogenase, quinone 1
Nr4a2	Nuclear receptor subfamily 4, group A, member 2
Pdgfb	Platelet derived growth factor, B polypeptide
Plau	Plasminogen activator, urokinase
Ptgs2	Prostaglandin-endoperoxide synthase 2
Rel	Reticuloendotheliosis oncogene
Rela	V-rel reticuloendotheliosis viral oncogene homolog A (avian)
Relb	Avian reticuloendotheliosis viral (v-rel) oncogene related B
Sele	Selectin, endothelial cell
Selp	Selectin, platelet
Snap25	Synaptosomal-associated protein 25
Sod2	Superoxide dismutase 2, mitochondrial
Stat1	Signal transducer and activator of transcription 1
Stat3	Signal transducer and activator of transcription 3
Stat5b	Signal transducer and activator of transcription 5B
Tnf	Tumor necrosis factor
Tnfrsf1b	Tumor necrosis factor receptor superfamily, member 1b

Tnfsf10	Tumor necrosis factor (ligand) superfamily, member 10
Traf2	Tnf receptor-associated factor 2
Trp53	Transformation related protein 53
Vcam1	Vascular cell adhesion molecule 1
Xiap	X-linked inhibitor of apoptosis

Table 2. Gene descriptions of all the genes tested during the NFκB target gene array. Taken from the PCR analysis tool on the SA biosciences website. Located at **http://pcrdataanalysis.sabiosciences.com/pcr/arrayanalysis.php**

9 Bibliography

Abbas, B. *et al.* (1989) 'Internal structure of the intestinal villus: morphological and morphometric observations at different levels of the mouse villus.', *Journal of anatomy*. Wiley-Blackwell, 162, pp. 263–73.

Abud, H. E., Watson, N. and Heath, J. K. (2005) 'Growth of intestinal epithelium in organ culture is dependent on EGF signalling', *Experimental Cell Research*, 303(2), pp. 252–262. doi: 10.1016/j.yexcr.2004.10.006.

Afghani, E. *et al.* (2017) 'Sphincter of Oddi Function and Risk Factors for Dysfunction.', *Frontiers in nutrition*. Frontiers Media SA, 4, p. 1. doi: 10.3389/fnut.2017.00001.

Al-Sadi, R. *et al.* (2016) 'TNF-α Modulation of Intestinal Tight Junction Permeability Is Mediated by NIK/IKK-α Axis Activation of the Canonical NF-κB Pathway', *The American Journal of Pathology*, 186(5), pp. 1151–1165. doi: 10.1016/j.ajpath.2015.12.016.

Alcaraz, J. *et al.* (2008) 'Laminin and biomimetic extracellular elasticity enhance functional differentiation in mammary epithelia.', *The EMBO journal*. European Molecular Biology Organization, 27(21), pp. 2829–38. doi: 10.1038/emboj.2008.206.

Alison, M. and Islam, S. (2009) 'Attributes of adult stem cells', *The Journal of Pathology*, 217(2), pp. 144–160. doi: 10.1002/path.2498.

Alkim, C. *et al.* (2011) 'Extension of ulcerative colitis.', *The Turkish journal of gastroenterology : the official journal of Turkish Society of Gastroenterology*, 22(4), pp. 382–7.

Allan, N., Richards, S. and Shepherd, P. (1995) 'UK Medical Research Council randomised, multicentre trial of interferon-alpha n1 for chronic myeloid leukaemia: improved survival irrespective of cytogenetic response. The UK Medical Research Council's Working Parties for Therapeutic Trials in Adult Leuka', *Lancet (London, England)*, 345(8962), pp. 1392–7.

Allen, I. C. *et al.* (2012) 'NLRP12 suppresses colon inflammation and tumorigenesis through the negative regulation of noncanonical NF-κB signaling.', *Immunity*. NIH Public Access, 36(5), pp. 742–54. doi: 10.1016/j.immuni.2012.03.012.

Ananthakrishnan, A. N. *et al.* (2013) 'A Prospective Study of Long-term Intake of Dietary Fiber and Risk of Crohn's Disease and Ulcerative Colitis', *Gastroenterology*, 145(5), pp. 970–977. doi: 10.1053/j.gastro.2013.07.050.

Anderson, C. A. *et al.* (2011) 'Meta-analysis identifies 29 additional ulcerative colitis risk loci, increasing the number of confirmed associations to 47', *Nature Genetics*, 43(3), pp. 246–252. doi: 10.1038/ng.764.

André, T. *et al.* (2009) 'Improved overall survival with oxaliplatin, fluorouracil, and leucovorin as adjuvant treatment in stage II or III colon cancer in the MOSAIC trial.', *Journal of clinical oncology : official journal of the American Society of Clinical Oncology*, 27(19), pp. 3109–16. doi: 10.1200/JCO.2008.20.6771.

Andresen, L. *et al.* (2005) 'Activation of nuclear factor kappaB in colonic mucosa from patients with collagenous and ulcerative colitis.', *Gut*. BMJ Publishing Group, 54(4), pp. 503–9. doi: 10.1136/gut.2003.034165.

Antoniou, E. *et al.* (2016) 'The TNBS-induced colitis animal model: An overview.', *Annals of medicine and surgery (2012)*. Elsevier, 11, pp. 9–15. doi: 10.1016/j.amsu.2016.07.019.

Apperley, J. F. (2015) 'Chronic myeloid leukaemia', *www.thelancet.com*. doi: 10.1016/S0140-6736(13)62120-0.

Ardite, E. *et al.* (1998) 'Effects of steroid treatment on activation of nuclear factor kappaB in patients with inflammatory bowel disease.', *British journal of pharmacology*, 124(3), pp. 431–433.

Arora, A. and Scholar, E. M. (2005) 'Role of tyrosine kinase inhibitors in cancer therapy.', *The Journal of pharmacology and experimental therapeutics*, 315(3), pp. 971–9. doi: 10.1124/jpet.105.084145.

Artis, D. (2008) 'Epithelial-cell recognition of commensal bacteria and maintenance of immune homeostasis in the gut', *Nature Reviews Immunology*, 8(6), pp. 411–420. doi: 10.1038/nri2316.

Arvikar, S. L. and Fisher, M. C. (2011) 'Inflammatory bowel disease associated arthropathy.', *Current reviews in musculoskeletal medicine*. Springer, 4(3), pp. 123–31. doi: 10.1007/s12178-011-9085-8.

Atreya, I., Atreya, R. and Neurath, M. F. (2008) 'NF-kappaB in inflammatory bowel disease.', *Journal of internal medicine*, 263(6), pp. 591–6. doi: 10.1111/j.1365-2796.2008.01953.x.

Axelrad, J. E., Lichtiger, S. and Yajnik, V. (2016) 'Inflammatory bowel disease and cancer: The role of inflammation, immunosuppression, and cancer treatment.', *World journal of gastroenterology*. Baishideng Publishing Group Inc, 22(20), pp. 4794–801. doi: 10.3748/wjg.v22.i20.4794.

Aya, K. *et al.* (2005) 'NF-(kappa)B-inducing kinase controls lymphocyte and osteoclast activities in inflammatory arthritis.', *The Journal of clinical investigation*. American Society for Clinical Investigation, 115(7), pp. 1848–54. doi: 10.1172/JCI23763.

Baccarani, M. *et al.* (2009) 'Chronic Myeloid Leukemia: An Update of Concepts and Management Recommendations of European LeukemiaNet', *Journal of Clinical Oncology*, 27(35), pp. 6041–6051. doi: 10.1200/JCO.2009.25.0779.

Baldwin, A. S. (1996) 'THE NF-κB AND IκB PROTEINS: New Discoveries and Insights', *Annual Review of Immunology*, 14(1), pp. 649–681. doi: 10.1146/annurev.immunol.14.1.649.

Barcellos-Hoff, M. H. *et al.* (1989) 'Functional differentiation and alveolar morphogenesis of primary mammary cultures on reconstituted basement membrane.', *Development (Cambridge, England)*, 105(2), pp. 223–35.

Barker, N. *et al.* (2007) 'Identification of stem cells in small intestine and colon by marker gene Lgr5', *Nature*, 449(7165), pp. 1003–1007. doi: 10.1038/nature06196.

Barker, N. *et al.* (2010) 'Lgr5+ve Stem Cells Drive Self-Renewal in the Stomach and Build Long-Lived Gastric Units In Vitro', *Cell Stem Cell*, 6(1), pp. 25–36. doi: 10.1016/j.stem.2009.11.013.

Barker, N. (2014) 'Adult intestinal stem cells: critical drivers of epithelial homeostasis and regeneration.', *Nature reviews. Molecular cell biology*, 15(1), pp.

19–33. doi: 10.1038/nrm3721.

Barkett, M. and Gilmore, T. D. (no date) ‘Control of apoptosis by Rel/NF-kB transcription factors’.

Barreiro-de Acosta, M. and Peña, A. S. (2007) ‘Clinical applications of NOD2/CARD15 mutations in Crohn’s disease.’, *Acta gastroenterologica Latinoamericana*, 37(1), pp. 49–54.

Bartek, J. and Lukas, J. (2007) ‘DNA damage checkpoints: from initiation to recovery or adaptation’, *Current Opinion in Cell Biology*, 19(2), pp. 238–245. doi: 10.1016/j.ceb.2007.02.009.

Beaugerie, L. and Itzkowitz, S. H. (2015) ‘Cancers Complicating Inflammatory Bowel Disease’, *New England Journal of Medicine*. Edited by D. L. Longo, 372(15), pp. 1441–1452. doi: 10.1056/NEJMra1403718.

Beg, A. A. *et al.* (1995) ‘Embryonic lethality and liver degeneration in mice lacking the RelA component of NF-κB’, *Nature*, 376(6536), pp. 167–170. doi: 10.1038/376167a0.

Behm, B. W. and Bickston, S. J. (2008) ‘Tumor necrosis factor-alpha antibody for maintenance of remission in Crohn’s disease’, in Bickston, S. J. (ed.) *Cochrane Database of Systematic Reviews*. Chichester, UK: John Wiley & Sons, Ltd, p. CD006893. doi: 10.1002/14651858.CD006893.

Beinke, S. and Ley, S. (2004) ‘Functions of NF-?B1 and NF-?B2 in immune cell biology’, *Biochemical Journal*, 382(2), pp. 393–409. doi: 10.1042/BJ20040544.

Belani, C. P. (2010) ‘The Role of Irreversible EGFR Inhibitors in the Treatment of Non-Small Cell Lung Cancer: Overcoming Resistance to Reversible EGFR Inhibitors’, *Cancer Investigation*, 28(4), pp. 413–423. doi: 10.3109/07357901003631072.

Belkhiri, A. and El-Rifai, W. (2015) ‘Advances in targeted therapies and new promising targets in esophageal cancer.’, *Oncotarget*, 6(3), pp. 1348–58. doi: 10.18632/oncotarget.2752.

Ben-Neriah, Y. *et al.* (1998) ‘Identification of the receptor component of the IkappaBalpha-ubiquitin ligase.’, *Nature*, 396(6711), pp. 590–594. doi: 10.1038/25159.

Berlanga-Acosta, J. *et al.* (2001) ‘Gastrointestinal cell proliferation and crypt fission are separate but complementary means of increasing tissue mass following infusion of epidermal growth factor in rats.’, *Gut*, 48(6), pp. 803–7.

Bernard, D. *et al.* (2002) ‘The c-Rel transcription factor can both induce and inhibit apoptosis in the same cells via the upregulation of MnSOD’, *Oncogene*, 21(28), pp. 4392–4402. doi: 10.1038/sj.onc.1205536.

Bernell, O., Lapidus, A. and Hellers, G. (2000) ‘Risk factors for surgery and postoperative recurrence in Crohn’s disease.’, *Annals of surgery*. Lippincott, Williams, and Wilkins, 231(1), pp. 38–45.

Bertelsen, L. S., Barrett, K. E. and Keely, S. J. (2004) ‘G_s Protein-coupled Receptor Agonists Induce Transactivation of the Epidermal Growth Factor Receptor in T_{84} Cells’, *Journal of Biological Chemistry*, 279(8), pp. 6271–6279. doi: 10.1074/jbc.M311612200.

Blakely, C. M. *et al.* (2015) 'NF-κB-activating complex engaged in response to EGFR oncogene inhibition drives tumor cell survival and residual disease in lung cancer.', *Cell reports*. NIH Public Access, 11(1), pp. 98–110. doi: 10.1016/j.celrep.2015.03.012.

Bleiberg, H. and Cvitkovic, E. (1996) 'Characterisation and clinical management of CPT-11 (irinotecan)-induced adverse events: the European perspective.', *European journal of cancer (Oxford, England : 1990)*, pp. S18-23.

Blume-Jensen, P. and Hunter, T. (2001) 'Oncogenic kinase signalling.', *Nature*, 411(6835), pp. 355–65. doi: 10.1038/35077225.

Bohuslav, J. *et al.* (1998) 'Regulation of an essential innate immune response by the p50 subunit of NF-kappaB.', *Journal of Clinical Investigation*, 102(9), pp. 1645–1652. doi: 10.1172/JCI3877.

Boland, M. P., Fitzgerald, K. A. and O'Neill, L. A. (2000) 'Topoisomerase II is required for mitoxantrone to signal nuclear factor kappa B activation in HL60 cells.', *The Journal of biological chemistry*, 275(33), pp. 25231–8.

Bonen, D. K. *et al.* (2003) 'Crohn's disease-associated NOD2 variants share a signaling defect in response to lipopolysaccharide and peptidoglycan', *Gastroenterology*, 124(1), pp. 140–146. doi: 10.1053/gast.2003.50019.

Bonizzi, G. *et al.* (2004) 'Activation of IKKalpha target genes depends on recognition of specific kappaB binding sites by RelB:p52 dimers.', *The EMBO journal*, 23(21), pp. 4202–10. doi: 10.1038/sj.emboj.7600391.

Bonizzi, G. and Karin, M. (2004) 'The two NF-kappaB activation pathways and their role in innate and adaptive immunity', *Trends Immunol*, 25(6), pp. 280–288. doi: 10.1016/j.it.2004.03.008.

Borm, M. E. A. *et al.* (2005) 'A NFKB1 promoter polymorphism is involved in susceptibility to ulcerative colitis', *International Journal of Immunogenetics*. Blackwell Science Ltd, 32(6), pp. 401–405. doi: 10.1111/j.1744-313X.2005.00546.x.

Boron, W. and Boulpaep, E. (2008) *Medical Physiology*, *Elsevier*. doi: 10.1136/pgmj.51.599.683-c.

Boschelli, D. H. *et al.* (2001) 'Optimization of 4-phenylamino-3-quinolinecarbonitriles as potent inhibitors of Src kinase activity.', *Journal of medicinal chemistry*, 44(23), pp. 3965–77.

Boussios, S. *et al.* (2012) 'Systemic treatment-induced gastrointestinal toxicity: incidence, clinical presentation and management.', *Annals of gastroenterology*, 25(2), pp. 106–118.

Bowen, J. M. *et al.* (2006) 'Irinotecan changes gene expression in the small intestine of the rat with breast cancer', *Cancer Chemotherapy and Pharmacology*. Springer-Verlag, 59(3), pp. 337–348. doi: 10.1007/s00280-006-0275-9.

Bowen, J. M. *et al.* (2007) 'Role of p53 in irinotecan-induced intestinal cell death and mucosal damage', *Anti-Cancer Drugs*, 18(2), pp. 197–210. doi: 10.1097/CAD.0b013e328010ef29.

Bowen, J. M. and M., J. (2014) 'Development of the rat model of lapatinib-induced diarrhoea.', *Scientifica*. Hindawi, 2014, p. 194185. doi: 10.1155/2014/194185.

Breese, E. *et al.* (1993) 'Interleukin-2- and interferon-gamma-secreting T cells in normal and diseased human intestinal mucosa.', *Immunology*, 78(1), pp. 127–31.

Broutier, L. *et al.* (2016) 'Culture and establishment of self-renewing human and mouse adult liver and pancreas 3D organoids and their genetic manipulation', *Nature Protocols*, 11(9), pp. 1724–1743. doi: 10.1038/nprot.2016.097.

Buchdunger, E. *et al.* (2000) 'Abl Protein-Tyrosine Kinase Inhibitor STI571 Inhibits In Vitro Signal Transduction Mediated by c-Kit and Platelet-Derived Growth Factor Receptors', *Journal of Pharmacology and Experimental Therapeutics*, 295(1).

Buettner, M. and Lochner, M. (2016) 'Development and Function of Secondary and Tertiary Lymphoid Organs in the Small Intestine and the Colon.', *Frontiers in immunology*. Frontiers Media SA, 7, p. 342. doi: 10.3389/fimmu.2016.00342.

Bullen, T. F. *et al.* (2006) 'Characterization of epithelial cell shedding from human small intestine', *Laboratory Investigation*, 86(10), pp. 1052–1063. doi: 10.1038/labinvest.3700464.

Burkitt, M. D. *et al.* (2013) 'Signaling mediated by the NF-kappaB sub-units NF-kappaB1, NF-kappaB2 and c-Rel differentially regulate Helicobacter felis-induced gastric carcinogenesis in C57BL/6 mice', *Oncogene*, 32(50), pp. 5563–5573. doi: 10.1038/onc.2013.334.

Burkitt, M. D. *et al.* (2015) 'NF-κB1, NF-κB2 and c-Rel differentially regulate susceptibility to colitis-associated adenoma development in C57BL/6 mice', *The Journal of Pathology*, 236(3), pp. 326–336. doi: 10.1002/path.4527.

Burotto, M. *et al.* (2015) 'Gefitinib and erlotinib in metastatic non-small cell lung cancer: a meta-analysis of toxicity and efficacy of randomized clinical trials.', *The oncologist*. AlphaMed Press, 20(4), pp. 400–10. doi: 10.1634/theoncologist.2014-0154.

Buttke, T. M. and Sandstrom, P. A. (1994) 'Oxidative stress as a mediator of apoptosis', *Immunology Today*, 15(1), pp. 7–10. doi: 10.1016/0167-5699(94)90018-3.

Caamaño, J. *et al.* (1999) 'The NF-κB Family Member RelB Is Required for Innate and Adaptive Immunity to Toxoplasma gondii', *The Journal of Immunology*, 163(8).

Caamaño, J. H. *et al.* (1998) 'Nuclear factor (NF)-kappa B2 (p100/p52) is required for normal splenic microarchitecture and B cell-mediated immune responses.', *The Journal of experimental medicine*, 187(2), pp. 185–96.

Calkins, B. M. (1989) 'A meta-analysis of the role of smoking in inflammatory bowel disease.', *Digestive diseases and sciences*, 34(12), pp. 1841–54.

Caprilli, R., Viscido, A. and Latella, G. (2007) 'Current management of severe ulcerative colitis', *Nature Clinical Practice Gastroenterology & Hepatology*. Nature Publishing Group, 4(2), pp. 92–101. doi: 10.1038/ncpgasthep0687.

Carter, M. J. (2004) 'Guidelines for the management of inflammatory bowel disease in adults', *Gut*, 53(suppl_5), pp. v1–v16. doi: 10.1136/gut.2004.043372.

Ceci, J. D. *et al.* (1997) 'Tpl-2 is an oncogenic kinase that is activated by carboxy-terminal truncation.', *Genes & development*, 11(6), pp. 688–700.

Chang, C.-T. *et al.* (2012) '5-Fluorouracil Induced Intestinal Mucositis via Nuclear

Factor-κB Activation by Transcriptomic Analysis and In Vivo Bioluminescence Imaging', *PLoS ONE*. Edited by U. M. Zanger, 7(3), p. e31808. doi: 10.1371/journal.pone.0031808.

Chassaing, B. *et al.* (2014) 'Dextran sulfate sodium (DSS)-induced colitis in mice.', *Current protocols in immunology / edited by John E. Coligan ... [et al.]*, 104, p. Unit 15.25. doi: 10.1002/0471142735.im1525s104.

Chen, L.-W. *et al.* (2003) 'The two faces of IKK and NF-κB inhibition: prevention of systemic inflammation but increased local injury following intestinal ischemia-reperfusion', *Nature Medicine*, 9(5), pp. 575–581. doi: 10.1038/nm849.

Chen, P. *et al.* (2011) 'EGFR-targeted therapies combined with chemotherapy for treating advanced non-small-cell lung cancer: a meta-analysis.', *European journal of clinical pharmacology*, 67(3), pp. 235–43. doi: 10.1007/s00228-010-0965-4.

Chen, R. *et al.* (2011) 'Interferon alfa versus interferon alfa plus cytarabine combination therapy for chronic myeloid leukemia: a meta-analysis of randomized controlled trials.', *Current therapeutic research, clinical and experimental*. Elsevier, 72(4), pp. 150–63. doi: 10.1016/j.curtheres.2011.06.002.

Chow, J. C. *et al.* (1999) 'Toll-like receptor-4 mediates lipopolysaccharide-induced signal transduction.', *The Journal of biological chemistry*. American Society for Biochemistry and Molecular Biology, 274(16), pp. 10689–92. doi: 10.1074/JBC.274.16.10689.

Chu, Z. L. *et al.* (1999) 'IKKgamma mediates the interaction of cellular IkappaB kinases with the tax transforming protein of human T cell leukemia virus type 1.', *The Journal of biological chemistry*, 274(22), pp. 15297–15300. doi: 10.1074/jbc.274.22.15297.

Chuang, S. E. *et al.* (2002) 'Basal levels and patterns of anticancer drug-induced activation of nuclear factor-kappaB (NF-kappaB), and its attenuation by tamoxifen, dexamethasone, and curcumin in carcinoma cells.', *Biochemical pharmacology*, 63(9), pp. 1709–16.

Cibor, D. *et al.* (2016) 'Endothelial dysfunction in inflammatory bowel diseases: Pathogenesis, assessment and implications.', *World journal of gastroenterology*. Baishideng Publishing Group Inc, 22(3), pp. 1067–77. doi: 10.3748/wjg.v22.i3.1067.

Cooper, H. S. *et al.* (1993) 'Clinicopathologic study of dextran sulfate sodium experimental murine colitis.', *Laboratory investigation; a journal of technical methods and pathology*, 69(2), pp. 238–49.

Cornish, J. A. *et al.* (2008) 'The Risk of Oral Contraceptives in the Etiology of Inflammatory Bowel Disease: A Meta-Analysis', *The American Journal of Gastroenterology*, 103(9), pp. 2394–2400. doi: 10.1111/j.1572-0241.2008.02064.x.

Cortes, J. E. *et al.* (2011) 'Safety and efficacy of bosutinib (SKI-606) in chronic phase Philadelphia chromosome-positive chronic myeloid leukemia patients with resistance or intolerance to imatinib', *Blood*, 118(17), pp. 4567–4576. doi: 10.1182/blood-2011-05-355594.

Courtois, G. and Gilmore, T. D. (2006) 'Mutations in the NF-?B signaling pathway: implications for human disease', *Oncogene*, 25(51), pp. 6831–6843. doi: 10.1038/sj.onc.1209939.

Courtois, G. and Smahi, a (2006) 'NF-kappaB-related genetic diseases.', *Cell death and differentiation*, 13(5), pp. 843–851. doi: 10.1038/sj.cdd.4401841.

le Coutre, P. *et al.* (2008) 'Nilotinib (formerly AMN107), a highly selective BCR-ABL tyrosine kinase inhibitor, is active in patients with imatinib-resistant or -intolerant accelerated-phase chronic myelogenous leukemia', *Blood*, 111(4), pp. 1834–1839. doi: 10.1182/blood-2007-04-083196.

Dai, C. *et al.* (2013) 'VSL#3 probiotics exerts the anti-inflammatory activity via PI3k/Akt and NF-?B pathway in rat model of DSS-induced colitis', *Molecular and Cellular Biochemistry*, 374(1–2), pp. 1–11. doi: 10.1007/s11010-012-1488-3.

Dai, X. M. *et al.* (2002) 'Targeted disruption of the mouse colony-stimulating factor 1 receptor gene results in osteopetrosis, mononuclear phagocyte deficiency, increased primitive progenitor cell frequencies, and reproductive defects', *Blood*, 99(1), pp. 111–120. doi: 10.1182/blood.V99.1.111.

Davé, S. H. *et al.* (2007) 'Amelioration of chronic murine colitis by peptide-mediated transduction of the IkappaB kinase inhibitor NEMO binding domain peptide.', *Journal of immunology (Baltimore, Md. : 1950)*, 179(11), pp. 7852–9.

Deininger, M., Buchdunger, E. and Druker, B. J. (2005) 'The development of imatinib as a therapeutic agent for chronic myeloid leukemia', *Blood*, pp. 2640–2653. doi: 10.1182/blood-2004-08-3097.

Deininger, M. W. N. *et al.* (2003) 'Practical Management of Patients With Chronic Myeloid Leukemia Receiving Imatinib', *Journal of Clinical Oncology*, 21(8), pp. 1637–1647. doi: 10.1200/JCO.2003.11.143.

Dejardin, E. *et al.* (2002) 'The lymphotoxin-beta receptor induces different patterns of gene expression via two NF-kappaB pathways.', *Immunity*, 17(4), pp. 525–35.

Dejardin, E. (2006) 'The alternative NF-??B pathway from biochemistry to biology: Pitfalls and promises for future drug development', *Biochemical Pharmacology*, 72(9 SPEC. ISS.), pp. 1161–1179. doi: 10.1016/j.bcp.2006.08.007.

DeRoche, T. C., Xiao, S.-Y. and Liu, X. (2014) 'Histological evaluation in ulcerative colitis.', *Gastroenterology report*. Oxford University Press, 2(3), pp. 178–92. doi: 10.1093/gastro/gou031.

Dianda, L. *et al.* (1997) 'T cell receptor-alpha beta-deficient mice fail to develop colitis in the absence of a microbial environment.', *The American journal of pathology*, 150(1), pp. 91–7.

Diasio, R. B. and Harris, B. E. (1989) 'Clinical Pharmacology of 5-Fluorouracil', *Clinical Pharmacokinetics*, 16(4), pp. 215–237. doi: 10.2165/00003088-198916040-00002.

Dominguez, J. A. *et al.* (2013) 'Inhibition of IKKβ in Enterocytes Exacerbates Sepsis-Induced Intestinal Injury and Worsens Mortality', *Critical Care Medicine*, 41(10), pp. e275–e285. doi: 10.1097/CCM.0b013e31828a44ed.

Dow, L. E. *et al.* (2015) 'Apc Restoration Promotes Cellular Differentiation and Reestablishes Crypt Homeostasis in Colorectal Cancer.', *Cell*. NIH Public Access, 161(7), pp. 1539–1552. doi: 10.1016/j.cell.2015.05.033.

Driehuis, E. and Clevers, H. (2017) 'CRISPR/Cas 9 genome editing and its applications in organoids', *American Journal of Physiology - Gastrointestinal and*

Liver Physiology, 312(3), pp. G257–G265. doi: 10.1152/ajpgi.00410.2016.

Druker, B. J. *et al.* (1996) 'Effects of a selective inhibitor of the Ab1 tyrosine kinase on the growth of Bcr-Ab1 positive cells', *Nature Medicine*, 2, pp. 561–566.

Duckworth, C. A., Clyde, D. and Pritchard, D. M. (2012) 'CD24 is expressed in gastric parietal cells and regulates apoptosis and the response to Helicobacter felis infection in the murine stomach', *American Journal of Physiology - Gastrointestinal and Liver Physiology*, 303(8).

Duckworth, C. A. and Pritchard, D. M. (2009) 'Suppression of Apoptosis, Crypt Hyperplasia, and Altered Differentiation in the Colonic Epithelia of Bak-Null Mice', *Gastroenterology*, 136(3), pp. 943–952. doi: 10.1053/j.gastro.2008.11.036.

Eckmann, L. *et al.* (2008) 'Opposing functions of IKKbeta during acute and chronic intestinal inflammation.', *Proceedings of the National Academy of Sciences of the United States of America*, 105(39), pp. 15058–63. doi: 10.1073/pnas.0808216105.

Egan, L. J. *et al.* (2004) 'IkappaB-kinasebeta-dependent NF-kappaB activation provides radioprotection to the intestinal epithelium.', *Proceedings of the National Academy of Sciences of the United States of America*, 101(8), pp. 2452–7.

Egger, B. *et al.* (2000) 'Mice harboring a defective epidermal growth factor receptor (waved-2) have an increased susceptibility to acute dextran sulfate-induced colitis.', *Scandinavian journal of gastroenterology*, 35(11), pp. 1181–7.

Ellinghaus, D. *et al.* (2012) 'Combined analysis of genome-wide association studies for Crohn disease and psoriasis identifies seven shared susceptibility loci', *American Journal of Human Genetics*, 90(4), pp. 636–647. doi: 10.1016/j.ajhg.2012.02.020.

Erdman, S. *et al.* (2001) 'Typhlocolitis in NF-kappa B-deficient mice.', *Journal of immunology (Baltimore, Md. : 1950)*, 166(3), pp. 1443–7.

Eri, R., McGuckin, M. A. and Wadley, R. (2012) 'T Cell Transfer Model of Colitis: A Great Tool to Assess the Contribution of T Cells in Chronic Intestinal Inflammation', in. Humana Press, pp. 261–275. doi: 10.1007/978-1-61779-527-5_19.

Farmer, R. G., Easley, K. A. and Rankin, G. B. (1993) 'Clinical patterns, natural history, and progression of ulcerative colitis. A long-term follow-up of 1116 patients.', *Digestive diseases and sciences*, 38(6), pp. 1137–46.

Farmer, R. G., Hawk, W. A. and Turnbull, R. B. (1975) 'Farmer, R. G., Hawk, W. A. and Turnbull, R. B. (1975) "Clinical patterns in Crohn"s disease: a statistical study of 615 cases.', Gastroenterology, 68(4 Pt 1), pp. 627–35. Available at: http://www.ncbi.nlm.nih.gov/pubmed/1123132 (Accessed: 11 September 201', *Gastroenterology*, 68(4 Pt 1), pp. 627–35.

Fatehullah, A., Tan, S. H. and Barker, N. (2016) 'Organoids as an in vitro model of human development and disease', *Nature Cell Biology*, 18(3), pp. 246–254. doi: 10.1038/ncb3312.

Feistle, D.-V. K. *et al.* (2012) 'NF-κB addiction and resistance to 5-fluorouracil in a multi-stage colon carcinoma model'. doi: 10.5414/CPP51035.

Finnberg, N. K. *et al.* (2016) 'Agonists of the TRAIL Death Receptor DR5 Sensitize Intestinal Stem Cells to Chemotherapy-Induced Cell Death and Trigger Gastrointestinal Toxicity', *Cancer Research*, 76(3).

van der Flier, L. G. and Clevers, H. (2009) 'Stem Cells, Self-Renewal, and Differentiation in the Intestinal Epithelium', *Annual Review of Physiology*, 71(1), pp. 241–260. doi: 10.1146/annurev.physiol.010908.163145.

Forbester, J. L. *et al.* (2015) 'Interaction of Salmonella enterica Serovar Typhimurium with Intestinal Organoids Derived from Human Induced Pluripotent Stem Cells.', *Infection and immunity*. American Society for Microbiology (ASM), 83(7), pp. 2926–34. doi: 10.1128/IAI.00161-15.

Fouquet, S. *et al.* (2004) 'Early Loss of E-cadherin from Cell-Cell Contacts Is Involved in the Onset of Anoikis in Enterocytes', *Journal of Biological Chemistry*, 279(41), pp. 43061–43069. doi: 10.1074/jbc.M405095200.

Franke, A. *et al.* (2010) 'Genome-wide meta-analysis increases to 71 the number of confirmed Crohn's disease susceptibility loci', *Nature Genetics*, 42(12), pp. 1118–1125. doi: 10.1038/ng.717.

Fukata, M. *et al.* (2006) 'Cox-2 Is Regulated by Toll-Like Receptor-4 (TLR4) Signaling: Role in Proliferation and Apoptosis in the Intestine', *Gastroenterology*, 131(3), pp. 862–877. doi: 10.1053/j.gastro.2006.06.017.

Fuss, I. J. *et al.* (1996) 'Disparate CD4+ lamina propria (LP) lymphokine secretion profiles in inflammatory bowel disease. Crohn's disease LP cells manifest increased secretion of IFN-gamma, whereas ulcerative colitis LP cells manifest increased secretion of IL-5.', *Journal of immunology (Baltimore, Md. : 1950)*, 157(3), pp. 1261–70.

Fuss, I. J. *et al.* (2004) 'Nonclassical CD1d-restricted NK T cells that produce IL-13 characterize an atypical Th2 response in ulcerative colitis', *Journal of Clinical Investigation*, 113(10), pp. 1490–1497. doi: 10.1172/JCI19836.

Gadjeva, M., Wang, Y. and Horwitz, B. H. (2007) 'NF-kappaB p50 and p65 subunits control intestinal homeostasis.', *European journal of immunology*, 37(9), pp. 2509–17. doi: 10.1002/eji.200737186.

Galenkamp, K. M. *et al.* (2015) 'TNFα sensitizes neuroblastoma cells to FasL-, cisplatin- and etoposide-induced cell death by NF-κB-mediated expression of Fas.', *Molecular cancer*. BioMed Central, 14, p. 62. doi: 10.1186/s12943-015-0329-x.

Gambacorti-Passerini, C. *et al.* (2011) 'Multicenter Independent Assessment of Outcomes in Chronic Myeloid Leukemia Patients Treated With Imatinib', *JNCI Journal of the National Cancer Institute*. Oxford University Press, 103(7), pp. 553–561. doi: 10.1093/jnci/djr060.

Garcia, S. *et al.* (2016) 'Colony-stimulating factor (CSF) 1 receptor blockade reduces inflammation in human and murine models of rheumatoid arthritis', *Arthritis Research & Therapy*, 18(1), pp. 1–14. doi: 10.1186/s13075-016-0973-6.

Garud, S. and Peppercorn, M. A. (2009) 'Ulcerative colitis: current treatment strategies and future prospects.', *Therapeutic advances in gastroenterology*. SAGE Publications, 2(2), pp. 99–108. doi: 10.1177/1756283X09102329.

Gerbe, F., Legraverend, C. and Jay, P. (2012) 'The intestinal epithelium tuft cells: specification and function.', *Cellular and molecular life sciences : CMLS*. Springer, 69(17), pp. 2907–17. doi: 10.1007/s00018-012-0984-7.

Gerondakis, S. *et al.* (2006) 'Unravelling the complexities of the NF-?B signalling

pathway using mouse knockout and transgenic models', *Oncogene*. Nature Publishing Group, 25(51), pp. 6781–6799. doi: 10.1038/sj.onc.1209944.

Gibson, R. J. *et al.* (2003) 'Irinotecan causes severe small intestinal damage, as well as colonic damage, in the rat with implanted breast cancer.', *Journal of gastroenterology and hepatology*, 18(9), pp. 1095–100.

Gilmore, T. D. (2006) 'Introduction to NF-κB: players, pathways, perspectives', *Oncogene*, 25(51), pp. 6680–6684. doi: 10.1038/sj.onc.1209954.

Giroux, V. and Rustgi, A. K. (2017) 'Metaplasia: tissue injury adaptation and a precursor to the dysplasia–cancer sequence', *Nature Reviews Cancer*. doi: 10.1038/nrc.2017.68.

Gjorevski, N. and Nelson, C. M. (2010) 'Endogenous patterns of mechanical stress are required for branching morphogenesis', *Integrative Biology*, 2(9), p. 424. doi: 10.1039/c0ib00040j.

Glasser, A. L. *et al.* (2001) 'Adherent invasive Escherichia coli strains from patients with Crohn's disease survive and replicate within macrophages without inducing host cell death.', *Infection and immunity*, 69(9), pp. 5529–37.

Greten, F. R. *et al.* (2004) 'IKKβ links inflammation and tumorigenesis in a mouse model of colitis-associated cancer', *Cell*, 118(3), pp. 285–296. doi: 10.1016/j.cell.2004.07.013.

Greten, F. R. *et al.* (2007) 'NF-κB Is a Negative Regulator of IL-1β Secretion as Revealed by Genetic and Pharmacological Inhibition of IKKβ', *Cell*, 130(5), pp. 918–931. doi: 10.1016/j.cell.2007.07.009.

Grimm, S. *et al.* (1996) 'Bcl-2 down-regulates the activity of transcription factor NF-kappaB induced upon apoptosis.', *The Journal of cell biology*, 134(1), pp. 13–23.

Groffen, J. *et al.* (1984) 'Philadelphia chromosomal breakpoints are clustered within a limited region, bcr, on chromosome 22', *Cell*, 36(1), pp. 93–99. doi: 10.1016/0092-8674(84)90077-1.

Grossmann, J. *et al.* (1998) 'New isolation technique to study apoptosis in human intestinal epithelial cells.', *The American journal of pathology*. Elsevier, 153(1), pp. 53–62. doi: 10.1016/S0002-9440(10)65545-9.

Guan, Y. *et al.* (2011) 'Redistribution of the tight junction protein ZO-1 during physiological shedding of mouse intestinal epithelial cells.', *American journal of physiology. Cell physiology*. American Physiological Society, 300(6), pp. C1404-14. doi: 10.1152/ajpcell.00270.2010.

Guinane, C. M. and Cotter, P. D. (2013) 'Role of the gut microbiota in health and chronic gastrointestinal disease: understanding a hidden metabolic organ.', *Therapeutic advances in gastroenterology*. SAGE Publications, 6(4), pp. 295–308. doi: 10.1177/1756283X13482996.

Gunawardene, A. R., Corfe, B. M. and Staton, C. A. (2011) 'Classification and functions of enteroendocrine cells of the lower gastrointestinal tract.', *International journal of experimental pathology*. Wiley-Blackwell, 92(4), pp. 219–31. doi: 10.1111/j.1365-2613.2011.00767.x.

Guo, J. *et al.* (2004) 'Enhanced Chemosensitivity to Irinotecan by RNA Interference-Mediated Down-Regulation of the Nuclear Factor- B p65 Subunit', *Clinical Cancer*

Research, 10(10), pp. 3333–3341. doi: 10.1158/1078-0432.CCR-03-0366.

Halfvarson, J. *et al.* (2003) 'Inflammatory bowel disease in a Swedish twin cohort: A long- term follow-up of concordance and clinical characteristics', *Gastroenterology*, 124(7), pp. 1767–1773. doi: 10.1016/S0016-5085(03)00385-8.

Hall, P. A. *et al.* (1994) 'Regulation of cell number in the mammalian gastrointestinal tract: the importance of apoptosis', *Journal of Cell Science*, 107(12).

Hamilton, J. A. (2008) 'Colony-stimulating factors in inflammation and autoimmunity', *Nature Reviews Immunology*, 8(8), pp. 533–545. doi: 10.1016/S1471-4906(02)02260-3.

Hampe, J. *et al.* (2007) 'A genome-wide association scan of nonsynonymous SNPs identifies a susceptibility variant for Crohn disease in ATG16L1', *Nature Genetics*, 39(2), pp. 207–211. doi: 10.1038/ng1954.

Hanedi, A. F. (2013) 'Physiological importance of various NFκB family members in regulating intestinal responses to injury', *Doctoral thesis University of Liverpool*.

Hare, K. J. *et al.* (2007) 'The intestinotrophic peptide, GLP-2, counteracts intestinal atrophy in mice induced by the epidermal growth factor receptor inhibitor, gefitinib', *Clinical Cancer Research*, 13(17), pp. 5170–5175. doi: 10.1158/1078-0432.CCR-07-0574.

Heller, F. *et al.* (2002) 'Oxazolone colitis, a Th2 colitis model resembling ulcerative colitis, is mediated by IL-13-producing NK-T cells.', *Immunity*. John Wiley & Sons, Inc, New York, 17(5), pp. 629–38. doi: 10.1016/S1074-7613(02)00453-3.

Hendrickson, B. A., Gokhale, R. and Cho, J. H. (2002) 'Clinical aspects and pathophysiology of inflammatory bowel disease.', *Clinical microbiology reviews*. American Society for Microbiology (ASM), 15(1), pp. 79–94. doi: 10.1128/cmr.15.1.79-94.2002.

Heusch, M. *et al.* (1999) 'The generation of nfkb2 p52: mechanism and efficiency', *Oncogene*, 18(46), pp. 6201–6208. doi: 10.1038/sj.onc.1203022.

Heymann, D. and Rédini, F. (2013) 'Targeted therapies for bone sarcomas', *BoneKEy Reports*. Springer Nature, 2. doi: 10.1038/bonekey.2013.112.

Hill, D. R. and Spence, J. R. (2017) 'Gastrointestinal Organoids: Understanding the Molecular Basis of the Host–Microbe Interface', *Cellular and Molecular Gastroenterology and Hepatology*, 3(2), pp. 138–149. doi: 10.1016/j.jcmgh.2016.11.007.

Hirsh, V. (2011) 'Managing treatment-related adverse events associated with egfr tyrosine kinase inhibitors in advanced non-small-cell lung cancer.', *Current oncology (Toronto, Ont.)*. Multimed Inc., 18(3), pp. 126–38.

Hobson, A. R. and Aziz, Q. (2011) 'Oesophagus and stomach motility', *Medicine*, 39(4), pp. 210–213. doi: 10.1016/j.mpmed.2011.01.007.

Hochhaus, A. *et al.* (2009) 'Six-year follow-up of patients receiving imatinib for the first-line treatment of chronic myeloid leukemia', *Leukemia*, 23(6), pp. 1054–1061. doi: 10.1038/leu.2009.38.

Hochhaus, A. *et al.* (2015) 'Frontline nilotinib in patients with chronic myeloid leukemia in chronic phase: results from the European ENEST1st study', *Leukemia,*

Published online: 06 October 2015; | *doi:10.1038/leu.2015.270*. Nature Publishing Group, 30(1), p. 57. doi: 10.1038/leu.2015.270.

Hoffmann, A., Natoli, G. and Ghosh, G. (2006) 'Transcriptional regulation via the NF-?B signaling module', *Oncogene*, 25(51), pp. 6706–6716. doi: 10.1038/sj.onc.1209933.

Hollenbach, E. *et al.* (2004) 'Inhibition of p38 MAP kinase- and RICK/NF- B-signaling suppresses inflammatory bowel diseaseHollenbach, E. et al. (2004) "Inhibition of p38 MAP kinase- and RICK/NF- B-signaling suppresses inflammatory bowel disease", The FASEB Journal, 18(13), pp. 1550–2.', *The FASEB Journal*, 18(13), pp. 1550–2. doi: 10.1096/fj.04-1642fje.

Holley, A. K. *et al.* (2010) 'RelB regulates manganese superoxide dismutase gene and resistance to ionizing radiation of prostate cancer cells', *Annals of the New York Academy of Sciences*, 1201(1), pp. 129–136. doi: 10.1111/j.1749-6632.2010.05613.x.

Houghton, J. A., Houghton, P. J. and Wooten, R. S. (1979) 'Mechanism of Induction of Gastrointestinal Toxicity in the Mouse by 5-Fluorouracil, 5-Fluorouridine, and 5-Fluoro-2′-deoxyuridine', *Cancer Research*, 39(7 Part 1).

Hsieh, M.-Y. and Van Etten, R. A. (2014) 'IKK-dependent activation of NF-κB contributes to myeloid and lymphoid leukemogenesis by BCR-ABL1.', *Blood*. American Society of Hematology, 123(15), pp. 2401–11. doi: 10.1182/blood-2014-01-547943.

Hubbard, S. R. and Till, J. H. (2000) 'Protein Tyrosine Kinase Structure and Function', *Annual Review of Biochemistry*, 69(1), pp. 373–398. doi: 10.1146/annurev.biochem.69.1.373.

Huen, M. S. and Chen, J. (2008) 'The DNA damage response pathways: at the crossroad of protein modifications', *Cell Research*, 18(1), pp. 8–16. doi: 10.1038/cr.2007.109.

Huxford, T. and Ghosh, G. (2009) 'A Structural Guide to Proteins of the NF-?B Signaling Module', *Cold Spring Harbor Perspectives in Biology*, 1(3), pp. a000075–a000075. doi: 10.1101/cshperspect.a000075.

Huynh, D. *et al.* (2013) 'CSF-1 Receptor-Dependent Colon Development, Homeostasis and Inflammatory Stress Response', *PLoS ONE*, 8(2). doi: 10.1371/journal.pone.0056951.

Hwang, B. *et al.* (2015) 'IPO3-mediated Nonclassical Nuclear Import of NF-κB Essential Modulator (NEMO) Drives DNA Damage-dependent NF-κB Activation', *Journal of Biological Chemistry*, 290(29), pp. 17967–17984. doi: 10.1074/jbc.M115.645960.

Hynds, R. E. and Giangreco, A. (2013) 'Concise review: the relevance of human stem cell-derived organoid models for epithelial translational medicine.', *Stem cells (Dayton, Ohio)*. Europe PMC Funders, 31(3), pp. 417–22. doi: 10.1002/stem.1290.

Ianaro, A. *et al.* (2009) 'NEMO-binding domain peptide inhibits proliferation of human melanoma cells', *Cancer Letters*, 274(2), pp. 331–336. doi: 10.1016/j.canlet.2008.09.038.

Ijiri, K. and Potten, C. S. (1987) 'Further studies on the response of intestinal crypt

cells of different hierarchical status to eighteen different cytotoxic agents.', *British journal of cancer*, 55(2), pp. 113–23.

Ijiri, K. and Pottent, C. S. (1983) 'Response of intestinal cells of differing topographical and hierarchical status to ten cytotoxic drugs and five sources of radiation', *Br. J. Cancer*, 47, pp. 175–185.

Ikuno, N. *et al.* (1995) 'Irinotecan (CPT-11) and characteristic mucosal changes in the mouse ileum and cecum.', *Journal of the National Cancer Institute*, 87(24), pp. 1876–83.

Inan, M. S. *et al.* (2000) 'Transcription factor NF-κB participates in regulation of epithelial cell turnover in the colon', *American Journal of Physiology - Gastrointestinal and Liver Physiology*, 279(6).

Ippolito, C. *et al.* (2016) 'Fibrotic and Vascular Remodelling of Colonic Wall in Patients with Active Ulcerative Colitis', *Journal of Crohn's and Colitis*, 10(10), pp. 1194–1204. doi: 10.1093/ecco-jcc/jjw076.

Ireland, H. *et al.* (2005) 'Cellular inheritance of a Cre-activated reporter gene to determine paneth cell longevity in the murine small intestine', *Developmental Dynamics*, 233(4), pp. 1332–1336. doi: 10.1002/dvdy.20446.

Ishikawa, H. *et al.* (1997) 'Gastric hyperplasia and increased proliferative responses of lymphocytes in mice lacking the COOH-terminal ankyrin domain of NF-kappaB2.', *The Journal of experimental medicine*, 186(7), pp. 999–1014.

Ishikawa, T. O., Oshima, M. and Herschman, H. R. (2011) 'Cox-2 deletion in myeloid and endothelial cells, but not in epithelial cells, exacerbates murine colitis', *Carcinogenesis*, 32(3), pp. 417–426. doi: 10.1093/carcin/bgq268.

Ito, R. *et al.* (2006) 'Interferon-gamma is causatively involved in experimental inflammatory bowel disease in mice', *Clinical and Experimental Immunology*, 146(2), pp. 330–338. doi: 10.1111/j.1365-2249.2006.03214.x.

Itzkowitz, S. H. and Yio, X. (2004) 'Inflammation and Cancer IV. Colorectal cancer in inflammatory bowel disease: the role of inflammation', *AJP: Gastrointestinal and Liver Physiology*, 287(1), pp. G7–G17. doi: 10.1152/ajpgi.00079.2004.

Janssens, S. and Tschopp, J. (2006) 'Signals from within: the DNA-damage-induced NF-κB response', *Cell Death and Differentiation*, 13(5), pp. 773–784. doi: 10.1038/sj.cdd.4401843.

Jenkins, D. *et al.* (1997) 'Guidelines for the initial biopsy diagnosis of suspected chronic idiopathic inflammatory bowel disease. The British Society of Gastroenterology Initiative.', *Journal of clinical pathology*. BMJ Publishing Group, 50(2), pp. 93–105.

Jeon, M. K. *et al.* (2013) 'Intestinal barrier: Molecular pathways and modifiers', *World Journal of Gastrointestinal Pathophysiology*, 4(4), p. 94. doi: 10.4291/wjgp.v4.i4.94.

Jerome, K. R., Vallan, C. and Jaggi, R. (2000) 'The tunel assay in the diagnosis of graft-versus-host disease: caveats for interpretation.', *Pathology*, 32(3), pp. 186–90.

Jess, T. *et al.* (2006) 'Risk of Intestinal Cancer in Inflammatory Bowel Disease: A Population-Based Study From Olmsted County, Minnesota', *Gastroenterology*, 130(4), pp. 1039–1046. doi: 10.1053/j.gastro.2005.12.037.

Jess, T. *et al.* (2006) 'Survival and cause specific mortality in patients with inflammatory bowel disease: a long term outcome study in Olmsted County, Minnesota, 1940-2004', *Gut*, 55(9), pp. 1248–1254. doi: 10.1136/gut.2005.079350.

Jess, T. *et al.* (2007) 'Changes in Clinical Characteristics, Course, and Prognosis of Inflammatory Bowel Disease during the Last 5 Decades: A Population-Based Study from Copenhagen, Denmark', *Inflammatory Bowel Diseases*, 13(4), pp. 481–489. doi: 10.1002/ibd.20036.

Jess, T., Frisch, M. and Simonsen, J. (2013) 'Trends in Overall and Cause-Specific Mortality Among Patients With Inflammatory Bowel Disease From 1982 to 2010', *Clinical Gastroenterology and Hepatology*, 11(1), pp. 43–48. doi: 10.1016/j.cgh.2012.09.026.

Johansson, M. E. V, Sjövall, H. and Hansson, G. C. (2013) 'The gastrointestinal mucus system in health and disease.', *Nature reviews. Gastroenterology & hepatology*. NIH Public Access, 10(6), pp. 352–61. doi: 10.1038/nrgastro.2013.35.

Josson, S. *et al.* (2006) 'RelB regulates manganese superoxide dismutase gene and resistance to ionizing radiation of prostate cancer cells', *Oncogene*, 25(10), pp. 1554–1559. doi: 10.1038/sj.onc.1209186.

Jung, P. *et al.* (2011) 'Isolation and in vitro expansion of human colonic stem cells', *Nature Medicine*, 17(10), pp. 1225–1227. doi: 10.1038/nm.2470.

Kaci, G. *et al.* (2011) 'Inhibition of the NF-kappaB pathway in human intestinal epithelial cells by commensal Streptococcus salivarius.', *Applied and environmental microbiology*. American Society for Microbiology (ASM), 77(13), pp. 4681–4. doi: 10.1128/AEM.03021-10.

Kanai, T. *et al.* (2006) 'TH1/TH2-mediated colitis induced by adoptive transfer of CD4+CD45RBhigh T lymphocytes into nude mice', *Inflammatory Bowel Diseases*, 12(2), pp. 89–99. doi: 10.1097/01.MIB.0000197237.21387.mL.

Kang, S. M. *et al.* (1992) 'NF-kappa B subunit regulation in nontransformed CD4+ T lymphocytes.', *Science (New York, N.Y.)*, 256(5062), pp. 1452–6.

Kantarjian, H. M. *et al.* (2011) 'Nilotinib versus imatinib for the treatment of patients with newly diagnosed chronic phase, Philadelphia chromosome-positive, chronic myeloid leukaemia: 24-month minimum follow-up of the phase 3 randomised ENESTnd trial', *The Lancet Oncology*, 12(9), pp. 841–851. doi: 10.1016/S1470-2045(11)70201-7.

Kantarjian, H. M. *et al.* (2014) 'Bosutinib safety and management of toxicity in leukemia patients with resistance or intolerance to imatinib and other tyrosine kinase inhibitors', *Blood*, 123(9), pp. 1309–1318. doi: 10.1182/blood-2013-07-513937.

Karin, M. and Ben-Neriah, Y. (2000) 'Phosphorylation Meets Ubiquitination: The Control of NF-κB Activity', *Annual Review of Immunology*, 18(1), pp. 621–663. doi: 10.1146/annurev.immunol.18.1.621.

Kaser, A. and Blumberg, R. S. (2011) 'Autophagy, microbial sensing, endoplasmic reticulum stress, and epithelial function in inflammatory bowel disease.', *Gastroenterology*. NIH Public Access, 140(6), pp. 1738–47. doi: 10.1053/j.gastro.2011.02.048.

Kasibhatla, S. *et al.* (1998) 'DNA damaging agents induce expression of Fas ligand and subsequent apoptosis in T lymphocytes via the activation of NF-kappa B and AP-1.', *Molecular cell*, 1(4), pp. 543–51.

Kasza, A. (2013) 'IL-1 and EGF regulate expression of genes important in inflammation and cancer', *Cytokine*, 62(1), pp. 22–33. doi: 10.1016/j.cyto.2013.02.007.

Kawai, T. *et al.* (1999) 'Unresponsiveness of MyD88-deficient mice to endotoxin.', *Immunity*, 11(1), pp. 115–22.

Kawai, T. *et al.* (2001) 'Lipopolysaccharide stimulates the MyD88-independent pathway and results in activation of IFN-regulatory factor 3 and the expression of a subset of lipopolysaccharide-inducible genes.', *Journal of immunology (Baltimore, Md. : 1950)*, 167(10), pp. 5887–94.

Keefe, D. M. *et al.* (2000) 'Chemotherapy for cancer causes apoptosis that precedes hypoplasia in crypts of the small intestine in humans.', *Gut*. BMJ Group, 47(5), pp. 632–7. doi: 10.1136/GUT.47.5.632.

Keller, G., Schafhausen, P. and Brummendorf, T. H. (2009) 'Bosutinib: a dual SRC/ABL kinase inhibitor for the treatment of chronic myeloid leukemia', *Expert Review of Hematology*, 2(5), pp. 489–497. doi: 10.1586/ehm.09.42.

Kerr, J. F., Wyllie, A. H. and Currie, A. R. (1972) 'Apoptosis: a basic biological phenomenon with wide-ranging implications in tissue kinetics.', *British journal of cancer*, 26(4), pp. 239–57.

Khalili, H. *et al.* (2016) 'Oral Contraceptive Use and Risk of Ulcerative Colitis Progression: A Nationwide Study.', *The American journal of gastroenterology*. NIH Public Access, 111(11), pp. 1614–1620. doi: 10.1038/ajg.2016.464.

Khanna, R. and Marshall, J. K. (2017) 'Sulfasalazine and 5-Aminosalicylates for Ulcerative Colitis', in *Crohn's Disease and Ulcerative Colitis*. Cham: Springer International Publishing, pp. 389–397. doi: 10.1007/978-3-319-33703-6_38.

Kharbanda, S. *et al.* (1995) 'Activation of the c-Abl tyrosine kinase in the stress response to DMA-damaging agents', *Nature*, 376(6543), pp. 785–788. doi: 10.1038/376785a0.

Khor, B., Gardet, A. and Xavier, R. J. (2011) 'Genetics and pathogenesis of inflammatory bowel disease.', *Nature*. NIH Public Access, 474(7351), pp. 307–17. doi: 10.1038/nature10209.

Kim, D. H. *et al.* (2013) 'Ginsenoside Rd inhibits the expressions of iNOS and COX-2 by suppressing NF-κB in LPS-stimulated RAW264.7 cells and mouse liver.', *Journal of ginseng research*. Elsevier, 37(1), pp. 54–63. doi: 10.5142/jgr.2013.37.54.

Kim, E. S. *et al.* (2008) 'Gefitinib versus docetaxel in previously treated non-small-cell lung cancer (INTEREST): a randomised phase III trial', *The Lancet*, 372(9652), pp. 1809–1818. doi: 10.1016/S0140-6736(08)61758-4.

Kim, K.-A. *et al.* (2005) 'Mitogenic Influence of Human R-Spondin1 on the Intestinal Epithelium', *Science*, 309(5738), pp. 1256–1259. doi: 10.1126/science.1112521.

Kim, Y. S. and Ho, S. B. (2010) 'Intestinal goblet cells and mucins in health and disease: recent insights and progress.', *Current gastroenterology reports*. Springer,

12(5), pp. 319–30. doi: 10.1007/s11894-010-0131-2.

King, K. E. *et al.* (2008) 'The p53 homologue DeltaNp63alpha interacts with the nuclear factor-kappaB pathway to modulate epithelial cell growth.', *Cancer research*. NIH Public Access, 68(13), pp. 5122–31. doi: 10.1158/0008-5472.CAN-07-6123.

Konopka, J. B., Watanabe, S. M. and Witte, O. N. (1984) 'An alteration of the human c-abl protein in K562 leukemia cells unmasks associated tyrosine kinase activity', *Cell*, 37(3), pp. 1035–1042. doi: 10.1016/0092-8674(84)90438-0.

Köntgen, F. *et al.* (1995) 'Mice lacking the c-rel proto-oncogene exhibit defects in lymphocyte proliferation, humoral immunity, and interleukin-2 expression.', *Genes & development*, 9(16), pp. 1965–77.

Körber, M. I. *et al.* (2016) 'NFκB-Associated Pathways in Progression of Chemoresistance to 5-Fluorouracil in an In Vitro Model of Colonic Carcinoma.', *Anticancer research*, 36(4), pp. 1631–9.

Krausova, M. and Korinek, V. (2014) 'Wnt signaling in adult intestinal stem cells and cancer', *Cellular Signalling*, 26(3), pp. 570–579. doi: 10.1016/j.cellsig.2013.11.032.

Kühn, R. *et al.* (1993) 'Interleukin-10-deficient mice develop chronic enterocolitis.', *Cell*, 75(2), pp. 263–74.

Kurzrock, R., Gutterman, J. U. and Talpaz, M. (1988) 'The Molecular Genetics of Philadelphia Chromosome–Positive Leukemias', *N. Engl. J. Med.*, 319(15), pp. 990–998. doi: 10.1056/NEJM198810133191506.

Lagadec, P. *et al.* (2008) 'Pharmacological targeting of NF-kappaB potentiates the effect of the topoisomerase inhibitor CPT-11 on colon cancer cells.', *British journal of cancer*. Nature Publishing Group, 98(2), pp. 335–44. doi: 10.1038/sj.bjc.6604082.

Lakhdari, O. *et al.* (2011) 'Identification of NF-κB modulation capabilities within human intestinal commensal bacteria.', *Journal of biomedicine & biotechnology*. Hindawi Publishing Corporation, 2011, p. 282356. doi: 10.1155/2011/282356.

Lambros, M. P. *et al.* (2015) 'Molecular signatures in the prevention of radiation damage by the synergistic effect of N-acetyl cysteine and qingre liyan decoction, a traditional chinese medicine, using a 3-dimensional cell culture model of oral mucositis.', *Evidence-based complementary and alternative medicine : eCAM*. Hindawi Publishing Corporation, 2015, p. 425760. doi: 10.1155/2015/425760.

Landre, T. *et al.* (2015) 'Doublet chemotherapy vs. single-agent therapy with 5FU in elderly patients with metastatic colorectal cancer. a meta-analysis.', *International journal of colorectal disease*, 30(10), pp. 1305–10. doi: 10.1007/s00384-015-2296-5.

Laroui, H. *et al.* (2012) 'Dextran sodium sulfate (DSS) induces colitis in mice by forming nano-lipocomplexes with medium-chain-length fatty acids in the colon.', *PloS one*. Public Library of Science, 7(3), p. e32084. doi: 10.1371/journal.pone.0032084.

de Lau, W. B. M., Snel, B. and Clevers, H. C. (2012) 'The R-spondin protein family.', *Genome biology*. BioMed Central, 13(3), p. 242. doi: 10.1186/gb-2012-13-3-242.

Lawrance, I. C. *et al.* (2003) 'A murine model of chronic inflammation-induced intestinal fibrosis down-regulated by antisense NF-kappa B.', *Gastroenterology*,

125(6), pp. 1750–61.

Lawrence, T. *et al.* (2001) ‘Possible new role for NF-kappaB in the resolution of inflammation.’, *Nature Medicine*, 7(12), pp. 1291–1297. doi: 10.1038/nm1201-1291.

Lawrence, T. (2009) ‘The Nuclear Factor NF-κB Pathway in Inflammation’, *About Cold Spring Harbor Perspectives in Biology*, pp. 1–10. doi: 10.1101/cshperspect.a001651.

LEBLOND, C. P. and WALKER, B. E. (1956) ‘Renewal of cell populations.’, *Physiological reviews*, 36(2), pp. 255–76.

Lee, H.-J. *et al.* (2013) ‘Diallyl trisulfide suppresses dextran sodium sulfate-induced mouse colitis: NF-?B and STAT3 as potential targets’, *Biochemical and Biophysical Research Communications*, 437(2), pp. 267–273. doi: 10.1016/j.bbrc.2013.06.064.

Lehouritis, P. *et al.* (2015) ‘Local bacteria affect the efficacy of chemotherapeutic drugs’, *Scientific Reports*, 5, p. 14554. doi: 10.1038/srep14554.

Lesage, S. *et al.* (2002) ‘CARD15/NOD2 mutational analysis and genotype-phenotype correlation in 612 patients with inflammatory bowel disease.’, *American journal of human genetics*. Elsevier, 70(4), pp. 845–57. doi: 10.1086/339432.

Lessard, L. *et al.* (2005) ‘Nuclear localisation of nuclear factor-kappaB transcription factors in prostate cancer: an immunohistochemical study.’, *British journal of cancer*. Nature Publishing Group, 93(9), pp. 1019–23. doi: 10.1038/sj.bjc.6602796.

Leushacke, M. *et al.* (2017) ‘Lgr5-expressing chief cells drive epithelial regeneration and cancer in the oxyntic stomach’, *Nature Cell Biology*. Nature Research, 19(7), pp. 774–786. doi: 10.1038/ncb3541.

Li, L. *et al.* (2015) ‘Prognostic impact of c-Rel nuclear expression and <i>REL</i> amplification and crosstalk between c-Rel and the p53 pathway in diffuse large B-cell lymphoma’, *Oncotarget*, 6(27), pp. 23157–23180. doi: 10.18632/oncotarget.4319.

Li, N. and Karin, M. (1998) ‘Ionizing radiation and short wavelength UV activate NF-kappaB through two distinct mechanisms.’, *Proceedings of the National Academy of Sciences of the United States of America*, 95(22), pp. 13012–7.

Li, X. *et al.* (2014) ‘Oncogenic transformation of diverse gastrointestinal tissues in primary organoid culture’, *Nature Medicine*, 20(7), pp. 769–777. doi: 10.1038/nm.3585.

Li, Y. *et al.* (2005) ‘Inactivation of Nuclear Factor B by Soy Isoflavone Genistein Contributes to Increased Apoptosis Induced by Chemotherapeutic Agents in Human Cancer Cells’, *Cancer Research*, 65(15), pp. 6934–6942. doi: 10.1158/0008-5472.CAN-04-4604.

Lin, C. and Zhang, J. (2017) ‘Inflammasomes in Inflammation-Induced Cancer.’, *Frontiers in immunology*. Frontiers Media SA, 8, p. 271. doi: 10.3389/fimmu.2017.00271.

Lin, L. and Ghosh, S. (1996) ‘A glycine-rich region in NF-kappaB p105 functions as a processing signal for the generation of the p50 subunit.’, *Molecular and cellular biology*, 16(5), pp. 2248–54.

Lin, W. *et al.* (2017) ‘Raf kinase inhibitor protein mediates intestinal epithelial cell

apoptosis and promotes IBDs in humans and mice', *Gut*, 66(4), pp. 597–610. doi: 10.1136/gutjnl-2015-310096.

Liu, W.-X. *et al.* (2015) 'Voluntary exercise prevents colonic inflammation in high-fat diet-induced obese mice by up-regulating PPAR-γ activity', *Biochemical and Biophysical Research Communications*, 459(3), pp. 475–480. doi: 10.1016/j.bbrc.2015.02.047.

Liu, Z. G. *et al.* (1996) 'Dissection of TNF receptor 1 effector functions: JNK activation is not linked to apoptosis while NF-kappaB activation prevents cell death.', *Cell*, 87(3), pp. 565–76.

Loftberg, R. *et al.* (2002) 'Topical NF-κB p65 antisense oligonucleotides in patients with active distal colonic IBD: a randomized, controlled pilot trial', *Gastroenterology*, 122.

Loftus, E. V (2004) 'Clinical epidemiology of inflammatory bowel disease: incidence, prevalence, and environmental influences', *Gastroenterology*, 126(6), pp. 1504–1517. doi: 10.1053/j.gastro.2004.01.063.

Logan, R. M. *et al.* (2008) 'Characterisation of mucosal changes in the alimentary tract following administration of irinotecan: implications for the pathobiology of mucositis', *Cancer Chemotherapy and Pharmacology*. Springer-Verlag, 62(1), pp. 33–41. doi: 10.1007/s00280-007-0570-0.

Logan, R. M. *et al.* (2009) 'Is the pathobiology of chemotherapy-induced alimentary tract mucositis influenced by the type of mucotoxic drug administered?', *Cancer Chemotherapy and Pharmacology*. Springer-Verlag, 63(2), pp. 239–251. doi: 10.1007/s00280-008-0732-8.

Lombardo, L. J. *et al.* (2004) 'Discovery of *N* -(2-Chloro-6-methyl- phenyl)-2-(6-(4-(2-hydroxyethyl)- piperazin-1-yl)-2-methylpyrimidin-4- ylamino)thiazole-5-carboxamide (BMS-354825), a Dual Src/Abl Kinase Inhibitor with Potent Antitumor Activity in Preclinical Assays', *Journal of Medicinal Chemistry*, 47(27), pp. 6658–6661. doi: 10.1021/jm049486a.

Longley, D. B., Harkin, D. P. and Johnston, P. G. (2003) '5-Fluorouracil: mechanisms of action and clinical strategies', *Nature Reviews Cancer*, 3(5), pp. 330–338. doi: 10.1038/nrc1074.

Lopez, J. *et al.* (2012) 'Src tyrosine kinase inhibits apoptosis through the Erk1/2-dependent degradation of the death accelerator Bik', *Cell Death and Differentiation*. Nature Publishing Group, 19(9), pp. 1459–1469. doi: 10.1038/cdd.2012.21.

Loriot, Y. *et al.* (2008) 'Drug Insight: gastrointestinal and hepatic adverse effects of molecular-targeted agents in cancer therapy', *Nature Clinical Practice Oncology*. Nature Publishing Group, 5(5), pp. 268–278. doi: 10.1038/ncponc1087.

Lu, H. *et al.* (2011) 'TNF- Promotes c-REL/ Np63 Interaction and TAp73 Dissociation from Key Genes That Mediate Growth Arrest and Apoptosis in Head and Neck Cancer', *Cancer Research*, 71(21), pp. 6867–6877. doi: 10.1158/0008-5472.CAN-11-2460.

Mabbott, N. A. *et al.* (2013) 'Microfold (M) cells: important immunosurveillance posts in the intestinal epithelium', *Mucosal Immunology*, 6(4), pp. 666–677. doi: 10.1038/mi.2013.30.

Madara, J. L. (1990) ‘Maintenance of the macromolecular barrier at cell extrusion sites in intestinal epithelium: physiological rearrangement of tight junctions.’, *The Journal of membrane biology*, 116(2), pp. 177–84.

Madison, B. B. *et al.* (2004) ‘Epithelial hedgehog signals pattern the intestinal crypt-villus axis’, *Development*, 132(2).

Marks, D. J. *et al.* (2006) ‘Defective acute inflammation in Crohn’s disease: a clinical investigation’, *The Lancet*, 367(9511), pp. 668–678. doi: 10.1016/S0140-6736(06)68265-2.

Marshall, D. *et al.* (2007) ‘Blockade of colony stimulating factor-1 (CSF-1) leads to inhibition of DSS-induced colitis’, *Inflammatory Bowel Diseases*, 13(2), pp. 219–224. doi: 10.1002/ibd.20055.

Marshman, E. *et al.* (2001) ‘Caspase activation during spontaneous and radiation-induced apoptosis in the murine intestine’, *The Journal of Pathology*. John Wiley & Sons, Ltd., 195(3), pp. 285–292. doi: 10.1002/path.967.

Mathes, E. *et al.* (2008) ‘NF-kappaB dictates the degradation pathway of IkappaBalpha.’, *The EMBO journal*. European Molecular Biology Organization, 27(9), pp. 1357–67. doi: 10.1038/emboj.2008.73.

McCole, D. F. and Barrett, K. E. (2009) ‘Decoding epithelial signals: critical role for the epidermal growth factor receptor in controlling intestinal transport function’, *Acta Physiologica*, 195(1), pp. 149–159. doi: 10.1111/j.1748-1716.2008.01929.x.

McCormick, D. A., Horton, L. W. and Mee, A. S. (1990) ‘Mucin depletion in inflammatory bowel disease.’, *Journal of clinical pathology*, 43(2), pp. 143–6.

McDaniel, D. K. *et al.* (2016) ‘Emerging Roles for Noncanonical NF-κB Signaling in the Modulation of Inflammatory Bowel Disease Pathobiology’, *Inflammatory Bowel Diseases*, 22(9), pp. 2265–2279. doi: 10.1097/MIB.0000000000000858.

McGovern, D. P. B. *et al.* (2010) ‘Genome-wide association identifies multiple ulcerative colitis susceptibility loci’, *Nature Genetics*, 42(4), pp. 332–337. doi: 10.1038/ng.549.

McNamee, E. N. *et al.* (2013) ‘Ectopic lymphoid tissue alters the chemokine gradient, increases lymphocyte retention and exacerbates murine ileitis’, *Gut*, 62(1), pp. 53–62. doi: 10.1136/gutjnl-2011-301272.

McNamee, E. N. and Rivera-Nieves, J. (2016) ‘Ectopic Tertiary Lymphoid Tissue in Inflammatory Bowel Disease: Protective or Provocateur?’, *Frontiers in immunology*. Frontiers Media SA, 7, p. 308. doi: 10.3389/fimmu.2016.00308.

McQuade, R. M. *et al.* (2016) ‘Chemotherapy-Induced Constipation and Diarrhea: Pathophysiology, Current and Emerging Treatments.’, *Frontiers in pharmacology*. Frontiers Media SA, 7, p. 414. doi: 10.3389/fphar.2016.00414.

Melgar, S. *et al.* (2008) ‘Validation of murine dextran sulfate sodium-induced colitis using four therapeutic agents for human inflammatory bowel disease’, *International Immunopharmacology*, 8(6), pp. 836–844. doi: 10.1016/j.intimp.2008.01.036.

Melgar, S., Karlsson, A. and Michaëlsson, E. (2005) ‘Acute colitis induced by dextran sulfate sodium progresses to chronicity in C57BL/6 but not in BALB/c mice: correlation between symptoms and inflammation.’, *American journal of physiology. Gastrointestinal and liver physiology*, 288(6), pp. G1328-38. doi:

10.1152/ajpgi.00467.2004.

Merker, S. R., Weitz, J. and Stange, D. E. (2016) 'Gastrointestinal organoids: How they gut it out', *Developmental Biology*, 420(2), pp. 239–250. doi: 10.1016/j.ydbio.2016.08.010.

Merritt, A. J. *et al.* (1995) 'Differential expression of bcl-2 in intestinal epithelia. Correlation with attenuation of apoptosis in colonic crypts and the incidence of colonic neoplasia.', *Journal of cell science*, 108 (Pt 6), pp. 2261–71.

Michail, S., Bultron, G. and Depaolo, R. W. (2013) 'Genetic variants associated with Crohn's disease.', *The application of clinical genetics*. Dove Press, 6, pp. 25–32. doi: 10.2147/TACG.S33966.

Miguel, J. C. *et al.* (2017) 'Epidermal growth factor suppresses intestinal epithelial cell shedding through a MAPK-dependent pathway', *Journal of Cell Science*, 130(1).

Mizoguchi, A. *et al.* (2016) 'Genetically engineered mouse models for studying inflammatory bowel disease.', *The Journal of pathology*. NIH Public Access, 238(2), pp. 205–19. doi: 10.1002/path.4640.

Mizoguchi, A. and Mizoguchi, E. (2010) 'Animal models of IBD: linkage to human disease.', *Current opinion in pharmacology*. NIH Public Access, 10(5), pp. 578–87. doi: 10.1016/j.coph.2010.05.007.

Mombaerts, P. *et al.* (1993) 'Spontaneous development of inflammatory bowel disease in T cell receptor mutant mice.', *Cell*, 75(2), pp. 274–82.

Montecucco, A. and Biamonti, G. (2007) 'Cellular response to etoposide treatment', *Cancer Letters*, 252(1), pp. 9–18. doi: 10.1016/j.canlet.2006.11.005.

Montecucco, A., Zanetta, F. and Biamonti, G. (2015) 'Molecular mechanisms of etoposide.', *EXCLI journal*. Leibniz Research Centre for Working Environment and Human Factors, 14, pp. 95–108. doi: 10.17179/excli2015-561.

Moorthy, A. K. *et al.* (2006) 'The 20S proteasome processes NF-kappaB1 p105 into p50 in a translation-independent manner.', *The EMBO journal*. European Molecular Biology Organization, 25(9), pp. 1945–56. doi: 10.1038/sj.emboj.7601081.

Morampudi, V. *et al.* (2014) 'DNBS/TNBS colitis models: providing insights into inflammatory bowel disease and effects of dietary fat.', *Journal of visualized experiments : JoVE*. MyJoVE Corporation, (84), p. e51297. doi: 10.3791/51297.

Morotti, A. *et al.* (2006) 'NF-kB inhibition as a strategy to enhance etoposide-induced apoptosis in K562 cell line', *American Journal of Hematology*. Wiley Subscription Services, Inc., A Wiley Company, 81(12), pp. 938–945. doi: 10.1002/ajh.20732.

Morson, B. S. (1968) 'Histopathology of Crohn's disease.', *Proceedings of the Royal Society of Medicine*. Royal Society of Medicine Press, 61(1), pp. 79–81.

Morteau, O. *et al.* (2000) 'Impaired mucosal defense to acute colonic injury in mice lacking cyclooxygenase-1 or cyclooxygenase-2', *Journal of Clinical Investigation*, 105(4), pp. 469–478. doi: 10.1172/JCI6899.

Mowat, A. M. and Agace, W. W. (2014) 'Regional specialization within the intestinal immune system', *Nature Reviews Immunology*. Nature Research, 14(10), pp. 667–685. doi: 10.1038/nri3738.

Murano, M. *et al.* (2000) 'Therapeutic effect of intracolonically administered nuclear factor kappa B (p65) antisense oligonucleotide on mouse dextran sulphate sodium (DSS)-induced colitis.', *Clinical and experimental immunology*. Wiley-Blackwell, 120(1), pp. 51–8. doi: 10.1046/j.1365-2249.2000.01183.x.

Nadiminty, N. *et al.* (2006) 'Stat3 activation of NF-{kappa}B p100 processing involves CBP/p300-mediated acetylation.', *Proceedings of the National Academy of Sciences of the United States of America*. National Academy of Sciences, 103(19), pp. 7264–9. doi: 10.1073/pnas.0509808103.

Nagata, S. and Golstein, P. (1995) 'The Fas death factor.', *Science (New York, N.Y.)*, 267(5203), pp. 1449–56.

NC3Rs/BBSRC/Defra/MRC/NERC/Wellcome (2017) 'Responsibility in the use of animals in bioscience research: expectations of the major research councils and charitable funding bodies.', *London: NC3Rs*.

Nedjic, J. *et al.* (2008) 'Autophagy in thymic epithelium shapes the T-cell repertoire and is essential for tolerance', *Nature*, 455(7211), pp. 396–400. doi: 10.1038/nature07208.

Neish, A. S. *et al.* (2000) 'Prokaryotic regulation of epithelial responses by inhibition of IkappaB-alpha ubiquitination.', *Science (New York, N.Y.)*, 289(5484), pp. 1560–3.

Nenci, A. *et al.* (2007) 'Epithelial NEMO links innate immunity to chronic intestinal inflammation', *Nature*, 446(7135), pp. 557–561. doi: 10.1038/nature05698.

Neurath, M. F. *et al.* (1995) 'Antibodies to interleukin 12 abrogate established experimental colitis in mice.', *The Journal of experimental medicine*, 182(5), pp. 1281–90.

Neurath, M. F. *et al.* (1996) 'Local administration of antisense phosphorothioate oligonucleotides to the p65 subunit of NF-kappa B abrogates established experimental colitis in mice.', *Nature medicine*, 2(9), pp. 998–1004.

Noort, A. R. *et al.* (2015) 'Tertiary Lymphoid Structures in Rheumatoid Arthritis: NF-κB-Inducing Kinase-Positive Endothelial Cells as Central Players', *American Journal of Pathology*, 185(7), pp. 1935–1943. doi: 10.1016/j.ajpath.2015.03.012.

Novack, D. V. *et al.* (2003) 'The IκB Function of NF-κB2 p100 Controls Stimulated Osteoclastogenesis', *The Journal of Experimental Medicine*, 198(5), pp. 771–781. doi: 10.1084/jem.20030116.

O'Dea, E. L. *et al.* (2007) 'A homeostatic model of IkappaB metabolism to control constitutive NF-kappaB activity.', *Molecular systems biology*. European Molecular Biology Organization, 3, p. 111. doi: 10.1038/msb4100148.

O'Hare, T. *et al.* (2005) 'In vitro Activity of Bcr-Abl Inhibitors AMN107 and BMS-354825 against Clinically Relevant Imatinib-Resistant Abl Kinase Domain Mutants', *Cancer Research*, 65(11).

Oeckinghaus, A. and Ghosh, S. (2009) 'The NF-kappaB family of transcription factors and its regulation.', *Cold Spring Harbor perspectives in biology*. Cold Spring Harbor Laboratory Press, 1(4), p. a000034. doi: 10.1101/cshperspect.a000034.

Okayasu, I. *et al.* (1990) 'A novel method in the induction of reliable experimental acute and chronic ulcerative colitis in mice.', *Gastroenterology*, 98(3), pp. 694–702. doi: S0016508590000725 [pii].

Olivier, B. J. *et al.* (2016) 'Vagal inervation is required for the formation of tertiary lymphoid tissue in colitis', *European Journal of Immunology*, pp. 1–41. doi: 10.1017/CBO9781107415324.004.

Olivier, I. *et al.* (2011) 'Is Crohn's creeping fat an adipose tissue?', *Inflammatory Bowel Diseases*, 17(3), pp. 747–757. doi: 10.1002/ibd.21413.

Ostanin, D. V *et al.* (2009) 'T cell transfer model of chronic colitis: concepts, considerations, and tricks of the trade.', *American journal of physiology. Gastrointestinal and liver physiology*. American Physiological Society, 296(2), pp. G135-46. doi: 10.1152/ajpgi.90462.2008.

Ostvik, A. E. *et al.* (2013) 'Enhanced expression of CXCL10 in inflammatory bowel disease: potential role of mucosal Toll-like receptor 3 stimulation.', *Inflammatory bowel diseases*, 19(2), pp. 265–74. doi: 10.1002/ibd.23034.

Pahl, H. L. (1999) 'Activators and target genes of Rel/NF-kappaB transcription factors.', *Oncogene*, 18(49), pp. 6853–66. doi: 10.1038/sj.onc.1203239.

Palombella, V. J. *et al.* (1994) 'The ubiquitin-proteasome pathway is required for processing the NF-kappa B1 precursor protein and the activation of NF-kappa B.', *Cell*. Cold Spring Harbor Laboratory Press, New York, 78(5), pp. 773–85. doi: 10.1016/S0092-8674(94)90482-0.

Parray, F. Q. *et al.* (2012) 'Ulcerative colitis: a challenge to surgeons.', *International journal of preventive medicine*. Wolters Kluwer -- Medknow Publications, 3(11), pp. 749–63.

Parsons, B. N. *et al.* (2014) 'Dietary Supplementation with Soluble Plantain Non-Starch Polysaccharides Inhibits Intestinal Invasion of Salmonella Typhimurium in the Chicken', *PLoS ONE*. Edited by M. Hensel. Public Library of Science, 9(2), p. e87658. doi: 10.1371/journal.pone.0087658.

Pasic, I. and Lipton, J. H. (2017) 'Current approach to the treatment of chronic myeloid leukaemia', *Leukemia Research*, 55, pp. 65–78. doi: 10.1016/j.leukres.2017.01.005.

Pasparakis, M. (2008) 'IKK/NF-κB signaling in intestinal epithelial cells controls immune homeostasis in the gut', *Mucosal Immunology*, 1(1s), pp. S54–S57. doi: 10.1038/mi.2008.53.

Pasternak, B. *et al.* (2013) 'Use of azathioprine and the risk of cancer in inflammatory bowel disease', *American Journal of Epidemiology*, 177(11), pp. 1296–1305. doi: 10.1093/aje/kws375.

Paul, G. *et al.* (2006) 'Profiling adipocytokine secretion from creeping fat in Crohn's disease.', *Inflammatory bowel diseases*, 12(6), pp. 471–7.

Paul, M. K. and Mukhopadhyay, A. K. (2004) 'Tyrosine kinase - Role and significance in Cancer.', *International journal of medical sciences*, 1(2), pp. 101–115. doi: 10.7150/ijms.1.101.

Perkins, N. D. and Gilmore, T. D. (2006) 'Good cop, bad cop: the different faces of NF-κB', *Cell Death and Differentiation*, 13(5), pp. 759–772. doi: 10.1038/sj.cdd.4401838.

Peterson, L. W. and Artis, D. (2014) 'Intestinal epithelial cells: regulators of barrier function and immune homeostasis', *Nature Reviews Immunology*, 14(3), pp. 141–

153. doi: 10.1038/nri3608.

Peyrin–Biroulet, L. *et al.* (2011) 'Increased Risk for Nonmelanoma Skin Cancers in Patients Who Receive Thiopurines for Inflammatory Bowel Disease', *Gastroenterology*, 141(5), p. 1621–1628.e5. doi: 10.1053/j.gastro.2011.06.050.

Pico, J.-L., Avila-Garavito, A. and Naccache, P. (1998) 'Mucositis: Its Occurrence, Consequences, and Treatment in the Oncology Setting.', *The oncologist*. AlphaMed Press, 3(6), pp. 446–451.

Pinto, D. *et al.* (2003) 'Canonical Wnt signals are essential for homeostasis of the intestinal epithelium.', *Genes & development*. Cold Spring Harbor Laboratory Press, 17(14), pp. 1709–13. doi: 10.1101/gad.267103.

Piret, B. and Piette, J. (1996) 'Topoisomerase poisons activate the transcription factor NF-kappaB in ACH-2 and CEM cells.', *Nucleic acids research*, 24(21), pp. 4242–8.

Potten, C. S. (1977) 'Extreme sensitivity of some intestinal crypt cells to X and gamma irradiation.', *Nature*, 269(5628), pp. 518–21.

Potten, C. S. *et al.* (1978) 'The segregation of DNA in epithelial stem cells.', *Cell*, 15(3), pp. 899–906.

Potten, C. S. *et al.* (1981) 'The correction of intestinal microcolony counts for variation in size.', *International journal of radiation biology and related studies in physics, chemistry, and medicine*, 40(3), pp. 321–6.

Potten, C. S. (1992) 'The significance of spontaneous and induced apoptosis in the gastrointestinal tract of mice.', *Cancer metastasis reviews*, 11(2), pp. 179–95.

Potten, C. S. *et al.* (2009) 'The stem cells of small intestinal crypts: where are they?', *Cell Proliferation*. Blackwell Publishing Ltd, 42(6), pp. 731–750. doi: 10.1111/j.1365-2184.2009.00642.x.

Potten, C. S. and Loeffler, M. (1990) 'Stem cells: attributes, cycles, spirals, pitfalls and uncertainties. Lessons for and from the crypt.', *Development (Cambridge, England)*, 110(4), pp. 1001–20.

Potten, C. S., Owen, G. and Roberts, S. A. (1990) 'The temporal and spatial changes in cell proliferation within the irradiated crypts of the murine small intestine.', *International journal of radiation biology*, 57(1), pp. 185–99.

Potten, C. S., Wilson, J. W. and Booth, C. (1997) 'Regulation and Significance of Apoptosis in the Stem Cells of the Gastrointestinal Epithelium', *Stem Cells*. John Wiley & Sons, Ltd., 15(2), pp. 82–93. doi: 10.1002/stem.150082.

Presland, R. B. and Dale, B. A. (2000) 'Epithelial structural proteins of the skin and oral cavity: function in health and disease.', *Critical reviews in oral biology and medicine : an official publication of the American Association of Oral Biologists*, 11(4), pp. 383–408.

Presland, R. B. and Jurevic, R. J. (2002) 'Making sense of the epithelial barrier: what molecular biology and genetics tell us about the functions of oral mucosal and epidermal tissues.', *Journal of dental education*, 66(4), pp. 564–74.

Pritchard, D. M. *et al.* (1997) 'Inhibition by uridine but not thymidine of p53-dependent intestinal apoptosis initiated by 5-fluorouracil: evidence for the

involvement of RNA perturbation.', *Proceedings of the National Academy of Sciences of the United States of America*. National Academy of Sciences, 94(5), pp. 1795–9.

Pritchard, D. M. *et al.* (1998) 'Chemically-induced apoptosis: p21 and p53 as determinants of enterotoxin activity.', *Toxicology letters*, 102–103, pp. 19–27.

Pritchard, D. M. *et al.* (2000) 'Bcl-w is an important determinant of damage-induced apoptosis in epithelia of small and large intestine', *Oncogene*, 19(34), pp. 3955–3959. doi: 10.1038/sj.onc.1203729.

Puttini, M. *et al.* (2006) 'In vitro and In vivo Activity of SKI-606, a Novel Src-Abl Inhibitor, against Imatinib-Resistant Bcr-Abl+ Neoplastic Cells', *Cancer Research*, 66(23), pp. 11314–11322. doi: 10.1158/0008-5472.CAN-06-1199.

Qi, Z. *et al.* (2017) 'BMP restricts stemness of intestinal Lgr5+ stem cells by directly suppressing their signature genes', *Nature Communications*, 8, p. 13824. doi: 10.1038/ncomms13824.

Qi, Z. and Chen, Y.-G. (2015) 'Regulation of intestinal stem cell fate specification', *Science China Life Sciences*, 58(6), pp. 570–578. doi: 10.1007/s11427-015-4859-7.

Qin, J. *et al.* (2010) 'A human gut microbial gene catalogue established by metagenomic sequencing.', *Nature*. Europe PMC Funders, 464(7285), pp. 59–65. doi: 10.1038/nature08821.

Qiu, W. *et al.* (2011) 'PUMA-mediated intestinal epithelial apoptosis contributes to ulcerative colitis in humans and mice', *Journal of Clinical Investigation*, 121(5), pp. 1722–1732. doi: 10.1172/JCI42917.

Rahman, K. *et al.* (2014) 'Crohn's Disease–associated Escherichia coli Survive in Macrophages by Suppressing NFκB Signaling', *Inflammatory Bowel Diseases*, 20(8), pp. 1419–1425. doi: 10.1097/MIB.0000000000000096.

Ramesh, M., Ahlawat, P. and Srinivas, N. R. (2010) 'Irinotecan and its active metabolite, SN-38: review of bioanalytical methods and recent update from clinical pharmacology perspectives', *Biomedical Chromatography*, 24(1), pp. 104–123. doi: 10.1002/bmc.1345.

Ranson, M. (2004) 'Epidermal growth factor receptor tyrosine kinase inhibitors', *British Journal of Cancer*, 90(12), pp. 2250–5. doi: 10.1038/sj.bjc.6601873.

Rao, J. N. and Wang, J.-Y. (2010) *Regulation of Gastrointestinal Mucosal Growth*, *Regulation of Gastrointestinal Mucosal Growth*. Morgan & Claypool Life Sciences.

Rasmussen, A. R. *et al.* (2010) 'The intestinotrophic peptide, GLP-2, counteracts the gastrointestinal atrophy in mice induced by the epidermal growth factor receptor inhibitor, Erlotinib, and cisplatin', *Digestive Diseases and Sciences*, 55(10), pp. 2785–2796. doi: 10.1007/s10620-009-1104-x.

Ren, R. (2005) 'Mechanisms of BCR–ABL in the pathogenesis of chronic myelogenous leukaemia', *Nature Reviews Cancer*. Nature Publishing Group, 5(3), pp. 172–183. doi: 10.1038/nrc1567.

Richard-Miceli, C. and Criswell, L. A. (2012) 'Emerging patterns of genetic overlap across autoimmune disorders.', *Genome medicine*. BioMed Central, 4(1), p. 6. doi: 10.1186/gm305.

Ritsma, L. *et al.* (2014) 'Intestinal crypt homeostasis revealed at single-stem-cell level by in vivo live imaging', *Nature*, 507(7492), pp. 362–365. doi: 10.1038/nature12972.

Romieu-Mourez, R. *et al.* (2003) 'Mouse mammary tumor virus c-rel transgenic mice develop mammary tumors.', *Molecular and cellular biology*, 23(16), pp. 5738–54.

von Roon, A. C. *et al.* (2007) 'The Risk of Cancer in Patients with Crohn's Disease', *Diseases of the Colon & Rectum*, 50(6), pp. 839–855. doi: 10.1007/s10350-006-0848-z.

Rosell, R. *et al.* (2009) 'Screening for Epidermal Growth Factor Receptor Mutations in Lung Cancer', *New England Journal of Medicine*, 361(10), pp. 958–967. doi: 10.1056/NEJMoa0904554.

Rosenblum, J. M. *et al.* (2010) 'CXC chemokine ligand (CXCL) 9 and CXCL10 are antagonistic costimulation molecules during the priming of alloreactive T cell effectors.', *Journal of Immunology*, 184(7), pp. 3450–3460. doi: 10.4049/jimmunol.0903831.

Rossi, R. *et al.* (2006) 'The Dispersal of Replication Proteins after Etoposide Treatment Requires the Cooperation of Nbs1 with the Ataxia Telangiectasia Rad3-Related/Chk1 Pathway', *Cancer Research*, 66(3), pp. 1675–1683. doi: 10.1158/0008-5472.CAN-05-2741.

Rothenberg, M. L. (2001) 'Irinotecan (CPT-11): recent developments and future directions--colorectal cancer and beyond.', *The oncologist*, 6(1), pp. 66–80.

Rowley, J. D. (1973) 'Letter: A new consistent chromosomal abnormality in chronic myelogenous leukaemia identified by quinacrine fluorescence and Giemsa staining.', *Nature*, 243(5405), pp. 290–3. doi: 10.1038/243290a0.

Roy, P. *et al.* (2016) 'Non-canonical NFκB mutations reinforce pro-survival TNF response in multiple myeloma through an autoregulatory RelB:p50 NFκB pathway', *Oncogene*. Nature Publishing Group. doi: 10.1038/onc.2016.309.

Rutter, M. D. *et al.* (2006) 'Thirty-Year Analysis of a Colonoscopic Surveillance Program for Neoplasia in Ulcerative Colitis', *Gastroenterology*, 130(4), pp. 1030–1038. doi: 10.1053/j.gastro.2005.12.035.

Sadlack, B. *et al.* (1993) 'Ulcerative colitis-like disease in mice with a disrupted interleukin-2 gene.', *Cell*, 75(2), pp. 253–61.

Sangiorgi, E. and Capecchi, M. R. (2008) 'Bmi1 is expressed in vivo in intestinal stem cells', *Nature Genetics*, 40(7), pp. 915–920. doi: 10.1038/ng.165.

Sato, T. *et al.* (2009) 'Single Lgr5 stem cells build crypt?villus structures in vitro without a mesenchymal niche', *Nature*, 459(7244), pp. 262–265. doi: 10.1038/nature07935.

Sato, T. *et al.* (2011) 'Paneth cells constitute the niche for Lgr5 stem cells in intestinal crypts', *Nature*, 469(7330), pp. 415–418. doi: 10.1038/nature09637.

Sato, T. and Clevers, H. (2013) 'Growing Self-Organizing Mini-Guts from a Single Intestinal Stem Cell: Mechanism and Applications', *Science*, 340(6137).

Savkovic, S. D., Koutsouris, a and Hecht, G. (1997) 'Activation of NF-kappaB in intestinal epithelial cells by enteropathogenic Escherichia coli.', *The American*

journal of physiology, 273(4 Pt 1), pp. C1160–C1167.

Scarminio, V. *et al.* (2012) 'Dietary intervention with green dwarf banana flour (Musa sp AAA) prevents intestinal inflammation in a trinitrobenzenesulfonic acid model of rat colitis', *Nutrition Research*, 32(3), pp. 202–209. doi: 10.1016/j.nutres.2012.01.002.

van Schaik, F. D. M. *et al.* (2012) 'Thiopurines prevent advanced colorectal neoplasia in patients with inflammatory bowel disease', *Gut*, 61(2), pp. 235–240. doi: 10.1136/gut.2011.237412.

Schreiber, S., Nikolaus, S. and Hampe, J. (1998) 'Activation of nuclear factor kappa B inflammatory bowel disease.', *Gut*. BMJ Publishing Group, 42(4), pp. 477–84.

Schubert, C. *et al.* (2017) 'The SCLtTAxBCR-ABL transgenic mouse model closely reflects the differential effects of dasatinib on normal and malignant hematopoiesis in chronic phase-CML patients.', *Oncotarget*. Impact Journals, LLC, 8(21), pp. 34736–34749. doi: 10.18632/oncotarget.16152.

Schwank, G. *et al.* (2013) 'Functional Repair of CFTR by CRISPR/Cas9 in Intestinal Stem Cell Organoids of Cystic Fibrosis Patients', *Cell Stem Cell*, 13(6), pp. 653–658. doi: 10.1016/j.stem.2013.11.002.

Sen, R. *et al.* (1986) 'Multiple nuclear factors interact with the immunoglobulin enhancer sequences', *Cell*. BioMed Central, 46(5), pp. 705–716. doi: 10.1016/0092-8674(86)90346-6.

Sen, R. and Baltimore, D. (1987) 'In vitro transcription of immunoglobulin genes in a B-cell extract: effects of enhancer and promoter sequences.', *Molecular and cellular biology*. American Society for Microbiology (ASM), 7(5), pp. 1989–94.

Senftleben, U. *et al.* (2001) 'Activation by IKKalpha of a Second, Evolutionary Conserved, NF-kappa B Signaling Pathway', *Science*, 293(5534), pp. 1495–1499. doi: 10.1126/science.1062677.

Seo, Y. H. (2015) 'Dual Inhibitors Against Topoisomerases and Histone Deacetylases', *Journal of Cancer Prevention*, 20(2), pp. 85–91. doi: 10.15430/JCP.2015.20.2.85.

Sha, W. C. *et al.* (1995) 'Targeted disruption of the p50 subunit of NF-kappa B leads to multifocal defects in immune responses.', *Cell*, 80(2), pp. 321–30.

Shamas-Din, A. *et al.* (2013) 'Mechanisms of action of Bcl-2 family proteins.', *Cold Spring Harbor perspectives in biology*. Cold Spring Harbor Laboratory Press, 5(4), p. a008714. doi: 10.1101/cshperspect.a008714.

Sharma, V., Hupp, C. D. and Tepe, J. J. (2007) 'Enhancement of chemotherapeutic efficacy by small molecule inhibition of NF-kappaB and checkpoint kinases.', *Current medicinal chemistry*, 14(10), pp. 1061–74.

Shattuck-Brandt, R. L. *et al.* (2000) 'Cyclooxygenase 2 expression is increased in the stroma of colon carcinomas from IL-10(-/-) mice.', *Gastroenterology*, 118(2), pp. 337–45. doi: http://dx.doi.org/10.1016/S0016-5085(00)70216-2.

Shepherd, F. A. *et al.* (2005) 'Erlotinib in previously treated non-small-cell lung cancer.', *The New England journal of medicine*, 353(2), pp. 123–32. doi: 10.1056/NEJMoa050753.

Sheth, S. G. and LaMont, J. T. (1998) ‘Toxic megacolon’, *The Lancet*, 351(9101), pp. 509–513. doi: 10.1016/S0140-6736(97)10475-5.

Shibata, W. *et al.* (2007) ‘Cutting edge: The IkappaB kinase (IKK) inhibitor, NEMO-binding domain peptide, blocks inflammatory injury in murine colitis.’, *Journal of immunology (Baltimore, Md. : 1950)*, 179(5), pp. 2681–5.

Shono, Y. *et al.* (2014) ‘A Small-Molecule c-Rel Inhibitor Reduces Alloactivation of T Cells without Compromising Antitumor Activity’, *Cancer Discovery*, 4(5).

Shrader, M. *et al.* (2007) ‘Gefitinib Reverses TRAIL Resistance in Human Bladder Cancer Cell Lines via Inhibition of AKT-Mediated X-Linked Inhibitor of Apoptosis Protein Expression’, *Cancer Research*, 67(4).

Siddique, M. M. *et al.* (2012) ‘Ablation of Dihydroceramide Desaturase Confers Resistance to Etoposide-Induced Apoptosis In Vitro’, *PLoS ONE*. Edited by R. Linden, 7(9), p. e44042. doi: 10.1371/journal.pone.0044042.

Siebenlist, U., Franzoso, G. and Brown, K. (1994) ‘Structure, regulation and function of NF- k B’, *Annu Rev Cell Biol*, 10, pp. 405–455.

da Silva, B. C. *et al.* (2014) ‘Epidemiology, demographic characteristics and prognostic predictors of ulcerative colitis.’, *World journal of gastroenterology*. Baishideng Publishing Group Inc, 20(28), pp. 9458–67. doi: 10.3748/wjg.v20.i28.9458.

De Silva, N. S. *et al.* (2016) ‘Transcription factors of the alternative NF-κB pathway are required for germinal center B-cell development.’, *Proceedings of the National Academy of Sciences of the United States of America*. National Academy of Sciences, 113(32), pp. 9063–8. doi: 10.1073/pnas.1602728113.

Simian, M. and Bissell, M. J. (2016) ‘Organoids: A historical perspective of thinking in three dimensions’, *The Journal of Cell Biology*.

Ślebioda, T. J. and Kmieć, Z. (2014) ‘Tumour Necrosis Factor Superfamily Members in the Pathogenesis of Inflammatory Bowel Disease’, *Mediators of Inflammation*, 2014, pp. 1–15. doi: 10.1155/2014/325129.

Slotta, C. *et al.* (2017) ‘CRISPR/Cas9-mediated knockout of c-REL in HeLa cells results in profound defects of the cell cycle’, *PLOS ONE*. Edited by M. F. Romano, 12(8), p. e0182373. doi: 10.1371/journal.pone.0182373.

Smith, R. (2017) ‘Colitis’, *Magill’s Medical Guide (online edition)*. EBSCOhost.

Snippert, H. J. *et al.* (2010) ‘Intestinal Crypt Homeostasis Results from Neutral Competition between Symmetrically Dividing Lgr5 Stem Cells’, *Cell*, 143(1), pp. 134–144. doi: 10.1016/j.cell.2010.09.016.

Soares, P. M. G. *et al.* (2008) ‘Gastrointestinal dysmotility in 5-fluorouracil-induced intestinal mucositis outlasts inflammatory process resolution.’, *Cancer chemotherapy and pharmacology*, 63(1), pp. 91–8. doi: 10.1007/s00280-008-0715-9.

Sobczac, L. (2017) ‘Crohn’s disease’, *Magill’s Medical Guide (online edition)*. Online edi. EBSCOhost.

Sobrero, A. *et al.* (2000) ‘Mechanism of action of fluoropyrimidines: relevance to the new developments in colorectal cancer chemotherapy.’, *Seminars in oncology*, 27(5

Suppl 10), pp. 72–7.

Sobrero, A. (2009) 'Medical Oncology: IROX as second-line therapy for metastatic colorectal cancer.', *Nature reviews. Clinical oncology*, 6(5), pp. 248–50. doi: 10.1038/nrclinonc.2009.43.

Soler, A. P. *et al.* (1999) 'Activation of NF-kappaB is necessary for the restoration of the barrier function of an epithelium undergoing TNF-alpha-induced apoptosis.', *European journal of cell biology*, 78(1), pp. 56–66.

Sonis, S. T. *et al.* (2004) 'Perspectives on cancer therapy-induced mucosal injury: pathogenesis, measurement, epidemiology, and consequences for patients.', *Cancer*, 100(9 Suppl), pp. 1995–2025. doi: 10.1002/cncr.20162.

Sonis, S. T. (2004) 'The pathobiology of mucositis', *Nature Reviews Cancer*. Nature Publishing Group, 4(4), pp. 277–284. doi: 10.1038/nrc1318.

Sonnenberg, A. (1986) 'Mortality from Crohn's disease and ulcerative colitis in England-Wales and the U.S. from 1950 to 1983', *Diseases of the Colon & Rectum*. Springer-Verlag, 29(10), pp. 624–629. doi: 10.1007/BF02560320.

Soria, J.-C. *et al.* (2012) 'EGFR-mutated oncogene-addicted non-small cell lung cancer: Current trends and future prospects', *Cancer Treatment Reviews*, 38(5), pp. 416–430. doi: 10.1016/j.ctrv.2011.10.003.

Sovak, M. A. *et al.* (1997) 'Aberrant nuclear factor-kappaB/Rel expression and the pathogenesis of breast cancer.', *Journal of Clinical Investigation*, 100(12), pp. 2952–2960. doi: 10.1172/JCI119848.

Steinbrecher, K. A. *et al.* (2008) 'Loss of epithelial RelA results in deregulated intestinal proliferative/apoptotic homeostasis and susceptibility to inflammation.', *Journal of immunology (Baltimore, Md. : 1950)*, 180(4), pp. 2588–99.

Stilmann, M. *et al.* (2009) 'A Nuclear Poly(ADP-Ribose)-Dependent Signalosome Confers DNA Damage-Induced IκB Kinase Activation', *Molecular Cell*, 36(3), pp. 365–378. doi: 10.1016/j.molcel.2009.09.032.

Stringer, A. M. *et al.* (2009) 'Gastrointestinal Microflora and Mucins May Play a Critical Role in the Development of 5-Fluorouracil-Induced Gastrointestinal Mucositis', *Experimental Biology and Medicine*. SAGE PublicationsSage UK: London, England, 234(4), pp. 430–441. doi: 10.3181/0810-RM-301.

Stringer, A. M. *et al.* (2009) 'Irinotecan-induced mucositis manifesting as diarrhoea corresponds with an amended intestinal flora and mucin profile', *International Journal of Experimental Pathology*, 90(5), pp. 489–499. doi: 10.1111/j.1365-2613.2009.00671.x.

Strober, W. (2011) 'Adherent-invasive E. coli in Crohn disease: bacterial ?agent provocateur?', *Journal of Clinical Investigation*, 121(3), pp. 841–844. doi: 10.1172/JCI46333.

Strober, W. and Fuss, I. J. (2011) 'Proinflammatory cytokines in the pathogenesis of inflammatory bowel diseases.', *Gastroenterology*. NIH Public Access, 140(6), pp. 1756–67. doi: 10.1053/j.gastro.2011.02.016.

Strong, S. A. (2010) 'Management of acute colitis and toxic megacolon.', *Clinics in colon and rectal surgery*. Thieme Medical Publishers, 23(4), pp. 274–84. doi: 10.1055/s-0030-1268254.

Sun, S.-C. (2011) ‘Non-canonical NF-κB signaling pathway’, *Cell Research*, 21(1), pp. 71–85. doi: 10.1038/cr.2010.177.

Sun, Y. *et al.* (2007) ‘The radiosensitization effect of parthenolide in prostate cancer cells is mediated by nuclear factor- B inhibition and enhanced by the presence of PTEN’, *Molecular Cancer Therapeutics*, 6(9), pp. 2477–2486. doi: 10.1158/1535-7163.MCT-07-0186.

Tannenbaum, J. and Bennett, B. T. (2015) ‘Russell and Burch’s 3Rs then and now: the need for clarity in definition and purpose.’, *Journal of the American Association for Laboratory Animal Science : JAALAS*. American Association for Laboratory Animal Science, 54(2), pp. 120–32.

Tato, C. M. *et al.* (2003) ‘Inhibition of NF-kappa B activity in T and NK cells results in defective effector cell expansion and production of IFN-gamma required for resistance to Toxoplasma gondii.’, *Journal of immunology (Baltimore, Md. : 1950)*, 170(6), pp. 3139–46.

Taub, D. D. *et al.* (1993) ‘Recombinant human interferon-inducible protein 10 is a chemoattractant for human monocytes and T lymphocytes and promotes T cell adhesion to endothelial cells.’, *The Journal of experimental medicine*, 177(6), pp. 1809–14. doi: 10.1084/jem.177.6.1809.

Thatcher, N. *et al.* (2005) ‘Gefitinib plus best supportive care in previously treated patients with refractory advanced non-small-cell lung cancer: results from a randomised, placebo-controlled, multicentre study (Iressa Survival Evaluation in Lung Cancer)’, *The Lancet*, 366(9496), pp. 1527–1537. doi: 10.1016/S0140-6736(05)67625-8.

Tien, M.-T. *et al.* (2006) ‘Anti-inflammatory effect of Lactobacillus casei on Shigella-infected human intestinal epithelial cells.’, *Journal of immunology (Baltimore, Md. : 1950)*, 176(2), pp. 1228–37.

Timmer, A. *et al.* (2016) ‘Azathioprine and 6-mercaptopurine for maintenance of remission in ulcerative colitis’, in Timmer, A. (ed.) *Cochrane Database of Systematic Reviews*. Chichester, UK: John Wiley & Sons, Ltd, p. CD000478. doi: 10.1002/14651858.CD000478.pub4.

Timmermans, W. M. C. *et al.* (2016) ‘Immunopathogenesis of granulomas in chronic autoinflammatory diseases.’, *Clinical & translational immunology*. Nature Publishing Group, 5(12), p. e118. doi: 10.1038/cti.2016.75.

Tinkum, K. L. *et al.* (2015) ‘Fasting protects mice from lethal DNA damage by promoting small intestinal epithelial stem cell survival.’, *Proceedings of the National Academy of Sciences of the United States of America*. National Academy of Sciences, 112(51), pp. E7148-54. doi: 10.1073/pnas.1509249112.

Toruner, M. *et al.* (2006) ‘Antianoikis Effect of Nuclear Factor-κB through Up-regulated Expression of Osteoprotegerin, BCL-2, and IAP-1’, *Journal of Biological Chemistry*, 281(13), pp. 8686–8696. doi: 10.1074/jbc.M512178200.

Triantafillidis, J. K., Nasioulas, G. and Kosmidis, P. A. (2009) ‘Colorectal cancer and inflammatory bowel disease: epidemiology, risk factors, mechanisms of carcinogenesis and prevention strategies.’, *Anticancer research*, 29(7), pp. 2727–37.

Troyer, K. L. *et al.* (2001) ‘Growth Retardation, Duodenal Lesions, and Aberrant

Ileum Architecture in Triple Null Mice Lacking EGF, Amphiregulin, and TGF-␣', *GASTROENTEROLOGY*, 121, pp. 68–78. doi: 10.1053/gast.2001.25478.

Tumang, J. R. *et al.* (1998) 'c-Rel is essential for B lymphocyte survival and cell cycle progression.', *European journal of immunology*, 28(12), pp. 4299–312. doi: 10.1002/(SICI)1521-4141(199812)28:12<4299::AID-IMMU4299>3.0.CO;2-Y.

Uhlen, M. *et al.* (2015) 'Tissue-based map of the human proteome', *Science*, 347(6220), pp. 1260419–1260419. doi: 10.1126/science.1260419.

Umar, S. (2010) 'Intestinal stem cells.', *Current gastroenterology reports*. NIH Public Access, 12(5), pp. 340–8. doi: 10.1007/s11894-010-0130-3.

Ungaro, R. *et al.* (2017) 'Ulcerative colitis', *The Lancet*, 389(10080), pp. 1756–1770. doi: 10.1016/S0140-6736(16)32126-2.

Uribe, J. M. *et al.* (1996) 'Epidermal growth factor inhibits Ca(2+)-dependent Cl- transport in T84 human colonic epithelial cells.', *The American journal of physiology*, 271, pp. C914-22.

Uribe, J. M. and Barrett, K. E. (1997) 'Nonmitogenic actions of growth factors: an integrated view of their role in intestinal physiology and pathophysiology.', *Gastroenterology*, 112(1), pp. 255–68.

Vadakara, J. and Borghaei, H. (2012) 'Personalized medicine and treatment approaches in non-small-cell lung carcinoma.', *Pharmacogenomics and personalized medicine*. Dove Press, 5, pp. 113–23. doi: 10.2147/PGPM.S24258.

Viennois, E., Chen, F. and Merlin, D. (2013) 'NF-κB pathway in colitis-associated cancers.', *Translational gastrointestinal cancer*, 2(1), pp. 21–29. doi: 10.3978/j.issn.2224-4778.2012.11.01.

Voboril, R. *et al.* (2004) 'Inhibition of NF-Kappa B augments sensitivity to 5-Fluorouracil/Folinic acid in colon cancer1', *Journal of Surgical Research*, 120(2), pp. 178–188. doi: 10.1016/j.jss.2003.11.023.

Wahl, C. *et al.* (1998) 'Sulfasalazine: a potent and specific inhibitor of nuclear factor kappa B.', *Journal of Clinical Investigation*, 101(5), pp. 1163–1174. doi: 10.1172/JCI992.

Wang, D. and Dubois, R. N. (2010) 'The role of COX-2 in intestinal inflammation and colorectal cancer.', *Oncogene*, 29(6), pp. 781–8. doi: 10.1038/onc.2009.421.

Wang, P. *et al.* (2009) 'PUMA is directly activated by NF-κB and contributes to TNF-α-induced apoptosis', *Cell Death and Differentiation*, 16(9), pp. 1192–1202. doi: 10.1038/cdd.2009.51.

Wang, X. *et al.* (2002) 'Manipulation of colonic bacteria and volatile fatty acid production by dietary high amylose maize (amylomaize) starch granules.', *Journal of applied microbiology*, 93(3), pp. 390–7.

Wang, X. *et al.* (2016) 'Oroxyloside prevents dextran sulfate sodium-induced experimental colitis in mice by inhibiting NF-κB pathway through PPARγ activation', *Biochemical Pharmacology*, 106, pp. 70–81. doi: 10.1016/j.bcp.2016.02.019.

Wang, Y. *et al.* (2004) 'Activation of Nuclear Factor B In vivo Selectively Protects the Murine Small Intestine against Ionizing Radiation-Induced Damage', *Cancer*

Research, 64(17), pp. 6240–6246. doi: 10.1158/0008-5472.CAN-04-0591.

Watson, A. J. M. *et al.* (2005) 'Epithelial Barrier Function In Vivo Is Sustained Despite Gaps in Epithelial Layers', *Gastroenterology*, 129(3), pp. 902–912. doi: 10.1053/j.gastro.2005.06.015.

Watson, A. J. M. *et al.* (2009) 'Mechanisms of Epithelial Cell Shedding in the Mammalian Intestine and Maintenance of Barrier Function', *Annals of the New York Academy of Sciences*, 1165(1), pp. 135–142. doi: 10.1111/j.1749-6632.2009.04027.x.

Watson, C. L. *et al.* (2014) 'An in vivo model of human small intestine using pluripotent stem cells', *Nature Medicine*, 20(11), pp. 1310–1314. doi: 10.1038/nm.3737.

Weber, C. K. *et al.* (2000) 'Suppression of NF-kappaB activity by sulfasalazine is mediated by direct inhibition of IkappaB kinases alpha and beta.', *Gastroenterology*, 119(5), pp. 1209–18.

Weih, F. *et al.* (1995) 'Multiorgan inflammation and hematopoietic abnormalities in mice with a targeted disruption of RelB, a member of the NF-kappa B/Rel family.', *Cell*, 80(2), pp. 331–40.

Weisberg, E. *et al.* (2005) 'Characterization of AMN107, a selective inhibitor of native and mutant Bcr-Abl.', *Cancer cell*. Elsevier, 7(2), pp. 129–41. doi: 10.1016/j.ccr.2005.01.007.

Wen, X.-D. *et al.* (2014) '*Panax notoginseng* Attenuates Experimental Colitis in the Azoxymethane/Dextran Sulfate Sodium Mouse Model', *Phytotherapy Research*, 28(6), pp. 892–898. doi: 10.1002/ptr.5066.

Williams, J. M. *et al.* (2013) 'A mouse model of pathological small intestinal epithelial cell apoptosis and shedding induced by systemic administration of lipopolysaccharide.', *Disease models & mechanisms*. Company of Biologists, 6(6), pp. 1388–99. doi: 10.1242/dmm.013284.

Williams, J. M. *et al.* (2015) 'Epithelial cell shedding and barrier function: a matter of life and death at the small intestinal villus tip.', *Veterinary pathology*. SAGE Publications, 52(3), pp. 445–55. doi: 10.1177/0300985814559404.

Wu, M. *et al.* (1996) 'Inhibition of NF-kappaB/Rel induces apoptosis of murine B cells.', *The EMBO journal*, 15(17), pp. 4682–90.

Wu, S. and Tong, L. (2010) 'Differential signaling circuits in regulation of ultraviolet C light-induced early- and late-phase activation of NF-κB.', *Photochemistry and photobiology*. NIH Public Access, 86(5), pp. 995–9. doi: 10.1111/j.1751-1097.2010.00767.x.

Wullaert, A., Bonnet, M. C. and Pasparakis, M. (2011) 'NF-κB in the regulation of epithelial homeostasis and inflammation.', *Cell research*. Nature Publishing Group, 21(1), pp. 146–58. doi: 10.1038/cr.2010.175.

Wyllie, A. H., Kerr, J. F. and Currie, A. R. (1980) 'Cell death: the significance of apoptosis.', *International review of cytology*, 68, pp. 251–306.

Xiao, G. *et al.* (2001) 'NF-kappaB-inducing kinase regulates the processing of NF-kappaB2 p100.', *Molecular cell*. Elsevier, 7(2), pp. 401–9. doi: 10.1016/S1097-2765(01)00187-3.

Xu, Y. *et al.* (2010) 'RelB-Dependent Differential Radiosensitization Effect of STI571 on Prostate Cancer Cells', *Molecular Cancer Therapeutics*, 9(4), pp. 803–812. doi: 10.1158/1535-7163.MCT-09-1001.

Yamaoka, T. *et al.* (2008) 'Transactivation of EGF receptor and ErbB2 protects intestinal epithelial cells from TNF-induced apoptosis.', *Proceedings of the National Academy of Sciences of the United States of America*. National Academy of Sciences, 105(33), pp. 11772–7. doi: 10.1073/pnas.0801463105.

Yan, D. *et al.* (2015) 'Gefitinib upregulates death receptor 5 expression to mediate rmhTRAIL-induced apoptosis in Gefitinib-sensitive NSCLC cell line.', *OncoTargets and therapy*. Dove Press, 8, pp. 1603–10. doi: 10.2147/OTT.S73731.

Yan, K. S. *et al.* (2012) 'The intestinal stem cell markers Bmi1 and Lgr5 identify two functionally distinct populations.', *Proceedings of the National Academy of Sciences of the United States of America*. National Academy of Sciences, 109(2), pp. 466–71. doi: 10.1073/pnas.1118857109.

Yan, Y. *et al.* (2009) 'Temporal and Spatial Analysis of Clinical and Molecular Parameters in Dextran Sodium Sulfate Induced Colitis', *PLoS ONE*. Edited by S. Bereswill, 4(6), p. e6073. doi: 10.1371/journal.pone.0006073.

Yang, J. *et al.* (2006) 'BMS-345541 Targets Inhibitor of B Kinase and Induces Apoptosis in Melanoma: Involvement of Nuclear Factor B and Mitochondria Pathways', *Clinical Cancer Research*, 12(3), pp. 950–960. doi: 10.1158/1078-0432.CCR-05-1220.

Yantiss, R. K. and Odze, R. D. (2006) 'Diagnostic difficulties in inflammatory bowel disease pathology', *Histopathology*, 48(2), pp. 116–132. doi: 10.1111/j.1365-2559.2005.02248.x.

Yasui, Y. *et al.* (2011) 'Dietary astaxanthin inhibits colitis and colitis-associated colon carcinogenesis in mice via modulation of the inflammatory cytokines', *Chemico-Biological Interactions*, 193(1), pp. 79–87. doi: 10.1016/j.cbi.2011.05.006.

Ye, X. and Sun, M. (2017) 'AGR2 ameliorates tumor necrosis factor-α-induced epithelial barrier dysfunction via suppression of NF-κB p65-mediated MLCK/p-MLC pathway activation', *International Journal of Molecular Medicine*, 39(5), pp. 1206–1214. doi: 10.3892/ijmm.2017.2928.

Yeung, C.-Y. *et al.* (2015) 'Amelioration of Chemotherapy-Induced Intestinal Mucositis by Orally Administered Probiotics in a Mouse Model', *PLOS ONE*. Edited by F. Cappello. Public Library of Science, 10(9), p. e0138746. doi: 10.1371/journal.pone.0138746.

Yin, W. *et al.* (2017) 'Inverse Association Between Poor Oral Health and Inflammatory Bowel Diseases', *Clinical Gastroenterology and Hepatology*, 15(4), pp. 525–531. doi: 10.1016/j.cgh.2016.06.024.

Yu, J. *et al.* (2005) 'Gene Expression Profiling of the Irinotecan Pathway in Colorectal Cancer', *Clinical Cancer Research*, 11(5), pp. 2053–2062. doi: 10.1158/1078-0432.CCR-04-1254.

Yu, J. (2013) 'Intestinal stem cell injury and protection during cancer therapy.', *Translational cancer research*. NIH Public Access, 2(5), pp. 384–396.

Zachos, N. C. *et al.* (2016) 'Human Enteroids/Colonoids and Intestinal Organoids

Functionally Recapitulate Normal Intestinal Physiology and Pathophysiology.', *The Journal of biological chemistry*. American Society for Biochemistry and Molecular Biology, 291(8), pp. 3759–66. doi: 10.1074/jbc.R114.635995.

Zaph, C. *et al.* (2007) 'Epithelial-cell-intrinsic IKK-β expression regulates intestinal immune homeostasis', *Nature*. Nature Publishing Group, 446(7135), pp. 552–556. doi: 10.1038/nature05590.

Zhang, H.-H. *et al.* (2014) 'Nemo-like kinase is critical for p53 stabilization and function in response to DNA damage', *Cell Death and Differentiation*, 21(10), pp. 1656–1663. doi: 10.1038/cdd.2014.78.

Zhang, Y.-J. *et al.* (2015) 'Impacts of gut bacteria on human health and diseases.', *International journal of molecular sciences*. Multidisciplinary Digital Publishing Institute (MDPI), 16(4), pp. 7493–519. doi: 10.3390/ijms16047493.

Zhou, D. *et al.* (1999) 'A high dose of ionizing radiation induces tissue-specific activation of nuclear factor-kappaB in vivo.', *Radiation research*, 151(6), pp. 703–9.